UNIVERSITÉ DU QUÉBEC À MONTRÉAL

ÉTUDE FONCTIONNELLE DE L'APOLIPOPROTÉINE D HUMAINE EN SITUATIONS DE STRESS

THÈSE
PRÉSENTÉE
COMME EXIGENCE PARTIELLE
DU DOCTORAT EN BIOLOGIE

PAR
SONIA DO CARMO

JANVIER 2009

REMERCIEMENTS

J'aimerais d'abord remercier le Dr Éric Rassart qui m'a accueillie dans son laboratoire pendant toutes ces années, pour sa confiance et son appui. Il m'a aidée à développer mon esprit scientifique et m'a conseillée à chacune des étapes de mon doctorat tout en me laissant une grande liberté. Je tiens aussi à remercier tous mes collègues de travail pour leur amitié, leurs conseils et leurs encouragements. Ils m'ont aidée à traverser les beaux moments comme les déceptions de la vie de doctorante. Je tiens à remercier tout spécialement ceux qui ont travaillé avec moi sur le projet apoD : Louis-Charles Levros avec qui j'ai eu le plaisir de collaborer, Wafa Najyb avec qui j'ai eu de grandes discussions et Azade Kashani qui m'a offert sa confiance. Je tiens aussi à remercier les nombreux chercheurs du département des sciences biologiques et leurs équipes qui ont contribué via leurs idées et l'accès à leur matériel à la réalisation de ce projet. Je pense plus spécialement à Julie Lafond, Catherine Mounier, Fathey Sarhan, Benoît Barbeau, Louise Brissette et François Dragon.

J'ai eu également la chance d'avoir d'excellents collaborateurs. Je remercie Diego Sanchez et Maria D. Ganfornina qui m'ont accueillie dans leur laboratoire comme dans leur vie privée. Ils m'ont aidée dans mes recherches, m'ont fait découvrir leur beau coin d'Espagne et sont devenus des amis proches. Je remercie aussi Pierre Talbot et Hélène Jacomy avec qui ça a été un réel plaisir de travailler. Je remercie finalement Julie Lafond et Maude Éthier-Chiasson qui m'ont fait découvrir l'apoD dans un tout nouveau contexte, la grossesse.

Je remercie aussi très fort mes parents, Maria Eugénia Dias et Manuel Antonio Carmo pour leur amour, leur présence dans les bons comme dans les mauvais moments, pour leurs conseils, pour leur soutien, ainsi que pour la confiance qu'ils me portent. Sans vous, rien n'aurait été possible. Un gros merci à mes amis qui sont restés à mes côtés et qui m'ont écoutée et encouragée alors qu'ils ne

comprenaient que très peu mes histoires de cellules et de souris. J'aimerais finalement remercier Jean-Benoît Charron avec qui je partage non seulement ma vie mais aussi ma passion de la science. Merci pour ton amour, pour tout ton soutien dans les moments difficiles, pour ta patience, pour ton aide, et pour ta présence tout simplement.

TABLE DES MATIÈRES

CHAPITRE II

LISTE DES TABLEAUX

CHAPITRE I

CHAPITRE II

CHAPITRE III

CHAPITRE V

ANNEXE II

LISTE DES FIGURES

CHAPITRE II

CHAPITRE III

CHAPITRE IV

CHAPITRE V

CHAPITRE VI

ANNEXE II

ANNEXE III

ANNEXE IV

ANNEXE V

LISTE DES ABRÉVIATIONS

AA	acide arachidonique
ABTS	2,2'-azino-bis(3-ethylbenzthiazoline-6-sulphonic acid)
ADN	acide désoxyribonucléique
ADNc	acide désoxyribonucléique complémentaire
AP	activating protein
ApoD	apolipoprotéine D
ApoE	apolipoprotéine E
APRE	acute phase responsive element
ARNm	acide ribonucléique messager
AtTIL	*Arabidopsis thaliana* temperature-induced lipocalin
BBB	blood-brain barrier
bFGF	basic fibroblast growth factor
BMI	body mass index
BrdU	5-bromo-2-deoxyuridine
BSA	bovine serum albumin
C/EBP	CCAAT/enhancer binding protein
CETP	cholesteryl ester transfer protein
CNS	central nervous system
COX	cycloxygenase
CSF	cerebrospinal fluid
DMEM	Dulbecco's modified Eagle's medium
DPI	days post-infection
DPN	days post-natal
EDTA	acide éthylène-diamine-tétraacétique
ELISA	enzyme-linked immunosorbent assay
ERE	estrogen response element

ERK 1/2	extracellular signal-regulated kinase-1/2
FAS	fatty acid synthase
FITC	fluorescein isothiocyanate
FSE	fat response element
GAPDH	glyceraldehyde 3-phosphate dehydrogenase
GCDFP-24	gross cystic disease protein-24 kDa
GFAP	glial fibrillary acidic protein
GFP	green fluorescent protein
GLaz	glial Lazarillo
GLUT	glucose transporter
GMCSF	granulocyte-macrophage colony-stimulating factor
GRE	glucocorticoid response element
GST	glutathione S-transferase
GWG	gestationla weight gain
H-apoD	human apoD, apoD humaine
HCoV-OC43	human coronavirus OC43
HDL	high density lipoprotein
HPLC	high performance liquid chromatography
HPRT	hypoxanthine-guanine phosphoribosyltransferase
HRP	horseradish peroxidase
HSV-1	herpes simplex virus
IC	intra-cérébral
IFNγ	interféron gamma
IL	interleukine
IPGTT	intraperitoneal glucose tolerance test
IRS	insulin receptor substrate
ITT	insulin tolerance test
KO	knock-out
LCAT	lécithine cholestérol acyltransférase

LDL	low density lipoprotein
LFABP	liver fatty acid-binding protein
LPS	lipopolysaccharide
LXR	liver X receptor
M-apoD	mouse apoD, apoD murine
MCP-1	monocyte chemoattractant protein 1
MEM	minimum essential medium
MMP	matrix metalloproteinase
MOPS	acide 3-(N-Morpholino)propanesulfonique
MRE	metal response element
MTS/PMS	3-(4,5-dimethylthiazol-2-yl)-5-(3-carboxymethoxyphenyl)-2-(4-sulfophenyl)-2H-tetrazolium/ phenazine methosulfate
NF-kB	nuclear factor kappa B
NFL	neurofilament light chain
NFT	neurofibrillary tangles
NLS	nuclear localization signal
NMDA	N-méthyl-D-aspartate
NPC	Niemann-Pick de type C
NPY/AGRP	neuropeptide Y/Agouti related peptide
NSE	neuron specific enolase
PBS	phosphate buffered saline
PCR	polymerase chain reaction
PDGF	platelet derived growth factor
PE	phycoerythrin
PKC	protein kinase C
PLA2	phospholipase A2
POMC/CART	pro-opiomelanocortin/ cocaine- and amphetamine-regulated transcript
PPAR	peroxisome proliferator-activated receptor
PQ	paraquat

PRE	progesterone response element
PVDF	polyvinylidene difluoride
RAR	retinoic acid receptor
ROS	reactive oxygen species
SDR	sterol dependent repressor
SDS-PAGE	sodium dodecyl sulfate-polyacrylamide gel electrophoresis
SNC	système nerveux central
SNP	système nerveux périphérique
SREBP	sterol regulatory element binding proteins
STAT	signal transducers and activators of transcription
STRE	stress response element
TBARS	thiobarbituric acid reactive substances
Tg	transgénique
TGFβ	transforming growth factor beta
TNFα	tumor necrosis factor alpha
TRE	thyroid-hormone response element
TUNEL	terminal deoxynucleotidyl transferase biotin-dUTP nick end labeling
UV	ultra-violet
VLDL	very low density lipoprotein
VSMC	vascular smooth muscle cells
WT	wild-type

RÉSUMÉ GÉNÉRAL

L'apolipoprotéine D (apoD) est une glycoprotéine sécrétée dont l'expression est modulée dans une multitude de situations incluant les cancers de différents tissus, les désordres métaboliques et les maladies neurodégénératives. Bien que la liste des conditions présentant une augmentation de l'apoD s'allonge chaque jour, les facteurs provoquant le déclenchement de son expression, de même que la fonction de celle-ci, restent inconnus. Les travaux présentés dans cette thèse ont permis de jeter un peu de lumière sur ces deux aspects. Dans un premier temps, ces travaux ont permis de déterminer que l'apoD est une protéine de stress spécifique et que son expression est déclenchée par des stress ayant une forte composante oxydante ou inflammatoire. Cependant, alors que l'expression de l'apoD en réponse au stress oxydatif est associée à un arrêt de croissance, en condition inflammatoire, elle est accompagnée d'une stimulation de la prolifération. De plus, ces stress modifient non seulement le niveau d'expression, mais aussi la localisation intracellulaire de l'apoD. L'apoD, qui est normalement sécrétée, est réinternalisée et s'accumule dans le cytoplasme et le noyau. L'entrée de l'apoD dans la cellule influence, de plus, la prolifération cellulaire. Ces travaux ont ensuite permis de mieux cerner le rôle de cette modulation de l'apoD en situations de stress chez l'animal. Pour cela, nous avons soumis des souris surexprimant l'apoD humaine dans leur système nerveux ou n'exprimant pas l'apoD à des conditions neurodégénératives. Nous avons ainsi établi que l'apoD serait impliquée dans les mécanismes régulant la protection contre diverses atteintes neurodégénératives, incluant le stress oxydatif et l'inflammation, favorisant donc la survie suite à ces atteintes. Ainsi, l'apoD joue un rôle dans la fonction neuronale basale tel que déterminé grâce à des tests comportementaux. De plus, l'apoD limite la peroxydation lipidique lors de l'exposition au paraquat, un générateur de stress oxydatif. De façon similaire, l'apoD contrôle la production de cytokines et de phospholipase A2, réduit l'infiltration de cellules T et induit l'activation gliale en réponse à l'infection par le coronavirus humain OC43, un modèle d'inflammation aiguë. Par ailleurs, la surexpression de l'apoD humaine chez la souris favorise l'accumulation de lipides dans le foie et les muscles, favorisant ainsi le développement de la résistance à l'insuline accompagnant souvent le vieillissement physiologique. Cette accumulation de lipides a été associée à une stimulation de gènes impliqués dans la synthèse d'acides gras. Les travaux présentés dans cette thèse contribuent donc à établir l'apoD comme un facteur bénéfique favorisant la survie suite à une atteinte cellulaire. Ils suggèrent aussi l'importance de contrôler les niveaux physiologiques de l'apoD afin de maintenir l'homéostasie métabolique.

Mots-clés : apolipoprotéine D, arrêt de croissance, inflammation, lipocaline, résistance à l'insuline, stress oxydatif.

CHAPITRE I

État des connaissances

1.1 Introduction

L'apolipoprotéine D (apoD) est une glycoprotéine de 29 kDa d'abord trouvée associée aux lipoprotéines de haute densité (HDL) dans le plasma humain. C'est une apolipoprotéine atypique qui, selon les caractéristiques de sa structure primaire, appartient à la famille des lipocalines. Les lipocalines sont une famille de petites protéines conservées au cours de l'évolution et impliquées dans plusieurs processus physiologiques. Ces protéines ont en commun une structure tertiaire en forme de barillet β leur permettant de lier et de transporter des petites molécules hydrophobes. Parmi les ligands connus de l'apoD, on retrouve entre autres l'acide arachidonique, les stéroïdes, la bilirubine et le cholestérol.

1.2 Propriétés de l'apoD

1.2.1 Structure du gène et de la protéine

L'analyse du promoteur humain de l'apoD a révélé la présence de plusieurs éléments potentiels de régulation. Parmi ceux-ci, on retrouve des éléments de réponse aux hormones stéroïdes, aux acides gras, au sérum et à la phase aiguë (Do Carmo *et al.* 2002, Lambert *et al.* 1993). La diversité de ces éléments de régulation reflète la complexité de la régulation de l'expression de l'apoD humaine. Par ailleurs, la région codante du gène de l'apoD contient 3 régions consensus et un modèle d'exons commun à tous les membres des lipocalines (Provost *et al.* 1990). Le gène humain est divisé en 5 exons et les 815 pb d'ARNm sont distribués sur plus de 12 kpb de génome. Le premier exon est non-codant. L'ADNc prédit une protéine mature de 169

acides aminés précédée d'un peptide signal de 20 acides aminés (Drayna *et al.* 1987). L'apoD a une structure tertiaire en forme de barillet β ouvert à son sommet et fermé à sa base, typique des lipocalines (Peitsch et Boguski 1990). Cette structure lui permet de transporter de petites molécules hydrophobes. Trois des 4 boucles de l'extrémité ouverte du barillet exposent des chaînes hydrophobes, ce qui est inhabituel chez une lipocaline. Cette particularité est sans doute responsable de l'insertion de l'apoD dans la phase lipidique des HDL. Cette région comporte aussi une cystéine libre qui peut stabiliser l'association de l'apoD aux HDL via la formation de ponts disulfure avec d'autres molécules présentes dans les HDL comme l'apoA-II (Eichinger *et al.* 2007, Yang *et al.* 1994).

1.2.2 Distribution tissulaire

Jusqu'à présent, l'apoD a été caractérisée chez cinq espèces mammifères et détectée chez le singe, le cochon et le poulet. La vaste distribution de l'expression de l'apoD reflète probablement son importance et son rôle de protéine multifonctionnelle. De plus, la découverte du gène de l'apoD aviaire, de même que des analyses phylogénétiques et la présence de séquences similaires à l'apoD chez les poissons et les céphalocordés suggèrent son importance évolutive dans la lignée des cordés (Ganfornina *et al.* 2005). De proches homologues ont également été trouvés dans la membrane externe de la bactérie *Escherichia coli* (Bishop *et al.* 1995), chez la drosophile (Sanchez *et al.* 2006, Walker *et al.* 2006), la chenille *Hyphantria cunea* (Kim *et al.* 2005), l'amphioxus (Wang *et al.* 2007) et chez les plantes (Frenette Charron *et al.* 2002)

Chez l'humain, l'apoD est faiblement exprimée dans le foie et l'intestin qui sont les sites majeurs de synthèse des autres apolipoprotéines. Elle est, par contre, hautement exprimée dans les glandes surrénales, les reins, le pancréas, le placenta, la

rate, les poumons, les ovaires, les testicules, le cerveau et les nerfs périphériques (Borghini *et al.* 1995, Drayna *et al.* 1986, Rassart *et al.* non publié). Chez le singe (Smith *et al.* 1990), le lapin (Provost *et al.* 1990a, Provost *et al.* 1991b) et le cobaye (Provost *et al.* 1995), la distribution de l'apoD est similaire à celle retrouvée chez l'humain (Drayna *et al.* 1986). Cependant, chez la souris (Cofer et Ross 1996, Séguin *et al.* 1995, Yoshida *et al.* 1996) et le rat (Boyles *et al.* 1990b), la distribution tissulaire de l'ARNm de l'apoD est différente avec une expression largement restreinte au système nerveux central (SNC) où elle est observée dans la moelle épinière, le cervelet et le cerveau (Table 1.1). Cependant, des analyses immunohistochimiques ont démontré la présence de cellules contenant des niveaux substantiels d'apoD dans pratiquement tous les organes (Boyles *et al.* 1990b). L'apoD aviaire est quant à elle préférentiellement associée aux lipoprotéines plasmatiques, mais est aussi présente dans l'oocyte en croissance rapide. Il a donc été suggéré qu'elle joue un rôle dans le transport et/ou la mobilisation des lipides et des molécules régulatrices durant l'embryogenèse chez les espèces ovipares (Vieira *et al.* 1995, Yao et Vieira 2002).

Table 1.1 : Distribution tissulaire de l'ARNm de l'apoD et de sa protéine dans différentes espèces[a].

organe	humain ARNm	singe rhésus protéine[b]	lapin ARNm	souris ARNm	rat ARNm	rat protéine[b]	cobaye ARNm
moelle	n.t.	n.t.	n.t.	+++++++++	++++	n.t.	n.t.
cervelet	+++	n.t.	+++	++++	+++	n.t.	n.t.
cerveau	++	+	++	+++	++	+	n.t.
ovaires	n.t.	n.t.	n.t.	+	-	n.t.	++++
surrénales	++++	n.t.	++++	+	-	+	+++
testicules	n.t.	+	++	+	+	+	+++
muscle	n.t.	+	+	+	-	n.t.	n.t.
thymus	n.t.	n.t.	+	+	-	n.t.	n.t.
poumons	n.t.	n.t.	++	+	-	+	+++
foie	+	+	+	+	-	+	+
rein	++	+	++	-[d]	-	+	++
coeur	n.t.	+	+	-	-	+	n.t.
intestin	+	+	+	-[d]	-	+	++
rate	+++	+	+++++	-[d]	-	+	++
pancréas	++	+	n.t.	-	n.t.	+	n.t.
placenta	+++	n.t.	n.t.	n.t.	n.t.	n.t.	n.t.
sérum[c]	oui	oui	oui	non		trace	n.t.
références	Drayna *et al.* 1986; non-publié	Smith *et al.* 1990	Provost *et al.* 1990	Séguin *et al.* 1990	Séguin *et al.* 1990	Boyles *et al.* 1990b	Provost *et al.* 1995

-, niveaux inférieurs à celui du foie; n.t., non-testé

[a] données provenant de diverses études, ne devraient pas être comparées entre elles

[b] les études protéiques n'étaient pas quantitatives

[c] mesure protéique

[d] présence d'une bande additionnelle plus petite

Tiré de Rassart *et al.* 2000.

1.2.3 Ligands

Lorsque identifiée comme la composante majeure (30 mg/ml) des fluides kystiques mammaires, l'apoD (GCDFP-24) a d'abord été caractérisée par sa capacité à lier la progestérone (Ka de 2.5 x 10^6 mol/l) et la prégnénolone (Ka de 1.32 x 10^6 mol/l), avec une très forte affinité (Balbin *et al.* 1990, Lea 1988, Pearlman *et al.* 1973). Le Ka relatif de l'apoD pour diverses classes de stéroïdes est : prégnénolone > progestérone > pregnanolone > pregnandione > androgènes > oestrogènes (Dilley *et al.* 1990, Simard *et al.* 1991).

De plus, à cause de son association avec la LCAT (lécithine cholestérol acyltransférase), le cholestérol et ses esters ont longtemps été considérés comme les principaux ligands de l'apoD (Drayna *et al.* 1986). Ainsi, l'apoD pourrait être impliquée dans le transfert des esters de cholestérol aux lipoprotéines accepteuses (Fielding et Fielding 1980, Francone *et al.* 1989) et dans le transport réverse du cholestérol des tissus périphériques vers le foie pour son catabolisme (Kostner *et al.* 1988, Spreyer *et al.* 1990). La modélisation moléculaire suggère toutefois que les composés dérivés de l'hème, comme la bilirubine, sont des ligands plus probables que les dérivés du cholestérol (Peitsch et Boguski 1990). Il a en effet été confirmé que l'affinité des HDL pour la bilirubine résulte de la liaison de celle-ci à l'apoD avec un ratio bilirubine:apoD de 0.8:1 (Goessling et Zucker 2000). Néanmoins, l'acide arachidonique est le ligand présentant la plus haute affinité pour l'apoD (Ka de 1.6 x 10^8 mol/l). Ceci suggère un rôle pour l'apoD dans la mobilisation de l'acide arachidonique, et donc dans la synthèse des prostaglandines. L'apoD pourrait également transporter l'acide arachidonique prévenant ainsi sa conversion en esters de cholestérol (Morais Cabral *et al.* 1995). La composante odorante des sécrétions axillaires, l'acide E-3-méthyl-2-héxénoïque (E-3M2H), est aussi transportée à la surface de la peau liée à l'apoD (Zeng *et al.* 1996). Il est possible que le ligand associé à l'apoD varie dépendamment des conditions ou du site d'expression lui

permettant ainsi d'exercer différentes fonctions. De plus, des études détaillées de liaison par titration de fluorescence effectuées sur des préparations d'apoD biochimiquement homogènes ont révélé que l'apoD peut discriminer des composés très semblables (Vogt et Skerra 2001).

1.3 Modulation de l'apoD et fonctions associées

La régulation de l'expression de l'apoD est très complexe et plusieurs auteurs ont démontré l'importance de facteurs biologiques dans la modulation de cette protéine.

1.3.1 Croissance et différenciation cellulaire

Il semble exister une relation inverse entre l'expression de l'apoD et la prolifération cellulaire. Par exemple, des études sur des cultures cellulaires primaires et immortalisées ont montré que l'arrêt de croissance provoqué par déprivation de sérum, confluence ou sénescence, induit l'expression de l'apoD (Do Carmo *et al.* 2002, Provost *et al.* 1991a). Au niveau du promoteur, les éléments responsables de cette induction ont été identifiés comme étant les SRE (serum response elements) et un APP (alternating purine-pyrimidine stretch) (Do Carmo *et al.* 2002). De façon similaire, dans des lignées cellulaires de cancer du sein ou de la prostate, la sécrétion de l'apoD est inhibée par les oestrogènes, stimulée par les androgènes et est inversement corrélée avec la prolifération cellulaire (Simard *et al.* 1990, Simard *et al.* 1991, Simard *et al.* 1992). De plus, l'exposition de cellules de cancer du sein à l'interleukin-1α diminue la prolifération cellulaire basale de même que celle induite par l'exposition aux oestrogènes. Parallèlement, elle stimule l'expression basale d'apoD et celle induite par les androgènes et les glucocorticoïdes (Blais *et al.* 1994). Tous ces effets peuvent être contrecarrés par l'ajout d'interleukine-6 aux cellules (Blais *et al.* 1995). Finalement, l'apoD supprime de façon sélective la réponse

proliférative des cellules musculaires vasculaires aux facteurs de croissance par un mécanisme relié à la translocation nucléaire de ERK1/2 (Sarjeant *et al.* 2003).

Cependant, l'expression de l'apoD peut également être reliée à la période de différenciation qui suit un arrêt prolifératif. En effet, l'addition d'acide rétinoïque (Lopez-Boado *et al.* 1994) ou de 1,25-dihydroxyvitamine D3 (Lopez-Boado *et al.* 1997), deux substances bien connues pour leurs propriétés différenciatives, peuvent induire l'expression d'apoD dans des cellules de cancer mammaire. Ultérieurement, il a été démontré que l'induction d'apoD est médiée par les récepteurs nucléaires à l'acide rétinoïque (RAR) menant à une inhibition significative de la prolifération cellulaire. Ainsi, l'apoD pourrait être un marqueur biochimique de différenciation et d'arrêt de prolifération médiés par RAR dans les cellules cancéreuses (Lopez-Boado *et al.* 1996).

Ces études suggèrent donc que l'expression de l'apoD pourrait être modulée directement ou indirectement par des changements dans la prolifération ou la différenciation cellulaires. Il existe également des preuves *in vivo* d'une telle corrélation. Ainsi, dans la prostate, l'apoD est principalement présente dans les cellules glandulaires épithéliales. Cette localisation peut être associée à l'état non-prolifératif ou différentié de ces cellules (Aspinall *et al.* 1995). Cependant, la relation entre la sécrétion de l'apoD et la prolifération cellulaire semble complexe et peut ne pas être respectée dans toutes les situations.

1.3.2 Métabolisme

L'apoD est également impliquée dans plusieurs aspects du métabolisme lipidique. Des polymorphismes dans le gène de l'apoD affectent le niveau de lipides dans le plasma (Desai *et al.* 2002) et peuvent être utilisés comme marqueurs génétiques pour l'obésité, l'hyperinsulinémie et le diabète non-insulino-dépendant ou

diabète de type 2 (Baker *et al.* 1994, Vijayaraghavan *et al.* 1994). De plus, l'apoD pourrait participer dans le transfert de lipides et le transport inverse du cholestérol en liant directement le cholestérol (Patel *et al.* 1997) ou via la formation de complexes avec l'apoA-I, la LCAT (lecithin-cholesterol acyltransferase) et le CETP (cholesteryl ester transfer protein) dans les fractions de HDL (Spreyer *et al.*1990, Steyrer et Kostner 1988). L'apoD a aussi été documentée comme un gène répondant au LXR (liver X receptor) (Hummasti *et al.* 2004) et pourrait jouer un rôle important dans l'équilibre entre la lipogenèse et la lipolyse dans les adipocytes (Bujalska *et al.* 2006, Zhang *et al.* 2007) en transportant des ligands pour LXR ou PPAR ou en participant au transport inverse du cholestérol dépendant de LXR (Hummasti *et al.* 2004).

À cause de sa capacité à lier l'acide arachidonique, l'apoD contribuerait aussi au métabolisme des phospholipides membranaires en stabilisant le niveau d'acide arachidonique dans les membranes cellulaires (Thomas *et al.* 2003d, Yao *et al.* 2005). Conformément à ceci, le cerveau de souris déficientes en apoD (apoD-KO) présente une composition en gras différente. Ainsi, leur cerveau a un plus petit ratio cholestérol/phospholipides totaux, mais une plus grande concentration d'acide docosahexaénoïque, d'acide linoléïque et de certains acides gras saturés comparativement aux souris de type sauvage (Thomas *et al.* 2007). L'implication dans la redistribution de lipides après des lésions nerveuses périphériques a également été suggérée (Boyles *et al.* 1990a).

Elle jouerait également un rôle dans le contrôle de l'homéostasie énergétique. Dans l'hypothalamus, l'apoD interagit spécifiquement avec la portion cytoplasmique de la forme longue du récepteur de la leptine Ob-Rb reconnu pour son implication dans le contrôle de la satiété et de la prise de poids. De plus, le niveau hypothalamique de l'ARNm de l'apoD est stimulé par le contenu en gras de l'alimentation et est fortement et positivement corrélé avec la masse adipeuse corporelle et les niveaux circulants de leptine. Cette corrélation avec l'adiposité

corporelle est cependant perdue chez les souris obèses ob-/ob- et db-/db-, qui possèdent des niveaux réduits d'apoD lorsque comparées avec les souris de type sauvage. Ceci suggère que l'apoD hypothalamique est impliquée dans les voies de signalisation du récepteur Ob-Rb de la leptine qui contrôle l'accumulation de gras lors d'une diète riche en gras (Liu *et al.* 2001).

Il n'est donc pas surprenant qu'une modulation de l'apoD soit trouvée dans des conditions présentant un défaut du métabolisme lipidique ou dans des conditions menant à l'accumulation de lipides. Parmi celles-ci, on retrouve la maladie de Tangier ou déficit familial en HDL (Alaupovic *et al.* 1981), le déficit familial en LCAT (Albers *et al.* 1985), les mutations dans le gène de l'apoA-I (Deeb *et al.* 1991), le diabète de type 2 (Hansen *et al.* 2004), l'alcoolisme (Lewohl *et al.* 2000, Saito *et al.* 2002) et les modèles animaux de la maladie de Niemann-Pick de type C (Yoshida *et al.* 1996). L'association de l'apoD avec ces maladies peut être directement reliée à l'accumulation de lipides. Elle peut également être reliée à des phénomènes entourant l'accumulation de lipides tels que l'activation des voies inflammatoires et pro-angiogéniques (Hummasti *et al.* 2004) qui modifient le métabolisme de l'acide arachidonique, le stress oxydatif ou la réponse à l'insuline. En effet, dans toutes ces maladies, on constate une résistance à l'insuline.

Des études ont démontré que la résistance à l'insuline est un prédicteur puissant de plusieurs maladies incluant l'accident vasculaire cérébral, le diabète de type 2, les maladies cardiovasculaires, l'hypertension et même le cancer (Facchini *et al.* 2001). La résistance à l'insuline est une diminution de l'effet biologique de l'insuline au niveau des tissus cibles tels que le muscle et le tissu adipeux. Elle résulte de défauts au niveau des récepteurs spécifiques à l'insuline ou des voies de signalisation intracellulaires répondant à l'insuline. Ces défauts inhibent la translocation des vésicules contenant le transporteur spécifique au glucose Glut-4 vers la surface cellulaire et donc l'entrée de glucose dans la cellule et son utilisation

subséquente dans les voies produisant de l'énergie. Ceci provoque une accumulation de glucose dans le sang au lieu de son absorption par les cellules. Comme le taux de glucose sanguin reste élevé, le pancréas continue à produire de plus en plus d'insuline, ce qui provoque une hyperinsulinémie, laquelle peut entraîner des conséquences graves sur la santé. Lorsque le pancréas n'est plus en mesure de produire la quantité d'insuline nécessaire pour contrôler le niveau de glucose sanguin, il y a apparition de diabète de type 2 non-insulinodépendant (Petersen et Shulman 2006).

1.3.3 Développement

L'apoD est également modulée durant la gestation et le développement fœtal, avec des niveaux d'expression plus bas chez le fœtus que chez l'adulte (Provost *et al.* 1995). L'apoD est surexprimée dans l'endomètre humain dans la fenêtre de réceptivité utérine à l'implantation embryonnaire qui recouvre les jours 20-24 du cycle menstruel (Kao *et al.* 2002) et est hautement exprimée dans le placenta (Drayna *et al.* 1986). Son expression est augmentée dans les trompes de Fallope et les ovaires de cobayes gestantes versus les non-gestantes (Provost *et al.* 1995) mais est diminuée dans la glande mammaire allaitante (Cofer et Ross 1996). Cependant, on retrouve de l'apoD dans le lait et le colustrum humains (Palmer *et al.* 2006). Chez la souris, l'apoD est sélectivement modulée du jour E9 à la naissance dans le mésenchyme et le neuroépithelium (Sanchez *et al.* 2002). Dans le cerveau de rat, durant le développement et durant la période néonatale précoce, l'induction de l'expression du gène de l'apoD est reliée à la maturation et coïncide avec la période de myélination active et la synaptogenèse (Ong *et al.* 1999).

L'apoD est également présente dans le vitellus de l'ovocyte en croissance rapide. D'abord associée au transport et la mobilisation des lipides durant l'embryogenèse chez les espèces ovipares (Vieira *et al.* 1995), il est plus probable

qu'elle transporte des molécules régulatrices telles que la vitamine A et les hormones thyroïdes (Yao et Vieira 2002). Chez le fœtus de poulet, l'apoD est exprimée dans les dérivés de l'ectoderme tels que les follicules de plumes et le système nerveux. Cependant, bien que retrouvée dans les neurones et la glie, l'apoD n'a pas été retrouvée dans les péricytes ni dans les méninges en développement tel que décrit chez la souris. Il a été suggéré que l'ancêtre commun des oiseaux et des mammifères exprimait l'apoD à la fois dans les dérivés mesenchymateux et neuroectodermiques. Cette distribution a possiblement changé lors de la séparation évolutive entre les oiseaux et les mammifères, restreignant l'expression de l'apoD de poulet aux dérivés neuroectodermiques. (Ganfornina *et al.* 2005).

1.3.4 Protection contre le stress

L'homologue de l'apoD chez la drosophile GLaz (Glial Lazarillo) a été démontré comme augmentant la résistance au stress. Son absence réduit la résistance au stress oxydatif et au manque de nourriture et diminue la durée de vie. Elle provoque aussi une réduction des lipides ce qui cause une diminution de la masse corporelle et affecte le comportement. Ces effets ont été corrélés avec une augmentation de la mort neuronale et de la quantité de lipides peroxydés (Sanchez *et al.* 2006). L'effet inverse a été observé chez la drosophile surexprimant GLaz ou l'apoD humaine avec une augmentation de la résistance au stress oxydatif et de la longévité (Muffat *et al.* 2008, Walker *et al.* 2006).

L'homologue de l'apoD chez la plante, AtTIL, démontre un rôle semblable. Les plantes déficientes en AtTIL sont très sensibles aux conditions oxydantes comme les variations de température ou le traitement au paraquat. Dans le même ordre d'idées, des plantes cultivées à la noirceur meurent peu de temps après leur transfert à la lumière. La complémentation de ces plantes avec l'ADNc de AtTIL rétablit le phénotype normal. De plus, la surexpression de AtTIL augmente la tolérance au

stress causé par le gel, la lumière, le traitement au paraquat et retarde le dévelopement normal de la plante notamment en perturbant les mécanismes de floraison et de sénescence. La différence de réponse des plantes en fonction de l'expression de AtTIL est expliquée par la modification de gènes impliqués dans la balance énergétique et la réponse au stress oxydatif tel que révélé par des analyses par micro-puces à ADN (Charron *et al.* 2008).

1.3.5 Cancer

Une modulation de l'apoD est présente dans plusieurs cancers. L'apoD est surexprimée dans les carcinomes du sein, des ovaires, de l'endomètre, de la prostate, de la rétine, de la peau, du pancréas, et du système nerveux central. Par contre, elle est réprimée dans les oncocytomes thyroïdiens (Baris *et al.* 2004) et le cancer colorectal (Ogawa *et al.* 2005). Il a été proposé que l'apoD soit un gène suppresseur de tumeurs. Ainsi, dans les carcinomes des cellules squameuses de l'oesophage, le gène de l'apoD est inactivé par méthylation et a été identifié comme un candidat de la suppression tumorale. L'ajout d'apoD à des cellules en culture a aussi démontré sa puissante activité suppresseur de croissance (Yamashita *et al.* 2002). Le rôle suppresseur de tumeur de l'apoD a également été démontré dans le cancer du sein. Ce rôle provient de la capacité de l'apoD à interagir avec et à inhiber l'ostéopontine, un gène important dans la formation de tumeurs et de métastases (Jin *et al.* 2006).

Cependant, la relation entre le degré de différenciation tumorale et l'expression de l'apoD reste ambiguë. Ainsi, dans les cancers du sein, du foie et du système nerveux central, la haute expression de l'apoD est principalement corrélée avec des carcinomes hautement différenciés non-invasifs, non-métastatiques et est associée à une diminution des chances de réapparition du cancer et une meilleure survie. De la même façon, l'expression de l'apoD est diminuée dans le cancer colorectal et cette diminution est associée à un stade tumoral avancé et métastatique

et un mauvais pronostic (Ogawa *et al.* 2005). La présence d'apoD dans ces tumeurs peut donc être une conséquence de l'arrêt de croissance cellulaire due à la différenciation (Diez-Itza *et al.* 1994, Hunter *et al.* 2002, Lamelas *et al.* 2000, Porter *et al.* 2003, Serra Diaz *et al.* 1999). Un contrôle est également exercé au niveau de la transcription, indépendamment ou non de l'arrêt de croissance. Ainsi, le gène de l'apoD est faiblement méthylé dans les tumeurs bien différenciées comparativement aux tumeurs peu différenciées (Utsunomiya *et al.* 2005).

Par ailleurs, une présence élevée d'apoD est associée à des cancers invasifs de la prostate (Ashida *et al.* 2004, Aspinall *et al.* 1995, Hall *et al.* 2004, Zhang *et al.* 1998), de la peau et du pancréas et peut donc être un facteur pronostique d'évolution défavorable (Iacobuzio-Donahue *et al.* 2002b, Miranda *et al.* 2003, Ryu *et al.* 2001, West *et al.* 2004). Dans d'autres cancers tels que les carcinomes de l'ovaire et de l'endomètre et les rétinoblastomes, il n'y a pas de relation significative entre l'immunocoloration de l'apoD et l'âge, le stade ni le degré histologique de la tumeur (Alvarez *et al.* 2004, Rojo *et al.* 2001, Vazquez *et al.* 2000). Ceci suggère l'activation de voies de signalisation différentes de celles qui sont impliquées dans la progression de la carcinogénèse. Ainsi, suite à la transformation maligne dans ces types de cancers, la relation inverse entre l'apoD et la prolifération cellulaire semble perdue, favorisant l'augmentation simultanée de l'expression de l'apoD et de la croissance tumorale. Il reste cependant à déterminer si ceci est relié à une augmentation du taux de prolifération cellulaire ou à la diminution de la mort cellulaire (Hall *et al.* 2004). De plus, l'activité protéase de l'apoD (Kesner *et al.* 1988), son implication dans la mobilité cellulaire en réponse à des facteurs de croissance (Leung *et al.* 2004) et son association avec la progression vers un stade tumoral plus différencié suggèrent un rôle pour l'apoD dans la capacité invasive d'une tumeur et pourrait expliquer pourquoi les cellules cancéreuses exprimant l'apoD pourraient avoir un comportement plus agressif (Alvarez *et al.* 2003). Il reste cependant à déterminer si

l'expression de l'apoD est une cause ou une conséquence de ces transformations cellulaires.

Cependant, il y a également des contradictions dans le même type de cancer. D'autres études portant sur le cancer du sein et de la prostate démontrent que l'expression de cette protéine n'est pas significativement associée au degré de différenciation tumorale mais montre une relation avec la survie du patient (Rodriguez *et al.* 2000, Selim *et al.* 2001). La modulation de l'apoD dans les cancers dépend également de l'échantillon analysé. Par exemple, dans le sein et la prostate, la protéine sécrétée est présente à la fois dans les fluides issus de tumeurs bénignes et malignes. Ainsi, les niveaux d'apoD ne sont pas significativement corrélés avec la présence de cancer (Alexander *et al.* 2004, Clements *et al.* 1999). L'utilité de cette protéine comme facteur pronostique est donc incertaine, mais il a été proposé qu'elle pourrait être utile dans le choix et le suivi des thérapies hormonales utilisées pour prévenir ou traiter le cancer du sein (Hall *et al.* 1996, Harding *et al.* 2000, Weber-Chappuis *et al.* 1996). En particulier, des différences dans l'expression de l'apoD entre les cancers mammaires mâles et femelles, le dernier ayant un plus grand niveau d'expression de l'apoD et de meilleures chances de rémission, ouvre la voie à des thérapies hormonales plus sélectives qui ne devraient pas seulement tenir compte de l'état des récepteurs d'oestrogènes mais aussi d'androgènes (Serra *et al.* 2000).

1.3.6 Système nerveux

1.3.6.1 Modèles neurodégénératifs du système périphérique

Chez le rat et la souris, l'apoD est normalement produite par les astrocytes et les oligodendrocytes dans le système nerveux central et par les cellules du neurilemme ou fibroblastiques (telles que les cellules de Schwann) dans le système nerveux périphérique (Boyles *et al.* 1990a, Patel *et al.* 1995). Puisque le tissu nerveux

périphérique est capable de synthèse locale de quelques apolipoprotéines comme l'apoD et l'apoE, il est probable qu'il possède son propre système de lipoprotéines servant de véhicule pour le mouvement lipidique entre les cellules et pour le maintien de l'homéostasie du cholestérol (Borghini *et al.* 1995). Ce système de transport lipidique serait plus actif dans les nerfs périphériques endommagés dans lesquels une quantité massive de lipides est libérée lors de la dégradation de la myéline, stockée puis réutilisée durant la régénération. Ainsi, seules de petites quantités d'ARNm d'apoD sont détectées dans le nerf mature de rat. Ces niveaux augmentent modérément dans des nerfs tranchés dont la régénération est rendue impossible par la ligature de ces nerfs. Par contre, dans des nerfs écrasés en régénération, les niveaux d'ARNm et de protéine de l'apoD augmentent transitoirement de 40- et de 500-fois respectivement au moment où les axones du cal proximal croissent dans le segment nerveux distal (Boyles *et al.* 1990a, Spreyer *et al.* 1990). Une augmentation d'apoD a aussi été constatée dans les nerfs sciatiques en régénération de deux autres espèces, le lapin et le singe marmouset (Boyles *et al.* 1990a). L'augmentation de l'apoD dans les sites en régénération après une lésion par écrasement du nerf sciatique suggère que l'apoD ait un rôle dans la régénération des nerfs périphériques et peut-être dans le maintien et la réparation du système nerveux (Boyles *et al.* 1990b). Ainsi, l'apoD pourrait prévenir l'accumulation locale de molécules toxiques, comme la bilirubine, produites par les nerfs endommagés. Elle pourrait également participer au trafic de lipides nécessaire à la régénération nerveuse, soit le transport de lipides de l'axone endommagé vers les cellules de Schwann et les macrophages puis, durant la phase de régénération, l'apport de lipides à partir de ces cellules vers les membranes nouvellement synthétisées.

1.3.6.2 Système nerveux central

Chez l'humain, dans des conditions normales, l'apoD est présente principalement dans le cytosol et dans la membrane externe de l'enveloppe nucléaire

des cellules gliales de la matière blanche. Dans la matière grise, l'apoD est présente dans quelques neurones dispersés et dans les astrocytes protoplasmiques. L'apoD est également associée au cytosol des cellules périvasculaires et le lysosome des péricytes dans les parois des vaisseaux sanguins suggérant un rôle de l'apoD dans le transport de stérols et de petites molécules hydrophobes de, ou vers, les vaisseaux sanguins du néocortex (Hu *et al.* 2001, Navarro *et al.* 1998, Navarro *et al.* 2004). L'utilisation d'une approche de criblage différentiel a également permis d'identifier l'apoD comme un gène spécifique à la myéline et aux oligodendrocytes pouvant jouer un rôle dans la synthèse et dans la formation de feuillets de myéline dans la moelle épinière de rat (Schaeren-Wiemers *et al.* 1995).

L'apoD peut être impliquée dans l'estérification du cholestérol ou d'autres stéroïdes par son association avec la LCAT (lécithine-cholestérol acétyltransférase) que l'on sait présente dans le système nerveux central (SNC). (Demeester *et al.* 2000). Deux ligands putatifs de l'apoD, la progestérone et la prégnénolone, sont synthétisés par les astrocytes et les oligodendrocytes dans le SNC, types cellulaires exprimant aussi l'apoD (Patel *et al.* 1995). La prégnénolone s'accumule aussi sous forme de sulfate de prégnénolone dans le cerveau et les nerfs sciatiques d'humain et de rat (Hu *et al.* 1987). L'apoD pourrait donc jouer un rôle dans le transport local de ces hormones et participer aux processus de réinnervation. Les récepteurs stéroïdes modulent la formation et le contrôle de la connectivité synaptique. Plus spécifiquement, des récepteurs à l'oestrogène et à la progestérone sont trouvés dans l'hippocampe et leur expression est induite par les oestrogènes. Puisque les oestrogènes modulent l'expression de l'apoD dans certaines situations et que l'apoD lie probablement la progestérone, il pourrait y avoir interaction entre ces différents éléments (McEwen 1994).

Chez l'humain, l'augmentation de la protéine et de l'ARNm d'apoD dans le cortex cérébral âgé est probablement due à l'augmentation du nombre d'astrocytes

réactifs et totaux (Belloir *et al.* 2001, del Valle *et al.* 2003, Kalman *et al.* 2000). Les dépôts d'apoD apparaissent d'abord en position périnucléaire puis s'étendent à l'ensemble du cytoplasme et aux processus cellulaires alors que la coloration d'apoD s'intensifie (del Valle *et al.* 2003). Une telle relation entre l'expression de l'apoD et l'activation de la microglie est aussi rapportée chez les souris déficientes en cystatine B, un modèle animal de la maladie de Unverricht-Lundborg qui est caractérisée par une dysfonction neurologique progressive et par des crises épileptiques (Lieuallen *et al.* 2001). De la même façon, alors qu'une augmentation de l'apoD est un phénomène normal dans le cerveau vieillissant, des super-augmentations telles que constatées dans les souris PDAPP âgées peut représenter une réponse gliale compensatoire à l'accumulation de bêta-amyloïde. Les souris PDAPP, un modèle de la maladie d'Alzheimer, expriment une forme mutée de la protéine précurseur d'amyloïde humain sous le contrôle du promoteur du facteur de croissance dérivé des plaquettes (PDGF). Ces souris présentent les dépôts de bêta-amyloïde caractéristiques de la maladie d'Alzheimer (Thomas *et al.* 2001c).

Plusieurs des polymorphismes d'apoD trouvés peuvent moduler le risque de développer la maladie d'Alzheimer dans certains groupes ethniques (Desai *et al.* 2003, Helisalmi *et al.* 2004). L'augmentation de l'apoD, dans la maladie d'Alzheimer, est corrélée avec le stade Braak de dégénération (Glockner et Ohm 2003), mais est indépendant des concentrations protéiques d'apoE (Terrisse *et al.* 1998). De plus, l'induction de l'apoD est corrélée avec le génotype d'apoE dans l'hippocampe et le liquide céphalorachidien (Terrisse *et al.* 1998, Glockner et Ohm 2003), mais pas dans le cortex préfrontal (Thomas *et al.* 2003e). Cette association différentielle avec le génotype d'apoE peut être expliquée par la progression de la maladie. Le cortex entorhinal et temporal de même que l'hippocampe sont les premières régions à accumuler les enchevêtrements neurofibrillaires (NFT) (Belloir *et al.* 2001, Kalman *et al.* 2000), alors que les lésions du cortex préfrontal, une région de grand intérêt puisque impliquée dans les fonctions cognitives, ne sont observées que

tard dans la maladie (Thomas *et al.* 2003e). Ainsi, au début de la maladie, l'augmentation de l'apoD en présence d'un allèle E4 est interprétée comme un mécanisme compensatoire et pourrait indiquer une réinnervation en cours plutôt que des dommages ou la mort cellulaire. Cependant, cette corrélation est perdue dans la progression de la maladie où l'expression de l'apoD serait sous le contrôle de mécanismes différents (Belloir *et al.* 2001, Kalman *et al.* 2000, Thomas *et al.* 2003e). Il a été observé que l'augmentation d'apoD correspond au nombre d'enchevêtrements fibrillaires mais pas avec celui de plaques séniles (Glockner et Ohm 2003). De plus, alors que l'apoE est toujours localisée au coeur de la plaque amyloïde, l'apoD se situe préférentiellement autour et près de l'amyloïde (Navarro *et al.* 2003). Plus récemment, l'apoD a été trouvée associée à un sous-groupe particulier de plaques amyloïdes. Dans ces plaques, les cellules immunoréactives pour l'apoD ont été identifiées comme étant de la microglie (Desai *et al.* 2005). La colocalisation de l'apoD et des enchevêtrements neurofibrillaires dans le même neurone est rare et il a été proposé que l'apoD soit présente dans les neurones en situation de stress avant l'accumulation de NFT et que lorsque les NFT se forment, la transcription de l'apoD est déjà altérée (Belloir *et al.* 2001).

Chez les patients atteints de schizophrénie, la concentration plasmatique d'apoD décroît significativement. Ceci est en accord avec de récentes hypothèses qui associent la schizophrénie avec des problèmes au niveau de la signalisation et du métabolisme des lipides. Cependant, chez les patients schizophrènes et bipolaires, les niveaux d'apoD sont significativement et sélectivement augmentés selon la région cérébrale permettant ainsi de distinguer entre les deux maladies (Thomas *et al.* 2003b). L'augmentation de l'apoD dans les régions cérébrales impliquées dans chacune de ces pathologies suggère une réponse compensatoire localisée que les traitements neuroleptiques peuvent augmenter (Thomas *et al.* 2001b). En effet, des niveaux élevés d'apoD ont été trouvés dans le cerveau post-mortem et le plasma de patients schizophrènes de même que dans les cerveaux de rats suite au traitement

chronique avec des antipsychotiques atypiques dont la clozapine (Thomas *et al.* 2001a, Khan *et al.* 2003, Thomas *et al.* 2003c). Cette augmentation était encore plus marquée chez les patients chroniques traités avec la clozapine comparativement à des patients contrôles et à des patients à leur premier épisode psychotique (Mahadik *et al.* 2002). L'augmentation d'apoD telle qu'induite par les médicaments neuroleptiques peut donc être bénéfique aux patients psychiatriques. Des études dans des cultures de cellules suggèrent que l'apoD lie et stabilise les niveaux d'acide arachidonique aux phospholipides de la membrane des globules rouges. Des déficiences en acide arachidonique, un ligand préférentiel de l'apoD, ont été constatées chez les patients atteints de schizophrénie (Thomas *et al.* 2003d, Yao *et al.* 2005).

Une modulation de l'apoD est aussi présente dans d'autres désordres de l'homéostasie des lipides. La maladie de Niemann-Pick de type C (NPC) est une maladie génétique impliquant des anomalies de transport intracellulaire du cholestérol, aboutissant à une accumulation de cholestérol non estérifié dans les compartiments endosomal tardif et lysosomal. La souris NPC, un modèle d'étude de cette maladie, présente des anomalies au niveau du métabolisme de l'apoD. Ses niveaux plasmatiques d'apoD sont augmentés de 6 fois et des niveaux élevés d'apoD sont également constatés dans le cerveau, le tissu adipeux, le cœur, le thymus et dans les astrocytes en culture (Suresh *et al.* 1998, Yoshida *et al.* 1996). Plus spécifiquement, des cellules fortement immunomarquées en apoD sont retrouvées dans les régions cérébrales précédemment identifiées comme démontrant les changements neurodégénératifs les plus importants (Ong *et al.* 1999, Ong *et al.* 2002). Or, l'apoD est un transporteur de cholestérol. Le cholestérol est important pour la synthèse, l'assemblage et le maintien de la myéline. L'altération de son métabolisme est associée à la dégénérescence neurofibrillaire dans les maladies d'Alzheimer et de Niemann-Pick de type C (Ohm *et al.* 2003). Ainsi, la séquestration de l'apoD pourrait expliquer à la fois la déficience en myéline et les défauts de transport du cholestérol caractérisant cette dernière. L'apoD semble donc impliquée

dans la neurodégénescence sélective observée dans cette maladie génétique (Kolodny 2000, Suresh *et al.* 1998).

Chez les souris déficientes en apoE, une perte de connexions synaptiques a été observée durant la réinnervation comparativement aux contrôles (Masliah *et al.* 1995). Puisque l'apoE semble essentielle dans les processus de réinnervation dans le SNC, l'induction de l'apoD chez les souris déficientes en apoE (Terrisse *et al.* 1999) représenterait un mécanisme compensatoire ou un indicateur de neuropathologie.

L'apoD est également augmentée dans le fluide céphalorachidien de patients atteints de : la méningo-encéphalite, l'accident vasculaire cérébral, la maladie des neurones moteurs, la démence (Terrisse *et al.* 1998), la maladie de Niemann-Pick (Suresh *et al.* 1998), la polyneuropathie démyélinisante inflammatoire chronique, le syndrome de Guillain-Barré, la sclérose en plaques (Reindl *et al.* 2001), la xanthomatose cérébrotendineuse (Salen *et al.* 1987) et l'hydrocéphalie à pression normale idiopathique (Li *et al.* 2006). L'apoD a également été proposée comme gène candidat pour le glaucome (Tomarev *et al.* 2003). Plus récemment, l'apoD a été trouvée augmentée dans le cerveau de patients atteints de la maladie de Parkinson et cette augmentation a été associée à une augmentation de la production d'apoD par les cellules gliales (Ordoñez *et al.* 2006). Elle augmente également dans le cortex préfrontal de gens atteints d'alcoolisme ou de tabagisme chroniques (Flatscher-Bader et Wilce 2006).

Par ailleurs, la transcription de l'apoD est induite dans le système nerveux de souris suite à l'infection virale avec les virus HSV-1 (Kang *et al.* 2003), de l'encéphalite japonaise, rabies, sindbis (Saha et Rangarajan 2003) et scrapie (Dandoy-Dron *et al.* 1998). Il a été proposé que l'augmentation de l'expression de cette protéine soit corrélée avec la synthèse accrue de d'autres molécules de transport et avec la réponse au stress observée pendant la maladie.

Tel que dit précédemment, l'apoD est normalement produite par les astrocytes et les oligodendrocytes. Cependant, suite à une atteinte cérébrale aiguë chez les rongeurs, son expression est augmentée dans les astrocytes et est aussi retrouvée dans les neurones. C'est le cas par exemple, dans l'hippocampe de rat suite à l'injection d'acide kainique (Montpied *et al.* 1999, Ong *et al.* 1997) ou à la lésion du cortex entorhinal (Terrisse *et al.* 1999). L'induction de l'apoD a également été notée dans le cortex et l'hippocampe de rat du côté ipsilatéral suite à un traumatisme crânien (Franz *et al.* 1999). Les traitements chroniques avec le MK-801, un antagoniste non-compétitif du récepteur au glutamate NMDA, induisent aussi une induction de l'apoD et des défauts d'apprentissage chroniques chez le rat, tel que déterminé par la piscine de Morris (O'Donnell *et al.* 2003).

Il semblerait que l'expression de l'apoD est reliée à des évènements distincts dans les cellules gliales et neuronales. L'activation astrocytaire est une réponse globale observée après une lésion cérébrale. La récupération du tissu nerveux après une lésion est probablement en partie le résultat de l'équilibre entre les effets négatifs de l'astroglie réactive sur la croissance axonale et les propriétés bénéfiques des substances relâchées par cette astroglie réactive, tels que les stéroïdes sexuels, qui peuvent promouvoir la survie neuronale (Garcia-Segura *et al.* 1999). Les stéroïdes sexuels produits par les astrocytes sont potentiellement responsables de l'augmentation locale de l'ARNm d'apoD et de sa protéine soit en activant directement l'expression du gène ou indirectement, en causant un arrêt de croissance des astrocytes. La protéine, telle que produite par les astrocytes peut participer aux effets bénéfiques des stéroïdes, en les redistribuant aux neurones. La production d'apoD par les neurones, par contre, peut être une tentative désespérée de récupérer des facteurs essentiels à la survie comme les stéroïdes ou les facteurs de croissance et de se débarrasser de molécules toxiques. Ceci est corroboré par des études suggérant que l'apoD est exprimée dans les neurones destinés à mourir (Franz *et al.* 1999, Ong

et al. 1997). Par contre, d'autres études démontrent qu'une expression accrue de l'apoD n'est pas toujours associée à la mort neuronale. Par exemple, l'induction du gène de l'apoD a été constatée dans des neurones en maturation du SNC qui avaient des caractéristiques de cellules viables plutôt qu'apoptotiques ou nécrotiques (Ong *et al.* 1999). De la même façon, dans un modèle expérimental d'accident vasculaire cérébral, la protéine mais pas l'ARNm de l'apoD était augmentée dans les neurones pyramidaux mourants indiquant la redistribution des lipides. L'apoD a de plus été localisée dans les zones de cicatrisation et d'élongation neuronale entourant les régions touchées suggérant un rôle actif dans la réparation (Rickhag *et al.* 2006).

Par ailleurs, le stress oxydatif jouerait un rôle dans la neurodégénération aiguë et chronique dans plusieurs désordres du SNC. Par exemple, les radicaux libres d'oxygène et les oxydes nitriques peuvent conduire à la dégénérescence neuronale suite à l'ischémie cérébrale aiguë et aux traumatismes crâniens *in vivo* (Chan *et al.* 1995). Puisque l'apoD lie la bilirubine et d'autres molécules reliées à l'hème, elle peut faire partie du système de défense antioxydant dans lequel la conversion de l'hème en biliverdine puis en bilirubine sert à protéger la cellule d'un dommage oxydatif après une lésion (Peitsch et Boguski, 1990). Donc, l'induction de l'apoD peut être important pour la protection neuronale suite à une maladie du SNC (Alvarez *et al.* 2003).

Ainsi, malgré la quantité d'études portant sur l'apoD, peu de choses sont connues à propos de ses fonctions physiologiques. Il est possible qu'à cause de ses propriétés multi-ligand, l'apoD agisse via différentes voies dans chacun des organes ou tissus dans lesquels son expression a été rapportée. Son implication dans les processus cellulaires et pathologiques souligne l'importance de la compréhension des mécanismes moléculaires contrôlant son expression afin de l'utiliser comme biomarqueur de pathologies et même, si possible, en tant qu'agent modulateur ou thérapeutique.

PROBLÉMATIQUE ET OBJECTIFS

Il est clair que l'apoD a une fonction importante dans l'organisme, particulièrement dans le système nerveux, durant le développement et la vie adulte. Elle est exprimée en conditions normales et surexprimée lors de lésions ou de pathologies tissulaires incluant les neuropathologies, les désordres métaboliques et le cancer. L'apoD peut donc faire partie intégrante des mécanismes entourant le développement de ces conditions pathologiques. Son expression peut, par ailleurs, être associée à une tentative de rémission par l'arrêt des dommages cellulaires et/ou la réparation des sites endommagés. Cependant, puisque les situations déclenchant son expression sont très hétérogènes, il a été proposé que la surexpression de l'apoD lors de pathologies reflète une réponse non-spécifique à un grand nombre de stimuli différents. L'augmentation de l'expression de cette protéine serait ainsi corrélée avec la synthèse accrue de d'autres molécules de transport et avec la réponse au stress observée pendant la maladie. Le rôle de l'apoD dans les pathologies en général et dans les situations neurodégénératives en particulier, qu'il soit direct ou indirect, reste donc à définir.

Afin d'élucider quelques aspects de la fonction de l'apoD, nous nous sommes fixés deux objectifs. Notre premier objectif était de déterminer ce qui provoque l'expression de l'apoD. Contrairement à ce qui a été suggéré, nous croyons que l'augmentation de l'expression de l'apoD lors de pathologies est reliée à un ou des déclencheurs spécifiques. Nous avons donc soumis des cultures de cellules à divers types de stress cellulaire et déterminé si ces stress avaient une influence sur l'apoD au niveau de son ARNm, de sa protéine et de sa localisation cellulaire. Nous avons aussi corrélé l'expression de l'apoD lors des stress avec des marqueurs de statut cellulaire comme la prolifération, l'apoptose et la sénescence.

Il s'agissait par la suite de déterminer si l'augmentation de l'expression de l'apoD est bénéfique ou non. En s'appuyant sur les résultats obtenus chez la drosophile, nous avons formulé l'hypothèse que l'apoD favorise une meilleure survie en réponse à des situations de stress cellulaire. Nous avons choisi de tester cette hypothèse dans un contexte neurodégénératif. Pour cela, nous avons utilisé des souris qui sont déficientes en apoD (ApoD-KO) ou qui surexpriment l'apoD humaine dans les neurones (H-apoD-Tg), le type cellulaire le plus affecté lors de maladies neurodégénératives. Nous avons opté pour la surexpression de l'apoD humaine afin de la différencier de l'apoD endogène de souris. Nous avons donc dans un premier temps caractérisé ces souris. Puis nous avons soumis ces souris à des traitements neurodégénératifs. Ces traitements ont été sélectionnés suite aux résultats obtenus lors du premier objectif. Nous avons utilisé l'injection de paraquat, un inducteur de stress oxydatif et l'infection avec le coronavirus humain OC43, un modèle d'inflammation aiguë du système nerveux. Il s'agissait donc de déterminer si les divers génotypes de souris survivaient de façon différente face à ces traitements et de corroborer ces différences dans la survie avec des paramètres biochimiques et moléculaires à l'aide de marqueurs d'inflammation et de stress oxydatif.

NOTE : Dans un souci d'économie, les références de chacun des chapitres apparaissent seulement dans la section intégrée des références à la fin de la thèse.

CHAPITRE II

Modulation of apolipoprotein D expression and translocation under specific stress conditions

Sonia Do Carmo, Louis-Charles Levros Jr, Eric Rassart

2007

Biochimica et Biophysica Acta (BBA)-Molecular Cell Research 1773: 954-969

Avant-propos

La compréhension des mécanismes impliqués dans le déclenchement de l'expression de l'apoD lors de pathologies nous fournira sans doute des éléments de réponse quant à sa fonction. Cet article a pour objectif de comprendre ce qui provoque l'expression de l'apoD lors de situations de stress cellulaire. Nous nous sommes donc intéressés à l'incidence de divers stress cellulaires sur la transcription, la traduction et la localisation de l'apoD ainsi qu'à la corrélation entre l'expression de l'apoD et des paramètres cellulaires comme la prolifération et l'apoptose. Ces travaux ont été faits sur des fibroblastes NIH/3T3. Ce sont des cellules faciles à manipuler et il a déjà été démontré que l'induction d'apoD dans ces cellules est semblable à celle observée dans d'autres types cellulaires tels que les cellules épithéliales et gliales.

J'ai été impliquée dans toutes les facettes des travaux associés à cet article. J'ai d'abord élaboré le design expérimental. Puis j'ai effectué les travaux en laboratoire. J'ai ainsi analysé l'expression de l'ARNm de l'apoD suite à l'application de divers stress sur des cultures de cellules et l'effet de ces stress sur des paramètres cellulaires comme la prolifération, l'apoptose et la sénescence. J'ai également déterminé, par délétion séquentielle de diverses sections du promoteur, la région du promoteur de l'apoD responsable de la réponse à l'application de lipopolysaccharide. J'ai aussi fait les études de localisation et de trafic de l'apoD lors de situations de stress cellulaire. J'ai finalement rédigé le manuscript et conçu les figures. Louis-Charles Levros a construit, par mutagénèse dirigée, les mutants qui ont servi à mieux cerner et confirmer les éléments du promoteur impliqués dans la réponse au lipopolysaccharide.

2.1 Résumé

L'apolipoprotéine D (apoD) est une lipocaline d'abord trouvée associée aux lipoprotéines de haute densité dans le plasma humain. L'expression de l'apoD est induite dans plusieurs situations pathologiques ou de stress cellulaire incluant l'arrêt de croissance suggérant qu'elle puisse agir comme une protéine de stress non-spécifique. L'étude d'un large éventail de stress cellulaires a démontré que ceux qui causent un arrêt de croissance prononcé tel le peroxyde d'hydrogène et les rayons ultraviolets augmentent l'expression de l'apoD. Par ailleurs, le lipopolysaccharide (LPS), un agoniste pro-inflammatoire, a démontré un effet dose et temps dépendant sur l'expression de l'apoD qui est corrélé avec une augmentation de la prolifération. Au niveau du promoteur, les éléments NF-kB, AP-1 et APRE-3 ont été identifiés comme impliqués dans la réponse au LPS. La colocalisation de la protéine de fusion apoDh-GFP avec des marqueurs spécifiques à l'ADN et à l'appareil de Golgi, l'immunohistochimie de la protéine endogène et le fractionnement cellulaire ont montré que la déprivation de sérum et le traitement au LPS causent un déplacement de la localisation de l'apoD. En conditions normales, l'apoD est majoritairement périnucléaire, mais elle s'accumule dans le cytoplasme et le noyau lors de conditions de stress. Puisque l'apoD nucléaire semble être dérivé de la protéine sécrétée, elle pourrait agir comme un transporteur de ligand extracellulaire ou comme un régulateur transcriptionnel selon sa localisation. Ce rôle de l'apoD à l'intérieur de la cellule ne dépend pas uniquement de l'apoD endogène, mais peut être fourni par de l'apoD exogène entrant dans la cellule.

Mots-clés : apolipoprotéine D, arrêt de croissance, inflammation, lipocaline, lipopolysaccharide, stress cellulaire, translocation nucléaire.

2.2 Abstract

Apolipoprotein D is a lipocalin, primarily associated with high-density lipoproteins in human plasma. Its expression is induced in several pathological and stressful conditions including growth arrest suggesting that it could act as a nonspecific stress protein. A survey of cellular stresses shows those causing an extended growth arrest, as hydrogen peroxide and UV light increase apoD expression. Alternatively, lipopolysaccharide (LPS), a pro-inflammatory agonist showed a time- and dose-dependent effect on apoD expression that correlates with an increase in proliferation. At the promoter level, NF-kB, AP-1 and APRE-3 proved to be the elements implicated in the LPS response. Colocalization of apoDh-GFP fusion constructs with DNA and Golgi markers, immunocytochemistry of the endogenous protein and cell fractionation showed that both serum starvation and LPS treatment caused a displacement of apoD localization. In normal conditions, apoD is mainly perinuclear but it accumulates in cytoplasm and nucleus under these stress conditions. Since nuclear apoD appears derived from the secreted protein, it may act as an extracellular ligand transporter as well as a transcriptional regulator depending on its location. This role of apoD inside the cell is not only dependent of endogenous apoD but may also be provided by exogenous apoD entering the cell.

Keywords: apolipoprotein D, growth arrest, inflammation, lipocalin, lipopolysaccharide, cellular stress, nuclear translocation.

2.3 Introduction

Apolipoprotein D (apoD) is a member of the lipocalin superfamily that is found associated with high-density lipoproteins in the plasma of humans and other species (Albers *et al.* 1981, Ayrault-Jarrier *et al.* 1963, Bojanovski *et al.* 1980, Provost *et al.* 1990, Rassart *et al.* 2000, Weech *et al.* 1986). Unlike most of the other plasma apolipoproteins whose expression is limited to the liver and/or the intestine, apoD, a 29 kDa glycoprotein, is expressed in almost all tissues that have been tested (Cofer and Ross 1996, Drayna *et al.* 1986, Provost *et al.* 1990, 1991, 1995, Séguin *et al.* 1995, Smith *et al.* 1990, Vieira *et al.* 1995) both during adulthood and during embryonic or postnatal development (Ganfornina *et al.* 2005, Sanchez *et al.* 2002). Although apoD has been shown to bind a number of small hydrophobic molecules, the physiological ligands of apoD have yet to be definitively identified, and it has been proposed that apoD may have multiple tissue-specific, physiological ligands and functions (Milne *et al.* 1993, Peitsch and Boguski 1990, Provost *et al.* 1991).

In cultured cells, apoD expression is modulated in response to various stimuli. It can be enhanced by growth arrest and senescence (Do Carmo *et al.* 2002, Provost *et al.* 1991) or by other factors such as steroids (Simard *et al.* 1991, 1992, Sugimoto *et al.* 1994), interleukin-1α (Blais *et al.* 1994), 1,25-dihydroxyvitamin D3 (Lopez-Boado *et al.* 1994), retinoic acid (Lopez-Boado *et al.* 1994, 1996), or 25-hydroxycholesterol (Patel *et al.* 1995). The promoter region of the human apoD gene contains several regulatory elements including serum response elements (SRE) and an alternating purine-pyrimidine stretch implicated in the response to growth arrest (Do Carmo *et al.* 2002). It also contains acute phase, estrogens, progesterone, glucocorticoids, fat, thyroid- hormone, metal and stress response elements (APRE, ERE, PRE, GRE, FSE, TRE, MRE, STRE), sterol dependent repressor (SDR), activation proteins 1 and 2 (AP-1, AP-2), and nuclear factor kappa B (NF-kB) binding sites (Do Carmo *et al.* 2002). There seems to be a significant biological role

for a tight physiological regulation of apoD, and an altered apoD expression has been reported in several pathological conditions.

ApoD is expressed at high levels in the normal central and peripheral nervous systems of various species (Boyles *et al.* 1990b, Drayna *et al.* 1986, Provost *et al.* 1990, 1991, Séguin *et al.* 1995, Smith *et al.* 1990). ApoD levels are further increased in human neuropathologies such as Alzheimer's disease, stroke, meningoencephalitis, motor neuron disease, dementia (Terrise *et al.* 1998), Niemann-Pick (Suresh *et al.* 1998), schizophrenia (Mahadik *et al.* 2002, Thomas *et al.* 2001b), Parkinson disease (Ordoñez *et al.* 2006) and multiple sclerosis (Reindl *et al.* 2001). ApoD is also increased in several animal models of brain injury (Boyles *et al.* 1990a, Franz *et al.* 1999, Montpied *et al.* 1999, Ong *et al.* 1997, Spreyer *et al.* 1990, Terrisse *et al.* 1999). In non-neurological pathologies, apoD protein accumulates in atherosclerotic plaques (Sarjeant *et al.* 2003), in the cyst fluid from women with breast gross cystic disease (Balbin *et al.* 1990, Diez-Itza *et al.* 1994), in various cancers and in metabolic diseases such as non-insulin dependent diabetes mellitus type II, obesity, and syndrome X (for review, see Van Dijk *et al.* 2006).

Other than the increase of apoD expression, these conditions share the presence of inflammation, oxidative stress and apoptosis. Inflammation is a physiological response to tissue injury, trauma, or infection and consists of a systemic reaction to fight further tissue damage, destroy infective organisms and activate repair processes. Chronic inflammation is associated with certain metabolic diseases and cancers. There is also an inflammatory component in Alzheimer's disease, multiple sclerosis, schizophrenia, traumatic brain injury and other neuropathologies (Giovannoni and Baker 2003). The long-term administration of nonsteroidal anti-inflammatory drugs (NSAIDs) or cycloxygenase (COX) inhibitors appears to reduce the incidence, or delay the onset, of Alzheimer's disease (Zandi *et al.* 2002). Both naproxen and ibuprofen (2 NSAIDs) inhibit the aggregation of β-amyloid peptides to

senile plaques ex vivo (Agdeppa *et al.* 2003). Also, apoE may play an isoform-specific role in mediating the systemic and brain inflammatory responses. ApoE4 has been associated with the early onset of Alzheimer's disease and poor prognosis in other disorders such as multiple sclerosis (Schmidt *et al.* 2002, Strittmatter and Roses 1996). ApoD levels in CSF and hippocampus increased as a function of inheritance of the apoE4 allele (Terrisse *et al.* 1998). Mice expressing the apoE4 allele and injected with LPS have significantly greater systemic and brain elevations of the pro-inflammatory cytokines TNFα and IL-6 as compared with their apoE3 counterparts (Lynch *et al.* 2001). Furthermore, oxidative modification of lipids occurs during inflammatory processes and leads to the formation and accumulation of biologically active lipid oxidation products that induce specific cellular reactions such as apoptosis. Moreover, oxidative stress has long been associated with the neuronal cell death in some neurodegenerative conditions. It is still unclear whether oxidative stress is the initiating event or a downstream consequence of the neurodegenerative process in Alzheimer's disease and multiple sclerosis, two degenerative diseases presenting apoD overexpression. The oxidant and antioxidant defense system may also be dysfunctional in schizophrenia and bipolar disorders, which also show apoD induction (Thomas *et al.* 2001b). Finally, oxidative stress resulting from an imbalance between pro-oxidants and anti-oxidants seems to play an important role in human breast carcinogenesis (Khanzode *et al.* 2004). Apoptosis has also been reported in situations showing apoD induction as kainate excitotoxicity, enthorinal cortex lesionning and traumatic brain injury (Franz *et al.* 1999, Montpied *et al.* 1999, Terrisse *et al.* 1999).

The heterogeneity of situations triggering apoD expression, although informative about the importance of apoD, leaves us in the dark about the primary event responsible for its induction. Thus, any stress situation may initiate apoD expression and it has been suggested that apoD is a nonspecific response to different stimuli and may be part of an antioxidant defense system (Alvarez *et al.* 2003).

The aim of this study is to determine which cellular stresses affect apoD expression and their effect on cell viability, apoptosis and senescence. The incidence of some of these stresses on apoD protein synthesis and localization is further examined. The responsive elements at the promoter level are also explored. Our results show that only those stresses causing an extended growth arrest increase apoD expression. Interestingly, lipopolysaccharide (LPS), a pro-inflammatory agonist in fibroblasts showed a time- and dose-dependent effect on apoD expression that correlates with an increase in proliferation. At the promoter level, NF-kB, AP-1 and APRE-3 proved to be the responsive elements. LPS exposure and growth arrest also induce a translocation of apoD to the nucleus.

2.4 Materials and methods

2.4.1 Cell culture

All cells were obtained from ATCC, Rockville, MD and maintained in DMEM (Invitrogen) supplemented with 10% calf serum (NIH/3T3), in MEM (Invitrogen) supplemented with 10% fetal calf serum (HepG2, HeLa and 293), in RPMI (Invitrogen) supplemented with 10% fetal calf serum (U373MG and U87). All cells were also supplemented with penicillin G (100 units/ml) and streptomycin (100 µg/ml), maintained at 37°C in a 5% CO_2 humidified atmosphere and were fed every 2 days with fresh medium. For the analysis of gene expression in sparsely growing cultures (normal condition), cells were maintained in medium supplemented with 10% calf serum and harvested at 50% of confluence. For analysis of growth arrest, cells were incubated in 0.2% serum when they reached 80% of confluence. Medium was changed after 24 h and cells were harvested after 4 days.

2.4.2 Stress induction

Cells were plated at 50 % confluency, allowed to recover 24 h then stressors were applied as follows. Two heat and two cold shocks, one of high and another of low intensity, were used. Cells were incubated at 42°C for 5 h (low heat) or at 45°C for 20 min (high heat). Cells were also exposed to 32°C for 4 h (low cold) or to 4°C (high cold) for 20 min. Cells were always maintained in a humidified atmosphere containing 5% CO_2 except for the 4°C condition were culture plates were tightly wrapped with parafilm and refrigerated for 20 min. Cells were allowed to recover for 6 h at 37°C before analysis. For hypo-osmotic shock, cell medium was reduced to 60% normosmotic strength by addition of sterile deionized water. Cells were exposed to this hypo-osmotic condition during 2h at 37°C then washed with PBS and replaced in normosmotic medium for 6h before harvest. For hyper-osmotic conditions, cells

were maintained for 4 days in regular growth medium supplemented with 150 mM NaCl before analysis and the medium was changed every day. Metal stress was caused by addition of metal salts to cells (100 µM $ZnCl_2$, 100 µM $CaCl_2$, 50 µM $MnCl_2$, 100 µM $MgCl_2$, 50 µM Alk $(SO_4)_2$, 50 µM LiCl) for 4 h at 37°C. After this treatment, cells were washed and were allowed to recover in fresh growth medium for 4 h at 37°C. Oxidative stress was induced by, unless otherwise indicated, addition of 100 µM or 300 µM H_2O_2 (Sigma-Aldrich) to the cells for 2 h at 37°C and cells were let to recover for 48 h after growth medium was replaced. Rose Bengal stress was produced by irradiating media containing 1 µM Rose Bengal with a 500 W lamp from a fixed distance of 66 cm for 15 min. To induce apoptosis, cells were incubated for 16 h at 37°C with 5 or 10 µM of camptothecin (CPT, Sigma-Aldrich) or for 8h with 0.1 µM staurosporine (Sigma-Aldrich) in serum free DMEM. For UV irradiation, medium and plate lids were removed and cells were irradiated with a Phillips® Sterilamp (256 nm, 15W) with a source-to-target distance of 70 cm. Then, cells were incubated for an additional 16 h at 37°C. For LPS treatment, cells were exposed to medium containing 2, 5, or 10 µg/ml of LPS (Sigma-Aldrich) for 4 days or as indicated. Medium was refreshed every day. Alternatively, cells were also exposed to 10 ng/ml or 100 ng/ml of bFGF or a combination of LPS 5 µg/ml, diclofenac 200 µM and bFGF (Sigma-Aldrich).

2.4.3 RNA extraction and northern blot analysis

For each condition, cells were washed in PBS, directly lysed in the culture dish by adding TRIZOL Reagent (Invitrogen) as recommended by the supplier and kept at -80°C until all samples were collected. For northern blots, 20 µg of total RNA was denatured in formaldehyde/formamide and migrated in 1.5 % agarose gel containing MOPS (20mM) and formaldehyde (17%). Nucleic acids were transferred to Osmonics Nylon Transfer Membranes (Fisher Scientific) and UV-fixed for 3 min. The membranes were hybridized with [α-32P] dCTP-labeled apoD, hsp70, caveolin-1

or GAPDH cDNAs, exposed to Biorad Imaging screen K and revealed with a PhosphorImager (Biorad Molecular Imager FX) and Quantity One software (Biorad). For each value, the optical density measured for each gene tested was divided by that of the GAPDH mRNA. The ratio obtained from sparse cultures was given an arbitrary value of one.

2.4.4 TUNEL assay

Apoptosis was monitored by TUNEL reaction using the *In situ* cell detection kit, fluorescein labeled (Roche, Mannheim, Germany) according to the manufacturer instructions. Cells were plated on 4 well-Sonic Seal Slides (Nunc, VWR) at 50% confluency, allowed to recover 24h then subjected to stress conditions as described above. Results are expressed as percentage of fluorescent apoptotic cells.

2.4.5 MTS/PMS viability test

Cell viability was measured using the CellTiter 96 AQueous Non-Radioactive Cell Proliferation Assay (Promega) according to the manufacturer instructions. Cells were plated as above and the results are expressed as percentage of proliferative cells.

2.4.6 BrdU incorporation

The proliferation assay was performed using colorimetric BrdU labeling and detection kit I according to the manufacturer's protocol (Roche, Mannheim, Germany). Results are expressed as BrdU incorporating cells relative to that of growing unstressed cells.

2.4.7 Beta-galactosidase staining of senescent cells

The β-galactosidase activity at pH 6.0, a known characteristic of senescent cells, was used to measure senescence. Cells were plated as above and the results are expressed as percentage of β-galactosidase expressing cells.

2.4.8 Construction and transfection of apoDh – GFP fusion protein expression vectors

The human apoD coding sequence, including the signal peptide, was cloned in frame in pEGFP-N1 and pEGFP-C1 vectors (BD Biosciences Clontech). The construct was transfected in NIH/3T3 cells with Qiagen's Polyfect transfection reagent as recommended by the supplier. Twenty-four hours later, cells were rinsed twice with phosphate-buffered saline and culture medium was changed for medium containing 10% serum supplemented with 5μg/ml of LPS or low-serum medium (containing 0.2% serum) or normal medium containing 10% serum.

2.4.9 Immunocytochemistry and cytochemistry

Cells were fixed with 4% paraformaldehyde 0, 3 or 6 days after stress induction and stained with propidium iodide (Sigma-Aldrich) or bodipy ceramide TR (Invitrogen). All fluorescent imaging was done at 40 X magnification using confocal microscopy. For control, cells were transfected with pEGFP-N1 vector alone. For immunofluorescence staining, NIH/3T3 or U373MG cells were grown on Labtek chamber slides (Fisher Scientific), subjected to stress conditions as above and fixed with 4% paraformaldehyde for 10 min at room temperature. After five washes with PBS, fixed cells were incubated in blocking and permeabilization solution (3% serum from the host animal of the secondary antibody and 0.2% Triton X-100 in PBS) for 1

h. Cells were sequentially incubated with primary antibody (polyclonal anti-mouse apoD raised against the bacterially expressed GST-fused mature mouse apoD, 1:50, Caro2 polyclonal anti-human apoD raised against human apoD purified from mammary cyst fluid, 1:50, or 2B9 monoclonal anti-human apoD, 1:200 (Terrisse *et al.* 1998) and then corresponding fluorophore-labeled secondary antibodies (Cy3- and FITC-labeled anti-rabbit IgG (Cedarlane laboratories limited), 1:100, for anti-human apoD and anti-mouse apoD polyclonal antibodies respectively and FITC-labeled anti-mouse IgG (Cedarlane laboratories limited), 1:200, for anti-human apoD monoclonal antibody) for 1 h, respectively. Cells were washed five times with PBS and then mounted with Slowfade Gold Antifade (Molecular Probes) before imaging. For inhibition of protein secretion by brefeldin A treatment, apoDh-GFP transfected cells were grown on chamber slides and subjected to stress conditions during 4 days. Cells were then treated with or without brefeldin A (5 μg/ml) (Sigma-Aldrich) for 1 h and fixed 24 h later for confocal microscopy.

2.4.10 Human apoD promoter-luciferase constructs and mutagenesis

Heterologous luciferase (LUC) reporter gene constructs containing different portions of the human apoD gene promoter were made by classic methods as previously described (Do Carmo *et al.* 2002). The APRE-3, the two NF-kB and the AP-1 elements present in region -816 to -471 were mutated by oligonucleotide-directed PCR mutagenesis (Table 2.1). For that purpose, PCR-amplified -816/-471 portion of the apoD promoter was cloned in the correct orientation upstream of position –179 upstream of the luciferase reporter gene in the pXP2 expression vector. Eight complementary mutated primers and two primers from the vector were used in two-step PCR (Table 2.1). Multiple mutants were constructed by the same technique using sequential mutagenesis. All of the luciferase reporter constructs were sequenced to confirm their integrity. Each construct was co-transfected in NIH/3T3 cells with a

β-galactosidase expression vector with Polyfect reagent. After transfection, the cells were maintained in either LPS containing (5 μg/ml) or LPS-free medium. The luciferase activity was analysed after 4 days, and the results were normalized for the β-galactosidase activity.

2.4.11 Luciferase and β-Galactosidase assays

Cells were washed with phosphate-buffered saline before adding 100 μl of Tris-HCl, 0.25 M, pH 7.8. Cells were then scraped with a cell lifter, transferred into microcentrifuge tubes, lysed by three cycles of freeze-thawing and the lysates were stored at -20 °C as described previously (Do Carmo *et al.* 2002). Luciferase assays were performed with a Wallac 1404 luminometer using the conditions and buffers recommended by the Luciferase assay system (Promega). β-Galactosidase assays were done as follows: each sample (30 μl) was adjusted to a final concentration of 1 mM $MgCl_2$, 45 mM β-mercaptoethanol, 0.88 mg/ml o-phenyl-β-D-galactopyranoside, and 0.1 M sodium phosphate (pH 7.5) and incubated at 37 °C for 30 min. Reactions were stopped by the addition of Na_2CO_3 to a final concentration of 625 mM, and the optical density was read at 420 nm. The results were standardized by calculating promoter activity relative to that of the co-transfected internal control plasmid pRSVβGAL. Each value is the average of at least three independent experiments performed in triplicate.

2.4.12 Extraction of total and nuclear proteins

For total protein extraction, 2.5 x 10^5 cells were lysed in 10 μl lysis buffer (50 mM Tris-HCl, pH 7.3, 150 mM NaCl, 5 mM EDTA, 0.2% Triton X-100, and 10% CompleteTM protease inhibitors (Roche, Indianapolis, IN)). After 30-min incubation at 4 °C, lysates were sonicated and cleared by 10 min of centrifugation at 20,000 g at

4 °C. For nuclear protein extraction, cells were washed twice with PBS and lysed in a solution containing 10 mM Tris, pH 7.4, 10 mM NaCl, 3 mM $MgCl_2$, 0.1 mM EDTA, 1 mM phenylmethylsulfonyl fluoride and 0.5% Nonidet P-40. Nuclei were pelleted by centrifugation at 2,000 x g for 2 min and washed once in the same buffer to remove residual cytoplasmic proteins. After removal of cytoplasmic proteins, cell nuclei were lysed at 37°C for 3 to 5 min in a hyperosmolar neutral-pH solution with 0.5 M NaCl, 50 mM MgCl2, 2 mM CaCl2, 10 mM Tris buffer, 100 U of DNase I/ml, and 10% CompleteTM protease inhibitors. The protein concentration was determined spectrophotometrically at 590 nm using the Bio-Rad protein assay reagents (Bio-Rad Laboratories). All extracts were stored at -70°C.

2.4.13 Immunoblotting

Protein extracts (10 μg) were heated for 10 min at 70°C before being loaded onto a 12% SDS- polyacrylamide gel. A prestained size marker (Biorad prestained SDS-PAGE standard, low range) was included in each run. The gel was subjected to electrophoresis for 1 h at 40 mA and then transferred by electroblotting to a polyvinylidene difluoride (PVDF, Millipore) membrane for 45 min at 300 mA. Membranes were blocked for 1 h at room temperature with blocking buffer (PBS containing 0.2% Tween 20 and 5% skim milk powder) and incubated for 1 h at room temperature with 1:1000 anti-human apoD (Caro2 polyclonal antibody), 1:1000 anti-GFP (Chemicon) or 1:4000 anti-GAPDH (Calbiochem) or overnight at 4°C with 1:1000 anti-mouse apoD polyclonal antibody in blocking buffer. Subsequently, the blots were incubated under gentle agitation at room temperature with a secondary horseradish peroxidase conjugated anti-rabbit antibody (GE Healthcare) diluted 1:5000 in blocking buffer. The blots were developed using the enhanced chemiluminescence method (Amersham-Pharmacia) with X-ray film.

2.4.14 Statistical analysis

Statistical significance of the apoD mRNA expression, apoptosis, cell viability and senescence levels in cells subjected to different stress in comparison with normal conditions was evaluated using an unpaired Student's t-test or a one-way ANOVA. Statistical differences between the different constructs used for the identification of LPS responsive elements in the apoD promoter were assessed by ANOVA. Differences identified by ANOVA were pinpointed by the Turkey-Kramer multiple comparison test.

2.5 Results

2.5.1 ApoD expression in response to cellular stress

Previous studies have shown that apoD mRNA is induced in cell cultures under specific conditions (for review, see Rassart *et al.* 2000, van Dijk *et al.* 2006) and that its expression could be part of an antioxidant defense system (Alvarez *et al.* 2003). Tatil, the plant apoD homolog is upregulated in response to temperature and water stress (Frenette Charron *et al.* 2002). However, in mammalian cells, no data are available regarding temperature or osmolarity stress. Also, no direct evidence of a relation between apoD and apoptosis, oxidative stress or inflammation has been reported. To analyze this aspect, we measured apoD mRNA expression in murine NIH/3T3 fibroblasts exposed to various stresses (Fig. 2.1A). Our team previously used these cells since they express apoD in a fashion similar to glial, epithelial and primary fibroblasts (Do Carmo *et al.* 2002). Endogenous apoD mRNA expression was very low in growing cells and in cells exposed to heat and cold shocks of high (Hs 45°C, Cs 4°C) or low (Hs 42°C, Cs 32°C) intensity. ApoD mRNA expression was also very low in cells grown in hypo- or hyper-osmotic conditions. Since the apoD promoter contains one putative metal responsive element (Do Carmo *et al.* 2002), a combination of metals was tested. However, no change in apoD mRNA levels was detected. For these conditions, longer exposures and recovery times were also tested and no further increase of apoD expression was observed. In contrast, H_2O_2 and UV light induced apoD transcripts accumulation in a dose-dependent manner (Fig. 2.1A). This was also observed with Rose Bengal another inducer of oxidative stress (data not shown). Lipopolysaccharide (LPS) also induces a dose-dependent response. Finally, camptothecin, an apoptosis inducer, had no effect on apoD mRNA expression. As expected, hsp70 is increased in the temperature, osmotic, metal, UV and H_2O_2 treatments revealing that the stress applied were effective. However, hsp70 is not activated by LPS. For comparison, serum starved

cells were included and they show a substantial apoD mRNA increase as previously reported (Do Carmo *et al.* 2002) (Fig. 2.1A).

It is interesting to note that, with the exception of LPS, those conditions that cause an apoD transcript accumulation also decrease cell proliferation (Fig. 2.1B). In fact, growing cells and cells exposed to temperature or osmotic shocks, metals or low concentrations of H_2O_2 (100μM) maintain a proliferative rate above 58% and a low level of apoD mRNA expression. At higher H_2O_2 concentration or long UV exposure, the results may suggest a relation between apoD transcript accumulation and apoptosis. However, no apoD mRNA induction was observed under treatments with various concentrations and time exposures of camptothecin, (Fig. 2.1A). Moreover, senescence, which is observed at high H_2O_2 concentration (300μM), has already been reported for its ability to induce apoD expression (Provost *et al.* 1991a). Finally, the conditions presenting the best induction, LPS exposure and serum starvation, both have apoptosis levels comparable (4% to 6% in LPS) or only slightly superior (12% in serum starvation) to those seen in growing cells (6%). Thus, our results clearly indicate that the important inducer of apoD mRNA accumulation is cellular growth arrest rather than apoptosis (Fig. 2.1B).

2.5.2 ApoD expression under oxidative stress correlates with decreased cell proliferation

To further assess the contribution of oxidative stress in the apoD mRNA expression observed in figure 2.1A, NIH/3T3 cell cultures were exposed to increasing concentrations of H_2O_2. ApoD transcripts accumulate from 100 μM to 300 μM in a dose-dependent manner (Fig. 2.2A). This apoD increase correlates well with a decrease in cell viability rather than an increased apoptotic rate (Fig. 2.2B). Indeed, no apoD accumulation is detected in low H_2O_2 concentrations already documented as being mitogenic (5 μM to 30 μM) (Davies 1999) nor in the highly apoptotic 500 μM

concentration. ApoD induction could also be caused by an increased senescence, which reach 40% in the 300 μM dose, although this situation is closely linked to a growth arrested state. Caveolin-1 is included as a control since its expression has been demonstrated to be upregulated by H_2O_2 treatment (Volonte *et al.* 2002). This inductive effect of H_2O_2 on apoD expression was also observed at lower doses, in a dose-dependent manner with HepG2, HeLa, 293, U373MG and U87 cultures (data not shown) indicating that the human apoD is subjected to the same regulation.

2.5.3 ApoD expression is associated with pro-inflammatory stimuli

Since the inductive effect of LPS on apoD transcription is dose-dependent (Fig. 2.1A), we decided to determine whether this effect was time-dependent. LPS induces a time-dependent transcript accumulation during 6 days and reaches a plateau (Fig. 2.3A). The decrease at day 7 coincided with a partial detachment of the cell monolayer. This inductive effect of LPS on apoD expression was also observed with HepG2, HeLa, 293, U373MG and U87 cultures although the LPS concentrations required to induce apoD expression were lower (data not shown).

Besides its pro-inflammatory properties, LPS has been extensively used as a potent inducer of proliferation and cytokine production in human T-lymphocyte, monocytes/macrophages, vascular cells, polymorphonuclear cells, and even B-lymphocytes (Ulmer *et al.* 2000). To determine which of the two LPS properties is responsible of apoD induction, we analyzed another proliferative molecule, basic fibroblast growth factor (bFGF) and an anti-inflammatory drug, diclofenac. Diclofenac has been previously used in fibroblast cultures to oppose inflammatory effects of LPS and it has an anti-proliferative effect (Nguyen and Lee 1993). The bFGF failed to induce apoD (Fig. 2.3B) whereas LPS and serum starvation showed a good increase in apoD mRNA expression, as expected (Fig. 2.1A, 2.3A). Furthermore, the proliferative effect of LPS was similar to that of bFGF with a 2 to 3

fold increase as documented by BrdU incorporation (Fig. 2.3C). The addition of diclofenac to the culture media slightly increases apoD transcript accumulation. This is most likely due to its anti-proliferative properties. Moreover, diclofenac decreases the proliferative action of bFGF but has no further influence on apoD transcription (Fig. 2.3B and C). More importantly, diclofenac decreases the LPS-induced apoD expression indicating that the pro-inflammatory rather than the mitogenic properties of LPS are responsible for activating apoD expression (Fig. 2.3B and C).

2.5.4 ApoD expression is associated with specific elements in the promoter

The apoD promoter contains an abundance of potential regulatory elements. It has already been established that a pair of serum-responsive elements and an alternating purine-pyrimidine stretch are the major determinants of growth arrest-induced apoD gene expression (Do Carmo *et al.* 2002). To identify those elements that regulate apoD expression in fibroblast cultures exposed to LPS, we used deletion mutants containing different portions of the apoD promoter (-1176 to -4) upstream of the luciferase reporter gene.

With the construct containing the entire promoter region (-1176 to -4), the LPS treatment resulted in an 8-fold induction of promoter activity when compared to normal conditions (Fig. 2.4A). This induction is significantly reduced to 3-fold when region -1176 to -558 is absent and totally abolished when only the minimal promoter is present (-179). The deletion of either region -352/-179 or -473/-191 resulted in a small decrease in induction suggesting a negligible contribution of APRE2 elements in response to LPS. This is further confirmed when comparing constructs -397/-176 and -266/-51, which differ only by one APRE2 element. Furthermore, the deletion of portions -558/-352 and -558/-179 resulted in a drastic reduction of induction (3- and 2-fold respectively) that underlines the importance of AP1 in the LPS response. The induction level can be greatly enhanced by the addition of the AP-1 element (compare

deletions -558/-179 and -473/-191). Although important, the AP-1 element alone is insufficient to restore the apoD induction by LPS. Thus, constructs -558 and -548/-321 still display only a 3-fold induction compared to -1176 suggesting that region -1176/-548 is at least as important as the AP-1 element. This region contains two AP2, an APRE3 and two NF-kB responsive elements. Again, this region alone is unable to restore completely the LPS induction as shown by deletion -558/-179 and construct -816/-597. Thus, it appears that AP-1 cooperates with NF-kB and possibly with APRE3, as suggested by construct -676/-471 and deletion -473/-191, to induce apoD expression under inflammatory conditions. Finally, comparison of deletion -1052/-558 with fragment -558 reveals the weak importance of the third NF-kB responsive element at position -1104.

Another construct was thus created that includes all the elements important to LPS response. It contains the region -816/-471 placed upstream of the minimal promoter -179 and presented an activity comparable to that of the -1176/-473 region of the promoter (Fig. 2.4A). Mutational analysis of the fragment -816/-471 (Fig. 2.4B) reveals that each of the APRE3, NF-kB and AP1 elements is important to LPS response and mutagenesis of APRE-3 or NF-kB1 or NF-kB2 is sufficient to abolish apoD response to LPS while inactivation of AP-1 only reduces the induction by half. Inactivation of NF-kB1 or NF-kB2 reduces apoD expression both in normal conditions and in presence of LPS. This phenomenon was also observed with the NF-kB element located at position -1104 (compare deletion -1052/-558 with -558 construct in Fig. 2.4A). Mutation of the APRE-3 increases significantly basal transcription and prevents LPS-induced transcriptional induction. When looking at double and triple mutants (Fig. 2.4B), the AP-1 mutation counteracts the effect of either NF-kB mutations but not both suggesting that the interaction between one NF-kB and the AP-1 element relies on the presence of the other NF-kB. This is clearly illustrated with the double mutants mNF-kB1, mAP-1 and mNF-kB2, mAP-1. However, AP-1 mutation cannot disable the APRE-3 mutation effect although the

promoter activity was reduced in both conditions. AP-1 seems to have a different effect on APRE-3 depending on the NF-kB mutations. When mutated AP-1 and APRE-3 sites are combined with a mutated NF-kB1 element, the basal promoter activity was increased whereas LPS-stimulated activity was not. This was not the case when the AP-1 and APRE-3 mutations were combined with a mutated NF-kB2 element.

2.5.5 ApoD protein localization is altered by serum starvation and LPS treatment

It is now clear that apoD transcription is modulated by specific stress signaling pathways. We then verified the protein induction and localization after LPS exposure and serum starvation-induced growth arrest. For this purpose, an expression vector containing the entire human apoD coding sequence, including the signal peptide, fused to the N-terminal end of the fluorescent GFP protein (apoDh-GFP), was transfected and the fusion protein was followed by western blot analysis and confocal imaging in stressed and unstressed cells (Fig. 2.5 and 2.6). As already observed with the transcripts (Fig. 2.1A and 2.3A), in total cell extracts, the endogenous mouse apoD increases in a time dependent manner after exposure to those stresses as detected with a polyclonal antibody against mouse apoD (Fig. 2.5A; apoDm). However, the protein increase was not as high as for the mRNA and after 6 days of serum starvation, the protein accumulation was 3.5 fold compared to 10 fold for the mRNA (Do Carmo *et al.* 2002). Similarly, after 6 days of LPS exposure, apoD transcript and protein levels are increased 7 fold and 1.5 fold, respectively. It is noteworthy that in addition to its accumulation in the cell, apoD is also found in the nucleus after stress exposure (Fig. 2.5B and 2.6). Interestingly, the nuclear apoD has a molecular mass similar to that of the secreted protein ($\approx$ 55 kDa for apoDh-GFP and 30 kDa for endogenous mouse apoD). Finally, it is also clear that apoD is secreted both in normal and LPS conditions. However, endogenous apoD is no longer secreted

after 3 and 6 days of serum starvation (Fig. 2.5C). When growth arrested cells are reallowed to proliferate by the addition of 10% serum to the culture medium, the endogenous mouse apoD returns to basal levels, is no longer found in the nucleus and is secreted again in the extracellular space (data not shown). In the same way, apoD was no longer found in the nucleus when the LPS treatment was interrupted. These changes in localization are also obvious in immunoblots with anti-GFP antibodies (Fig. 2.5). In total cell extracts (Fig. 2.5A), apoDh-GFP is detected in all conditions as expected since it is transcribed from the CMV promoter. In nuclear extracts, however, apoDh-GFP is absent in normal conditions, most likely because it is secreted but it is detected after 3 and 6 days after LPS exposure and serum deprivation (Fig. 2.5B). This localization is directly correlated with that of the endogenous apoD.

The subcellular localization of apoDh-GFP fusion protein was further examined using confocal fluorescence microscopy. In unstressed normal cells, (Fig. 2.6A, a-c), apoD is found in the perinuclear area. This localization is consistent with the Golgi apparatus as demonstrated by overlaid fluorescence of GFP and Bodipy TR ceramide (Fig. 2.6B, a-c). Similar to immunoblotting results, no apoDh-GFP is present in the nucleus as established by the lack of colocalization with the nuclear marker propidium iodide (PI) (Fig. 2.6A, a-c). After 3 days of serum starvation or LPS treatment, this localization is altered. ApoDh-GFP distribution is extended in the cytoplasm and becomes visible in the nucleus (Fig. 2.6A, e-g and m-o). Interestingly, during serum starvation, apoDh-GFP appears as a dotted localization in the cytoplasm (Fig. 2.6A, e). The nuclear localization of apoDh-GFP intensifies after 6 days of stress exposure (Fig. 2.6A, i-k and q-s) as showed by merged images with PI staining of the nucleus. We also produced the reverse fusion protein containing the human apoD coding sequence linked to the C-terminus of GFP (GFP-apoDh). Since the apoD peptide signal is now in the middle of the fusion protein, the fluorescence patterns indicated a subcellular distribution identical to the GFP alone (results not

shown). The subcellular distribution of endogenous apoD was also probed with a polyclonal mouse apoD antibody. Confocal microscopy confirmed that apoD is perinuclear in normal conditions (Fig. 2.6A, d) and translocates to the nucleus as stress is prolonged (Fig. 2.6A, h, l, p, t). Together, these results indicate that apoD drives GFP into the nucleus. Finally, immunofluorescence staining of human glioma cell line U373MG using a polyclonal human apoD antibody shows that the nuclear localization pattern is not restricted to NIH/3T3 cell line. As a matter of fact, fluorescence is clearly concentrated in the nucleus of cells exposed to serum starvation or LPS conditions during 6 days but appears diffuse in normal conditions.

2.5.6 Exogenous apoD enters cells and affects cellular status

ApoD is a glycosylated and secreted protein. Its presence in the nucleus might be explained by its re-entry in the cell after secretion and its transport to the nucleus. It has already been shown that human apoD, purified from breast cyst fluid, enters ovine vascular smooth muscle cells when added to the culture medium (Sarjeant *et al.* 2003). Moreover, it interacts specifically with the cytoplasmic portion of the leptin long form receptor Ob-Rb (Liu *et al.* 2001). In the same way, human apoD, purified from cyst fluid, also enters NIH/3T3 cells when added to the culture medium, as detected with human apoD specific antibody (Fig. 2.7A and 2.8B). Moreover, the human apoD localization is dependent on cellular status. In normal growing cells, human apoD is detected in the cytoplasm but not in the nucleus (Fig. 2.7A, d-f). In comparison, in serum starved and LPS exposed cells, human apoD accumulates in the cytoplasm but also in the nucleus as demonstrated by merged images of the fluorescence of the anti-human apoD antibody and the nuclear marker PI (Fig. 2.7A, g-l). However, in absence of human apoD, no signal could be detected demonstrating the high specificity of the antibody towards human apoD (Fig. 2.7A, a-c). Similarly, when conditioned media from apoDh-GFP transfected cells was added to cells that were further exposed to normal or stress conditions during 5 days, fluorescence could

be detected in the cytoplasm of normal growing cells (Fig. 2.7B, a-c). In serum starved and LPS exposed cells, the fluorescence accumulated inside the nucleus as demonstrated by a strong colocalization with nucleus staining (Fig. 2.7B, d-i). The weaker nuclear localization obtained with the addition of human cyst fluid apoD in comparison with the addition of apoDh-GFP is explained by the fact that an earlier time point is shown (3 days and 6 days post-treatment respectively).

The ability of apoD to enter the cell and its nucleus also suggests an implication in nuclear processes such as transcription activation, cell cycling or apoptosis. We investigated further the effect of extracellular apoD in growing and stressed mouse fibroblast cultures using antibodies that recognize specifically the human protein. The presence of human apoD has no influence on apoD mRNA or mouse protein expression (Fig. 2.8A and B), although, it can modulate cell proliferation and apoptosis. When human apoD is added to growing cells, we observed no effect on apoptosis but a 2-fold increase in cell proliferation. Similarly, the addition of human apoD to LPS-treated cells does not affect the apoptotic rate but further increases the proliferation level already enhanced by LPS addition. However, when applied to serum-starved cells, human apoD had no effect on cell proliferation but increased apoptosis (Fig. 2.8C and D).

2.5.7 Nuclear apoD is derived from secreted protein

To further confirm that the presence of apoD in the nucleus under stress conditions is due to a reentry of the secreted protein, apoDh-GFP transfected cells were subjected to stress and to brefeldin A (BFA) treatment. Brefeldin A disrupts the structure and function of the Golgi apparatus. Immunoblot analysis of the conditioned media from apoDh-GFP transfected cells confirmed the presence of the secreted fusion protein (55kDa) in both normal and LPS-treated cells but not in serum starved cultures (Fig. 2.5C and 2.9A). When BFA was added, apoDh-GFP disappeared from

the conditioned media in both normal and LPS conditions (Fig. 2.9A) confirming that the apoDh-GFP detected originated from secretion via the Golgi apparatus. As expected, this inhibition of apoDh-GFP secretion abolished the nuclear localization of apoDh-GFP but caused an accumulation in the cytoplasm both in serum starvation and in LPS conditions (Fig. 2.9B). All together, these results strongly suggest that the nuclear apoD is derived from the secreted protein. This conclusion can be extended to the endogenous protein since all localization studies (Fig. 2.5 and 2.6) show that apoDh-GFP behaves identically to endogenous apoD.

2.6 Discussion

In this study, we demonstrate that some but not all stress conditions activate apoD expression. Temperature, osmotic pressure, metal exposition and pro-apoptotic agents such as camptothecin did not affect apoD transcription. However, classical inducers of oxidative stress, H_2O_2, Rose Bengal and UV light did induce apoD mRNA accumulation in a dose-dependent manner. This response was very closely associated with a decrease in cell proliferation and viability as demonstrated with increasing concentrations of H_2O_2. Indeed, induced apoD expression was observed specifically at those H_2O_2 concentrations that caused growth arrest. This strongly suggests that the capacity of some specific stresses to trigger apoD expression is more related to their capacity to activate growth arrest pathways. The relation between apoD and growth arrest is well established. When analyzed in cell cultures, apoD induction seems always inversely correlated to cell proliferation (Blais *et al.* 1994, Do Carmo *et al.* 2002, Lopez-Boado *et al.* 1994, 1996, Patel *et al.* 1995, Provost *et al.* 1991a, Simard *et al.* 1991, 1992, Sugimoto *et al.* 1994).

This study is also the first to our knowledge that establishes a relation between apoD expression and inflammation. Indeed, the only stress that increased apoD without inhibiting cell proliferation was LPS. This molecule, derived from the outer membrane of Gram-negative bacteria, is well documented as being both a mitogen and a pro-inflammatory agonist in several cell types participating to inflammatory responses, including fibroblasts (Smith *et al.* 2001, Tardif *et al.* 2004, Warner *et al.* 2004). It is also capable to induce oxidative stress through the activation of NADPH oxidase and antioxidant enzymes. In spite of this, we believe that apoD expression is related to inflammatory pathways because of the capacity of diclofenac to reverse the LPS-associated induction. Our results also show that the LPS function on the apoD expression is mediated at the promoter level, through the APRE-3, NF-kB and AP-1 binding sites. AP-1 and NF-kB are well documented as regulators of numerous genes

involved in immune and inflammatory responses (Lee *et al.* 2003). In different cell and promoter contexts, AP-1 binds DNA as Jun/Jun homodimers or Jun/Fos heterodimers and alters gene expression in response to growth factors, cytokines, oxidative stress, and phorbol esters (Kushner *et al.* 2000). Less information is available concerning acute-phase responsive elements (APRE) having a consensus sequence similar to the one present on the apoD promoter. Some studies reported that APREs have an important role during inflammation and infection and to bind IL-1α (Brasier *et al.* 1990), IFN-γ (Strhlow *et al.* 1993), IL-6 (Yuan *et al.* 1994) and NF-kB1 isoforms (Jamaludin *et al.* 2000). The APRE could also bind C/EBPβ, which is mobilized upon LPS administration in mice. C/EBPβ is an important regulator of genes involved in immune and inflammatory responses and has been shown to bind the IL-6 gene promoter as well as several other acute-phase and cytokine genes (Hu *et al.* 2004). This pathway is not yet fully understood but allows the production of prostaglandin E2 (Uematsu *et al.* 2002), a member of the pro-inflammatory eicosanoids family. Interestingly, arachidonic acid, the preferential ligand for apoD, is the dominant substrate for eicosanoid synthesis (Calder 2005). In addition to C/EBPβ, the APRE could also bind STAT3 (Song *et al.* 2004), which is known to play important roles in cell differentiation, proliferation, survival, and angiogenesis promotion.

The accumulation of apoD under growth arrest and in presence of LPS is also observed at the protein level. However, the protein accumulation is more modest than that of the mRNA. Our results clearly show for the first time that apoD subcellular localization undergoes modifications upon stress exposure: it is mainly secreted and found perinuclear in the Golgi apparatus under basal conditions but accumulates in the cytoplasm and the nucleus in stress conditions. Perinuclear localization of apoD has been reported in oligodendrocyte precursor-like cells and astrocytes of mouse brain of Niemann-Pick type C disease model (Ong *et al.* 2002) and in vascular

smooth muscle cells (VSMC) after wounding (Leung *et al.* 2004). The accumulation of apoD in the cytoplasm and its translocation to the nucleus when growth arrest or pro-inflammatory stimuli are applied was supported by several independent experimental approaches. This included colocalization of apoDh-GFP fusion constructs with DNA and Golgi markers, immunocytochemistry of the endogenous protein, and cell fractionation. Thus, immunoblotting of apoDh-GFP transfected cells confirms that, upon serum starvation and LPS treatment, there is an accumulation of apoD both in the cell and in the nucleus. No detectable secretion in the extracellular space was obtained in growth-arrested cells although easily detectable in the extracellular space upon LPS treatment. The experiment presented the advantage that we could follow the endogenous mouse apoD and the exogenous human apoD linked to GFP. Interestingly, both the mouse and human apoD behave similarly, suggesting a common response pattern upon stress exposure including similar pathways for nuclear transport.

Nuclear apoD may have several possible sources. It is unlikely that apoD enters the nucleus by passive diffusion since the fusion protein used in our study was generated by fusing EGFP to the C-terminus of the entire coding region of human apoD. The molecular mass of the resulting fusion protein is $\approx$ 55 kDa and therefore, it cannot enter the nucleus by diffusion. Furthermore, apoD does not contain any common putative nuclear localization signal (NLS) that could direct its translocation to the nucleus. Still, the binding of apoD to a transmembrane receptor or a protein containing a NLS cannot be excluded. Retrograde trafficking from ER to the nucleus is a more plausible mechanism of translocating the intracellular apoD from cytoplasm to the nuclear compartment. It has been suggested that misfolded proteins that would classically undergo degradation in the ER can be back-translocated from the ER to the cytoplasm. However, if misfolding occurs, it is not the consequence of the overexpression of the apoDh-GFP since a similar localization of endogenous apoD was found in cells transfected or not with the apoDh-GFP construct. Misfolding could

then be associated with the stress itself. In spite of this, we provided evidences that nuclear apoD originates from the extracellular compartment. Indeed, as a glycoprotein harboring a peptide signal, apoD should be entirely secreted. Its presence within cells exposed to specific stress suggests a protein re-uptake, most likely by an endocytosis-dependent pathway, and transport to the nucleus. This is in agreement with several observations: (1) the apoD present in the nucleus has a molecular mass similar to that of the secreted protein; this would not be the case if apoD had bypassed the Golgi and ER glycosylation (2) apoDh-GFP is secreted as well as localized in the nucleus; (3) when untransfected stressed cells (LPS exposed or serum starved) are exposed to conditioned media containing apoDh-GFP, the fusion protein is translocated to the nucleus; (4) inhibition of protein secretion by BFA abolishes the nuclear presence of apoDh-GFP, whereas it increases its cytoplasmic content. Thus, apoD nuclear localization is dependent on the functional Golgi apparatus; (5) human apoD, purified from cyst fluid, is internalized in normal and stressed cells but translocation to the nucleus is observed only after stress; (6) finally, there is accumulating evidence that secreted proteins are present in the nucleus under specific circumstances. The fact that apoD is found in the nucleus of serum starved cells although we could not detect its presence in the media may appear as a contradiction but we cannot rule out that very low levels of apoD are secreted and immediately reabsorbed under these conditions. Indeed, the media was only concentrated twice before analysis.

Eventhough, apoD is translocated differentially in normal and stress conditions, its possible function in the cells remains to be determined. The data obtained by confocal imaging and immunoblotting of apoDh-GFP transfected cells and cells exposed to exogenous human apoD suggest that, in normal growing cells, apoD is modified in the Golgi apparatus and secreted before reinternalization in the cytoplasm, possibly transporting one of its ligand. The exposition of cells to exogenous apoD followed by its internalization results in an increased proliferation

and points to an interaction of apoD or its ligand or both with early targets of proliferative signals. The function of apoD in the nucleus during stress is less clear. Its accumulation in the nucleus of both serum starved and LPS treated cells raised the possibility that it may regulate gene expression directly or indirectly. In particular, it suggests a role for apoD in the balance between apoptosis and cell proliferation. This balance might be dependent of the interaction of apoD or its ligand or both with cell-cycle regulators that affect both the proliferative and non-proliferative processes. Consequently, the addition of exogenous apoD has a strong incidence on cellular proliferation in LPS treated cells but apoptosis is observed when added to growth-arrested cells. Both mitogenic and growth arrest conflicting signals are known to initiate apoptosis as this could be the case in growth arrested cells treated with purified apoD. Yet, exogenous apoD does not influence endogenous apoD protein or mRNA expression, excluding the possibility of self-regulation.

Inflammation, oxidative stress and apoptosis are part of many if not all the pathological situations where apoD is found increased. Chronic inflammation is associated with certain metabolic diseases such as non-insulin dependent diabetes mellitus type II and metabolic syndrome X (for review, see Rassart *et al.* 2000, Van Dijk *et al.* 2006) There is also an emerging consensus of the inflammatory and/or oxidative stress hypothesis of Alzheimer's disease, multiple sclerosis, schizophrenia, bipolar disorder, traumatic brain injury and other neuropathologies (Dakhale *et al.* 2004, Giovannoni and Baker 2003, Thomas *et al.* 2001b). Moreover, apoptosis was reported in situations showing apoD overexpression (Lieuallen *et al.* 2001, Montpied *et al.* 1999, Thomas *et al.* 2003c). Thus, it might be difficult to distinguish the incidence of each of these pathways on apoD induction since most of them are intimately linked. However, the present study suggests that those conditions responsible for apoD expression are more related to an antiproliferative and inflammatory signals than to oxidation and apoptosis. It remains to be determined whether apoD accumulation in inflammation is protective or detrimental. ApoD could

be part of the protective component of a mild inflammation, particularly at the neuronal level. It could also trap inflammatory mediators. In particular, apoD could trap arachidonic acid, which is released from the cellular membrane after inflammatory stimuli, and prevent its subsequent conversion in pro-inflammatory eicosanoids.

In conclusion, apoD induction is specific to ongoing cellular stress. Only pathological and/or stressful situations tested here having an inflammatory or growth arrest component have the capacity to increase apoD expression. We have provided some lines of evidence indicating that these stresses induce a displacement of apoD localization and that the nuclear apoD is derived from the secreted protein. ApoD binds several quite different molecules. Within the cell, apoD could have many functions such as the transport of specific molecules to the various compartments and evacuation of toxic metabolites. It could also play a role in the modulation of signal transduction pathways and in the regulation of nuclear processes such as transcription activation, cell cycling and apoptosis. More studies are needed to identify potential target genes of apoD and to elucidate the molecular events that trigger its cell entry and nuclear translocation.

2.7 Acknowledgments

We thank Ross Milne, Diego Sanchez and Maria Dolores Ganfornina for helpful discussions. The anti-mouse antibody was raised by Olivier Guinard in our lab. We gratefully acknowledge support from the Canadian Institutes for Health Research (Grant MOP-15677). SDC was supported by FRSQ and NSERC studentships.

Table 2.1 : Sites implicated in apoD transcription induction following LPS exposure.

Element	Sequence	Position	Orientation	Primers used for mutagenesis
APRE-3	AACTTTTAGCCCCAGTT	-681 to -665	(+)	**Forward:** 5'-CTCAACTTTcgGCCaaAGTTGTTAGA-3'
				Reverse: 5'-TCTAACAACTttGGCcgAAAGTTGAGA-3'
NF-kB1	ACTGGTATCTCCCCT	-656 to -642	(-)	**Forward :** 5'-ACTGGTATCTaaaCTACACGTCTGGC-3'
				Reverse : 5'-GCCAGACGTGTAGtttAGATACCAGT-3'
NF-kB2	GGGGGCTGCCC	-568 to -558	(+)	**Forward :** 5'-GAGAAGTTAGtttGCTGCCCAGG-3'
				Reverse : 5'-CTGGGCAGCaaaCTAACTTCTC-3'
AP-1	TTGACTCAT	-535 to -527	(+)	**Forward :** 5'-CAGCTTTGACTtgTAACCCTCGC-3'
				Reverse : 5'-GCGAGGGTTAcaAGTCAAAGCTG-3'

The primers used for mutagenesis of the region -816/-417 cloned upstream of the minimal promoter -179/-4 are indicated. The mutated nucleotides are indicated in lower case.

2.8 Figure legends

Figure 2.1: ApoD mRNA modulation under stress conditions is associated with variations in proliferation, senescence and apoptosis. A) ApoD mRNA expression in NIH/3T3 cells after exposure to various stresses. Untreated growing cultures (N) and serum-starved cultures (0.2 %) are included as controls. The following lanes are, respectively, RNA from cultures exposed to high temperatures (Hs 42°C and Hs 45°C), low temperatures (Cs 32°C and Cs 4°C), hypo- and hyper-osmotic conditions (H_2O and NaCl), metal salts, hydrogen peroxide (H_2O_2 100 μM and 300 μM), lipopolysaccharide (LPS 2, 5 and 10 μg/ml), UV light (1 and 2 min) or camptothecin (CPT 5 and 10μM). Blots were hybridized with mouse apoD, hsp70 and GAPDH cDNAs. B) Apoptosis, viability and senescence were measured by the TUNEL assay, by the MTS/PMS mitochondrial respiration assay and by the β-galactosidase activity, respectively. Data are represented as mean ± S.D. of at least three experiments. Asterisk indicates statistical difference compared to normal conditions (unpaired Student's t-test, $*p < 0.001$).

Figure 2.2: ApoD mRNA expression after H_2O_2 treatment is concentration-dependent. A) Total RNAs were isolated from NIH/3T3 untreated (N) or treated with increasing concentrations of H_2O_2. Serum starved cells are included as control. Hybridization was performed with mouse apoD, caveolin-1 and GAPDH cDNAs. B) Quantification of apoptosis, viability and senescence after H_2O_2 exposure was performed as in Figure 1B. Data are represented as mean ± S.D. of at least three experiments. Asterisk indicates statistical difference compared to normal conditions (unpaired Student's t-test, $*p < 0.001$).

Figure 2.3: ApoD mRNA expression after LPS treatment and relation with inflammation and proliferation. A) NIH/3T3 cells were exposed to LPS (5μg/ml)

during the indicated number of days. Northern analysis was performed with total RNAs probed with mouse apoD and GAPDH cDNAs. B) ApoD expression in cells treated with LPS diclofenac or basic fibroblast growth factor (bFGF) for 4 days. Untreated growing cells (N) and serum-starved cells (0.2%) were included as controls. Northern analysis was performed with total RNAs probed with mouse apoD and GAPDH cDNAs. C) Analysis of proliferation by BrdU incorporation in cells treated as in B. Data are represented as mean $\pm$ S.D. of at least three experiments. Asterisk indicates statistical difference compared to normal conditions or as indicated (One-way ANOVA, *$p < 0.001$).

Figure 2.4: Identification of LPS responsive elements in the apoD promoter. A) A serie of luciferase reporter constructs was made that contained progressive deletions of the 5'-flanking regions of the apoD gene promoter. B) Site-directed mutagenesis of APRE-3, NF-kB1, NF-kB2 and AP-1 responsive elements. Each element was mutated alone or in combination with the others in a construct containing the -816/-471 region of the promoter cloned upstream of the minimal promoter -179/-4. The mutated sequences are summarized in Table 2.1. All constructs were transfected into NIH/3T3 cells, which were maintained in media with (black bars) or without (gray bars) 5µg/ml LPS. Luciferase activities were assayed 4 days after transfection. The induction represents the ratio of luciferase activity in cells treated with LPS to that of cells without LPS. Each value represents the mean $\pm$ S.D. of at least three experiments performed in triplicate (One-way ANOVA, *$p< 0.05$, **$p< 0.01$, ***$p < 0.001$). Letters at the right of the induction numbers represent statistical significance; different letters indicate statistically different -fold induction.

Figure 2.5: Effects of LPS exposure and serum starvation on the intracellular localization of endogenous apoD and apoDh-GFP. NIH/3T3 cells were kept in normal growing conditions (N), treated with 5µg/ml LPS or grown in low-serum

medium (0.2%) for 0, 3, or 6 days and then subjected to Western blot analyses. Total (A), nuclear (B), and secreted (C) fractions of endogenous apoD and apoDh-GFP were detected with an anti-mouse apoD (apoDm) and an anti-GFP antibody, respectively. An anti-GAPDH antibody was included as a loading control. Each experiment was repeated at least 3 times.

Figure 2.6: Intracellular localization of apoD after exposure to LPS or serum starvation. A) Confocal microscopy analysis of NIH/3T3 cells transfected with the human apoD-coding region fused to GFP (apoDh-GFP) and treated with 5 μg/ml LPS (m-o; q-s) or 0.2% serum medium (e-g; i-k). All fluorescent imaging was done 3 (a-c; e-g; m-o) or 6 (i-k; q-s) days after normal or stress conditions at 40 X magnification and each experiment was done at least three times. Green fluorescence (GFP) indicates the position of apoDh-GFP, whereas the red fluorescence (propidium iodide; PI) indicates the position of the nucleus. The extent of nuclear localization of apoDh-GFP is indicated by yellow in the merged images. Results were confirmed by immunofluorescence staining of untransfected cells using a polyclonal mouse apoD antibody in the same stress conditions (d, h, l, p, t). B) GFP (a), Bodipy TR ceramide (b) and overlaid fluorescence of apoDh-GFP and Bodipy ceramide (c) in NIH/3T3 cells transfected with apoDh-GFP and kept 3 days in normal conditions before being treated with Bodipy TR ceramide. C) Immunofluorescence staining of human glioma cell line U373MG using a Caro2 polyclonal human apoD antibody. Normal cells (a) were exposed during 6 days to serum starvation (b) or LPS (5 μg/ml; c).

Figure 2.7: Internalization of exogenous human apoD or apoDh-GFP. A) Immunofluorescence staining of cells exposed to purified human apoD using a monoclonal human apoD antibody. Staining was performed 3 days after the addition of human apoD (200 ng/ml) to the culture media of cells in normal (d-f), in low serum (0.2%; g-i) or in LPS (5μg/ml; j-l) conditions. As a control, staining was conducted on cells without the addition of human apoD (a-c). Green fluorescence

(anti-apoDh) indicates the position of human apoD, whereas the red fluorescence (propidium iodide; PI) indicates the position of the nucleus. The extent of nuclear localization of human apoD is indicated by yellow in the merged images. B) Confocal imaging of extracellular apoDh-GFP. Conditioned media from cells transfected with apoDh-GFP was added to cells in normal (a-c) or stress conditions (d-i) during 6 days.

Figure 2.8: Effect of exogenous human apoD on endogenous apoD expression, apoptosis and proliferation. Induction of apoD mRNA (A) and protein (B) expressions was tested 3 days after the addition (+) or not (-) of 200 ng/ml of human apoD to the culture media. Northern analysis was performed with total RNAs probed with mouse apoD and GAPDH cDNAs. Western immunoblot analysis for human and mouse apoD protein was performed on total cell lysates and is representative of two separate experiments. Apoptosis (C) and proliferation (D) levels were determined by TUNEL assay and by BrdU incorporation, respectively in the presence (+) or absence (-) of 200 ng/ml of human apoD in growing cells compared with serum starved (0.2%) and LPS treated (5µg/ml) cultures. Each bar represents the mean ratio of fluorescent apoptotic cells ± SD in each condition of three separate experiments performed in triplicate. Asterisk indicates statistical difference compared to conditions without addition of human apoD (unpaired Student's t-test, *$p < 0.001$).

Figure 2.9: Intracellular localization of apoDh-GFP in brefeldin A exposed cells. ApoDh-GFP transfected cells were subjected to growing (N), serum starved (0.2%) and LPS (5µg/ml) conditions during 4 days. A) Western immunoblot analysis for human apoD was performed on the culture media of cells treated with or without BFA (5 µg/ml) for 1 h and processed 24 h later for immunoblotting. B) Confocal fluorescence imaging of cells transfected with apoDh-GFP, exposed to stress conditions and treated or not with BFA as in A).

Figure 2.1

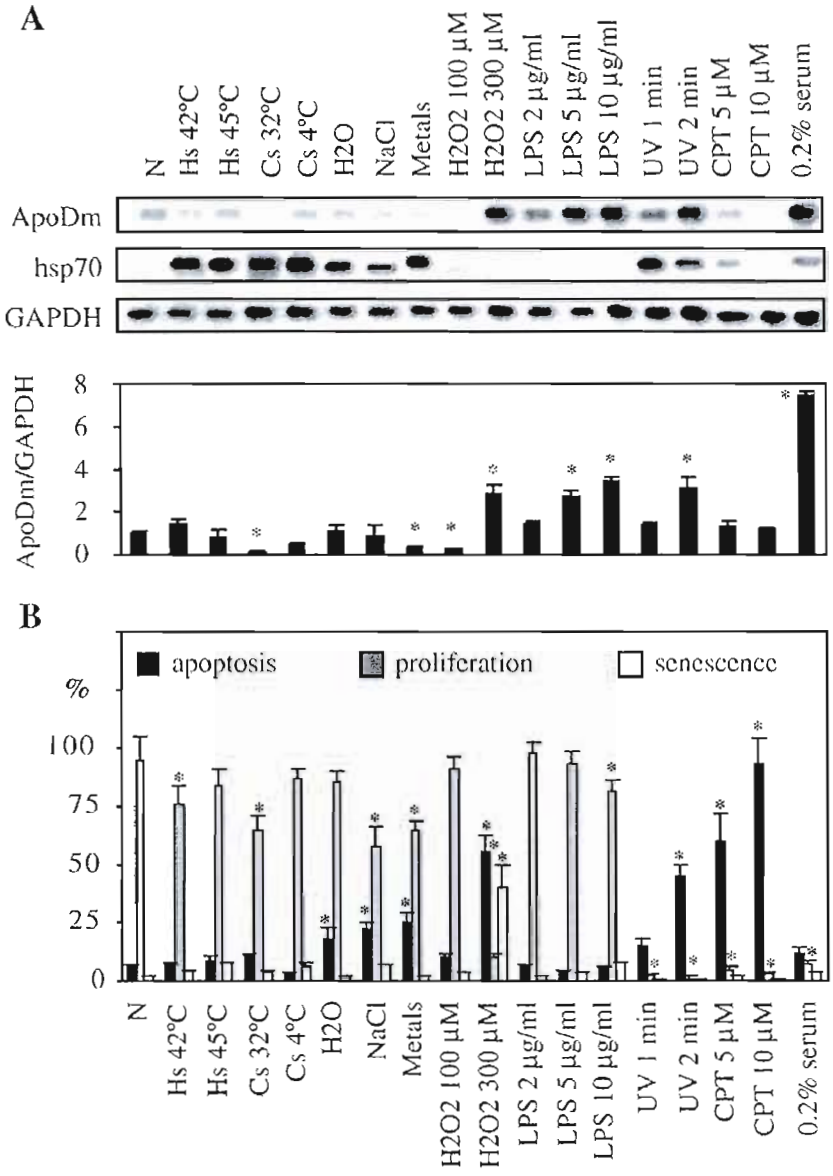
A
N
Hs 42°C
Hs 45°C
Cs 32°C
Cs 4°C
H2O
NaCl
Metals
H2O2 100 µM
H2O2 300 µM
LPS 2 µg/ml
LPS 5 µg/ml
LPS 10 µg/ml
UV 1 min
UV 2 min
CPT 5 µM
CPT 10 µM
0.2% serum
ApoDm
hsp70
GAPDH
ApoDm/GAPDH
8
6
4
2
0
B
apoptosis
proliferation
senescence
%
100
75
50
25
0

Figure 2.2

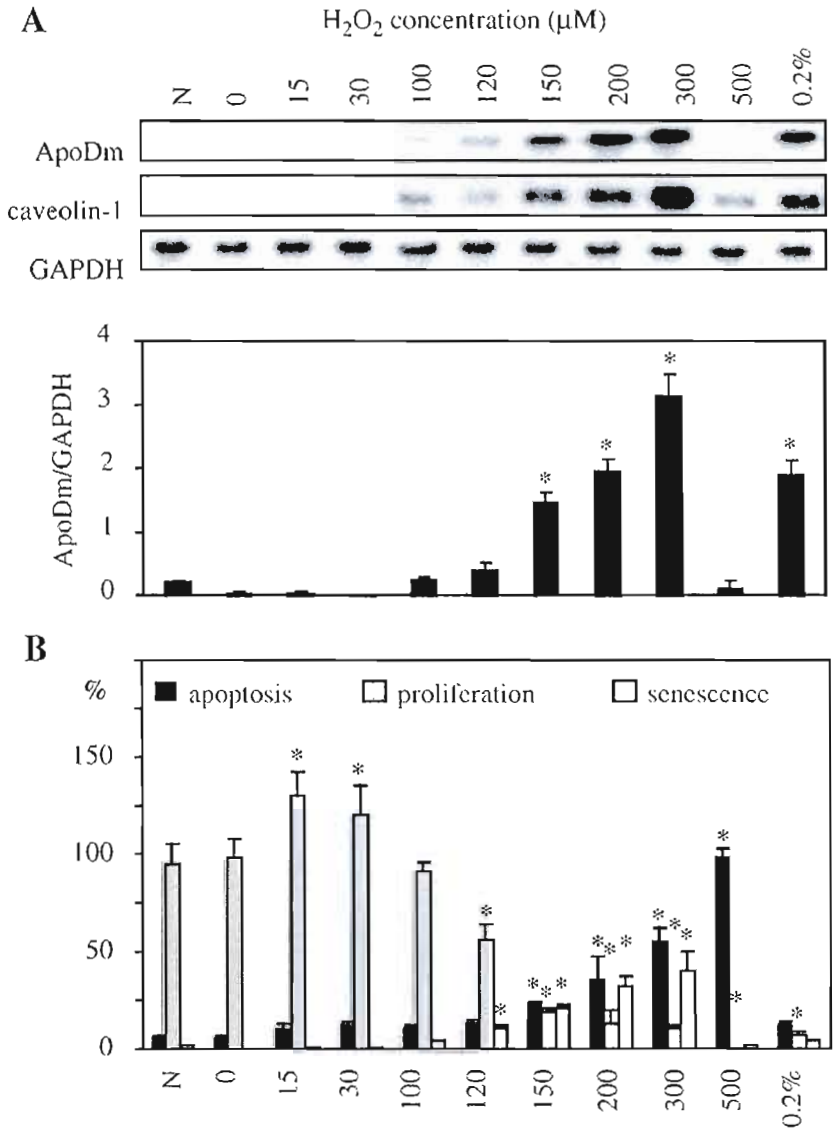
A
H_2O_2 concentration (μM)
N
0
15
30
100
120
150
200
300
500
0.2%
ApoDm
caveolin-1
GAPDH
ApoDm/GAPDH
4
3
2
1
0
B
%
apoptosis
proliferation
senescence
150
100
50
0
N
0
15
30
100
120
150
200
300
500
0.2%

Figure 2.3

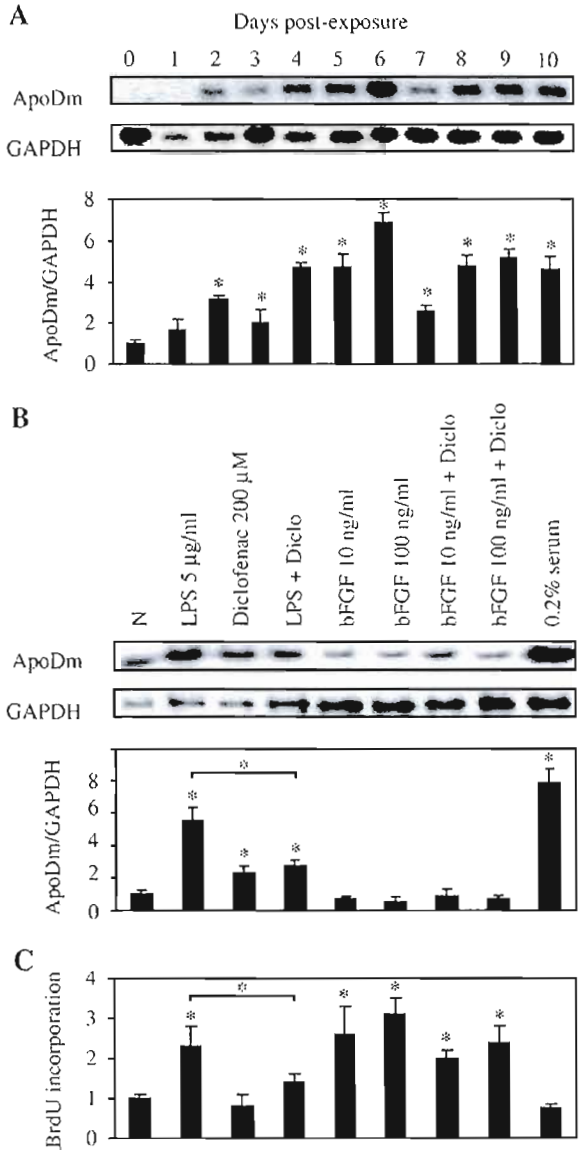
A
Days post-exposure
0 1 2 3 4 5 6 7 8 9 10
ApoDm
GAPDH
ApoDm/GAPDH
0 2 4 6 8
B
N
LPS 5 µg/ml
Diclofenac 200 µM
LPS + Diclo
bFGF 10 ng/ml
bFGF 100 ng/ml
bFGF 10 ng/ml + Diclo
bFGF 100 ng/ml + Diclo
0.2% serum
ApoDm
GAPDH
ApoDm/GAPDH
0 2 4 6 8
C
BrdU incorporation
0 1 2 3 4

Figure 2.4

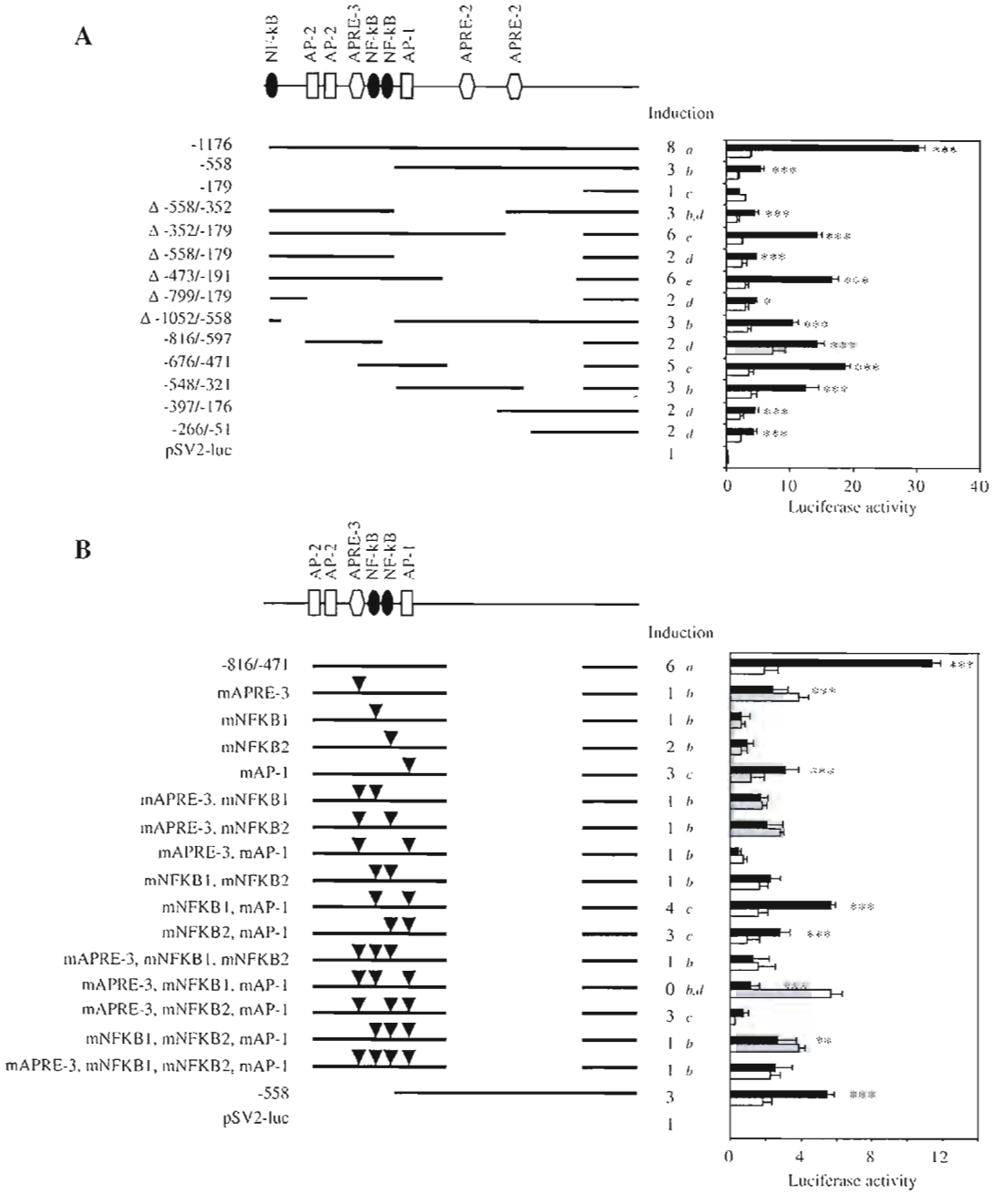
A
NF-kB
AP-2
AP-2
APRE-3
NF-kB
NF-kB
AP-1
APRE-2
APRE-2
Induction
-1176
-558
-179
Δ -558/-352
Δ -352/-179
Δ -558/-179
Δ -473/-191
Δ -799/-179
Δ -1052/-558
-816/-597
-676/-471
-548/-321
-397/-176
-266/-51
pSV2-luc
8 a
3 b
1 c
3 b,d
6 c
2 d
6 e
2 d
3 b
2 d
5 c
3 b
2 d
2 d
1
0
10
20
30
40
Luciferase activity
B
AP-2
AP-2
APRE-3
NF-kB
NF-kB
AP-1
Induction
-816/-471
mAPRE-3
mNFKB1
mNFKB2
mAP-1
mAPRE-3, mNFKB1
mAPRE-3, mNFKB2
mAPRE-3, mAP-1
mNFKB1, mNFKB2
mNFKB1, mAP-1
mNFKB2, mAP-1
mAPRE-3, mNFKB1, mNFKB2
mAPRE-3, mNFKB1, mAP-1
mAPRE-3, mNFKB2, mAP-1
mNFKB1, mNFKB2, mAP-1
mAPRE-3, mNFKB1, mNFKB2, mAP-1
-558
pSV2-luc
6 a
1 b
1 b
2 b
3 c
1 b
1 b
1 b
1 b
4 c
3 c
1 b
0 b,d
3 c
1 b
1 b
3
1
0
4
8
12
Luciferase activity

Figure 2.5

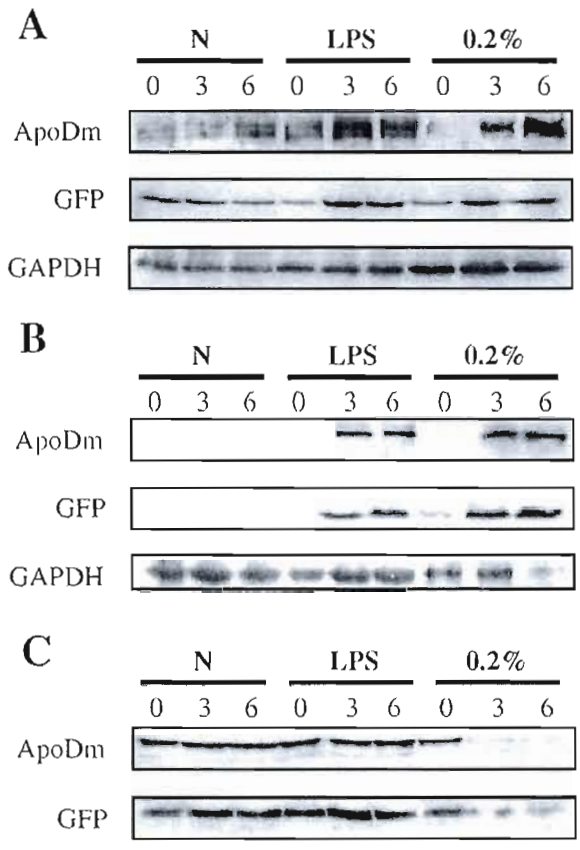
A
N
LPS
0.2%
0 3 6 0 3 6 0 3 6
ApoDm
GFP
GAPDH
B
N
LPS
0.2%
0 3 6 0 3 6 0 3 6
ApoDm
GFP
GAPDH
C
N
LPS
0.2%
0 3 6 0 3 6 0 3 6
ApoDm
GFP

Figure 2.6

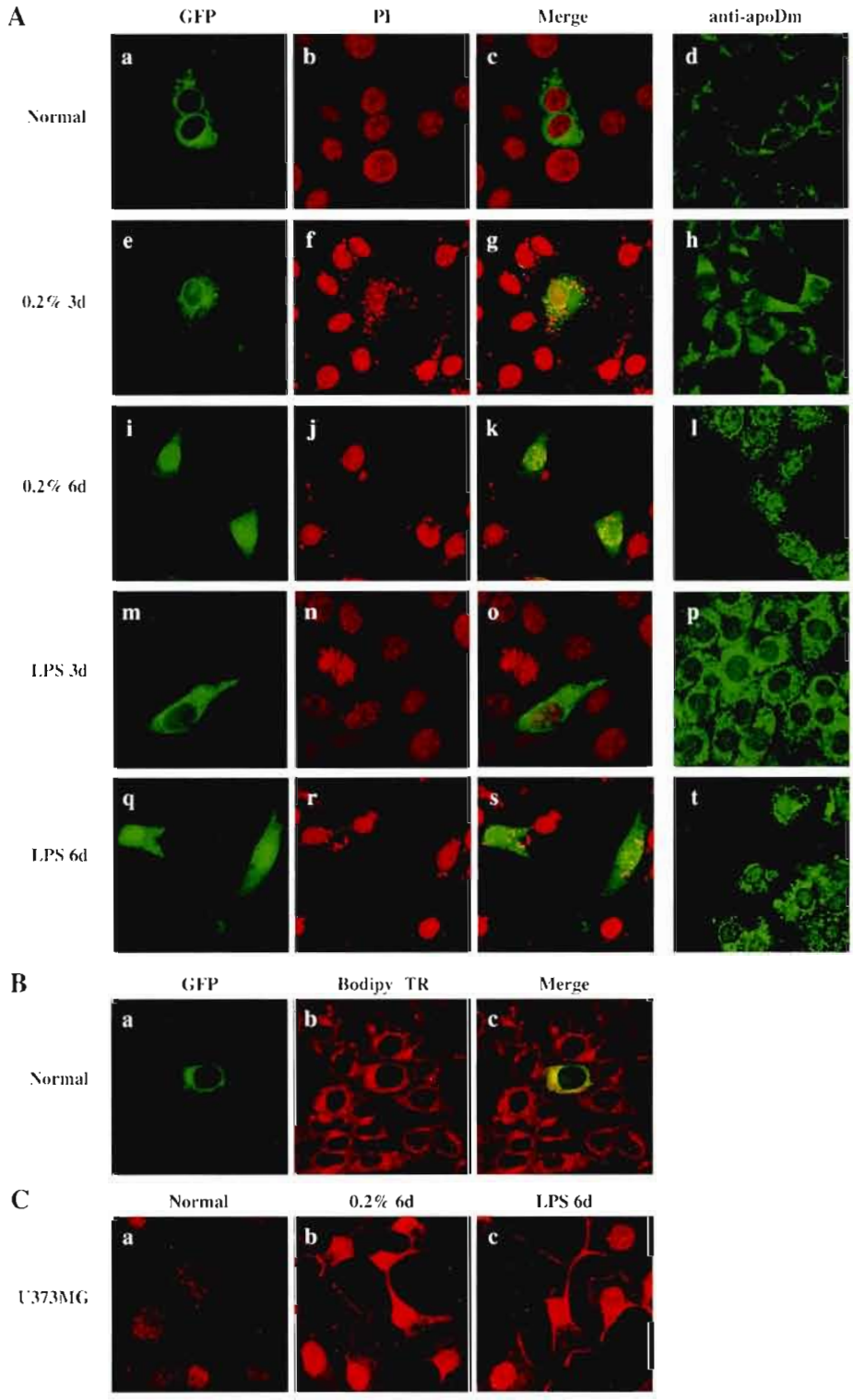
A
GFP
PI
Merge
anti-apoDm
Normal
0.2% 3d
0.2% 6d
LPS 3d
LPS 6d
a
b
c
d
e
f
g
h
i
j
k
l
m
n
o
p
q
r
s
t
B
GFP
Bodipy TR
Merge
Normal
a
b
c
C
Normal
0.2% 6d
LPS 6d
U373MG
a
b
c

Figure 2.7

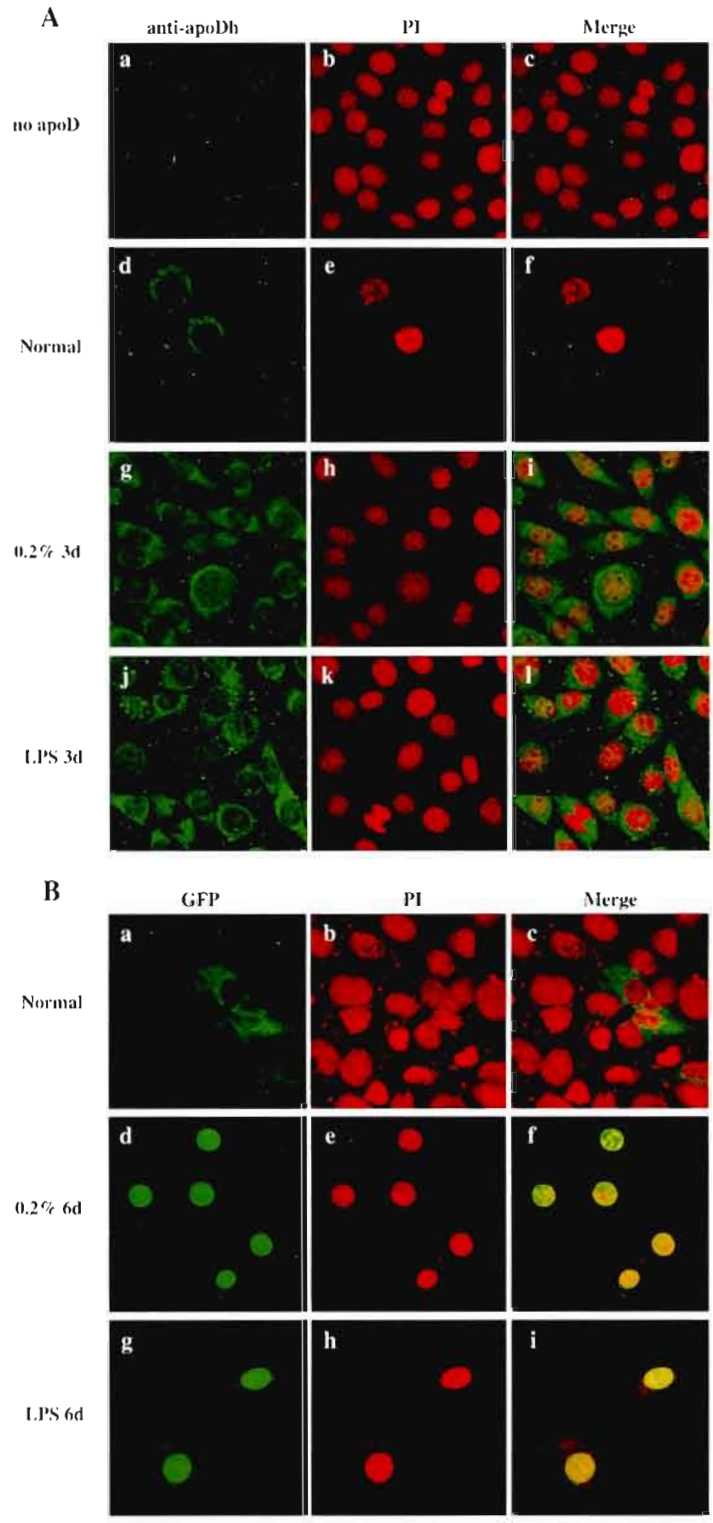
A
anti-apoDh
PI
Merge
no apoD
Normal
0.2% 3d
LPS 3d
B
GFP
PI
Merge
Normal
0.2% 6d
LPS 6d

Figure 2.8

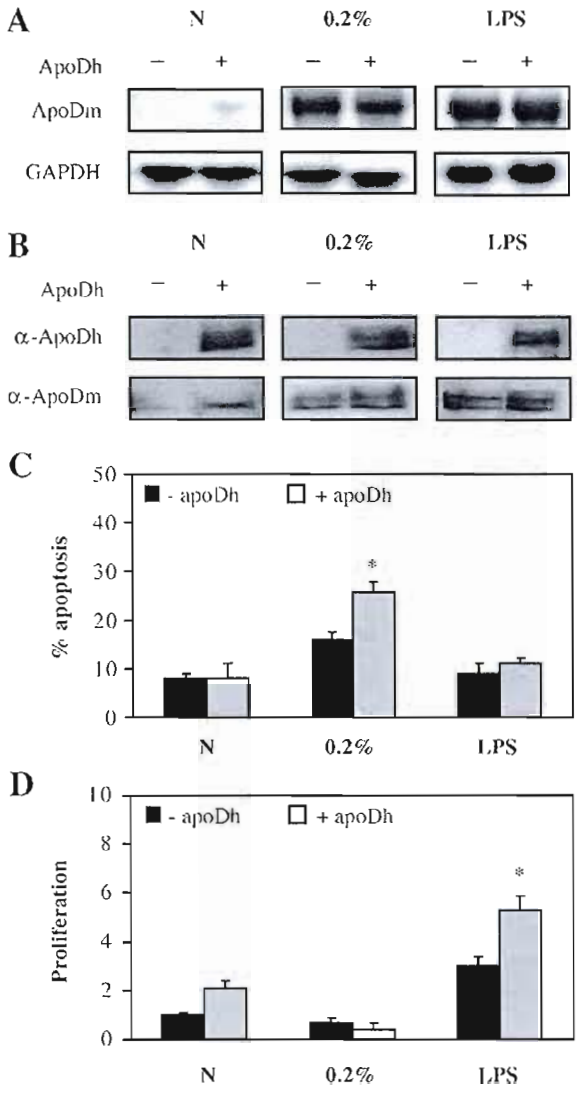
A
N
0.2%
LPS
ApoDh
– + – + – +
ApoDm
GAPDH
B
N
0.2%
LPS
ApoDh
– + – + – +
α-ApoDh
α-ApoDm
C
- apoDh
+ apoDh
% apoptosis
50
40
30
20
10
0
*
N
0.2%
LPS
D
- apoDh
+ apoDh
Proliferation
10
8
6
4
2
0
*
N
0.2%
LPS

Figure 2.9

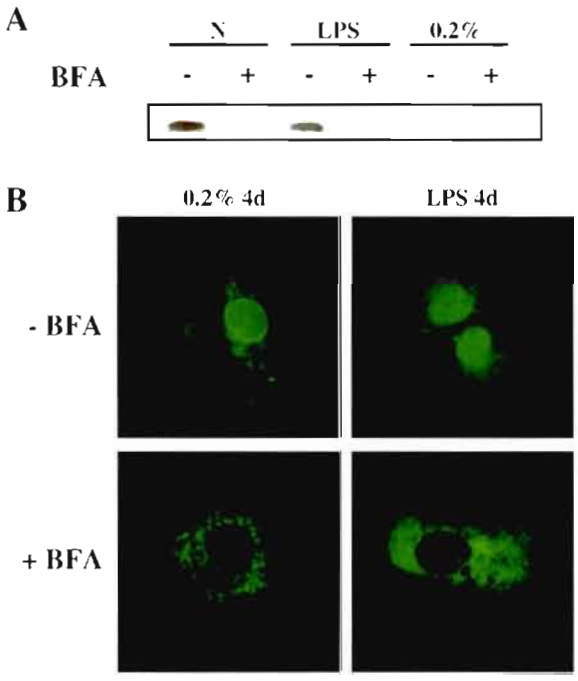

CHAPITRE III

Human apolipoprotein D overexpression in transgenic mice induces insulin resistance and alters lipid metabolism

Sonia Do Carmo, David Fournier, Catherine Mounier, Eric Rassart

2009

American Journal of Physiology-Endocrinology and Metabolism
Sous presse

Avant-propos

Nous avons démontré en chapitre II que l'expression de l'apoD était déclenchée en réponse à des stress spécifiques. Cependant, la fonction de cette modulation de l'expression de l'apoD reste inconnue. Nous avons émis comme hypothèse que l'apoD favorise une meilleure survie en réponse à des situations de stress cellulaire. Étant donné l'importance de l'apoD dans le développement du sytème nerveux et sa modulation dans la plupart des maladies neurodégénératives dont certaines ont été étudiées dans notre laboratoire, nous avons choisi de tester cette hypothèse dans un contexte neurodégénératif. Pour cela, nous avons d'abord généré les souris H-apoD-Tg qui surexpriment l'apoD humaine dans les neurones, le type cellulaire le plus affecté lors de maladies neurodégénératives. Nous avons opté pour la surexpression de l'apoD humaine afin de la différencier de l'apoD endogène de souris. Cependant, avant de soumettre ces souris à des traitements neurodégénératifs, il était important de caractériser ces souris. Ces souris ne présentent pas de différences morphologiques majeures au niveau du cerveau. Cependant, elles ont des différences au niveau comportemental tel que présenté dans le chapitre IV suggérant que l'apoD joue un rôle dans la fonction neuronale. De façon intéressante, nous avons constaté que l'expression de l'apoD humaine ne se limitait pas au système nerveux. Nous avons donc exploré l'influence de l'apoD humaine sur la composition cellulaire et la biochimie sanguines de même que sur divers paramètres morphométriques et tissulaires.

David Fournier a construit les transgènes et généré les souris transgéniques. Il a aussi monté les colonies de souris transgéniques. J'ai ensuite repris le projet et j'ai caractérisé les souris. J'ai donc été impliquée dans toutes les facettes de ce travail. J'ai élaboré le design expérimental et fait la totalité du travail pratique. J'ai également rédigé le manuscrit.

3.1 Résumé

L'apolipoprotéine D, une lipocaline largement exprimée, a la capacité de transporter de petites molécules hydrophobes. Même s'il a été proposé que l'apoD puisse avoir plusieurs fonctions et ligands et ce de façon tissu-spécifique, ceux-ci n'ont pas encore été clairement identifiés. Afin d'élucider quelques-unes de ces fonctions, nous avons généré des souris transgéniques surexprimant l'apoD humaine (H-apoD) sous le contrôle de promoteurs spécifiques aux neurones. Chez les souris Thy-1/ApoD et NSE/ApoD, l'expression de H-apoD est forte dans le système nerveux bien que détectée aussi faiblement dans les tissus périphériques comme le foie et les cellules sanguines. Ces souris démontrent des défauts métaboliques non entièrement anticipés. Ainsi, bien qu'elles ne soient pas obèses et qu'elles aient un niveau normal de lipides en circulation, les souris Thy-1/ApoD et NSE/ApoD sont intolérantes au glucose, résistantes à l'insuline et elles développent une stéatose hépatique. Cette stéatose et la résistance à l'insuline qui lui est associée sont corrélées avec des déficiences dans les voies signalétiques de l'insuline et dans la lipogenèse hépatique. Cependant, elles ne sont pas fortement corrélées à la présence d'inflammation. Par ailleurs, l'altération de la réponse à l'insuline n'est pas causée par une diminution de la leptine circulante ni par une modulation des niveaux d'adiponectine ou de résistine. Ces résultats suggèrent que des variations des niveaux et/ou des sites d'expression de l'apoD influencent les métabolismes des lipides et du glucose, consolidant ainsi l'apoD comme une cible pour les maladies reliées à la résistance à l'insuline.

Mots-clés : résistance à l'insuline, métabolisme lipidique, stéatose hépatique, inflammation, longévité.

3.2 Abstract

Apolipoprotein D (apoD), a widely expressed lipocalin, has the capacity to transport small hydrophobic molecules. Although it has been proposed that apoD may have multiple tissue-specific, physiological ligands and functions, these have yet to be identified. To gain insight in some of its functions, we generated transgenic mice overexpressing human apoD (H-apoD) under the control of neuron-specific promoters. In Thy-1/ApoD and NSE/ApoD mice, expression of H-apoD was strong in the nervous system although weakly detected in peripheral organs such as the liver and blood cells. These mice displayed not entirely anticipated metabolic defects. Although they are not obese and have normal lipid concentration in circulation, Thy-1/ApoD and NSE/ApoD mice are glucose intolerant, insulin resistant and develop hepatic steatosis. The steatosis and its associated insulin resistance are correlated with impairments in insulin signaling and hepatic lipogenesis. However, they are not strongly related with inflammation. This impaired insulin response is not caused by a decrease in circulating leptin or a modulation of adiponectin and resistin levels. These results suggest that variations in the levels and/or sites of apoD expression influence the lipid and glucose metabolism, consolidating apoD as a target for insulin resistance related disorders.

Keywords : insulin resistance, lipid metabolism, hepatic steatosis, inflammation, longevity.

3.3 Introduction

Apolipoprotein D (apoD) is a member of the lipocalin superfamily of small hydrophobic molecule transporters. ApoD was first detected in 1963, in association with plasma lipoproteins (Ayrault-Jarrier *et al.* 1963b). Since then, apoD was related with many physiological and pathological conditions and several potential ligands were identified: arachidonic acid (AA), progesterone, pregnenolone, bilirubin, cholesterol and E-3-methyl-2-hexenoic acid (reviewed in Rassart *et al.* 2000).

ApoD is widely expressed in vertebrates both during development and adulthood. In humans, it is poorly expressed in liver and intestines, the major sites of synthesis of other apolipoproteins. It is mainly expressed in the adrenal glands, kidneys, pancreas, placenta, spleen, lungs, ovaries, testes, brain, peripheral nerves and cerebrospinal fluid (Drayna *et al.* 1986). In mouse, apoD is mostly expressed in the central nervous system (CNS) (Séguin *et al.* 1995), mainly in glia but also in neurons. It is also found at high levels in adipose tissue and at lower levels in other tissues (Cofer and Ross 1996, Yoshida *et al.* 1996). Therefore, it has been proposed that apoD may have multiple tissue-specific, physiological ligands and functions (Rassart *et al.* 2000, van Dijk *et al.* 2006).

Both the apoD transcript and/or protein are altered in a broad range of conditions. Those include cellular growth, differentiation and stress response (Provost *et al.* 1991a, Lopez-Boado *et al.* 1994, Do Carmo *et al.* 2002, 2007), different types of cancer (van Dijk *et al.* 2006) and several neurological disorders such as Alzheimer' disease, stroke (Terrisse *et al.* 1998), schizophrenia (Thomas *et al.* 2001b), Parkinson's disease (Ordoñez *et al.* 2006) and animal models of nervous system pathology (Boyles *et al.* 1990a, Terrisse *et al.* 1999). ApoD is also involved in diverse aspects of lipid metabolism. ApoD gene polymorphisms affect plasma lipid levels (Desai *et al.* 2002) and can be used as a genetic marker for obesity,

hyperinsulinemia and non-insulin-dependent diabetes mellitus (Baker *et al.* 1994, Vijayaraghavan *et al.* 1994). Furthermore, apoD may participate in lipid transfer and reverse cholesterol transport by directly binding cholesterol (Patel *et al.* 1997) or by its association with apoA-I, lecithin-cholesterol acyltransferase (LCAT) and cholesteryl ester transfer protein (CETP) in high-density lipoprotein (HDL) fractions (Steyrer and Kotner 1988). Because of its capacity to bind AA, apoD contributes to membrane phospholipid metabolism by stabilizing AA levels in cellular membranes (Thomas *et al.* 2003d). An involvement in lipid redistribution after peripheral nerve injury was also suggested (Boyles *et al.* 1990a). Moreover, apoD was documented as a liver X receptor (LXR) responsive gene (Hummasti *et al.* 2004) and could play an important role in the modulation of the lipogenesis/lipolysis balance in adipocytes by transporting ligands for LXR or PPAR or participating in LXR-dependent reverse cholesterol transport (Hummasti *et al.* 2004). Finally, apoD plays a role in the control of food intake and body weight by interacting specifically with the cytoplasmic portion of the long form of the leptin receptor Ob-Rb (Liu *et al.* 2001). Therefore, it is not surprising to find apoD modulation in conditions presenting a deregulation of lipid metabolism such as Tangier disease (Alaupovic *et al.* 1981), familial LCAT deficiency (Albers *et al.* 1985), mutations in the apoA-I gene (Deeb *et al.* 1991) or in conditions leading to lipid accumulation as type 2 diabetes (Hitman *et al.* 1992) and mouse models of Niemann-Pick disease type C (Yoshida *et al.* 1996).

Abnormal lipid metabolism contributes to several neurodegenerative disorders, including Alzheimer's and Parkinson's diseases. The involvement of apoD in both lipid metabolism and neurological disorders suggest a central role in neurodegeneration and/or repair. Still, the precise role of apoD remains undetermined. Recent reports indicate a protective effect as it counteracts aging and oxidative stress (Ganfornina *et al.* 2008, Sanchez *et al.* 2006, Walker *et al.* 2006). In an attempt to reveal some aspects of the apoD function, we generated mice overexpressing human apoD (H-apoD) in the CNS. We chose to overexpress H-apoD

because it allows its discrimination from the endogenous apoD. During the characterization process, we observed that H-apoD overexpression affects the metabolism of glucose and lipids of these mice in a promoter's strength depending manner and also expression pattern. These defects correlate with impaired insulin signaling and hepatic lipogenesis. However, they do not correlate with increased inflammation or altered adipokine signaling. It therefore appears that a slight modulation of apoD expression in specific tissues could alter the glucose and lipid metabolisms.

3.4 Materials and methods

3.4.1 Animals

All the experimental procedures were approved by the Animal Care and Use Committee of Université du Québec à Montréal. Animals were housed at 24 ± 1°C in a 12 h light/dark cycle and fed a standard rodent chow ad libitum (Charles River rodent chow #5075, St-Hubert, QC) with free access to water. Experiments were carried out with 11-13 month old male animals, unless otherwise noted. Blood samples were collected for hematology and serum analysis. Tissues were collected, frozen in dry ice, and kept at -80°C. Sections of tissues were also frozen in HistoPrep Frozen Tissue Embedding medium (Fisher Scientific, Ottawa, ON) or fixed in 4% paraformaldehyde and embedded in paraffin for histological analysis.

3.4.2 Generation of H-apoD transgenic mice

The plasmid ApoD/BGH/pBSSK generated in our lab and comprising the human apoD coding sequence followed by the bovine growth hormone (BGH) polyadenylation signal in pBluescript II SK (Stratagene-VWR, Ville Mont-Royal, QC) was used for the transgene construction. Briefly, for the Thy-1/ApoD construct, the promoter, the first exon, the first intron and the 5' non-coding region of the second exon of the human Thy-1 gene (~ 3.5 kb) (generous gift from J. Silver, New York University Medical Center) were cloned upstream of the apoD coding sequence in plasmid ApoD/BGH/pBSSK (Ganfornina *et al.* 2008). The NSE/ApoD construct was generated similarly with the 5' non-coding region of the rat neuron-specific enolase (NSE) gene (~ 1.8 kb) (generous gift from G. Sutcliffe, Scripps Research Institute, La Jolla). Each transgene fragment was excised from its plasmid by digestion and prepared for microinjection by agarose gel electrophoresis and extraction with QIAEX II Gel extraction kit (Qiagen, Mississauga, ON).

Microinjection into the pronuclei of fertilized C57BL/6 x CBA zygotes was performed by standard procedures at the McGill transgenic facility (Montreal, QC). Transgenic animals were identified by PCR and Southern blot analysis of genomic DNA isolated from 3 weeks-old mouse tail biopsies. All mice were backcrossed into C57BL/6 genetic background for at least 8 generations to ensure phenotype stability. Genotyping was performed by PCR using an apoD-specific primer (5' CCC AAT CCT CCG GTG CAG GAG AA 3') and a BGH-specific primer (5' GAA GGC ACA GTC GAG GCT GAT CAG 3'), producing a 0.6 kb fragment in transgenic mice (Fig. 3.1C).

3.4.3 Southern blot analysis

BamHI-digested genomic DNA was separated on a 0.8% agarose/TAE gel, denatured, transferred to Osmonics Nylon Transfer Membrane (Fisher Scientific, Ottawa, ON) and UV-fixed for 3 min. The membranes were hybridized with [α-32P]dCTP-labeled probe corresponding to each transgene, exposed to Biorad Imaging screen K and revealed with a PhosphorImager (Biorad Molecular Imager FX). Copy standards are prepared by mixing non-transgenic tail DNA with a known amount of transgene DNA.

3.4.4 RNA extraction, northern blot analysis and semi-quantitative RT-PCR

Extraction of total RNA was performed with the Trizol reagent (Invitrogen, Burlington, ON). Total RNA (10μg) was separated on 1.5% (wt/vol) agarose-formaldehyde gels and blotted to a nylon membrane. The membranes were hybridized with [α-32P]dCTP-labeled human ApoD, mouse apoE or mouse GAPDH cDNAs as described above. Total RNA was also reverse transcribed using Omniscript RT kit (Qiagen) and amplified with human apoD, PPARα, PPARγ, FAS, LFABP, SREBP-1c or HPRT specific primers (Table 3.1). A control amplification of reverse

transcription reaction without the addition of reverse transcriptase was used to ensure that there was no DNA contamination.

3.4.5 Immunoblotting

Tissues were homogenized in lysis buffer (50 mM Tris-HCl pH 7.3, 150 mM NaCl, 5 mM EDTA, 0.2% Triton X-100, and 10% Complete protease inhibitors (Roche, Mississauga, ON)). After 30 min. of incubation at 4°C, lysates were sonicated and cleared by centrifugation. The protein concentration was determined using a protein assay reagent (Bio-Rad Laboratories, Mississauga, ON). All extracts were stored at -80°C. For each sample, 10 μg of protein were loaded and separated on a 12% SDS-polyacrylamide gel. The proteins were then transferred to PVDF membranes blocked with 10% milk and incubated with the primary antibodies: human apoD mouse monoclonal antibody (2B9), 1:100000; GAPDH rabbit polyclonal antibody (Calbiochem, La Jolla, CA), 1:4000; phospho-Akt (Ser473) rabbit polyclonal antibody (Cell signaling-NEB, Pickering, Ontario), 1:1000, Akt rabbit polyclonal antibody (Cell signaling), 1:1000. These primary antibodies were then detected with appropriate HRP-conjugated secondary antibodies and visualized by chemiluminescence (Amersham ECL, GE-Healthcare, Baie d'Urfé, QC) and X-ray film.

3.4.6 Blood analysis

Blood hematology and serum biochemistry were carried out by the Diagnostic and research support service of McGill University Animal Resources Center (Montreal, QC). Levels of cytokines and adipokines in serum were determined by SearchLight technology at the SearchLight Sample Testing Service of Pierce Biotechnology (Woburn, MA). Free fatty acids (FFA) levels were measured using a colorimetric kit (MBL International, Woburn, MA).

3.4.7 Competitive ELISA

Human apoD in plasma was quantified by ELISA using the human apoD monoclonal antibody 2B9 as previously described (Terrisse *et al.* 1998). Briefly, microtiter plates were coated with antigen (1 µg apoD/ml) in 5 mM glycin buffer (pH 9.2) and incubated overnight at 4°C. The wells were washed with PBS-Tween 0.25% and saturated with PBS-BSA 1% for 1 h. A mixture that was previously incubated overnight and containing diluted plasma and 2B9 antibody in PBS-BSA 1% then replaced the saturation solution. After 2 h of incubation, wells were washed. Bound 2B9 antibody was detected by peroxidase labeled anti-mouse IgG (KPL, Gaithersburg, MD) and revealed with ABTS substrate (KPL). Optical density was measured at 410 nm. All quantifications were performed in triplicate with 10 mice/genotype.

3.4.8 Liver lipid content

Fresh tissues were weighed in a precision balance, cut in small pieces and dried in glass vials placed in bell jar with dessicant under vacuum for 24 h. Tissues were then re-weighed to calculate dry tissue weight. Neutral lipids were extracted from tissues with diethyl ether for 24 h (2 extractions with 10 ml). Tissues were dried again for 24 h and re-weighed to obtain the fat-free dry weight. Total lipid content was calculated as: (dry tissue weight- fat-free dry tissue weight) x 100/dry tissue weight. Total cholesterol (cholesterol and cholesteryl ester) and triglycerides were quantified using colorimetric kits according to the manufacturer's instructions (Biovision Cedarlane, Burlington, ON).

3.4.9 TBARS assay

The extent of oxidation in transgenic tissues was determined by the thiobarbituric acid reactive substance (TBARS) assay. Liver tissue was homogenized in cold PBS 1X (3 µl PBS per mg of tissue) in presence of 5 mM butylated hydroxytoluene. A 12 µl aliquot of tissue extract was incubated with 390 µl of 0.2 M glycine-HCL, pH 3.6 and 250 µl of fresh TBA reagent (0.5% TBA, 0.5% SDS). Samples were incubated 15 min at 90°C and cooled on ice prior to a triplicate reading of the absorbance at 532 nm. Values were normalized by the lipid content of each sample.

3.4.10 Histology

The paraformaldehyde-fixed liver tissue was processed and embedded in paraffin and 5 µm-thick paraffin sections were stained with hematoxylin and eosin for histological analysis. To visualize lipids, frozen sections (10 µm thick) were stained with 0.5% Oil RedO in propylene glycol.

3.4.11 Intraperitoneal glucose and insulin tolerance tests (IPGTT and ITT)

For the glucose tolerance test, mice fasted overnight (12-15 h) were injected intraperitoneally with D-glucose (2 g/kg body weight). For the insulin tolerance test, mice were fasted for 5h before intraperitoneal injection of human regular insulin Humulin R (Elli Lilly Canada Inc., St-Laurent, QC) (1.5 U/kg body weight). Their body weights before and after fasting were recorded to the nearest gram unit. Blood samples were collected from the saphen vein 0, 15, 30, 45, 60, 90, and 120 min after the injections. Blood glucose and serum insulin levels were measured with the Accu-Chek Advantage Glucose Monitor and test strips (Roche) and the rat/mouse insulin ELISA kit (Linco/Millipore, MA), respectively. The area under the glucose curve in

the IPGTT was calculated by the trapezoid rule from the glucose measurements. Glucose levels in the ITT were expressed as percentages of initial blood glucose concentrations. The mice were allowed to recover for 2 weeks between experiments.

3.4.12 In vivo hepatic VLDL-triglyceride production

VLDL secretion was measured in 10 hours-fasted animals (1 year old). Control and H-apoD Tg mice were injected via the tail vein with 12% (v/v) Triton WR1339 (Tyloxapol; Sigma-Aldrich, Oakville, ON; 5 ml/kg body weight) diluted in PBS. Blood samples were taken before (t 0) and 30, 60 and 90 min after Triton injection. Triglyceride content was measured as described above. The secretion rate was calculated from the slope of the individual lines and expressed as µmol/kg/h.

3.4.13 Statistical analysis

Results are expressed as mean ± SE. Statistical analysis was performed with Prism 5 software (GraphPad, San Diego, CA). The statistical significance from control values was determined by Student's t-test. Values were considered to be significant at $p<0.05$.

3.5 Results

3.5.1 Generation of H-apoD transgenic mice

We generated and used two transgenic mouse lines overexpressing H-apoD in neurons under the control of the Thy-1 (Ganfornina *et al.* 2008) or the NSE promoters (Fig. 3.1A). We chose to overexpress the H-apoD because it allows its discrimination from the endogenous apoD and because the two proteins are highly homologous and are believed to achieve the same function both in humans and mice. For each transgene, three independent mouse lines that had integrated and were able to transmit the transgene were generated and analyzed. However, since the behavioral, molecular, biochemical and general health characterization demonstrated similar phenotypes, only one line for each transgene was included in this study (Thy-1/ApoD-555; NSE/ApoD-182-4). The presence and the number of integrations of the transgene fragment and its transmission through the germline was first verified by Southern blot analysis. Thy-1/ApoD and NSE/ApoD integrated 8 and 12 copies of the corresponding transgene, respectively, as determined by densitometric comparison with copy standards (Fig. 3.1B). Subsequently, H-apoD transgenic (H-apoD Tg) mice were identified by PCR genotyping. Only those mice where the apoD and BGH primers amplified a 0.6 kb band were considered transgenic (Fig. 3.1C).

3.5.2 Expression of human apoD in H-apoD Tg mice

The expression of each transgene was then analyzed in different tissues. By northern blot analysis, H-apoD was found expressed mainly in the nervous system, as expected (Fig. 3.2A). Immunoblotting on total brain extracts confirmed the presence of H-apoD protein in these tissues (Fig. 3.2B). As anticipated, in Thy-1/ApoD mice, H-apoD expression is stronger and is expressed in all brain regions (Gordon *et al.* 1987). The weaker expression in NSE/ApoD mice (Fig. 3.2B) is explained by the

strong expression of this gene in the grey but not in the white matter of the brain (Forss-Peter *et al.* 1990). H-apoD protein was also weakly detected in the liver with a slightly stronger signal in Thy-1/ApoD mice (Fig. 3.2B) but was undetectable in adipose tissue (data not shown). H-apoD protein was also detected in circulation in the plasma (Thy-1/ApoD: 5.35 ± 0.93 μg/ml, NSE/ApoD: 4.69 ± 0.71 μg/ml, as measured by ELISA.

Because of its greater sensitivity, semi-quantitative RT-PCR was also used to analyze the transgene expression. Using H-apoD and internal control HPRT specific primers, we could determine that, in the Thy-1/apoD mice, H-apoD is expressed in all the central nervous system regions tested but at lower levels in spinal cord and in midbrain (Fig. 3.2C). H-apoD expression was also detected in thymus, heart and liver and to a lower extent in ovaries, testis, eyes and blood cells. In NSE/ApoD, H-apoD was detectable in all the nervous system except in the olfactive bulb with a stronger expression in hippocampus, cerebellum and spinal cord. It was also detected in blood cells, muscle, liver and spleen (Fig. 3.2C). H-apoD expression was not observed in white adipose tissue from inguinal and mesenteric fat pads (data not shown). These expression patterns are in full agreement with the promoters used on the transgenes. Even though Thy-1 and NSE promoters were chosen to drive apoD expression into neurons, they are also expressed by other tissues. Thus, human Thy-1 expression was also reported in fibroblasts, myofibroblasts, endothelial cells, smooth muscle cells, renal glomerular mesangial cells, NK cells and a subset of CD34+ cells in the bone marrow, blood and thymus (Craig *et al.* 1993, McKenzie et Fabre 1981, Saalbach *et al.* 1998). In the same way, a NSE expression was already reported in blood and marrow leucocytes (Pechumer *et al.* 1993). NSE expression in the skeletal muscle was unexpected and could be imputed on nerve fascicles running throughout the muscle (Busacchi *et al.* 1999).

3.5.3 H-apoD overexpression has an effect on morphometric, serum and hematological parameters

The two transgenic lines develop and breed normally. They have external phenotype and food and water consumption similar to wild-type (WT) mice at all ages (data not shown). However, some phenotypic differences appeared with aging. One-year-old Thy-1/ApoD and NSE/ApoD mice presented a liver significantly larger than WT mice (30% and 21% respectively). This modification did not significantly affect the total body weight (Table 3.2). It is noteworthy that these transgenic mice express H-apoD in the liver (Fig. 3.2C). Serum parameters of non-fasting mice did reflect some of these differences (Table 3.3). Thus, NSE/ApoD mice presented increased ALT (alanine aminotransferase) and AST (aspartate aminotransferase) levels which are indicative of liver congestion or damage. These increases were not observed in Thy-1/ApoD mice which also present a larger liver (Table 3.2). However, the later showed a slight although not significant increase in alkaline phosphatase which also reflects liver function. In addition, Thy-1/ApoD and NSE/ApoD mice showed elevated serum insulin suggesting insulin resistance. Of note, 3-months-old H-apoD Tg mice did not show hyperinsulinemia (data not shown). Moreover, the hyperinsulinemia was connected with feeding as H-apoD Tg mice displayed normal basal fasting insulin levels (Fig. 3.3C) but developed fed hyperinsulinemia (Table 3.3). Furthermore, NSE/ApoD mice presented high creatinine levels often seen in kidney dysfunction or muscle degeneration (Table 3.3). It is noteworthy that NSE/ApoD mice express the transgene in muscle (Fig. 3.2C). In spite of that, circulating cholesterol, HDL, triglycerides and free fatty acids levels remained unaffected (Table 3.3). Also of note, adipocyte diameter in inguinal fat was similar in the two transgenics and WT mice (data not shown). Blood cell populations were also affected by the H-apoD overexpression in transgenic mice (Table 3.4). H-apoD Tg and especially NSE/ApoD mice presented an elevated leukocyte number (WBC, white blood cells) caused by increased neutrophil and lymphocyte concentrations. In

NSE/ApoD mice, the raised WBC count was also associated with an increased monocyte count. Thy-1/ApoD and NSE/ApoD mice also had an augmented platelet count.

3.5.4 H-apoD Tg mice show glucose intolerance and insulin resistance

The increased fed plasmatic insulin levels in H-apoD Tg mice (Table 3.3) can be related to abnormal glucose homeostasis and we examined this by IPGTT (Fig. 3.3). After intraperitoneal glucose injection to fasting mice, the serum glucose raised significantly in Thy-1/ApoD mice and to a lesser extent in NSE/ApoD mice, compared to WT littermates. The hyperglycemia was sustained up to 120 min in Thy-1/ApoD but was no longer observed at 90 min in NSE/ApoD mice (Fig. 3.3A). The integrated net rise in glucose levels above the fasting levels, calculated as the area under the IPGTT curve (Fig. 3.3B), further demonstrated the glucose intolerance in H-apoD Tg mice. These two transgenic lines also showed increased insulin levels during IPGTT at 30 min after glucose administration (Fig. 3.3C). The increased insulin levels of these two transgenic lines during IPGTT (Fig. 3.3C) suggest that glucose intolerance must be due to the resistance of tissues to the insulin action. The presence of insulin resistance in Thy-1/ApoD and, less importantly, in NSE/ApoD mice was confirmed by the reduced decline of blood glucose after the administration of insulin in ITT (Fig. 3.3D).

3.5.5 H-apoD Tg mice develop hepatic steatosis

Since Thy-1/ApoD and NSE/ApoD mice exhibited hepatomegaly (Table 3.2) and altered levels of indicators of hepatic function (Table 3.3), liver histology was examined. As shown by hematoxylin-eosin and Oil RedO staining, Thy-1/ApoD and NSE/ApoD livers showed severe steatosis (Fig. 3.4B-C, E-F). The steatosis was further confirmed by the quantification of the liver lipid content (Fig. 3.4G). This

steatosis corresponded to an increase in triglycerides but not in total cholesterol levels (Fig. 3.4I-J). However, the lipid peroxidation levels, measured as thiobarbituric acid reactive substances, were similar in WT and H-apoD Tg mice, when normalized by the total lipid content (Fig. 3.4H). Lipid accumulation in muscle was also examined. A mild muscle steatosis appeared in Thy-1/ApoD, and NSE/ApoD mice (data not shown).

3.5.6 Mechanisms of insulin resistance and steatosis

To investigate the mechanisms underlying lipid accumulation impaired glucose tolerance and insulin sensitivity in H-apoD Tg mice, we examined the effect of H-apoD overexpression on lipid metabolism and insulin signaling components in the liver of mice fed ad libitum. Akt is a key molecule downstream of PI3-kinase, which mediates the metabolic activity of insulin. Both Thy-1/ApoD and NSE/ApoD mice exhibited a 40% decrease in Akt phosphorylation at Ser473 in liver (Fig. 3.5A). All tissues were collected in the early morning, which may explain the high pAkt levels. Hepatic steatosis can be caused by a decrease in lipid secretion. Apolipoprotein E (apoE) deficiency was already associated with the development of hepatic steatosis because of impairment in very low density lipoprotein (VLDL)-triglyceride secretion (Mensenkamp *et al.* 2001). Only NSE/ApoD mice showed differences in this process with a 30% decrease of apoE transcription (Fig. 3.5C). The rate of plasma triglyceride accumulation in fasting mice after intravenous injection of Triton WR1339 was also measured. The VLDL-triglyceride secretion rate, calculated from the slope of each individual lines, was not statistically different (Fig. 3.5I).

Mice with hepatic steatosis also exhibited significantly increased expression of liver-specific fatty acid binding protein (LFABP), fatty acid synthase (FAS), peroxisome proliferator-activated receptor gamma (PPARγ) and sterol regulatory element binding protein-1c (SREBP-1c), providing evidence that lipogenesis is

stimulated in these mice (Fig. 3.5D-G). Peroxisome proliferator-activated receptor alpha (PPARα), which is involved in the lipid beta oxidation pathway, was also stimulated in these mice (Fig. 3.5H). Muscle tissue also plays an important role in glucose metabolism and thus, the Akt phosphorylation at Ser473 was also tested in this tissue. As in the liver, phosphorylation of Akt was inhibited by 60% in Thy-1/ApoD and by 40% in NSE/ApoD mice (Fig. 3.5B).

High serum levels of cytokines and adipokines were previously reported in insulin resistance and steatosis and the modulation of leukocyte counts in H-apoD Tg mice could have predict an immune response. Interestingly, H-apoD Tg mice displayed similar or even decreased levels of most of the cytokines tested compared with WT mice (Fig. 3.1S). The circulating levels of the adipokines leptin, adiponectin and resistin were also measured. Only leptin showed variations in its levels with a 2-fold increase in NSE/ApoD mice (Fig. 3.1S).

3.6 Discussion

Since its isolation from HDL particles in 1976 (McConathy and Alaupovic 1976), apoD was reported associated with many processes. However, the precise physiological function(s) of this protein still remains unclear. Some beneficial roles were assigned to apoD. ApoD is thought to be involved in the regeneration and reinnervation processes after nervous tissue injury (Boyles *et al.* 1990a, Ong *et al.* 1999, Rickhag *et al.* 2006, Terrisse *et al.* 1999). In addition, apoD has been described as a marker of differentiation and good prognosis in cancer (Diez-Itza *et al.* 1994). It also plays a protective role in stress situations (Ganfornina *et al.* 2008, Sanchez *et al.* 2006, Walker *et al.* 2006). Paradoxically, apoD was also associated with neuronal death (Franz *et al.* 1999), oxidative stress (Alvarez *et al.* 2003) and tumor progression (Ryu *et al.* 2001).

In order to gain insight into some aspects of the apoD function, we generated two transgenic mice lines overexpressing H-apoD. Here, we demonstrate that overexpression of H-apoD driven by neuronal promoters in mice results in an interesting, although not entirely anticipated alteration of the glucose/insulin metabolism. More precisely, the presence of H-apoD amplifies the insulin resistance that occurs with aging, as 3 months-old mice have similar insulin levels independently of genotype. This was first suggested by elevated insulin plasma concentration in non-fasting one-year-old mice and explored by IPGTT and ITT. The results show that, although H-apoD Tg mice are not obese and present normal food intake and normal lipid levels in circulation, they develop glucose intolerance and insulin resistance with aging. This insulin resistance is associated with lipid accumulation in the liver, where it causes hepatomegaly, as evidenced by histology and abnormal liver function parameters in serum. A strong connection between lipid accumulation in liver and insulin resistance was already reported (Kraegen *et al.* 2001).

The slight H-apoD expression in the liver might contribute to fat, predominantly triglycerides, accumulation and insulin resistance. Being a secreted protein, and expressed namely by blood cells, H-apoD was found circulating in the plasma and thus, it could also account for lipid accumulation in the liver. Accumulation of lipids in the liver is generally multifactorial.

One possible mechanism is the trapping of arachidonic acid, a well-known apoD ligand, or other fatty acids by H-apoD, therefore creating an imbalance favoring fat accumulation versus its elimination by the liver. In addition, given that polyunsaturated fatty acids can inhibit SREBP-1c expression (Yoshikawa *et al.* 2002), the trapping of fatty acids by H-apoD could support the activation of SREBP-1c expression induced by insulin resistance and thus favor lipid accumulation in the liver. Another potential source of lipid accumulation is an increase in the hepatic lipid uptake, but this seems unlikely as the circulating free fatty acids, triglycerides, cholesterol and HDL levels are similar in all mice. Still, we cannot rule out an increased transport of lipids towards the liver by the circulating H-apoD because of the potential apoD participation in lipid transfer and reverse cholesterol transport (Patel *et al.* 1997, Steyrer *et al.* 1988). A defect in lipid oxidation can also be involved in lipid accumulation. However, since the levels of PPARα, known to control the expression of many genes involved in lipid oxidation, are increased in Thy-1/ApoD and NSE/ApoD mice, probably as a compensatory mechanism, it seems unlikely that defective lipid oxidation is the cause of liver steatosis. Moreover, lipid accumulation can result from decreased removal of lipids from the liver. ApoE is essential for VLDL-triglyceride synthesis and secretion, a main pathway of lipid elimination in the liver and apoE deficiency promotes the development of hepatic steatosis (Mesenkamp *et al.* 2001). The decreased apoE expression in NSE/ApoD mice suggested that an impaired lipid secretion might account for liver steatosis in these mice. However, this possibility was ruled out, as the VLDL-triglyceride secretion rate after Triton WR1339 administration was similar in H-ApoD Tg and

WT mice. Together with the fact that the decrease in apoE transcription was absent in Thy-1/ApoD mice, this suggests that the apoE modulation unlikely results from H-apoD overexpression but could be related to another lipid-associated event and is then of low pathologic importance. More likely, the mechanism for hepatic steatosis development resides in an enhanced de novo lipogenesis by hepatocytes as LFABP, FAS, SREBP-1c and PPARγ transcripts are overexpressed. Given that Thy-1/ApoD mice showed the strongest H-apoD expression in brain as well as the strongest insulin resistance, and given that, although weak, the H-apoD levels in the liver of these mice were superior to the ones in NSE/ApoD mice, we expected these mice to have a greater hepatic steatosis. The surprisingly similar levels of fat accumulation in the liver of both lines of H-apoD Tg mice suggests that the apoD effect on lipid accumulation is subjected to a tight regulation. Still, the connection between H-apoD expression in the liver and liver steatosis is not clear and requires further examination.

The nature of the connection between steatosis and insulin resistance remains unclear. The accumulation of lipid metabolites such as ceramides, diacylglycerol or long chain acyl-CoA, inside skeletal muscle and liver, results in the downregulation of insulin signaling and therefore in insulin resistance (Schinner *et al.* 2005). Phosphorylation on serine 473 of Akt, a key event of the insulin-signaling pathway, is decreased in liver and in muscles of NSE/ApoD and Thy-1/ApoD mice. This confirms the involvement of impaired insulin signaling in apoD-induced insulin resistance. Counteracting mechanisms may explain the lower insulin resistance of NSE/ApoD mice. These mice show insulin-signaling (pAkt) impairment both in liver and muscles. However, as these processes would predict a strong insulin resistance, they may be tempered by the increased circulating leptin, which promotes lipid oxidation.

Several studies also suggest a link between oxidative stress and insulin resistance. Indeed, intracellular accumulation of fatty acid metabolites contributes to the production of reactive oxygen species (ROS). ROS contribute to hepatic insulin resistance through the activation of PKCs (Schinner *et al.* 2005). They also attack polyunsaturated fatty acids and initiate lipid peroxidation. However, although H-apoD Tg mice featured hepatic steatosis, their lipid peroxidation levels were not increased. This suggests on one hand, that oxidative stress is not the cause of insulin resistance and on the other, that H-apoD prevents the oxidative stress caused by lipid accumulation. ApoD was already reported to play a protective role in oxidative stress situations (Ganfornina *et al.* 2008, Sanchez *et al.* 2006, Walker *et al.* 2006).

In addition, insulin resistance in humans is associated with chronic low-grade inflammation (Pacifico *et al.* 2006, Tilg *et al.* 2008). Whether inflammation causes insulin resistance or is an epiphenomenon of fat accumulation is still unknown. In this perspective, increased leukocyte counts in Thy-1/ApoD and NSE/ApoD mice predicted higher serum cytokines levels. The absence of upregulation of most of the cytokines tested would be in agreement with previous studies suggesting that apoD may have anti-inflammatory properties as its expression is upregulated in response to inflammatory stimuli (Blais *et al.* 1994, Do Carmo *et al.* 2007, 2008). However, the presence of inflammation cannot be completely excluded.

It is also noteworthy that H-apoD is primarily expressed in neurons and that H-apoD levels are directly correlated with the incidence of insulin resistance, as Thy-1/ApoD mice are more insulin resistant than NSE/ApoD mice. H-apoD could interfere directly with leptin or insulin receptors in the arcuate (ARC), paraventricular (PVH) and other hypothalamic nuclei. ApoD is involved in the leptin receptor signal transduction pathway that controls appetite and body fat accumulation. It interacts specifically with the cytoplasmic portion of the long form of the leptin receptor, Ob-Rb. In hypothalamus, apoD transcription is stimulated by dietary fat and correlates

positively with adipose tissue mass and circulating leptin levels. However, this positive association is lost in mice carrying a mutant leptin or Ob-Rb gene, in which levels of hypothalamic apoD mRNA are reduced compared to those of WT mice (Liu *et al.* 2001). H-apoD overexpression in the ARC or PVH could cause a partial desensibilization of the leptin receptor leading to a leptin resistance and further to an insulin resistance. However, as H-apoD Tg mice do not show increased weight gain or hyperphagia, a downregulation of the leptin pathway seems unlikely. Still, the presence of H-apoD in neurons could interfere with the central regulation of insulin sensitivity.

Apart from lipid accumulation, H-apoD Tg mice display other insulin-resistance-associated features such as abnormal hematological parameters. Therefore, in H-apoD Tg mice, insulin resistance is associated with abnormal leukocyte and platelet concentration in blood. Hematological abnormalities are often associated with insulin resistance in humans and an increased leukocyte count, particularly T cells, was associated with the progression of atherosclerosis (Tanigawa *et al.* 2004). It was also reported that human platelets have insulin receptors that participate in the regulation of platelet function. Insulin resistance, and its associated hyperinsulinemia, promotes platelet activation, thus increasing the risk of cardiovascular disease.

In conclusion, these results pinpoint to the importance of a complex regulation of apoD levels and sites of expression, which may influence apoD function and its impact on glucose and lipid metabolism. Consequently, these results bring new evidence for apoD as a potential target for glucose and lipid metabolism related disorders. However, the molecular basis for the apoD role in steatosis and insulin resistance, as well as its contribution to other components of the metabolism control such as energy expenditure and response to high-fat diet have yet to be defined.

3.7 Acknowledgments

We are thankful to Diego Sanchez, Maria D. Ganfornina and Louise Brissette for helpful discussions. We thank Marie Trudel for advises with the transgenic mice. This work was supported by a Canadian Institutes for Health Research Grant (MOP-15677). DF was supported by FCAR and NSERC studentships. SDC was supported by FRSQ, NSERC and UQAM studentships.

Table 3.1: Primers used in semi-quantitative RT-PCR.

Gene	Forward primer	Reverse primer
Human apoD	TGC AGG AGA ATT TTG ACG TG	AGG TTA ACT GGG GTG GCT TC
PPAR α	CAT GTG AAG GCT GTA AGG GCT T	TCT TGC AGC TCC GAT CAC ACT
PPAR γ	CTG CTC AAG TAT GGT GTC CAT GA	TGA GAT GAG GAC TCC ATC TTT ATT CA
FAS	TAC CAA GCC AAG CAC ATT CG	TGG CTT CGG CGA TGA GA
LFABP	AAG TCA AGG CAG TCG TCA AGC T	TGA GTT CAG TCA CGG ACT TTA TGC
SREBP-1c	TGG ATT GCA CAT TTG AAG ACA TG	TGT CTC ACC CCC AGC ATA GG
HPRT	GTG ATG AAG GAG ATG GGA GGC C	GGT GAA AAG GAC CCC ACG AAG

Table 3.2: Morphometric parameters of H-apoD Tg mice and WT littermates.

	WT	Thy-1/ApoD	NSE/ApoD
Body weight (g)	38.95 ± 4.57	44.06 ± 5.42	43.83 ± 4.16
Body lenght (cm)	9.86 ± 0.40	10.11 ± 0.36	10.00 ± 0.18
Body mass index (g/cm2)	0.40 ± 0.03	0.43 ± 0.05	0.44 ± 0.04
Weights of tissue (g/g of body weight, x 100)			
Brain	1.07 ± 0.08	0.97 ± 0.08	0.96 ± 0.07
Liver	4.03 ± 0.58	5.24 ± 0.68 **	4.91 ± 0.73 *
Inguinal fat	4.87 ± 1.54	4.40 ± 0.68	5.19 ± 0.90
Mesenteric fat	5.26 ± 1.01	4.77 ± 0.83	5.37 ± 0.95
Epididymal fat	0.88 ± 0.26	0.82 ± 0.23	0.68 ± 0.31

Data are means ± SE of 12 mice per group. * $p<0.05$, ** $p<0.01$ vs WT mice.

Table 3.3: Serum parameters in non-fasting H-apoD Tg mice and WT littermates.

	WT	Thy-1/ApoD	NSE/ApoD
Total protein (g/L)	52.20 ± 4.09	52.33 ± 5.16	55.40 ± 11.61
Albumin (g/L)	27.40 ±7.50	27.83 ± 6.71	30.20 ± 8.47
Glucose (mmol/L)	10.90 ± 0.75	12.52 ± 3.44	11.28 ± 2.95
Insulin (ng/ml)	1.44 ± 0.37	3.15 ± 0.56 ***	2.32 ± 0.37 *
BUN urea (mmol/L)	8.28 ± 1.01	7.98 ± 1.79	7.62 ± 1.09
Creatinine (μmol/L)	13.33 ± 0.58	15.33 ± 5.13	17.67 ± 2.52 **
Total bilirubin (μmol/L)	2.92 ± 0.94	2.82 ± 1.48	3.56 ± 1.36
ALT (U/L)	39.00 ± 1.00	38.00 ± 2.65	72.00 ± 26.29 *
AST (U/L)	86.00 ± 20.88	78.67 ± 2.08	173.67 ± 65.26 *
Alkaline phosphatase (U/L)	82.40 ± 14.96	120.80 ± 62.50	73.00 ± 29.51
Creatine kinase (U/L)	85.33 ± 47.51	102.67 ± 27.01	94.00 ± 49.12
Cholesterol (mmol/L)	2.98 ± 0.36	3.13 ± 0.63	4.25 ± 1.98
HDL (mmol/L)	2.42 ± 0.31	2.60 ± 0.63	3.07 ± 1.57
Triglycerides (mmol/L)	1.15 ± 0.31	1.71 ± 0.89	1.14 ± 0.50
Free fatty acids (mmol/L)	0.63 ± 0.38	0.65 ± 0.16	0.69 ± 0.28

ALT, alanine aminotransferase; AST, aspartate aminotransferase; HDL, high density lipoprotein. Data are means ± SE of 6 mice per group. * $p<0.05$, ** $p<0.01$, *** $p<0.001$ vs WT mice.

Table 3.4: Hematological parameters in H-apoD Tg mice and WT littermates.

	WT	Thy-1/ApoD	NSE/ApoD
Hemoglobin (g/L)	123.50 ± 9.19	123.50 ± 13.44	133.00 ± 7.07
RBCs (x 10^{12}/L)	8.07 ± 0.18	8.31 ± 1.01	8.28 ± 0.14
WBCs (x 10^9/L)	3.75 ± 0.21	4.75 ± 0.35 ***	6.65 ± 1.06 ***; ◇◇
Neutrophils (x 10^9/L)	0.42 ± 0.34	0.87 ± 0.33 *	0.93 ± 0.05 **
Lymphocytes (x 10^9/L)	3.27 ± 0.16	3.59 ± 0.30 *	4.99 ± 0.37 ***; ◇◇◇
Monocytes (x 10^9/L)	0.02± 0.03	0.05 ± 0.06	0.11 ± 0.06 **
Eosinophils (x 10^9/L)	0.04 ± 0.06	0.26 ± 0.22	0.64 ± 0.57
Platelets (x 10^9/L)	747.00 ± 241.83	1139.00 ± 53.74 **	1203.00 ± 205.06 **

RBC, red blood cells, WBC, white blood cells. Data are means ± SE of 6 mice per group.
* $p<0.05$, ** $p<0.01$, *** $p<0.001$ vs WT mice. ◇◇ $p<0.01$, ◇◇◇ $p<0.001$ vs Thy-1/ApoD mice

3.8 Figure legends

Figure 3.1: Structure of the H-apoD transgene and analysis of transgenic mice. A) The promoter/enhancer region (open box) of the Thy-1 or Neuron Specific Enolase (NSE) genes were fused to the H-apoD coding sequence (black) followed by the bovine growth hormone (BGH) polyadenylation signal (grey). B: BamHI, H: HindIII, K: KpnI, RI: EcoRI, S/X: SalI/XhoI, X: XbaI. The transgenes were excised by digestion with EcoRI/XhoI (Thy-1/ApoD; 4,5 Kbp) or EcoRI/KpnI (NSE/ApoD; 3 Kbp). B) Southern analysis of transgenic mice. BamHI-digested genomic DNA (10 μg) was analyzed using the corresponding transgene as a probe. Copy standards (left) corresponding to 1 (1c) or 10 (10c) copies of the transgenes are used to estimate the transgene copy number. C: Representative PCR genotyping of the mice. A band (0.6 kbp) is amplified with H-apoD and BGH primers in the two transgenic, but not in WT mice.

Figure 3.2: Analysis of the transgene expression. A) Northern blot analysis of total RNA with a H-apoD specific probe. Equal loading was determined by subsequent hybridization with a GAPDH probe. H-apoD is mainly expressed in the CNS. B) Immunoblot showing H-apoD protein expression in the transgenic brains and livers. An anti-GAPDH polyclonal antibody was used for normalization. C) Semi-quantitative RT-PCR analysis of different tissues with H-apoD specific primers. HPRT amplification was used as an internal control. Medulla: medulla oblongata. Muscle: skeletal muscle. Results are representative of three separate experiments.

Figure 3.3: In vivo analysis of glucose tolerance and insulin sensitivity. A) Blood glucose levels during the intraperitoneal glucose tolerance test (IPGTT), demonstrating the hyperglycemic response to the load in Thy-1/ApoD and NSE/ApoD transgenic mice (2 g/kg body weight on 12-15h fasting animals). B) Net glucose release above basal levels quantified by the integration of the area under the

curve during IPGTT. C) Insulin concentration at 0 and 30 min during IPGTT showing hyperinsulinemia in Thy-1/ApoD and NSE/ApoD transgenic mice. D) Glucose levels during an intraperitoneal insulin tolerance test (ITT; 1.5 U/kg body weight on 5h fasting animals) showing insulin resistance in Thy-1/ApoD and NSE/ApoD transgenic mice. Data are expressed as percentage of initial blood concentration. Values are means ± SE of 6 mice per group. * $p<0.05$, ** $p<0.01$, *** $p<0.001$ of Thy/ApoD vs WT mice. # $p<0.05$, ## $p<0.01$, ### $p<0.001$ of NSE/ApoD vs WT mice.

Figure 3.4: Hepatic steatosis in H-apoD Tg mice. A-C) Hematoxylin-eosin stained liver paraffin sections. D-F) Oil RedO staining of cryosected liver. Photomicrographs show normal histology in WT mice (A, D) and strong lipid accumulation in Thy-1/ApoD (B, E) and NSE/ApoD (C, F). Original magnification, x 100; n=6. Hepatic total lipid content (G), lipid peroxidation (H), total cholesterol (I) and triglycerides (J) levels in transgenic and WT mice. Values are means ± SE of 6 mice per group. *** $p<0.001$ vs WT mice.

Figure 3.5: Analysis of hepatic steatosis and insulin resistance pathways. Total liver (A) or muscle (B) extracts from non-fasting animals were subjected to immunoblot analysis with anti-Ser473-phospho-specific Akt antibody and anti-Akt1 antibody. Graphs were normalized by Akt1 levels. C) Northern blot analysis of apoE expression in liver tissues of H-apoD Tg and WT mice. ApoE expression was normalized by GAPDH levels. Steatosis is associated with enhanced LFABP (D), FAS (E), PPARγ (F), SREBP-1c (G) and PPARα (H) transcription in Thy-1/ApoD and NSE/ApoD mice as explored by semi-quantitative RT-PCR. Gene levels were normalized by HPRT expression. For each graph, the H-apoD Tg values were normalized by the WT values, which was given an arbitrary value of one. A-H) Values are means ± SE of 6 mice per group. * $p<0.05$, ** $p<0.01$, *** $p<0.001$ vs WT mice. I) Plasma triglyceride production rates were measured in fasting H-apoD

Tg and WT mice after Triton WR1339 injection. Data represent mean triglyceride concentrations (in mM) ± SE, n = 5 per group. The VLDL-triglyceride secretion rate, calculated from the slope of each individual line, was not statistically different (WT: 53,04 ± 5,69; Thy-1/ApoD: 39,0 ± 2,47; NSE/ApoD: 45,0 ± 4,64 μmol/kg/h).

Figure 3.1

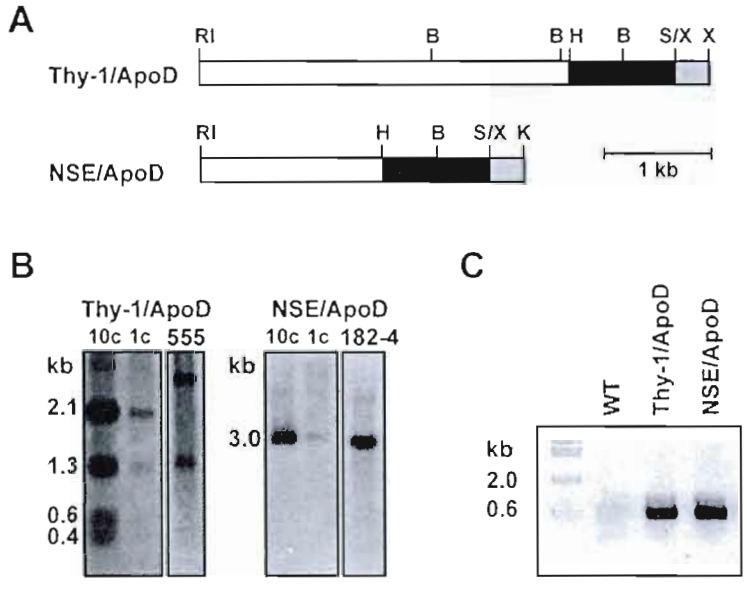
A
RI
B
B H
B
S/X X
Thy-1/ApoD
RI
H
B
S/X K
NSE/ApoD
1 kb
B
Thy-1/ApoD
10c 1c 555
NSE/ApoD
10c 1c 182-4
kb
2.1
1.3
0.6
0.4
kb
3.0
C
WT
Thy-1/ApoD
NSE/ApoD
kb
2.0
0.6

Figure 3.2

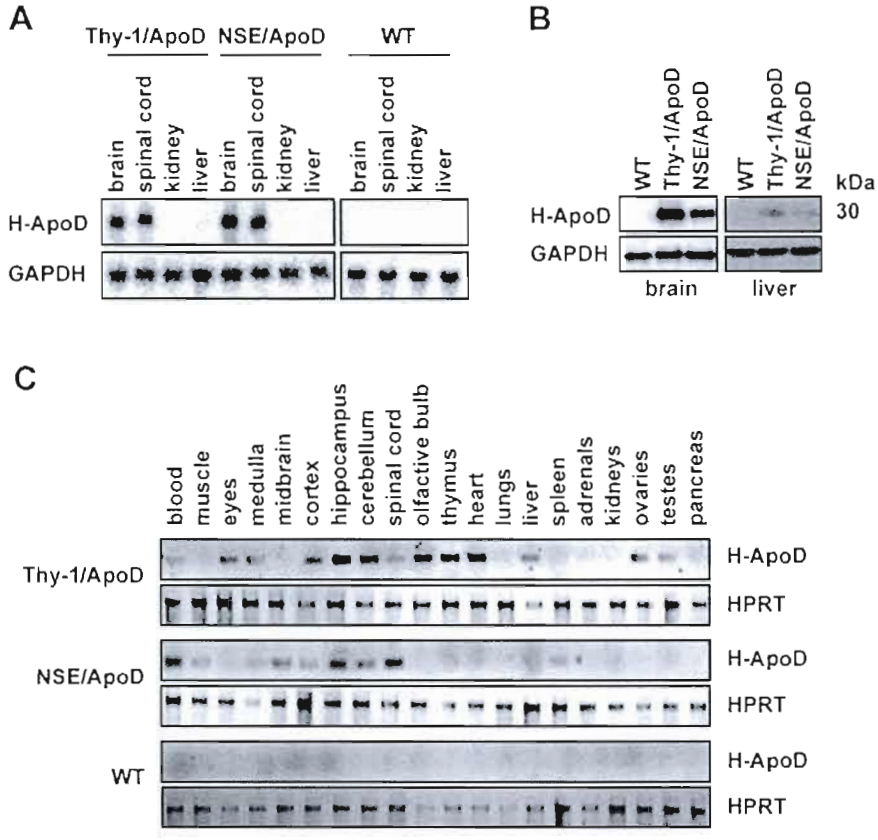
A
Thy-1/ApoD
NSE/ApoD
WT
brain
spinal cord
kidney
liver
H-ApoD
GAPDH
B
WT
Thy-1/ApoD
NSE/ApoD
kDa
30
H-ApoD
GAPDH
brain
liver
C
blood
muscle
eyes
medulla
midbrain
cortex
hippocampus
cerebellum
spinal cord
olfactive bulb
thymus
heart
lungs
liver
spleen
adrenals
kidneys
ovaries
testes
pancreas
Thy-1/ApoD
NSE/ApoD
WT
H-ApoD
HPRT

Figure 3.3

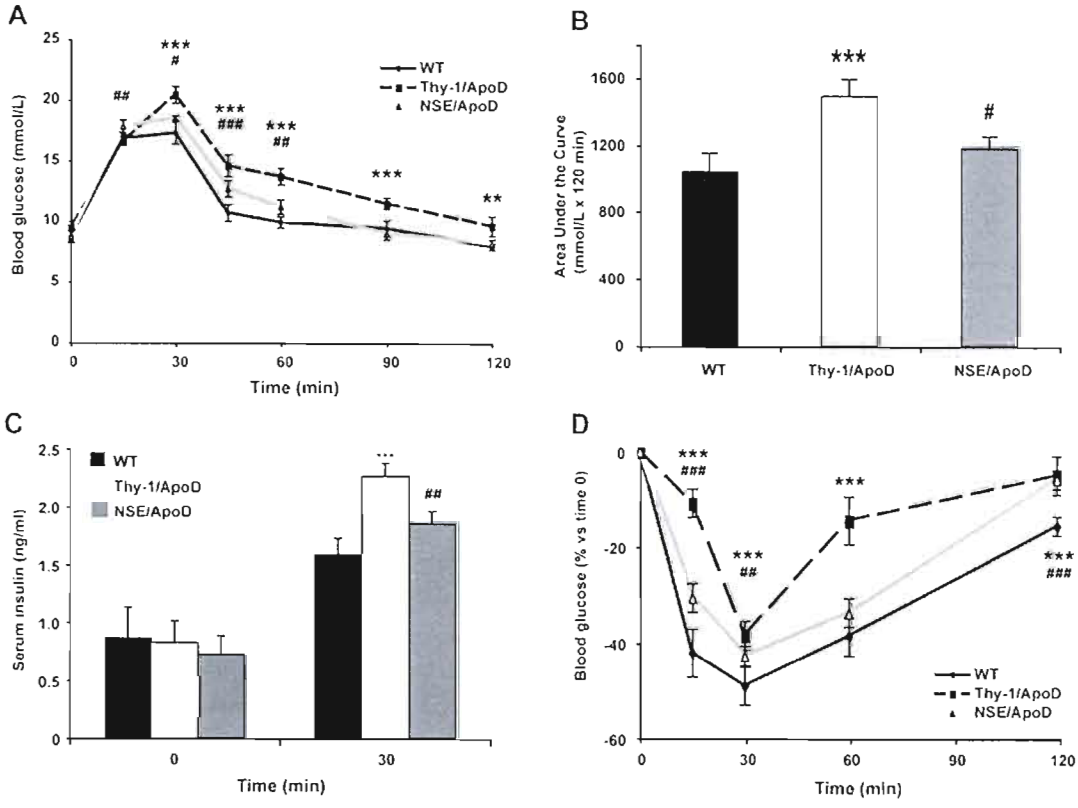
A
Blood glucose (mmol/L)
Time (min)
WT
Thy-1/ApoD
NSE/ApoD
B
Area Under the Curve (mmol/L x 120 min)
WT
Thy-1/ApoD
NSE/ApoD
C
Serum insulin (ng/ml)
Time (min)
WT
Thy-1/ApoD
NSE/ApoD
D
Blood glucose (% vs time 0)
Time (min)
WT
Thy-1/ApoD
NSE/ApoD

Figure 3.4

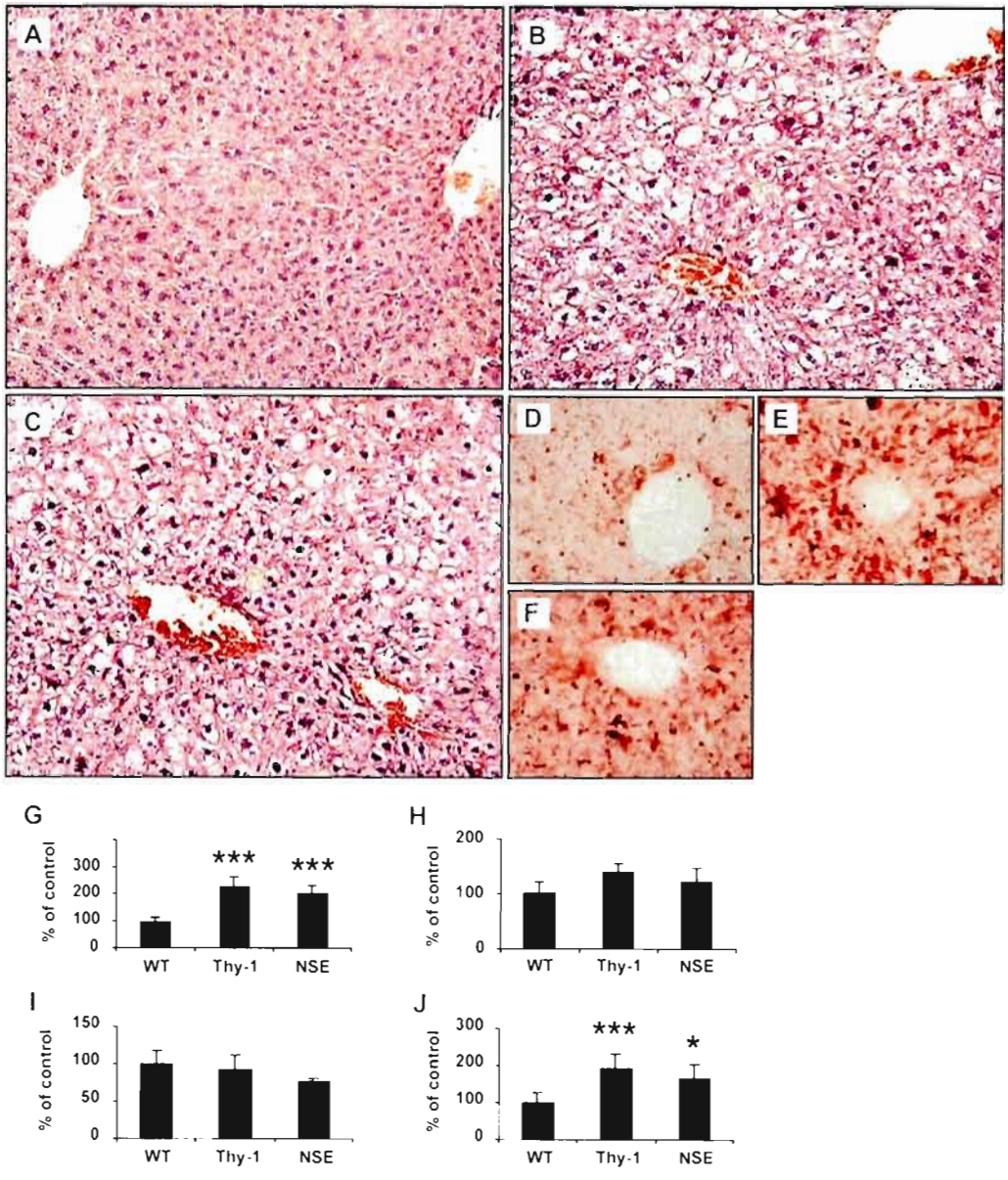
A
B
C
D
E
F
G
% of control
300
200
100
0
***
***
WT
Thy-1
NSE
H
% of control
200
100
0
WT
Thy-1
NSE
I
% of control
150
100
50
0
WT
Thy-1
NSE
J
% of control
300
200
100
0
***
*
WT
Thy-1
NSE

Figure 3.5

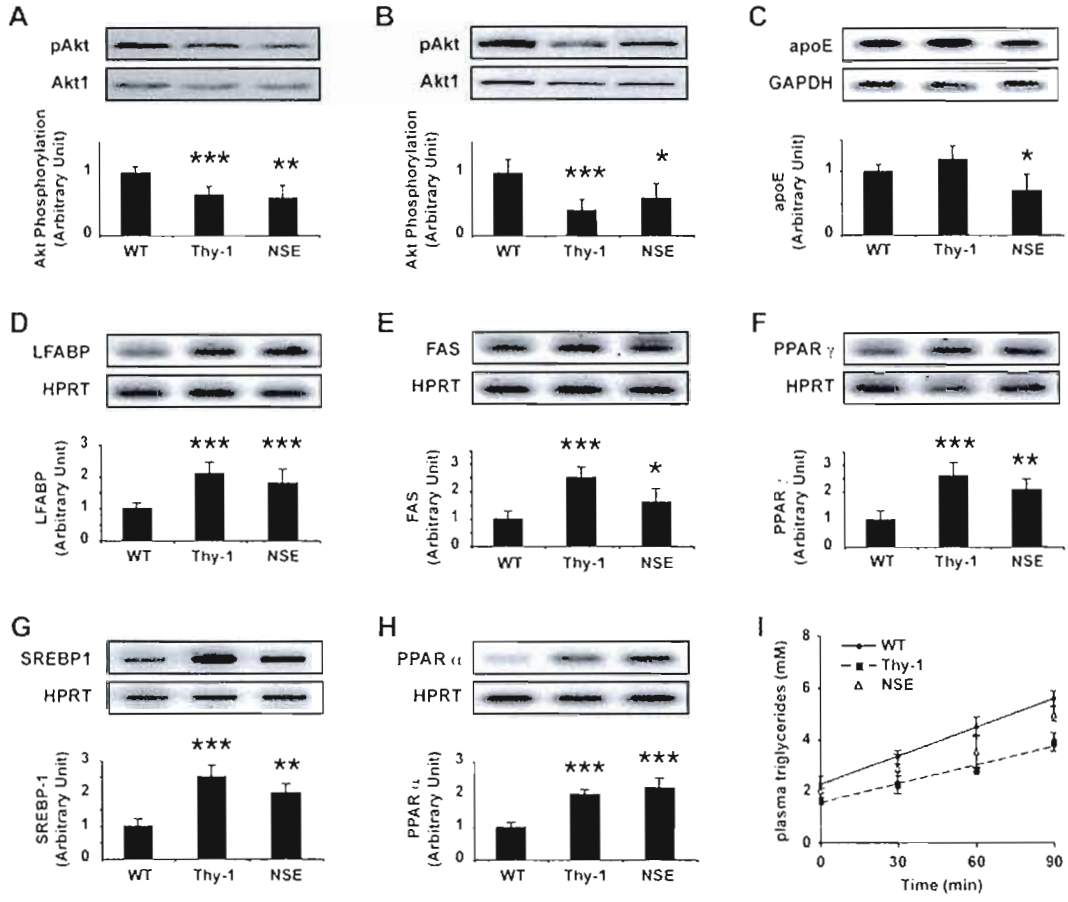
A
pAkt
Akt1
Akt Phosphorylation (Arbitrary Unit)
***
**
WT
Thy-1
NSE
B
pAkt
Akt1
Akt Phosphorylation (Arbitrary Unit)
***
*
WT
Thy-1
NSE
C
apoE
GAPDH
apoE (Arbitrary Unit)
*
WT
Thy-1
NSE
D
LFABP
HPRT
LFABP (Arbitrary Unit)
***
***
WT
Thy-1
NSE
E
FAS
HPRT
FAS (Arbitrary Unit)
***
*
WT
Thy-1
NSE
F
PPAR γ
HPRT
PPAR γ (Arbitrary Unit)
***
**
WT
Thy-1
NSE
G
SREBP1
HPRT
SREBP-1 (Arbitrary Unit)
***
**
WT
Thy-1
NSE
H
PPAR α
HPRT
PPAR α (Arbitrary Unit)
***
***
WT
Thy-1
NSE
I
WT
Thy-1
NSE
plasma triglycerides (mM)
Time (min)
0
30
60
90

3.9 Supplemental material

Figure 3.1S : Serum levels of cytokines and adipokines in transgenic and WT mice. Interleukin-1α, interleukin-6 and -10, TNFα, IFNγ, TGFβ, leptin, adiponectin and resistin concentrations were tested by Searchlight arrays. Values are means ± SE of 6 mice per group. * $p<0.05$, ** $p<0.01$ vs WT mice.

Figure 3.1S

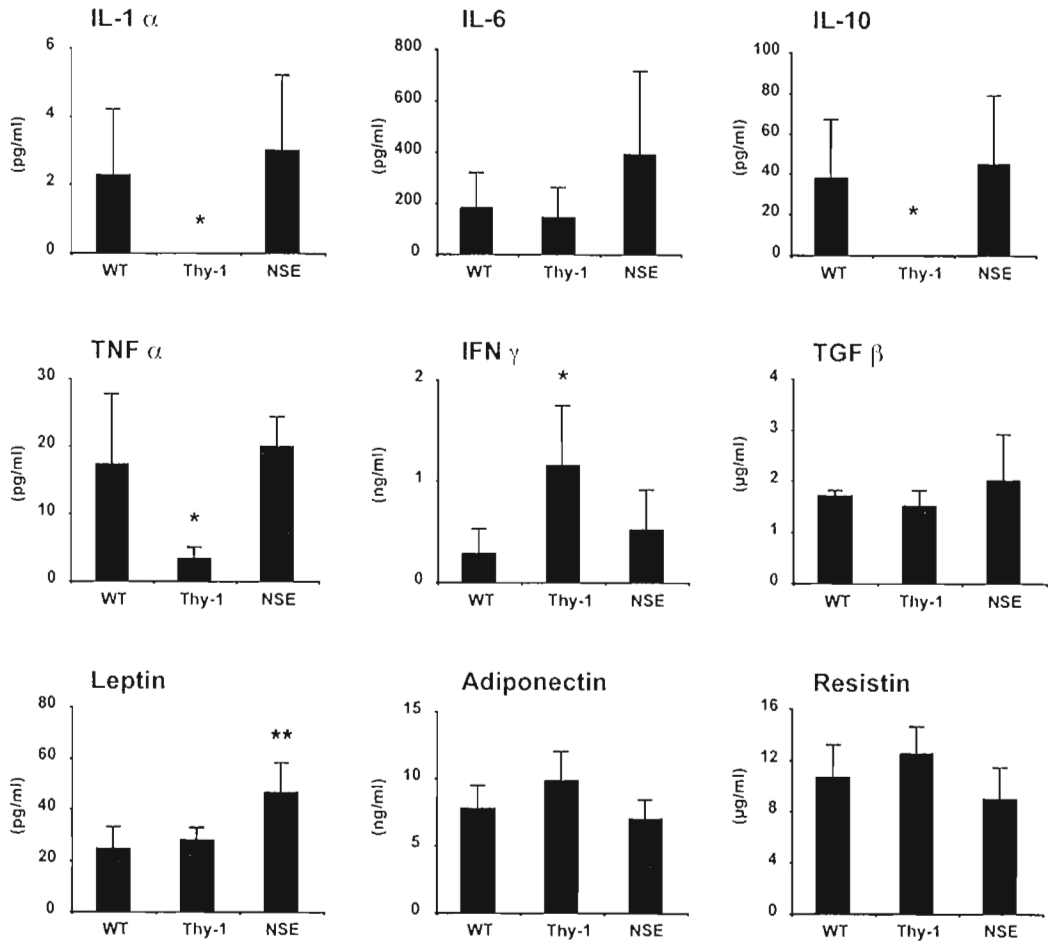
IL-1 α
(pg/ml)
6
4
2
0
*
WT
Thy-1
NSE
IL-6
(pg/ml)
800
600
400
200
0
WT
Thy-1
NSE
IL-10
(pg/ml)
100
80
60
40
20
0
*
WT
Thy-1
NSE
TNF α
(pg/ml)
30
20
10
0
*
WT
Thy-1
NSE
IFN γ
(ng/ml)
2
1
0
*
WT
Thy-1
NSE
TGF β
(µg/ml)
4
3
2
1
0
WT
Thy-1
NSE
Leptin
(pg/ml)
80
60
40
20
0
**
WT
Thy-1
NSE
Adiponectin
(ng/ml)
15
10
5
0
WT
Thy-1
NSE
Resistin
(µg/ml)
16
12
8
4
0
WT
Thy-1
NSE

CHAPITRE IV

Apolipoprotein D is involved in the mechanisms regulating protection from oxidative stress

Maria D. Ganfornina*, Sonia Do Carmo*, Jose M. Lora, Sonia Torres-Schumann, Marci Vogel, Maria Allhorn, Constancio González, Michael J. Bastiani, Eric Rassart, Diego Sanchez

2008

Aging Cell 7: 506-515

*Ces auteurs ont contribué de façon équivalente à ce travail.

Avant-propos

L'étude *in vitro* présentée en chapitre II nous a permis de déterminer que l'induction de l'apoD lors de pathologies est sans doute initiée par un événement spécifique. Le stress oxydatif est l'une des conditions capables d'induire l'expression de l'apoD. De plus, le stress oxydatif est intimement lié à la plupart des neuropathologies présentant une induction de l'apoD. Afin de comprendre pourquoi l'apoD est induite dans certaines pathologies, nous avons donc décidé d'étudier, dans un premier temps, l'importance de l'apoD en situation normale et dans un contexte neurodégénératif induit par un produit oxydant, le paraquat. Pour ce faire, nous avons injecté du paraquat de façon intrapéritonéale à des souris n'exprimant pas (ApoD-KO) ou surexprimant l'apoD humaine dans leurs neurones sous le contrôle du promoteur du gène Thy-1 humain (HApoD-Tg). Nous avons ainsi examiné l'influence de l'apoD sur la survie des souris et sur la peroxydation lipidique suite à l'administration de paraquat. Puis nous avons étudié l'influence du paraquat sur l'induction de l'apoD.

L'herbicide paraquat (dichlorure de 1,1'-diméthyl-4,4'-bipyridinium) a été établi comme facteur de risque potentiel pour le développement de la maladie de Parkinson, l'une des neuropathologies présentant une augmentation de l'apoD. Le lien entre le paraquat et la maladie de Parkinson est basé à la fois sur les études épidémiologiques qui lient le parkinsonisme et l'exposition à cet agent et sur la similarité de sa structure chimique avec le MPTP (1-methyl-4-phenyl-1,2,3,6-tetrahydropyridine). Il a été démontré que les utilisateurs du substitut d'héroïne MPTP développaient la maladie de Parkinson. Le paraquat génère un stress oxydatif par la production de radicaux d'oxygène libres. Ces radicaux superoxydes réagissent avec les lipides membranaires insaturés, tuant ainsi les neurones dopaminergiques par apoptose. La voie des JNK (c-jun-N-terminal kinase) serait impliquée dans cette mort

par apoptose (Peng *et al.* 2004). Bien qu'il n'existe pas d'études liant le paraquat et l'expression de l'apoD, il a été largement utilisé comme modèle neurodégénératif.

J'ai contribué à toutes les facettes de cette étude. J'ai participé à l'élaboration du design expérimental, au travail pratique et à l'élaboration des figures et du manuscrit. Plus particulièrement, j'ai fait le travail concernant les souris transgéniques surexprimant l'apoD humaine. J'ai donc étudié leur comportement en situations normales puis j'ai déterminé leur survie et leur niveau de peroxydation lipidique suite à l'injection de différentes doses de paraquat. J'ai également fait le travail (northerns) concernant l'induction de l'apoD suite à l'administration de paraquat. Maria D. Ganfornina et Diego Sanchez ont été les initiateurs de cette étude et ont fait toutes les expériences sur les souris ApoD-KO dans les locaux de Constancio González. Jose M. Lora, Sonia Torres-Schumann, Marci Vogel et Maria Allhorn ont été impliqués dans la création et la caractérisation des souris ApoD-KO dans le laboratoire de Michael J. Bastiani.

4.1 Résumé

Plusieurs pathologies du système nerveux sont associées avec une augmentation des niveaux de l'Apolipoprotéine D (ApoD), une lipocaline également exprimée durant le développement normal et le vieillissement. Un homologue du gène de l'ApoD chez la drosophile, Glial Lazarillo, régule la résistance au stress et la neurodégénérescence du cerveau âgé. Nous étudions ici pour la première fois le potentiel protecteur de l'ApoD chez un organisme modèle vertébré. La perte fonctionnelle de l'ApoD chez la souris augmente la sensibilité au stress oxydatif et le niveau de peroxydation lipidique dans le cerveau et altère les capacités locomotrices et d'apprentissage. La surexpression de l'ApoD humaine dans le cerveau de souris produit les effets inverses, augmentant la survie et prévenant l'accumulation de lipides peroxydés après le traitement oxydant. Ces observations, conjointement avec l'augmentation de la transcription de l'ApoD dans le cerveau après une lésion oxydative, identifient l'ApoD comme une protéine de phase aiguë ayant une fonction protectrice et donc bénéfique médiée par le contrôle des lipides peroxydés.

Mots-clés : apprentissage, comportement locomoteur, lipocaline, paraquat, peroxydation lipidique, stress oxydatif.

4.2 Abstract

Many nervous system pathologies are associated with increased levels of Apolipoprotein D (ApoD), a lipocalin also expressed during normal development and aging. An ApoD homologous gene in Drosophila, Glial Lazarillo, regulates resistance to stress, and neurodegeneration in the aging brain. Here we study for the first time the protecting potential of ApoD in a vertebrate model organism. Loss of mouse ApoD function increases the sensitivity to oxidative stress and the levels of brain lipid peroxidation, and impairs locomotor and learning abilities. Human ApoD over-expression in the mouse brain produces opposite effects, increasing survival and preventing the raise of brain lipid peroxides after oxidant treatment. These observations, together with its transcriptional up-regulation in the brain upon oxidative insult, identify ApoD as an acute response protein with a protective and therefore beneficial function mediated by the control of peroxidated lipids.

Keywords: learning, locomotor ability, lipocalin, paraquat, lipid peroxidation, oxidative stress.

4.3 Introduction

Apolipoprotein D (ApoD) is a Lipocalin, an ancient family of small proteins engaged in a diverse array of physiological processes, whose general molecular function is binding and transporting hydrophobic ligands. ApoD is known to bind arachidonic acid, progesterone, retinol, cholesterol and other lipophilic ligands. Elevations in its expression level have been associated with a number of pathological and tissue damage conditions including neurodegenerative diseases. Its levels increase as well during physiological aging (see Rassart *et al.* 2000; van Dijk *et al.* 2006 for review). Although the correlation between those states and increased gene expression is consistent, the causal link with ApoD function is still unclear. Whether ApoD is one of the factors contributing to the degenerative or aging processes, or its function is part of a defense mechanism providing protection to cells must be solved. Our previous work on an ApoD homologue in insects, the Drosophila Glial Lazarillo (GLaz), shows that it regulates longevity, resistance to stress, locomotor behavior, and degeneration in brain and other tissues upon aging (Sanchez *et al.* 2006; see also Walker *et al.* 2006). We therefore undertook a genetic analysis of the ApoD function in a vertebrate model organism by generating knockout and transgenic over-expressing mice.

4.4 Results and discussion

An ApoD knockout mouse (ApoD-KO) was generated by standard homologous recombination techniques. We replaced the wild-type ApoD gene with a copy interrupted by the insertion of the neomycin resistance gene (Neo) in the opposite direction to ApoD transcription (Fig. 4.1S A), which rendered a transcriptional null mutant (Fig. 4.1S B-D) without deleting any genomic fragment potentially containing regulatory regions. We also generated transgenic mice over-expressing the human orthologue of ApoD (HApoD) under the control of the neuronal human Thy-1 promoter (HApoD-Tg line; Fig. 4.2S A), thus expressing HApoD in neurons in all regions of the nervous system (Fig. 4.2S B-E). General features of ApoD-KO and HApoD-Tg mice are described in Supporting Information available online.

Both ApoD-KO and HApoD-Tg mice are viable and breed normally. Three independent lines were obtained for the Thy-1 transgenic, but a single line was used in this work due to their similar phenotypes based on general health, and biochemical and molecular characterization (Do Carmo and Rassart, unpublished observations). No apparent genotypic differences were observed during development when comparing sibling ApoD-KO and WT mice (see Supporting Online Information). We therefore turn to study ApoD function during adulthood, both in normal conditions, and when exposing the organism to oxidative stress situations mimicking the many pathological situations in which ApoD is up-regulated.

4.4.1 ApoD alters locomotor activity and learning abilities in young adult animals

Open field analysis revealed a significant decrease in horizontal and vertical locomotor activity in ApoD-KO mice (25% and 36% mean reduction in horizontal

and vertical activity respectively; Fig. 4.1A, left and right panels), while no differences were observed in anxiety related parameters (relative time spent in the center vs. periphery of the open field arena; Fig. 4.1A central panel). On the other hand, over-expression of human ApoD causes an increase in vertical activity (number of rearings, Fig. 4.1B, left panel), while differences in horizontal activity were not significant (Fig. 4.1B, right panel).

Visual ability, assessed by darkness preference and object recognition, was not significantly affected. Other behavioral tests exploring pain and touch sensitivity, gait, and muscular strength gave no significant differences between ApoD-KO mice and their wild-type littermates. Similarly, the walking pole test exploring sensory-motor coordination gave no differences in ApoD-KO nor HApoD-Tg mice (see Supporting Online Material).

ApoD-KO mice and their wild-type control perform equally well in the Rotarod test (also exploring sensory-motor coordination) when first tested on the accelerated rod after a set of training sessions. However, a parameter that estimates the ability to learn a motor task (improvement of performance over consecutive trials) was much smaller in the ApoD-KO mice (Fig. 4.1C).

Hippocampal-dependent memory was assessed with the spatial version of the Barnes maze. Wild-type mice showed an average learning time of 64 days, while none of the ApoD-KO mice were able to meet the learning criteria (7 out of 8 sessions with 3 or less errors) for the test period of 70 days (Fig. 4.1D).

Therefore, mice lacking ApoD expression reduce their locomotor and exploratory activity, while over-expression of HApoD in the brain renders the animals slightly more active. In addition, ApoD-KO mice show deficits in learning either a motor task or an orientation-based task (dependent on visual cues). Decreased

locomotor performance was also shown for Drosophila GLaz null mutants (Sanchez *et al.* 2006), illustrating interesting functional conservation of these homologous genes throughout evolution.

4.4.2 Resistance to experimentally induced oxidative stress is undermined in the absence of ApoD and increased by the over-expression of human ApoD

The regulation of ApoD in physiological and pathological states where reactive oxygen species (ROS) are generated (reviewed in Rassart *et al.* 2000), and the higher sensitivity to oxidative stress experienced by the Drosophila GLaz mutants (Sanchez *et al.* 2006) motivated us to test the overall survival of ApoD-KO and HApoD-Tg mice exposed to an oxidative insult. Sensitivity to the ROS generator 1,1'-dimethyl-4,4'-bypiridinium (paraquat; PQ) was assayed using different paradigms of intraperitoneal injections (see Methods in Supporting Online Material). The ApoD null mutant mice show a higher sensitivity to PQ-induced chronic oxidative stress than wild-type controls (Fig. 4.2A). The survival curves show a reduction in both the median and the maximum lifespan (26% and 56% respectively, Fig. 4.2A) reflecting an early onset of functional decline in the ApoD-KO mice. This effect is observed independently of the genetic background (C57BL6/J or Balb/C), indicating that the reduction observed is originated by the lack of ApoD.

These results will predict that mice over-expressing ApoD would be more protected against the stress produced by PQ. Indeed, HApoD-Tg mice showed improved survival upon single systemic exposures to PQ at two different concentrations, with an increase in median survival time of 41.6 and 27.5% respectively (Fig. 4.2B, C). Thus the human ApoD protein is able to exert a protective role when expressed in the mouse brain. This general effect on survival might be due to either the presence of the neuron-expressed ApoD in the systemic circulation, or to low levels of non-neuronal ApoD expression in other tissues.

The protective effect of ApoD is also consistent with the results obtained in Drosophila over-expressing the endogenous ApoD homologue GLaz (Walker *et al.* 2006) or the human ApoD gene (Muffat *et al.* personal communication). All these results strongly suggest that the protecting role in oxidative stress-compromised survival is a common factor in all ApoD homologues, reflecting that it is probably part of the ancestral function of this lipocalin. Therefore, the analyses in model organisms can be very useful to understand the human ApoD function.

4.4.3 ApoD expression is induced in the brain upon experimental oxidative stress

The up-regulation of ApoD in ROS-related pathological conditions predicts that an experimentally produced oxidative stress would also regulate ApoD mRNA expression in the mouse. Since ApoD is up-regulated in neurological pathologies, and our behavioral studies in the mouse indicate that nervous system functionality is compromised in the absence of ApoD, we assayed the transcription of ApoD in mouse brain after a single exposure to PQ. An acute up-regulation of ApoD (1.86-fold induction) is detected 3 hours after exposure, and the expression returns to baseline by 24 hours (Fig. 4.3A).

Similar transient effects of PQ on gene transcription have been shown in lung and kidney for several genes with antioxidant roles (Tomita *et al.* 2006a, 2006b). We therefore assayed the transcription of ApoD in several tissues 3 hours after PQ exposure, when the expression peaks in the brain. No up-regulation is produced in the lung or the liver, while the brain tissue shows a strong ApoD induction upon PQ treatment (Fig. 4.3B). These results suggest a specific function of ApoD in the response of the nervous system to oxidative injury.

The higher sensitivity to oxidative stress of mice lacking ApoD parallels our results obtained in the Drosophila GLaz null mutant (Sanchez *et al.* 2006) and in null mutants of the ApoD homologue in plants (Frenette-Charron *et al.* personal communication) which are more sensitive to oxidative and other forms of stress. We can therefore predict that the regulation of these lipocalin genes must also be conserved (a transient up-regulation of GLaz also occurs in Drosophila, our unpublished observations also confirmed by J. Muffat *et al.* personal communication), and that the ApoD up-regulation in the mouse brain upon PQ-induced ROS generation is part of the normal protective response to stress.

The increased survival of the transgenic animals over-expressing human ApoD in the nervous system should be due to a higher and longer-lasting presence of ApoD in the tissues. Since the human transgene is placed in a wild-type genetic background (C57BL6/J mice), we measured the expression level of the mouse endogenous ApoD gene in the brain of transgenic animals. Mouse ApoD transcript levels are not affected by the presence of the human transgene either under normal conditions or upon PQ treatment. As expected, the human transgene does not show a response by PQ (Fig. 4.3C).

4.4.4 ApoD controls the levels of brain lipid peroxidation under normal conditions

PQ treatment is known to generate protein and lipid peroxidation (Beal 2002). By evaluating the oxidation state of these macromolecules in the brain, both in the control situation and in the presence of PQ-induced oxidative stress, we should gain insight into the biochemical actions of ApoD in the brain tissue when it is exerting the protecting effects described above at the organism level.

We assayed lipid peroxidation levels upon the different paradigms used for PQ injection. In agreement with McCormack (McCormack *et al.* 2005), lipid peroxide adducts accumulate in the wild type brain over time at a relatively slow pace (Fig. 4.3S A). As it is the case for tissues like lung, kidney and liver (Sato *et al.* 1992), no increase in lipid peroxidation is observed in the brain 3 hours after a single high dose of PQ (acute PQ treatment, protocol B), while a low-dose chronic treatment (protocol C) does produce a significant increase after two weeks. In contrast, protein carbonylation, a marker of oxidative modification of proteins, is much faster, showing a patent increase by 3 hours upon acute treatment (Fig. 4.3S B).

In control conditions (sham injection, Fig. 4.4A) we observe that the lack of ApoD results in increased levels of lipid peroxides in the brain, but not in the lung, in accordance with the normal tissue distribution of ApoD. Moreover, as expected for a lipid managing lipocalin, the effect is specific for lipids, since no alterations are seen in protein carbonylation. On the other hand, the amount of lipid peroxidation in the brain of HApoD-Tg mice is similar to the wild-type levels (Fig. 4.4C), indicating that an excess of human ApoD cannot reduce the basal levels of oxidation products related to normal cellular metabolic activity. As expected, lung lipid peroxidation levels are also unchanged by the human transgene (not shown).

An increased level of lipid peroxidation under basal conditions was also observed in the GLaz null mutant fruit flies (Sanchez *et al.* 2006). These results suggest that ApoD and its homologues can condition the peroxidation state of lipids, even in normal non-stress situations. The maintenance of cellular membrane integrity can be expected to be compromised in the ApoD-KO and, since ApoD absence is particularly noticed in the brain, it can result in neural functional alterations that we are able to detect by behavioral tests.

The data by Thomas and Yao (Thomas and Yao 2007) also support the above proposal. They performed a brain lipid profile analysis in our ApoD-KO mice to understand the role of ApoD in the mechanisms of antipsychotic drug action. Their results in the control animals (without drug addition) show that ApoD-KO brains have increased levels of some polyunsaturated fatty acids (dienes and hexanenes). Since polyunsaturated fatty acids are more prone to peroxidation, the susceptibility of membranes to peroxidation (Hulbert 2005) must be increased in the ApoD-KO brains, and therefore membranes could be more susceptible to the effects of normal oxidative metabolism.

4.4.5 ApoD is able to prevent the lipid peroxidation increase upon oxidative insult

Upon oxidative insult (either acute or low-dose chronic PQ treatment) lipid peroxidation increases (33% and 43% respectively) over the wild-type levels in the ApoD-KO brain (Fig. 4.4B). This change can be correlated with the decrease in survival time observed in the ApoD-KO mice upon PQ treatment. Again, no genotype-dependent differences in protein carbonylation were observed under PQ treatment (Fig. 4.4B), suggesting that the function of ApoD is confined to lipid management. On the other hand, human ApoD over-expression abolishes the long-term accumulation of lipid peroxides after 2 weeks of PQ treatment, maintaining the levels at control values (Fig. 4.4C). These results show that an excess of human ApoD in the brain can counteract the exogenously-induced oxidative damage to lipids. Therefore, we can expect that a supplement of ApoD might be beneficial for human conditions where lipid oxidation is a key factor in the functional decline associated to physiological aging or neural pathologies.

4.4.6 Lipocalins as part of the oxidative stress response system

Our data support the notion that ApoD is part of the mechanisms regulating protection from diverse forms of stress, including oxidation. We show in this report that ApoD specifically controls the levels of lipid peroxidation in an organ as vulnerable as the brain. The structural property of ApoD shared with all other lipocalins is the presence of a binding pocket that can bind diverse molecules, mostly hydrophobic (Akerstrom *et al.* 2006, Flower *et al.* 2000), therefore it is probable that its mechanism of action involves this lipid-binding property. The control of lipid peroxidation can be exerted directly, either a priori by preventing the oxidation of bound lipids, or a posteriori by removing peroxidated lipids from membranes, and therefore avoiding the positive feedback loops leading to more oxidative damage. Alternatively, the control of lipid oxidation can be a consequence of the regulation of lipid composition in membranes, which will determine the susceptibility of membranes to peroxidation. Scavenging roles have been proposed for other lipocalins. Lcn-1 (tear lipocalin), expressed in secretory glands, has been shown to bind lipid peroxidation products in vitro and is also up-regulated upon oxidative stress in an epithelial cell line (Lechner *et al.* 2001). α-1 microglobulin is able to reduce and then trap ABTS radicals by covalent binding (Akerstrom *et al.* 2007).

However, can our data also be compatible with a direct antioxidant activity of ApoD?

The antioxidant defense system is currently known to comprise low molecular mass agents (e.g. glutathione or melatonin), iron or copper sequestration proteins (such as transferrin, ferritin, or albumin) and antioxidant enzymes (like superoxide dismutase or catalase). With the data available so far, ApoD belongs to none of these categories. While other lipocalins are well known for their iron sequestration properties (Flo *et al.* 2004, Goetz *et al.* 2002), binding to toxic heme (Allhorn *et al.*

2002) or antioxidant catalytic activities (Allhorn *et al.* 2005), neither metal sequestration properties nor enzymatic activity have been shown for ApoD, or its orthologues in fruitflies or plants.

The lipocalin α-1 microglobulin (Akerstrom *et al.* 2007, Allhorn *et al.* 2002, Allhorn *et al.* 2005) exerts reductase and dehydrogenase activities through a free cysteine group located in a flexible loop. ApoD has four cysteine residues that form two disulfide bonds at the core of the protein fold in all species studied so far. However, human ApoD has an extra cysteine (Cys116) known to bind covalently to Apolipoproteins A-II and B-100 (Blanco-Vaca *et al.* 1992). Whether the thiol group of Cys116 confers additional antioxidant properties to human ApoD remains to be investigated. If this were the case, then this property would be human-specific. In order to explain the results obtained in mouse (this study), fly (Sanchez *et al.* 2006) and plants (Frenette-Charron *et al.* personal communication), additional antioxidant properties of ApoD that are conserved among these divergent species must be invoked. Moreover, the fact that only lipid peroxidation, but not protein carbonylation, is altered in the absence of ApoD argues against a direct antioxidant activity of mouse ApoD.

The oxidative modification of membrane lipids also triggers intracellular signaling cascades that direct the cell fate after an oxidative insult. Particularly, arachidonic acid (AA) is known to be mobilized from membranes upon oxidative stress (Balboa and Balsinde 2006). ApoD is able to bind a variety of lipidic ligands (Breustedt *et al.* 2006, Eichinger *et al.* 2007, Rassart *et al.* 2000) of which the highest affinity is shown for AA. Data supporting the participation of ApoD in regulating the mobilization of AA has been shown in a cell culture system (Thomas *et al.* 2003d), and both ApoD and AA are regulated in patients with schizophrenia in response to antipsychotic drug treatment (Thomas *et al.* 2001b, 2003a, 2003c). The lipid analysis of ApoD-KO brains upon treatment with clozapine (Thomas and Yao 2007) has

shown that the absence of ApoD alters the levels of AA upon drug treatment (even though levels are not modified by the mutation in basal conditions). Thus by modulating important signaling lipids like AA, ApoD can influence the patient's response to different treatments.

All data available so far point to a common biochemical function for ApoD, directly linked to membrane physiology, which is essential for a proper nervous system function. By controlling the levels of lipid peroxidation ApoD could influence parameters as important as neurotransmitter release, in turn affecting learning abilities or locomotor activity (Vajragupta *et al.* 2000) throughout life. Likewise, by performing the same biochemical function, ApoD can control the rate of brain functional decline upon normal aging or in pathological conditions, although it is unlikely to be the only such factor.

4.4.7 Functional significance of ApoD: its influence on normal and pathological nervous system decline upon aging

We have shown that ApoD expression in the mouse brain is boosted by experimental oxidative stress, mimicking what happens in many human neurodegenerative and psychiatric diseases, nervous system injuries, as well as during normal aging. The main known effect of lacking ApoD is to become more vulnerable to stress, while an ApoD overdose makes animals less sensitive to the same stress. The fact that the human ApoD gene can produce effects that oppose those observed in the ApoD-KO mouse strongly suggests a conserved function, and therefore the utility of the mouse model to test potential therapeutic uses of ApoD. This study is the first showing that an excess of ApoD results in seemingly beneficial effects upon experimental oxidative stress in the mouse. Testing the effects of over-expressing ApoD in mouse models of disease should therefore become a priority.

4.5 Experimental procedures

4.5.1 Animals

The experimental procedures were approved by the Animal Care and Use Committees of the University of Utah, University of Valladolid and Université du Québec à Montréal, and were in accordance with the Guidelines for the Care and Use of Mammals in Neuroscience and Behavioral Research (2001). Mice were maintained in positive pressure-ventilated racks at 25±1°C with a 12 h light/dark cycle, fed a standard rodent pellet diet (Global Diet 2014; Harlan), and allowed free access to filtered and UV-irradiated water. Experiments were carried out with 3-5 months old animals of mixed sexes.

4.5.2 Targeted disruption of the mouse ApoD gene

In order to silence the mouse ApoD gene we constructed a targeting vector with the neomycin phosphotransferase (Neo) gene interrupting exon 6 of the ApoD gene (Fig. 4.1S A). G418r-GANCs 129/SvJ ES cells were transfected with the construct and tested for the presence of the disrupted ApoD allele by BamHI digestion of their genomic DNA followed by Southern hybridization with an external probe comprising exon 4 (Fig. 4.1S A). Genomic DNA sequence of the region surrounding the targeting vector confirmed the proper homologous recombination of the positive lines injected into female mouse blastocysts at the U. of Utah Transgenics Facility. Subsequent crosses with the chimeric mice showing germline transformation of the targeted allele generated heterozygous ApoD+/- mice that were further confirmed by Southern blot with a 3' probe (Fig. 4.1S A). Standard genotyping was performed from tail DNA and PCR with Neo and ApoD-specific primers: ApoD-for: 5' CCA CCG GCA CCC TAC TGG ATC 3'; ApoD-rev: 5' CGG GCA GTT CGC TTG ATC TGT 3'; and Neo-for: 5' CGA TTG TCT GTT GTG

CCC AGT 3'. Phenotype stability was assessed by backcrossing and outcrossing the ApoD mutated allele into the C57BL6/J and Balb/C genetic backgrounds respectively. The mutant allele was selected for ten generations of crosses with the corresponding wild type females. An additional generation was performed by crossing mutant females with wild type males to introduce the Y chromosome of the wild type strain.

4.5.3 Generation of human ApoD transgenic mouse

The human ApoD transgenic mouse (HApoD-Tg) carries a construct (~ 4.5 kb) containing the promoter, the first exon, the first intron and the 5' non-coding region of the second exon of the human Thy-1 gene (generous gift from J. Silver, New York University Medical Center). This fragment was fused to the human ApoD coding sequence followed by the bovine growth hormone (BGH) polyadenylation signal (Fig. 4.2S A). The presence of the transgene was verified by PCR using an ApoD-specific primer (5' CCC AAT CCT CCG GTG CAG GAG AA 3') and a BGH-specific primer (5' GAA GGC ACA GTC GAG GCT GAT CAG 3'), producing a 0.6 kb fragment (Fig. 4.2S B). The HApoD-Tg mice used in this study were backcrossed onto C57/BL6 wild-type mice as explained above.

4.5.4 RNA extraction and northern blot analysis

Animals were euthanized by inhalation of CO2/O2 (2:1). Tissues were collected, frozen in dry ice, and kept at -80°C until extraction of total RNA using the Trizol reagent™ (Invitrogen). Total RNA (10μg) was separated on 1.5% (wt/vol) agarose-formaldehyde gels and blotted to a nylon membrane. The membranes were hybridized with [α-32P]dCTP-labeled mouse or human ApoD, or GAPDH cDNAs, exposed to Biorad Imaging screen K and revealed with a PhosphorImager (Biorad Molecular Imager FX) and Quantity One software (Biorad). For each value, the

optical density measured for each gene tested was divided by that of the GAPDH mRNA.

4.5.5 Protein extraction and western blot analysis

Frozen tissues were thawed on ice and homogenized in lysis buffer (50 mM Tris-HCl pH 7.3, 150 mM NaCl, 5 mM EDTA, 0.2% Triton X-100, and 10% Complete protease inhibitors (Roche)). After 30 min of incubation at 4°C, lysates were sonicated and cleared by centrifugation. The protein concentration was determined using a protein assay reagent (Bio-Rad Laboratories). All extracts were stored at -80°C. For western blot analysis, protein extracts (10µg) were separated on a 12% SDS- polyacrylamide gel and transferred to a polyvinylidene difluoride (PVDF) membrane. A prestained size marker (Biorad prestained SDS-PAGE standard, low range) was included in each run. Membranes were blocked in PBS containing 0.2% Tween-20 and 5% skim milk powder before incubation with the primary antibodies diluted as follows: polyclonal anti-human ApoD (Caro2), 1:4000; anti-GAPDH, 1:4000. Subsequently, the blots were incubated under gentle agitation at room temperature with a HRP-conjugated secondary antibody diluted 1:5000 in blocking buffer. The blots were developed using the enhanced chemoluminescence method (Amersham-Pharmacia) with X-ray film.

4.5.6 Behavioral analyses

Open field tests in the ApoD-KO and their wild type controls were performed by video recording in a 1m2 arena for a single session of 10 min. A total of 6 mice of each genotype and sex were analyzed. The subsequent analysis explored horizontal (Number of squares visited) and vertical (Number of rearings) activities, as well as anxiety, measured as relative time spent in the central area of the arena. Horizontal

and vertical activity was measured in the HApoD-Tg mice and control littermates in an open field arena measuring 30 x 44.5 cm.

A novel-object recognition test was used to assay for visual ability and short-term memory recognition. Mice habituated to the test arena are presented with two plastic objects of different shapes. The object recognition was evaluated by the ratio of time spent exploring the novel vs. the familiar object 10 sec and 1 min after first exposure.

Hippocampal-dependent memory was explored in six WT and six ApoD-KO mice subjected to the spatial version of Barnes maze test (Barnes 1979), where the mouse needs to learn and remember distal cues in the environment, and associate them with the location of an escape tunnel. The mice were tested daily for 70 days, and the number of holes searched, perseverations and time was recorded. The average for each genotype was recorded and grouped into session blocks of 5 testing days.

Rotarod analysis was performed in a Ugo Basile (Varese, Italy) apparatus with acceleration from 4 to 40 rpm over 5 minutes. Each mouse was subjected to two training sessions separated by a 15 min rest. Each session consisted of a 2 min period of exposure to the rod rotating at minimum speed (4 rpm). After another 15 min resting period a first test was performed, consisting of three runs with the rod accelerating from the starting 4 rpm speed. Time of permanence in the rod was recorded. A second test of three runs was performed 2 hours later, after the mice had been injected intraperitoneally either with PBS or paraquat (see Protocol B below).
Other tests such as pain and touch sensitivity, gait, and muscular strength were performed as detailed in (Crawley 2000).

4.5.7 Oxidative stress toxicity by 1,1'-dimethyl-4,4'-bypiridinium (paraquat)

The following protocols of doses, administration patterns and analysis have been used:

Protocol A: Chronic paraquat (PQ) treatment. Mice were daily injected intraperitoneally with a solution of PQ in phosphate buffered saline (PBS) at 15 mg/kg of body weight. Death occurrence was scored at least every 12 hours for the survival analysis. Morphological analyses were performed on brains from mice euthanized on day 5 of treatment (when the ApoD-KO mice survival is at the 50% level).

Protocol B: Acute PQ treatment. A single dose of either 30 or 50 mg/kg of PQ was injected as described above. Behavioral tests were performed just before injection (t =0), 1.5 hours after injection, and 24 hours after injection. Mice were then euthanized either 3 hours or 24 hours post-injection, and their brains extracted for biochemical and immunohistochemical analyses.

Protocol C: Low-dose, neurotoxic chronic PQ treatment. Following Thyruchelvam *et al.* (Thiruchelvam *et al.* 2000), mice were injected twice a week, for a total of 2 weeks, with a 15 mg/kg of PQ as described before. Animals were euthanized 3 hours after the last injection, and their brains extracted for biochemical and immunohistochemical analyses. We confirmed the absence of lung toxicity by histopathological analysis looking for alterations in alveoli, respiratory ducts, and bronchioles (results not shown).

4.5.8 Lipid and protein oxidation assays

4.5.8.1 TBARS assay

The concentration of thiobarbituric acid (TBA) reactive species was assayed to monitor the level of lipid peroxidation. Brain tissue was homogenized in PBS in the presence of an antioxidant (butylated hydroxytoluene, BHT) to prevent new lipid peroxidation to occur during homogenization. A 12µl aliquot of each extract was incubated with 390µl of 0.2 M glycine-HCL, pH 3.6 and 250µl of fresh TBA reagent (0.5% TBA, 0.5% SDS). After 15 min incubation at 90°C, samples were cooled on ice and transferred to a 96 well microplate for triplicate readings. Absorbance was monitored at 532 nm in a Versamax microplate reader (Molecular Devices). Values were normalized to the protein concentration of each sample, measured with the Micro BCA Protein Assay (Pierce).

4.5.8.2 Protein carbonylation-ELISA assay

Protein carbonylation was performed as previously reported (Buss *et al.* 1997). Briefly, triplicate protein samples were allowed to react with dinitrophenylhydrazine (DNP) and then adsorbed to wells of an ELISA plate. A biotinylated anti-DNP antibody (Molecular Probes Inc.) was used for detection of the protein-bound DNP followed by an amplification step with streptavidin-biotinylated horseradish peroxidase (Amersham). Color reaction was performed by supplying o-phenylenediamine, hydrogen peroxide and citric acid in phosphate buffer. Absorbance at 490 nm was measured in a Versamax microplate reader (Molecular Devices). Values were normalized to the protein concentration of each sample.

4.6 Acknowledgements

We thank J.R. Acebes, V. Pomies and S. Thompson for technical assistance. Polyclonal antibody anti-rat ApoD was kindly provided by Dr. S. Patel. This work was supported by start-up grants to D.S. and M.D.G. from the "Ramon y Cajal Program"(MEC-Spain and FEDER-FSE); the SGFRH Foundation; NIH grant 2/R01/NS25387-10A1 to M.J.B.; CIHR grant MOP-15677 to E.R.; FRSQ and CRSNG studentships to S.D.C.; STINT fellowship KU2003-4308 to M.A.; DGICyT grant BFU2004-06394 and JCyL grant VA011C05 to C.G.; and MEC grant BFU2005-00522 and JCyL grant VA049A05 to M.D.G. and D.S.

4.7 Figure legends

Figure 4.1: Alterations in behavioral output in ApoD-KO and HApoD-Tg mice. (A) Open field test on locomotor exploratory behavior in ApoD-KO mice. Both horizontal (number of squares visited) and vertical (number of rearings) activities are decreased in the ApoD-KO mice, while an anxiety-related behavior (exploration of the center of the 1 m2 arena) is not altered. N= 12 mice/genotype (6th backcross generation onto C57BL/6 background). Unpaired two-sided Student's t-test, *$p < 0.05$, **$p < 0.01$. (B) Open field test in HApoD-Tg mice. Vertical activity increase in HApoD-Tg mice (left panel), while horizontal activity differences are not significant (right panel). A smaller arena was used in this case, and the anxiety parameter was not measured. WT: N = 16; HApoD-Tg: N = 13 (11th backcross generation onto C57BL/6 background). Unpaired two-sided Student's t-test, *$p < 0.05$. (C) Motor learning abilities were tested as the increment of the Rotarod test score over a 2 hours interval, and is represented normalized to the score of the first test. ApoD-KO mice show a lower learning ability under normal conditions. N= 14 mice/genotype (11th backcross generation onto C57BL/6 background). Sign non-parametric test, *$p < 0.05$. (D) Barnes maze test on spatial learning. ApoD-KO mice fail to increase their rate of success in finding a safe escape hole, while wild type mice learn and remember using distal spatial clues. Mice were tested daily for 70 days. Results from each five consecutive daily sessions were combined in blocks. N= 6 mice/genotype (5th backcross generation onto C57BL/6 background). ANOVA test, $p < 0.0001$. (A-D) Data are represented as mean ± SD.

Figure 4.2: Oxidative stress-compromised survival is decreased in the absence of ApoD and increased when human ApoD is over-expressed in the mouse brain. (A) Survival analysis of mice treated daily with the ROS generator paraquat (15 mg/kg of body weight; Protocol A). KO and WT genotypes in C57BL/6 background (8th backcross generation) are compared. N= 11 mice/genotype. The absence of

ApoD shortens the mice survival (Gehan-test, p = 0.026; Cox's F-test, p = 0.028). A decrease of 26% in mean lifespan and 56% in maximum lifespan is observed. The survival phenotype is stable after changing the genetic background (Balb/C, 8th outcross generation) with 11% decrease in mean lifespan and 9% in maximum lifespan. N= 12 mice/genotype. Gehan-test, p = 0.031; Cox's F-test, p = 0.043 (curve not shown). (B and C) Survival analysis of WT and transgenic (HApoD-Tg) mice treated with single PQ doses of 30 (B) or 50 (C) mg/kg of body weight (Protocol B). Death occurrence was recorded up to 10 days. Surviving animals were sacrificed at day 10. Data was fitted to a Gompertz function. (B) Over-expression of ApoD increases the mice survival. WT: N = 16; HApoD-Tg: N = 13. Gehan-test, p = 0.029; Cox's F-test, p = 0.043. (C) Over-expression of ApoD also protects mice at higher doses of paraquat. WT: N = 12; HApoD-Tg: N = 9. Gehan-test, p = 0.045; Cox's F-test, p = 0.033. All transgenic mice are backcrossed on the C57Bl/6 background (11th generation).

Figure 4.3: The endogenous mouse ApoD is transiently up-regulated by exposure to PQ while the human transgene is expressed constitutively in the brain. (A) Northern blot analysis of mouse ApoD mRNA shows a transient increase in response to a single injection of paraquat (30 mg/kg; Protocol B). Quantification of mRNA expression by band densitometry. Values were normalized with the GAPDH gene. Error bars represent SD (N=3). (B) Mouse ApoD is specifically up-regulated in the brain upon acute PQ treatment (3 hours after a single PQ dose; 30mg/kg; Protocol B). No induction is observed in liver or lung. The GAPDH gene was used as a control. (C) Northern blot analysis shows a comparable expression of the mouse ApoD endogenous mRNA in the brain of WT and HApoD-Tg mice 3 hours after a single PQ dose (30mg/kg; Protocol B), and the absence of response to PQ of the human transgene. The GAPDH gene was used as a control.

Figure 4.4: Loss of ApoD function specifically alters lipid peroxidation in the brain and an over-dose of human ApoD prevents their accumulation upon oxidative insult. (A) Oxidation of proteins (Carbonyls-ELISA assay) and lipids (TBARS assay) in control conditions (sham injection of PBS). Lipid peroxidation, and not protein carbonylation, is increased in the ApoD-KO brains, while lipid peroxidation in the lung remains unchanged. (B) Brain oxidation status assayed upon acute (3 hours, Protocol B) or chronic (2 weeks low-dose, Protocol C) exposure to paraquat. ApoD-KO mouse brain show a higher level of lipid peroxidation while protein carbonylation levels do not change with genotype. (A and B) N= 7 mice/genotype/sex (11th backcross generation onto C57BL/6 background). Data are represented as mean ± SD normalized to the wild-type value. Unpaired two-sided Student's t-test, *$p < 0.05$, **$p < 0.01$ ***$p < 0.001$. (C) Analysis of lipid peroxidation two weeks after PQ treatment (30 mg/kg of body weight). Human ApoD expression prevents the rise of oxidized lipids accumulation in the brain. WT: N = 16; HApoD-Tg: N = 13 (11th backcross generation onto C57BL/6 background). Unpaired two-sided Student's t-test, ***$p < 0.001$. Data are represented as mean ± SD normalized with respect to the control values (sham injection of PBS).

Figure 4.1

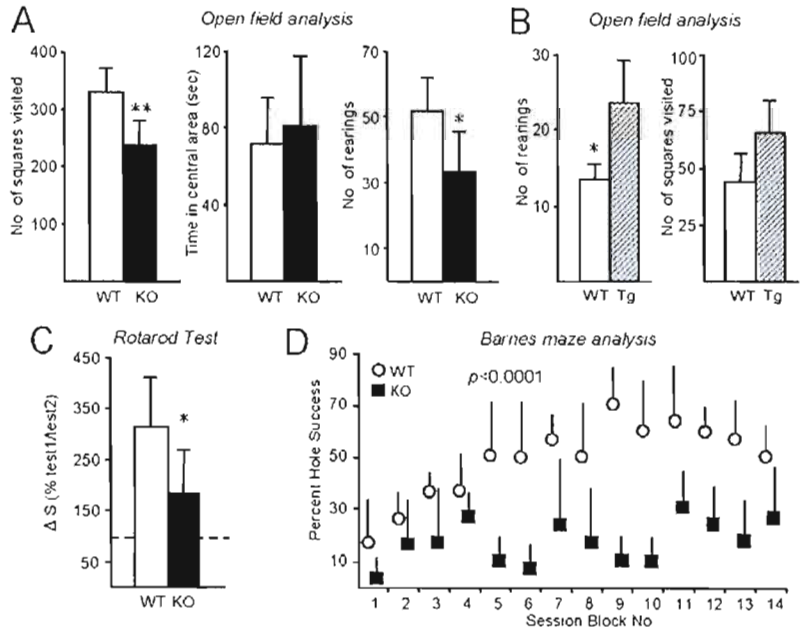
A
Open field analysis
No of squares visited
400
300
200
100
**
WT KO
Time in central area (sec)
120
80
40
WT KO
No of rearings
70
50
30
10
*
WT KO
B
Open field analysis
No of rearings
30
20
10
*
WT Tg
No of squares visited
100
75
50
25
WT Tg
C
Rotarod Test
Δ S (% test1/test2)
450
350
250
150
50
*
WT KO
D
Barnes maze analysis
WT
KO
p<0.0001
Percent Hole Success
90
70
50
30
10
1 2 3 4 5 6 7 8 9 10 11 12 13 14
Session Block No

Figure 4.2

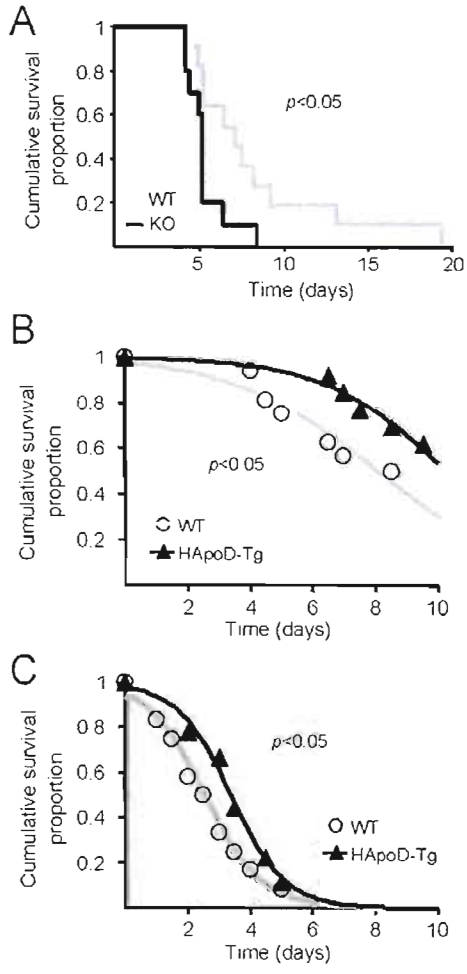
A
Cumulative survival proportion
1
0.8
0.6
0.4
0.2
p<0.05
WT
KO
5
10
15
20
Time (days)
B
Cumulative survival proportion
p<0 05
WT
HApoD-Tg
2
4
6
8
10
Time (days)
C
Cumulative survival proportion
p<0.05
WT
HApoD-Tg
Time (days)

Figure 4.3

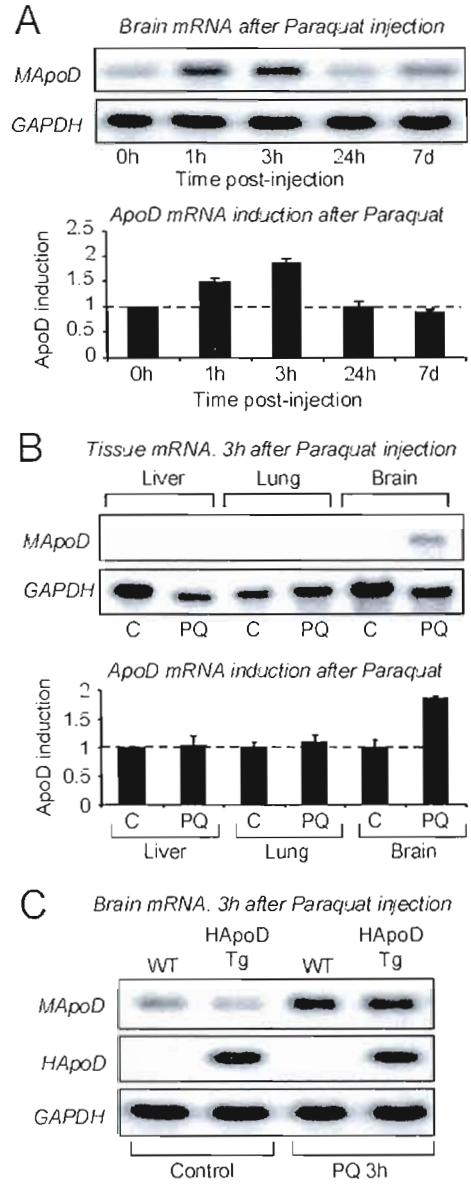
A
Brain mRNA after Paraquat injection
MApoD
GAPDH
0h 1h 3h 24h 7d
Time post-injection
ApoD mRNA induction after Paraquat
ApoD induction
2.5
2
1.5
1
0.5
0
0h 1h 3h 24h 7d
Time post-injection
B
Tissue mRNA. 3h after Paraquat injection
Liver Lung Brain
MApoD
GAPDH
C PQ C PQ C PQ
ApoD mRNA induction after Paraquat
ApoD induction
2
1.5
1
0.5
0
C PQ C PQ C PQ
Liver Lung Brain
C
Brain mRNA. 3h after Paraquat injection
HApoD Tg
HApoD Tg
WT WT
MApoD
HApoD
GAPDH
Control
PQ 3h

Figure 4.4

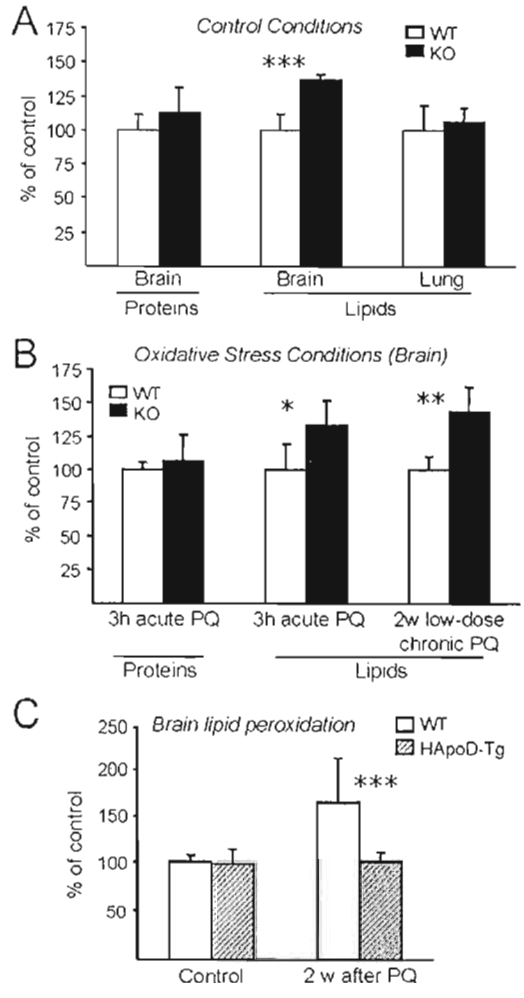
A
Control Conditions
WT
KO
***
% of control
175
150
125
100
75
50
25
Brain
Brain
Lung
Proteins
Lipids
B
Oxidative Stress Conditions (Brain)
WT
KO
*
**
% of control
3h acute PQ
3h acute PQ
2w low-dose chronic PQ
Proteins
Lipids
C
Brain lipid peroxidation
WT
HApoD-Tg
***
% of control
250
200
150
100
50
Control
2 w after PQ

4.8 Supplementary online material

4.8.1 Supplementary results

4.8.1.1 General features of ApoD-KO and HApoD-Tg mice

ApoD-KO mice are viable, develop, and breed normally with litters of similar size. Frequency analysis of appearance of the mutated allele in litters from heterozygous couples demonstrated a standard Mendelian inheritance ($\chi 2=0.57$, n=142, C57BL6/J background). Variables related to metabolism (size and weight, effects of high fat diet, and serum lipid profile), as well as to the general cytoarchitecture of the brain, did not show significant differences between genotypes (see below). Likewise, transgenic HApoD-Tg mice live and reproduce normally.

4.8.1.2 Compensation by other lipocalins

Given the mild phenotypes of ApoD-KO mice, we tested a functional compensation by other lipocalins. We studied with immunoblot and immunohistochemistry the expression of two other members of the lipocalin family that can be found in the neural tissue: the prostaglandin D-synthase and alpha-1 microglobulin. The expressions of these lipocalins were not altered in the ApoD-KO brains under normal conditions (results not shown).

4.8.1.3 Nervous system cellular architecture in ApoD-KO mice

Cytoarchitecture of cortical, hippocampal and cerebellar brain regions were explored using standard histochemistry and immunohistochemistry with neuronal (calretinin, Tuj1), astroglial (GFAP) and oligodendroglial (PLP) antibody markers.

No apparent differences were observed in ApoD-KO mice with respect to their wild-type siblings (results not shown).

4.8.1.4 Behavioral tests

The results of the behavioral explorations (Crawley 2000) of the sensory domain (visual ability, pain and touch sensitivity), footprint analysis and muscular strength (hanging wire test) are shown below. No differences are observed between genotypes.

Novel-object recognition test (1 min after pre-test):

Ratio WT=0.65±0.03; Ratio KO=0.67±0.04 (p=0.63; t-Test)

Hot plate:

WT=9.2±2.4 sec; KO=11.4±6.1 sec (p=0.27; t-Test)

Tail Flick:

WT=2.6±0.9 sec; KO=2.9±1.1 sec (p=0.52; t-Test)

Mecanoception by Von Frey hairs test with 1.6, 3.98, 6.78, 14.4, 20 and 35.5 mN hairs:

WT=0.25±0.6; 1.42±1.32;1.83±1.32; 4.17±1.99; 6.42±2.56; 8.67±1.11

KO=0.42±0.86; 1.58±1.26; 2.58±1.38; 5.08±2.06; 7.67±1.84; 9.17±1.34

t-Test p values: 0.6, 0.76, 0.24, 0.30, 0.2, and 0.35

Footprint analysis (stride length, overlap and width):

WT=77.29±9.49; 5.28±1.08; 18.24±2.43.

KO=77.78±5.7; 5.39±0.96; 17.51±2.76.

t-Test p values: 0.88; 0.81; 0.21.

Hanging wire:

WT=36.5±28.7 sec; KO=35.9±33 sec (p=0.97; t-Test)

4.8.2 Supplementary figure legends

Figure 4.1S : Generation of ApoD knockout mice and molecular assessment of the null allele. (A) Targeted disruption of the mouse ApoD gene by insertion of the inverted Neo gene. Schematic maps of the wild-type allele, targeting vector and mutated allele. ApoD exons are shown as white boxes. BamHI restriction fragments expected for the wild-type and mutant loci are shown with brackets. Genomic DNA from transfected G418r-GANCs ES cells was digested with BamHI and analyzed by Southern blot using the 5' probe (striped box). B, Bam HI. (B) PCR primers in exon 6 were used to test ApoD transcription in brains of ApoD+/+ (WT) and ApoD-/- (KO) mice. Absence of the ApoD band in the mutant allele proves the null transcriptional mutation. Absence of genomic DNA contamination was proved by omitting the reverse transcriptase from the reaction mixture (RT- control lanes). An expected genomic fragment (gDNA) was amplified for comparison. Negative PCR control was performed in the presence of an unrelated DNA template. (C) Northern blot analysis of total RNA from brainstems of WT and KO mice probed with a P32-labeled ApoD cDNA probe. Hybridization shows the expected 0.9 kb ApoD band in wild type mouse and the lack of signal in the RNA from ApoD-KO mice, confirming the null transcriptional allele. (D) Protein expression test by immunohistochemistry in cryostat sections of brain regions of WT and ApoD-KO mice. Arrows point to cells expressing ApoD, that appear to be (according to their shape and size) oligodendrocytes in the corpus callosum, astrocytes and neurons in the brainstem, and pericytes in the blood vessel shown.

Figure 4.2S : Generation of transgenic mice overexpressing human ApoD in the CNS. (A) Schematic representation of HApoD transgene. It contains first a 3.5 kb of the human Thy-1 promoter/enhancer upstream of a 0.7 kb fragment representing the human ApoD cDNA followed by 0.2 kb BGH consensus polyadenylation signal. It was microinjected into the pronucleus of fertilized CBA x C57Bl/6 mouse eggs using

standard techniques. (B) PCR genotyping of tail DNA for identification of transgenic mice (abbreviated hereafter as HApoD-Tg). An expected 0.6 kb band is amplified with human ApoD and BGH primers in transgenic, but not in WT mice. Control lane shows a PCR reaction in the presence of an unrelated DNA template. (C) Analysis of the transgene expression in multiple tissues by northern hybridization with a P32-labeled human ApoD specific probe. Human ApoD appears to be mostly expressed in the CNS, with a weak expression in the thymus and heart. Total RNA of WT mouse brain is included as control. Equal loading was determined by subsequent hybridization with a GAPDH cDNA probe. (D) Comparison of transgene expression in various brain subregions by northern blot analysis. All regions, except the pons, express good levels of the human transgene. (E) Western blot analysis of the transgene product in the brain with a polyclonal anti-human ApoD (Caro2) antibody. Equal loading is shown by subsequent staining with an antibody against GAPDH.

Figure 4.3S : Effects of PQ treatment in lipid and protein oxidation in the wild type brain. (A) Lipid peroxide adducts (TBARS assay) accumulate in the wild type brain over time at a relatively slow pace. No increase is observed 3 hours after a single high dose of PQ (acute PQ treatment, protocol B), while a low-dose chronic treatment (protocol C) does produce a significant increase after two weeks. (B) Protein oxidation in brain (carbonyl groups detected by ELISA assay) occur faster with a significant increase after 3h (acute PQ treatment, protocol B). (A and B) Data are represented as mean ± SD normalized with respect to the control values (sham injection of PBS).

Figure 4.1S

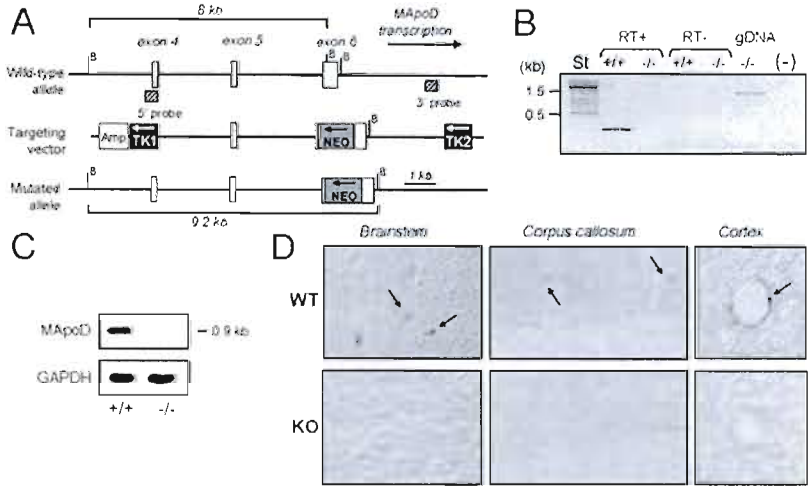
A
8 kb
exon 4
exon 5
exon 6
MApoD transcription
Wild-type allele
5' probe
3' probe
Targeting vector
Amp
TK1
NEO
TK2
Mutated allele
1 kb
9.2 kb
B
RT+
RT-
gDNA
St
+/+
-/-
+/+
-/-
-/-
(-)
(kb)
1.5
0.5
C
MApoD
~ 0.9 kb
GAPDH
+/+
-/-
D
Brainstem
Corpus callosum
Cortex
WT
KO

Figure 4.2S

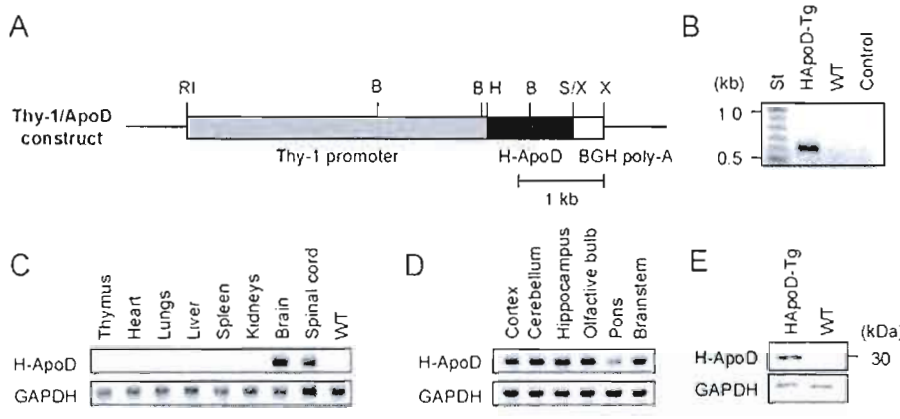
A
RI
B
B H
B
S/X
X
Thy-1/ApoD construct
Thy-1 promoter
H-ApoD
BGH poly-A
1 kb
B
(kb)
St
HApoD-Tg
WT
Control
1 0
0.5
C
Thymus
Heart
Lungs
Liver
Spleen
Kidneys
Brain
Spinal cord
WT
H-ApoD
GAPDH
D
Cortex
Cerebellum
Hippocampus
Olfactive bulb
Pons
Brainstem
H-ApoD
GAPDH
E
HApoD-Tg
WT
(kDa)
H-ApoD
30
GAPDH

Figure 4.3S

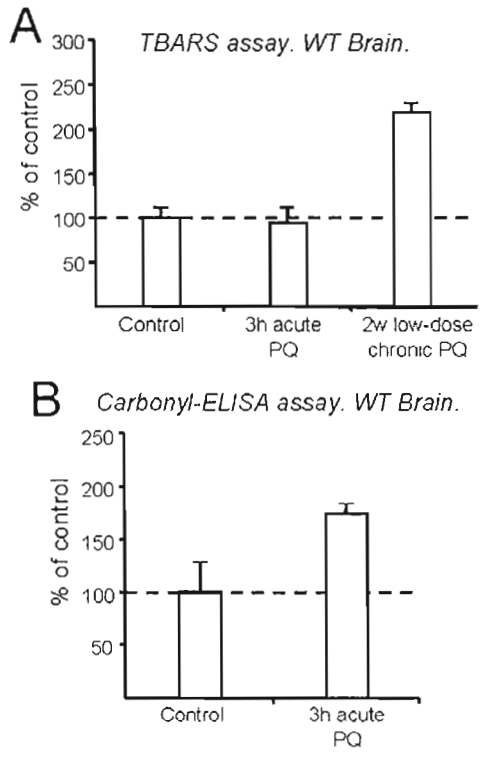
A
TBARS assay. WT Brain.
% of control
300
250
200
150
100
50
Control
3h acute PQ
2w low-dose chronic PQ
B
Carbonyl-ELISA assay. WT Brain.
% of control
250
200
150
100
50
Control
3h acute PQ

CHAPITRE V

Neuroprotective effect of Apolipoprotein D against human coronavirus OC43-induced encephalitis in mice

Sonia Do Carmo*, Hélène Jacomy*, Pierre J. Talbot, Eric Rassart

2008

Journal of Neuroscience 28 : 10330-10338

*Ces auteurs ont contribué de façon équivalente à ce travail.

Avant-propos

Les travaux présentés en chapitre IV nous ont démontré que l'apoD a un effet protecteur face aux effets oxydants du paraquat. Puisque l'étude *in vitro* présentée en chapitre II nous a démontré que l'apoD répondait aussi très fortement au stress inflammatoire, nous avons voulu vérifier si la surexpression de l'apoD humaine était également capable de contrer les effets neurodégénératifs d'un traitement déclenchant une inflammation aiguë. Pour ce faire, nous avons injecté le coronavirus humain-OC43 (HCoV-OC43) de façon intracérébrale à des souris H-apoD-Tg. Nous avons ainsi examiné l'influence du HCoV-OC43 sur l'expression de l'apoD. Nous avons par la suite déterminé l'effet de l'apoD sur la survie des souris et sur différentes composantes de l'encéphalite virale soit la réplication virale, l'activation des astrocytes et de la microglie, l'infiltration des cellules T dans le cerveau, la production de cytokines et de chemokines et enfin l'activité de la phospholipase A2 qui régule beaucoup de processus inflammatoires impliqués dans les dommages neuronaux.

Les coronavirus humains sont des virus enveloppés possédant un génome à ARN simple brin de polarité positive. Ils infectent surtout l'appareil respiratoire et sont responsables du rhume. Ils ont de plus la capacité d'infecter, de se répliquer et de persister dans les cellules neuronales. L'un des sérotypes de coronavirus humains, HCoV-OC43, ressemble aux coronavirus murins. Ceux-ci sont capables de causer une inflammation démyélinisante du SNC rappelant la sclérose en plaques (Jacomy and Talbot 2003). Lorsque injecté de façon intracrânienne chez la souris, le HCoV-OC43 provoque une encéphalite aiguë qui tue 80% des souris C57/bl6 en environ 13 jours. Les souris restantes se remettent de l'infection. Ces dernières sont habituellement des femelles puisque celles-ci sont plus résistantes à l'infection que les mâles. L'infection est retrouvée partout à travers le SNC. Elle affecte les neurones causant leur vacuolisation et dégénération. Les régions affectées présentent également

une réaction inflammatoire aiguë et une activation de la microglie (macrophages cérébraux) contribuant encore plus à la dégénérescence nerveuse.

J'ai contribué à toutes les facettes de ce travail. J'ai d'abord élaboré le design expérimental qui a ensuite été approuvé et amélioré par Hélène Jacomy. J'ai fait les études d'expression d'apoD en réponse à HCoV-OC43. J'ai également fait tous les immunobuvardages concernant l'expression de l'apoD, des marqueurs d'activation gliale et de cellules T. J'ai également fait les études de FACS et d'activité de la phospholipase A2. J'ai aussi fourni les animaux transgéniques à Hélène Jacomy qui s'est occupée de l'injection et de la surveillance régulière des animaux injectés. Elle a de plus prélevé les tissus utilisés dans les différentes expériences, quantifié les virus dans le cerveau des souris suite à l'injection et homogénéisé les cerveaux pour l'analyse des cytokines. Hélène et moi avons partagé la rédaction du manuscrit.

5.1 Résumé

L'apolipoprotéine D (apoD) est une lipocaline surexprimée dans le système nerveux suite à une lésion ou à des pathologies comme l'Alzheimer ou le Parkinson et la sclérose en plaques. Nous avons déjà démontré que l'apoD protège contre la neuropathologie en contrôlant le niveau de lipides peroxydés. Ici, nous avons exploré davantage la fonction biologique de l'apoD dans un modèle murin d'encéphalite aiguë. Nos résultats démontrent que les transcrits et la protéine de l'apoD sont augmentés pendant l'encéphalite aiguë causée par l'infection par le coronavirus humain OC43 (HCoV-OC43). La surexpression de l'apoD coïncide avec l'activation gliale et son expression revient aux niveaux de base lorsque le virus et l'activation gliale sont résorbés. Par ailleurs, la surexpression de l'apoD humaine dans les neurones des souris transgéniques Thy-1/ApoD a triplé le nombre de souris survivant à l'infection par HCoV-OC43. Ce meilleur taux de survie est corrélé à la fois avec l'augmentation de l'activation gliale, la diminution de la réponse immune innée (cytokines, chemokines) et l'infiltration de cellules T dans le cerveau. De plus, la protection semble associée à une activité de la phospholipase A2 restreinte. Ces résultats révèlent un rôle pour l'apoD dans la régulation de l'inflammation et suggèrent qu'elle protège de l'encéphalite induite par HCoV-OC43 sans doute via les voies signalétiques de la phospholipase A2.

Mots-clés : inflammation, encéphalite virale, phospholipase A2, infiltration de cellules T.

5.2 Abstract

Apolipoprotein D (apoD) is a lipocalin up-regulated in the nervous system following injury or pathologies such as Alzheimer's disease, Parkinson's disease and multiple sclerosis. We previously demonstrated that apoD protects against neuropathology by controlling the level of peroxidated lipids. Here, we further investigated the biological function of apoD in a mouse model of acute encephalitis. Our results show that apoD transcript and protein are up-regulated during acute encephalitis induced by the human coronavirus OC43 (HCoV-OC43) infection. The apoD up-regulation coincides with glial activation and its expression returns to normal levels when the virus is cleared, concomitantly to a resolved glial reactivity. In addition, the overexpression of human apoD in the neurons of Thy-1/ApoD transgenic mice results in a 3-fold increase of the number of mice surviving to HCoV-OC43 infection. This increased survival rate is correlated with an up-regulated glial activation associated with a limited innate immune response (cytokines, chemokines) and T-cell infiltration into infected brains. Moreover, the protection seems to be associated with a restricted phospholipase A2 activity. These data reveal a role for apoD in the regulation of inflammation and suggest that it protects from HCoV-OC43-induced encephalitis, most likely through the phospholipase A2 signaling pathways.

Keywords : inflammation, viral encephalitis, phospholipase A2, T-cell infiltration.

5.3 Introduction

Apolipoprotein D (apoD) is a lipocalin widely expressed in human tissues including the central nervous system (CNS) where it is expressed mainly in glia but also in neurons (Hu *et al.* 2001, Provost *et al.* 1991, Smith *et al.* 1990). ApoD expression is increased in several neuropathologies such as Alzheimer's (Terrisse *et al.* 1998), Parkinson's (Ordoñez *et al.* 2006) and Niemann-Pick's type C diseases (Yoshida *et al.* 1996), meningoencephalitis (Terrisse *et al.* 1998) and multiple sclerosis (Reindl *et al.* 2001) (reviewed in Rassart *et al.* 2000, van Dijk *et al.* 2006). Nevertheless, the precise role of apoD in the CNS remains unknown. Early studies suggested that apoD promotes repair. Indeed, after nervous tissue injury, its expression correlated well with removal and redistribution of lipids (Boyles *et al.* 1990a, Terrisse *et al.* 1999), active myelination and axonal outgrowth (Ong *et al.* 1999, Rickhag *et al.* 2008). Moreover, apoD favors survival upon an oxidative insult by controlling the levels of peroxidated lipids (Ganfornina *et al.* 2008).

ApoD has been shown to bind with high affinity to arachidonic acid (AA) (Morais Cabral *et al.* 1995), an abundant component of neural membranes (Diau *et al.* 2005). The liberation of AA from membrane phospholipids by phospholipases A2 (PLA2s) is an upstream regulator of many inflammatory processes involved in neuronal damage (Farooqui *et al.* 1997). As apoD seems to stabilize membrane-associated AA (Thomas *et al.* 2003d), it could restrain inflammation by limiting free AA. ApoD was already associated with inflammation as its expression is modulated in response to lipopolysaccharide in non-neuronal cells (Do Carmo *et al.* 2007) and in response to interleukin-1, interleukin-6 and glucocorticoids in human breast-cancer cells (Blais *et al.* 1994, 1995). This modulation could be related to the presence of specific binding sites on the apoD promoter (Do Carmo *et al.* 2002, 2007).

Human coronaviruses (HCoV) are enveloped positive-stranded RNA viruses that primarily infect the upper respiratory tract, leading to common colds (Myint *et al.* 1994). Moreover, they have neuroinvasive properties in human brains (Arbour *et al.* 2000), and could initiate neurological disorders such as multiple sclerosis (Boucher *et al.* 2007, Talbot *et al.* 2001, 2008). We previously characterized HCoV OC43-mediated neuropathogenesis in mice (Jacomy and Talbot 2003; Jacomy *et al.* 2006). C57BL/6 mice infected by an intracerebral inoculation of HCoV OC43 developed signs of acute encephalitis. Neurons, which are the main target of infection, underwent vacuolation and degenerated by necrosis and apoptosis. Infected regions also presented microglial activation and astrogliosis, signs of a strong inflammatory reaction.

The main objective of this study was to investigate the biological role of apoD during acute viral encephalitis in a mouse model. Here we show that following HCoV-OC43 infection, endogenous apoD is up-regulated and mice overexpressing human apoD (H-apoD) in neurons have an increased survival rate. This increased survival was correlated with an up-regulated inflammatory reaction associated with a limited T-cell infiltration into infected brains. These data revealed a role for apoD in the regulation of inflammatory reactions in the brain and suggest that apoD protects from HCoV-OC43 induced encephalitis, at least in part, through the activation of signaling pathways involving PLA2.

5.4 Materials and methods

5.4.1 Mice

Human apoD transgenic mice carry a construct containing the H-apoD cDNA fused to the bovine growth hormone (BGH) polyadenylation signal under the control of three different neuron-specific promoters/enhancers. In Thy-1/ApoD mice, the H-apoD expression is controlled by the promoter, the first exon, the first intron and the 5' non-coding region of the second exon of the human Thy-1 gene (~ 3.5 kb) (gift from J. Silver, New York University Medical Center). In NSE/ApoD mice, the rat neuron-specific enolase (NSE) promoter (~ 1.8 kb) (gift from G. Sutcliffe, Scripps Research Institute, La Jolla) controls the H-apoD expression. Finally, in NFL/ApoD mice, the H-apoD/BGH fragment was inserted after the promoter in the complete human neurofilament light chain (NFL) gene (gift from J.-P. Julien, CHUL, Université Laval). Thus, H-apoD is expressed in neuronal cells in all regions of the nervous system. All mice were backcrossed into C57BL/6 background for at least 10 generations. Genotyping was performed on tail biopsies as already described (Ganfornina *et al.* 2008). All the experimental procedures were approved by the Animal Care and Use Committees of Université du Québec à Montréal and INRS-Institut Armand-Frappier.

5.4.2 Virus and inoculations

The ATCC HCoV-OC43 strain (ATCC number VR-759) was grown on the HRT-18 cell line and virus stocks ($10^{6.5}$ $TCID_{50}$/ml) were kept at -80°C as previously described (Jacomy and Talbot 2003). Mice were infected at 22 days post-natal (DPN) with intra-cerebral (IC) inoculation of 10 µl containing 10 $TCID_{50}$ of HCoV-OC43. Control mice received an intra-cerebral inoculation of 10 µl of cell culture medium.

Mice were sacrificed at different days post-infection (DPI) and brain and spinal cord were collected.

5.4.3 Survival curves

Litters were weaned at 21 days postnatal (DPN) and separated by sex, maintaining strain identification. The next day, all separated litters were inoculated with virus and during anesthesia ears were punch for identification and piece of tail sectioned for genotype analysis. Then, infected mice were observed daily up to 20 DPI to monitor survival. Forty-eight transgenic Thy-1/ApoD mice and 45 wild-type (WT) littermates, as well as 32 transgenic NSE/ApoD versus 51 WT littermates and 53 transgenic NFL/ApoD versus 46 WT littermates were used to establish survival curves. Survival rate was calculated at 20 days after HCoV-OC43 inoculation.

5.4.4 Infectious virus assays

Five transgenic mice and 5 WT littermates for each genotype were dissected at 11 DPI for infectious virus assays. Brains were homogenized to 10% (w/v) sterile PBS, centrifuged at 4°C, 20 min at 1,000 x g, and supernatants were immediately frozen at -80°C and stored until assayed. The extracts were processed for the presence and quantification of infectious virus by an indirect immunocytotochemistry assay, as previously described (Jacomy and Talbot 2003).

5.4.5 RNA extraction and Northern blot analysis

Total RNA was extracted from brain or spinal cord by homogenization in the Trizol reagent (Invitrogen, Burlington, ON). RNA (10µg) was separated on 1.5% (w/v) agarose-formaldehyde gels and blotted to a nylon membrane. The membranes

were hybridized with [α-32P] dCTP-labeled human or mouse apoD, and mouse GAPDH cDNAs. The hybridization signal was detected with a Bio-Rad Imaging screen K, read with a PhosphorImager and analyzed with the QuantityOne software (Bio-Rad Molecular Imager FX, Bio-Rad Laboratories, Mississauga, ON).

5.4.6 Protein extraction and Western blot analysis

Brain and spinal cords were homogenized in lysis buffer (50 mM Tris-HCl pH 7.3, 150 mM NaCl, 5 mM EDTA, 0.2% (v/v) Triton X-100, and 10% (w/v) Complete protease inhibitor (Roche, Laval, QC)). After 30 min of incubation at 4°C, lysates were sonicated and cleared by centrifugation. Protein concentration was determined using the Bio-Rad protein assay (Bio-Rad Laboratories). Proteins (10 μg per sample) were separated on a 12% (w/v) SDS-polyacrylamide gel and transferred to PVDF membranes. Membranes were incubated with the primary antibodies: human apoD mouse monoclonal antibody (2B9), 1:100000; mouse apoD rabbit polyclonal antibody, 1:500; HCoV-OC43 nucleocapsid N protein (OC43 (N)) mouse monoclonal antibody 1:100; GFAP rabbit polyclonal antibody (Cell signaling-NEB, Pickering, ON), 1:5000; Mac-2 rat monoclonal antibody (ATCC-Cedarlane, Burlington, ON), 1:100; CD4 rat monoclonal antibody (BD Pharmingen, Mississauga, ON), 1:500; GAPDH mouse monoclonal antibody (Calbiochem, San Diego, CA), 1:500000. Binding of these primary antibodies was detected with appropriate horseradish peroxidase-conjugated secondary antibodies and visualized by chemiluminescence (Amersham ECL, GE-Healthcare, Baie d'Urfé , QC) and X-ray film.

5.4.7 Immunohistochemistry

Serial vibratome sections (40 μm) of paraformadehyde-perfused brains were subjected to immunohistochemistry as already described (Jacomy and Talbot 2003).

Viral antigens were detected with 4-E11.3 mouse monoclonal antibody (1:1000) (Bonavia *et al.* 1997). Astrocytes and microglia/macrophages were identified respectively with GFAP rabbit polyclonal antibody (1:50; DAKO, Mississauga, ON) and Mac-2 rat monoclonal antibody (1:100; ATCC).

5.4.8 Flow cytometry

Brain cell suspensions were prepared and analyzed for CD4 and CD8 cell surface expression. Briefly, brains were ground between frosted glass slides, suspended in cold RPMI and passed through nylon mesh. Percoll (GE Healthcare) was added to a final concentration of 30% (v/v) and the homogenate was centrifuged at 1,300 x *g* for 30 min at 4°C. The cell pellet was washed and cells counted. Antibodies (BD Pharmingen) used for immunophenotyping were fluorescein isothiocyanate (FITC)-conjugated rat anti-mouse CD4 and phycoerythrin (PE) anti-mouse CD8a. Isotype controls (BD Pharmingen) were included for each antibody used. Flow cytometric analyses were done with a fluorescence-activated cell sorter scanner (FACScan; Becton Dickinson), and the data were processed with the WinMDI software.

5.4.9 Total PLA2 activity

Brains were homogenized in cold buffer (50 mM HEPES, pH 7.4, containing 1 mM EDTA; 10 ml per g of tissue) and centrifuged at 10,000 x *g* for 15 min at 4°C. The supernatant was used to quantify total phospholipase activity using the cPLA2 colorimetric assay kit (Cayman Chemical, Ann Arbor, MI) without the addition of specific PLA2 inhibitors according to the manufacturer's total PLA2 activity protocol.

5.4.10 Cytokine quantification

Brains from Thy-1/ApoD and WT littermate mice were dissected at 8 and 11 DPI for cytokine assays. Brains were weighed and homogenized in 10% (w/v) sterile PBS (pH 7.4) containing Halt protease inhibitor cocktail (Pierce-Fisher Scientific, Ottawa, ON). Following homogenization, tissues were centrifuged at 4°C, 15 min at 1,500 x *g*, then supernatants were immediately collected and stored frozen at -80°C until assayed. The extracts were processed for the presence and quantification of cytokines using SearchLight Chemiluminescent Protein Arrays and were performed by the SearchLight Sample Testing Service of Pierce Biotechnology (Woburn, MA).

5.4.11 Statistical analyses

Survival rates were plotted as Kaplan-Meier survival curves and were compared using the log-rank (Mantel-Cox) test or Student's t-test for the survival rate at 20 DPI. One-way ANOVA was used for histogram analyses. Statistical significance was defined as $P < 0.05$.

5.5 Results

5.5.1 Clinical status of mice following HCoV-OC43 infection

During the first week post-infection, mice ate and drank normally and did not loose weight. Between 8 to 9 DPI, infected mice presented ruffed fur and, one day later, showed humped back posture, as previously described (Jacomy and Talbot 2003). At around 11 DPI, mice either recovered rapidly and showed no further symptoms of encephalitis (classified as having mild signs) or they became anorexic, inactive, dehydrated and start to die from encephalitis (classified as having severe signs). Mice with severe signs of impairment, lethargy or eating/drinking difficulty were immediately euthanized.

5.5.2 ApoD is induced in the CNS of HCoV-OC43- infected mice

To investigate whether HCoV-OC43 infection modulated apoD gene transcription, infected WT mice were sacrificed at 7, 12 and 20 DPI and different parts of the brain were processed for the detection of apoD gene expression. Results show that apoD transcription was increased in response to HCoV-OC43 infection (Fig. 5.1). The CNS regions showing the highest apoD up-regulation were the cortical area (cortex) and hippocampus with a 5- and 6-fold increase in expression at 7 DPI, respectively. At this time post infection, mice did not yet show pathological symptoms of infection. ApoD expression was further increased at 12 DPI, when mice began to present morbidity and reached 11- and 13-fold induction, respectively, when compared to non-infected (control) mice. At 12 DPI, apoD gene expression reached its maximum in all CNS regions tested. Its expression was increased 2- to 3-fold in the medulla and olfactory bulb and 6-fold in cerebellum and spinal cord. At 20 DPI,

apoD transcription returned to baseline levels in mice which survived the infection (Fig. 5.1).

5.5.3 ApoD induction correlates with virus load and astrocytic and microglial activation

ApoD protein levels were closely consistent with mRNA levels and were highest in cortex and hippocampus. Maximal protein levels were also observed at 12 DPI in all CNS tissues (Fig. 5.2), which corresponded to the time of acute phase of the encephalitis. Increased apoD levels were also consistent with the presence of HCoV-OC43. Actively replicating HCoV-OC43 could be detected at 7 DPI as well, as seen by the additional band above the OC43 (N) band, as previously described (Jacomy and Talbot 2003). Delayed expression of apoD protein in the cerebellum and spinal cord was also correlated with delayed HCoV-OC43 replication, in accordance to virus spread and invasion of the remote areas, located far from the initial inoculation site (Fig. 5.2). HCoV-OC43 and apoD increases were also concomitant with astrocyte and microglia activation as detected with antibodies against the astrocyte-specific marker glial fibrillary acidic protein (GFAP) and the microglia activation marker Mac-2, respectively. Indeed, ApoD, GFAP, Mac-2 and virus levels were closely regulated in all analyzed CNS regions. At 20 DPI, in those mice that survived the infection, HCoV-OC43 proteins disappeared totally and apoD, GFAP and Mac-2 returned to baseline levels, confirming that mice had recovered from the acute infection.

5.5.4 Transgenic mice expressing H-apoD are more resistant to acute encephalitis

To investigate the role of apoD during viral encephalitis, three different transgenic mice over-expressing H-apoD in neurons and WT littermates were

infected by HCoV-OC43. Survival curves were established for each transgenic mouse group and compared to corresponding WT littermates (Fig. 5.3). Survival rates were almost three times higher in transgenic mice. Nineteen percent of the Thy-1/ApoD mice (9 mice on 48) survived following infection while only 7% ($p = 0.0112$) of WT littermates (3 mice on 45) survived the infection (Fig. 5.3A). Moreover, males were significantly better protected by apoD overexpression even though these are more sensitive to infection. Indeed, male Thy-1/ApoD mice had a survival rate of 21% compared to 7% for WT ($p = 0.0041$) (Fig. 5.3B). Still, female Thy-1/ApoD mice were also less susceptible than female WT mice (Thy-1/ApoD, 16%; WT, 7%; $p = 0.0458$) (Fig. 5.3C). However, survival rates were similar for NSE/ApoD and NFL/ApoD as compared to WT littermates, with 84% deaths for NSE/ApoD (Fig. 5.3D) and 79% deaths for NFL/ApoD (Fig. 5.3E), with no apparent difference between females and males. It is noteworthy that NSE/ApoD and NFL/ApoD mice produce respectively moderate and low levels of H-apoD in their CNS when compared to Thy-1/ApoD mice, in accordance with the relative strength and expression pattern of each promoter in neuronal cells (Fig. 5.3F). Interestingly, the NSE/apoD transgenic mice presented a survival curve that was slightly shifted in relation to time suggesting that these mice died less rapidly from infection (Fig. 5.3D).

5.5.5 H-apoD increases infection-induced CNS glial activation

Since only Thy-1/ApoD expression seemed to confer protection against acute viral encephalitis, further experiments were carried out with these mice only. Presence of the H-apoD transgene did neither affect endogenous mouse apoD mRNA expression in response to HCoV-OC43 infection (Fig. 5.4A) nor its protein levels (Fig. 5.4B). Brain infectious virus titers showed no statistical difference between Thy-1/ApoD mice and its littermates as measured at 11 DPI (Fig. 5.4C). Accordingly, viral nucleocapsid protein levels, in the brain and spinal cord (Fig. 5.4B) were also

similar in Thy-1/ApoD and in WT mice. However, astrogliosis (increased GFAP staining) and microgliosis (increased Mac-2 staining), signs of an inflammatory reaction, were observed following infection and were more evident in the CNS of Thy-1/ApoD than in WT littermates. In contrast, a decreased CD4 infiltration was evident in H-apoD over-expressing (Thy-1/ApoD) mice as compared to WT (Fig. 5.4B). Of note, in non-infected tissues, GFAP, Mac-2 and CD4 levels remained similar in WT and Thy-1/apoD mice (data not shown). Immunohistochemistry on brain slices revealed a quite similar increase of activated microglial cells and astrocytes for all genotypes. Astrogliosis and microgliosis were diffused in CNS regions and found mainly in infected regions, as illustrated for hippocampus in figure 5.4D. Mac-2 and GFAP staining were dependant upon the region observed, the presence of virus in the region and the intensity of the disease, mild versus severe, in WT and H-apoD mice.

5.5.6 Phospholipase A2 activity during infection

Total levels of PLA2 activity were measured in the brains of non-infected mice (controls) to determine baseline levels in all groups of studied mice. Quantification revealed that baseline levels were similar in WT versus transgenic mice (Fig. 5.5). However, following HCoV-OC43 infection, there was a 100% (2-fold) increase of PLA2 activity in WT mice. In comparison, PLA2 activity in infected-Thy-1/ApoD mice was also up-regulated but significantly less than in infected WT mice (40%; Fig. 5.5). Interestingly, NSE/ApoD and NFL/ApoD mice, which displayed the same survival curve than WT mice after infection, have levels of PLA2 activity comparable to WT mice. In addition, PLA2 activity levels were higher in NFL/ApoD than in Thy-1/ApoD mice. However, PLA2 levels in NSE/ApoD were not statistically different from those in Thy-1/ApoD mice.

5.5.7 H-apoD reduces T-cell infiltration into the CNS

Immunoblots already showed that CD4 was downregulated in Thy-1/ApoD compared to WT mice after HCoV-OC43 infection (Fig. 5.4B). To further examine T-cell infiltration, FACS analyses were conducted on total brain extracts from mice dissected at 4, 6, 8 and 11 DPI (Table 5.1 and supplemental Fig. 5.1). In infected WT mice, both CD4- and CD8- expressing cells entered the CNS and increased significantly with time. At 11 DPI, there was a clear split between animals that will probably have survived the infection (showing mild signs of encephalitis; 11 DPI-mild) and those that will most likely have died (showing severe signs of encephalitis; 11 DPI-severe). T-cell infiltration correlated with the outcome of the infection, as T-cell infiltration was more prominent in 11-DPI-severe than in 11 DPI-mild animals. Accordingly, a similar modulation of T-cell infiltration was observed in Thy-1/ApoD mice. Moreover, H-apoD (Thy-1/ApoD) expression in neurons significantly lowered the T-cell infiltration after infection in mice with mild as well as severe encephalitis as compared to WT mice (Table 5.1 and supplemental Fig. 5.1).

5.5.8 H-apoD reduces inflammatory cytokine and chemokine production

Activated microglial and astroglial cells, as well as leukocytes infiltrating the CNS can secrete cytokines and chemokines. Therefore, we measured CNS levels of several of these proteins during the acute phase of viral encephalitis. At 8 and 11 DPI, most of inflammatory cytokines could be detected in infected brains, such as IL-1ß, IL-2, IL-6, TNF-α, INF-γ or GMCSF. Although IL-1ß and TNF-α protein levels were similar in WT and Thy-1/ApoD mice at 8 DPI, an upregulation of IL-1ß and TNF-α was maintained in WT as compared to Thy-1/ApoD at 11 DPI. (Fig. 5.6A and B). By contrast, IL-6 levels were downregulated in WT versus Thy-1/ApoD mice. Interleukin-6 (IL-6) acts as both a pro-inflammatory and anti-inflammatory cytokine

(Stoll *et al.* 2000). The role of IL-6 as an anti-inflammatory cytokine role is mediated through its inhibitory effects on IL-1 and this could explain the reduction of IL1-ß in Thy-1/ApoD brain. As the matrix metalloproteinase (MMP) family members are involved in the breakdown of extra-cellular matrix in normal physiological processes, as well as in disease processes, we investigated the levels of MMP. Although levels of MMP-9 and MMP-3 were high in infected brains, no differences were seen between genotypes (Fig. 5.6C). The high levels of MMP-9 and MMP-3 could favor the trafficking of leukocytes into infected brains. We then investigated inflammatory chemokines that can modulate the recruitment of leukocytes into infected tissues. At 8 DPI, the monocyte chemoattractant protein-1 (MCP-1 or CCL2) was detected at similar levels in WT and Thy-1/ApoD mice. MCP-1 stimulates monocytes to leave the bloodstream, enter the surrounding tissue and become tissue macrophages (Calvo *et al.* 1996). MCP-1 facilitates the migration of T cells towards the CNS, as well (Biernacki *et al.* 2004). At 11 DPI, MCP-1 levels were down-regulated in Thy-1/ApoD mice but remained unchanged in WT mice. At 8 DPI, T cell-attracting ((RANTES (CCL-5) and IP-10 (CXCL-10)) chemokine levels were quite similar for both mouse genotypes (Fig. 5.6D). At 11 DPI, similarly to MCP-1, levels of RANTES showed a decrease in Thy-1/ApoD mice, probably resulting from a reduction of T cell and macrophage infiltration, whereas high levels remained in WT littermates. These data are consistent with the higher T-cell infiltration observed in WT at 11 DPI (Table 5.1).

5.6 Discussion

Host survival to viral infections mainly depends on the ability to trigger and regulate innate and adaptive inflammatory responses, which promote clearance of virus and cell debris, as well as on its capacity to repair and/or replace damaged cells. An up-regulation of apoD gene expression was already reported in humans with meningoencephalitis (Terrisse *et al.* 1998) and in the CNS of mice infected by encephalitis-associated viruses such as herpes simplex type-1 virus (HSV-1) (Kang *et al.* 2003), Sindbis virus (Johnston *et al.* 2001), Japanese encephalitis virus (JEV) (Saha and Rangarajan 2003) or rabies virus (Prosniak *et al.* 2001). These observations support the hypothesis that common host cell pathways are activated in the CNS by different neurotropic and neuroinvasive viruses. Here, we report for the first time, that apoD mRNA and protein are up-regulated after acute viral encephalitis caused by HCoV-OC43 infection. Until now, functional up-regulation of apoD during infection has remained unclear. We demonstrate that up-regulation of apoD in CNS seems to confer a neuroprotective effect. Indeed, neuronal overexpression of apoD in H-apoD transgenic mice resulted in a statistically significant 3-fold increase in the number of mice surviving to HCoV-OC43 infection.

Neuroinflammation was already reported after infection with HCoV-OC43 (Butler *et al.* 2006, Jacomy and Talbot 2003, Jacomy *et al.* 2006). A key component of neuroinflammation is the activation of astrocytes and microglia. Upon activation, these cells proliferate, increase in size, change morphology and produce cytokines. Activated microglia can also migrate to the injury site and phagocyte dead cells and cellular debris (Farooqui *et al.* 2007). Here, we demonstrate that during acute encephalitis, the up-regulation of endogenous apoD coincides perfectly with glial activation and that its expression returned to normal levels after clearance of the acute viral infection, concomitantly to a resolved glial reactivity.

The expression of H-apoD in neurons of Thy-1/ApoD mice, which we showed to result in an increased survival rate following acute encephalitis, was associated with an increased activation of glial cells during the acute phase of the infection. The function of activated glia in neurological disorders is a highly controversial subject. Chronic activation of glia is deleterious, in contrast to limited acute activation of glia, which is generally accepted as a beneficial response favoring organism repair. Indeed, controlled microgliosis restricts brain damage following acute brain injury probably by removing cellular debris, neurotoxic molecules, and hence providing an environment that promotes repair, neuron regeneration, and associated neuritic outgrowth (Simard and Rivest 2007). Activated microglia can also serve as a source of trophic and growth factors (Elkabes *et al.* 1996). Several studies also demonstrated that astrocyte activation protects neurons by circumscribing the damaged area by the formation of a scar, by limiting leukocyte infiltration, by promoting blood-brain barrier (BBB) repair and by sustaining neuronal survival through nutrient contribution and regulation of cell-to-cell communication (Bush *et al.* 1999, Faulkner *et al.* 2004). In other respects, it was previously reported that, following HCoV-OC43 infection, non-infected cells in close proximity to infected ones exhibited signs of apoptosis, suggesting that some inflammatory molecules, released by activated glial cells adjacent to infected neurons are deleterious to neurons (Jacomy *et al.* 2006). The fact that neuronal H-apoD expression promotes both glial activation and limited leukocyte infiltration into CNS, as well as increased mouse survival to infection suggests that apoD-induced glial activation was neuroprotective against viral damage. It has already been demonstrated that endogenous apoD expression was increased in activated microglia cells (Gebicke-Haerter 2005) and also during inflammatory brain disorders (Franz *et al.* 1999, Reindl *et al.* 2001, Rickhag *et al.* 2006).

During reactive gliosis, PLA2, an important enzyme for the production of AA is up-regulated (Sandhya *et al.* 1998, Stephenson *et al.* 1996, Walton *et al.* 1997). The ability of specific PLA2 inhibitors to reduce neuronal damage supports an important

role for AA in neurodegeneration (Farooqui *et al.* 2004). It was already suggested that apoD plays an important role in the regulation of AA signaling and metabolism. ApoD could influence the availability of free AA in the cell, first by stabilizing it in cell membrane, thus preventing its liberation by PLA2; or second by binding/chelating free AA in the cytosol, thus making it unavailable for further use in enzymatic pathways (Thomas *et al.* 2003d). The present study suggests another way for apoD to control free AA concentration in cell: by modulating PLA2 activity. Indeed, H-apoD in Thy-1/ApoD mice prevented in part the increase of PLA2 activity following HCoV-OC43 infection. The effect on PLA2 activity is dependent on the levels of H-apoD expression. Indeed, NSE/ApoD and NFL/ApoD mice, which express lower levels of H-apoD, displayed similar levels of PLA2 activity and survival rate than WT mice following infection. The decreased PLA2 activity in Thy-1/ApoD mice is most probably related to the decreased cytokine production in these mice, as IL-1α, IL-1β and TNFα stimulate PLA2 activity (Adibhatla and Hatcher 2007).

It has already been demonstrated that, following HCoV-OC43 infection, a large fraction of cells infiltrating into the CNS of the animals consists of CD4 and CD8 T-cells (Butler *et al.* 2006). The role played by the infiltration of inflammatory cells in HCoV-OC43 encephalitis is not well defined. Immunosuppression by cyclosporin A resulted in the acceleration of the pathology onset and increased the percentage of acute animal deaths (Jacomy and Talbot 2003). On the other hand, HCoV-OC43 induced death is delayed in mice lacking normal B and T cell responses (Rag -/-), even if, at the time of death, these mice had higher virus loads (Butler *et al.* 2006). This data illustrate the precarious balance between immune mediated viral clearance and immunopathogenesis. Some chemokines are considered pro-inflammatory and can be induced during an immune response to recruit cells of the immune system to the site of infection. Interleukin-1 (IL-1) produced by

macrophages forms an important part of the inflammatory response of the body against infection (O'Neill 2000). We demonstrated a maintained up-regulation of IL-1β, particularly in WT mice at 11 DPI. This cytokine increases the expression of adhesion factors on endothelial cells to enable transmigration of leukocytes to sites of infection. Peripheral lymphocyte infiltration into the CNS was previously reported to either protect against or exacerbate encephalitic disease in CNS infection models (Irani and Griffin 1996, Stohlman *et al.* 1995). We propose that an uncontrolled immune response may contribute to neuropathology, as seen in WT mice following viral encephalitis. In the same way, an increased MCP-1 was reported to contribute to virus-induced neuropathogenesis (Nakajima *et al.* 2001, Peterson *et al.* 1997). RANTES, IP-10 and MCP-1 have been previously characterized for their role in the recruitment of activated T cells to the site of infection (Babcock *et al.* 2003, Klein 2004, Weiss *et al.* 1998). These pro-inflammatory chemokines act in the development of inflammatory response and may also induce neurological damages if their synthesis is maintained. Indeed, IP-10 or MCP-1 neutralizing antibodies were shown to reduce pathology but not viral titers (Carr *et al.* 2003, Marques *et al.* 2006, Nakajima *et al.* 2001).

In the present study, the increased survival of Thy-1/ApoD mice correlates with a decreased number of infiltrating T-cells, associated with decreased T-cell-attracting chemokine levels (MCP-1). T-cell infiltration into CNS indicates a compromised BBB (Streit *et al.* 2004) and the decreased infiltration observed in transgenic mice suggests a role for apoD in BBB integrity. In support of this, apoD is expressed in pericytes and perivascular cells in the brain (Hu *et al.* 2001) and it controls proliferation and migration of vascular smooth muscle cells (Leung *et al.* 2004, Sargeant *et al.* 2003,). Furthermore, another lipocalin, the neutrophil gelatinase-associated lipocalin is produced by the choroid plexus as a component of

the innate immune response that protects the central nervous system from infection (Marques *et al.* 2008).

On top of its influence on inflammatory reactions, apoD could also positively affect the host survival by promoting CNS repair either by supporting myelination (Boyles *et al.* 1990a, Ong *et al.* 1999, Terrisse *et al.* 1999), or by evacuating toxic metabolites such as peroxidated lipids (Ganfornina *et al.* 2008) or by supplying nutrients and neuroprotective factors such as estrogens and progesterone (Ghoumari *et al.* 2003, Suzuki *et al.* 2007).

A beneficial role of apoD up-regulation in nervous system pathology and/or injury has often been suggested. However, although it is indeed increased in several neuropathologies, the link between apoD expression and neuronal processes remains obscure. In the present study, we demonstrate for the first time that apoD does protect from the damaging consequences of viral encephalitis, most likely by modulating inflammatory reactions. Therefore, our results, in combination with our recent study involving apoD in the defense mechanisms against oxidative stress (Ganfornina *et al.* 2008), suggests that apoD, as an acute phase protein, could restore the homeostatic balance following injury.

5.7 Acknowledgments

We are thankful to Diego Sanchez and Maria D. Ganfornina for helpful discussions. We gratefully acknowledge support from the Canadian Institutes for Health Research (Grants MT-9203 to PJT and MOP-15677 to ER). SDC was supported by FRSQ, NSERC and UQAM studentships.

Table 5.1: FACS analysis of CD4+ and CD8+ T cells in total brain extracts of mice at various times after intracranial inoculation with HCoV-OC43 or saline solution (control). Data represent mean values ± SD of three mice per genotype, expressed in percentage. All analyses were performed in triplicate.

	Percentage of cells			
	WT		Thy-1/ApoD	
	CD4	CD8	CD4	CD8
control	0.19 ± 0.05	0.10 ± 0.02	0.05 ± 0.02 ***	0 ± 0 ***
4 DPI	2.29 ± 0.54	1.15 ± 0.19	0.23 ± 0.08 ***	0.46 ± 0.14 ***
6 DPI	2.18 ± 0.43	3.93 ± 0.55	1.93 ± 0.43	1.95 ± 0.32 ***
8 DPI	2.40 ± 0.21	2.48 ± 0.46	1.31 ± 0.41 ***	1.31 ± 0.37 ***
11 DPI-mild	1.79 ± 0.98	4.60 ± 1.13	1.99 ± 0.50	2.53 ± 0.63 **
11 DPI-severe	13.26 ± 2.07	6.23 ± 1.34	4.67 ± 1.98 ***	4.32 ± 1.69

* $p<0.05$, ** $p<0.01$, *** $p<0.001$ vs WT mice.

5.8 Figure legends

Figure 5.1: Effect of HCoV-OC43 infection on CNS apoD mRNA expression. Endogenous apoD expression (M-apoD) was examined by Northern blot analysis in several CNS regions of non-infected WT mice (c) and in HCoV-OC43 infected WT mice 7, 12 and 20 days post-infection. GAPDH expression was included as an internal control. Top: Representative autoradiograms. Bottom: Quantification of mRNA expression by densitometry. Values were normalized by the GAPDH expression and by the respective non-infected control which was given an arbitrary value of 1. Values represent means ± SD (n=3, performed in triplicate). * $p < 0.05$, ** $p < 0.01$, *** $p < 0.001$ compared to the respective non-infected control. Hippoc: hippocampus, olfac. bulb: olfactory bulb.

Figure 5.2: Western immunoblot analysis of HCoV-OC43 infected WT mice. Endogenous apoD expression (M-apoD) was examined by immunoblot in several CNS regions of non-infected control mice (c) and in HCoV-OC43 infected mice 7, 12 and 20 days post-infection. HCoV-OC43 nucleocapsid N protein (OC43 (N)), GFAP, and Mac-2 were also tested. GAPDH expression was included as an internal control. Experiments were performed in triplicate (n=3). Hippoc: hippocampus, olfac. bulb: olfactive bulb.

Figure 5.3: Survival curves of H-apoD Tg mice after HCoV-OC43 infection. Thy-1/ApoD mice present an increased survival as compared to WT mice. This effect is observed in curves containing mixed sexes (A) and also when males (B) are analyzed separately from females (C). Survival curves of NSE/ApoD (D) or NFL/ApoD (E) mice (mixed sexes curves are presented). * $p < 0.05$, ** $p < 0.01$ compared to corresponding WT for survival rate at 20 DPI.. F) Immunoblot showing H-apoD protein expression in transgenic brains. GAPDH was used for normalization.

Figure 5.4: Analysis of Thy-1/ApoD mice 11 days after HCoV-OC43 infection. Expression levels in total brain and spinal cord of Thy-1/ApoD HCoV-OC43 infected mice are compared to non-infected (c) and infected WT mice. A) Northern blot analysis of M-apoD. H-apoD is also presented. GAPDH was included as a loading control. M-apoD expression was quantified by densitometry. Values were normalized by the GAPDH expression and by the non-infected control. Values are means ± SD (n=3, performed in triplicate). * $p < 0.001$ compared to the non-infected control. B) Western blot analysis of M-apoD. H-apoD, HCoV-OC43 nucleocapsid N protein (OC43 (N)), GFAP, Mac-2, and CD4 expression were also tested. GAPDH expression was included as a loading control. Experiments were performed in triplicate (n=3). Note that the GFAP intensities for Thy-1/ApoD in brain and spinal cord are not statistically different. C) Amount of infectious virus detected in brain. Values are means ± SD (n=3). D) Immunohistochemistry of inflammatory response in hippocampus. Astrogliosis (revealed by GFAP staining) and microgliosis (revealed by Mac-2 staining) were evident in regions where cells are positive for viral antigens (OC43) in both WT and Thy-1/ApoD mice.

Figure 5.5: Total PLA2 activity. PLA2 activity was measured 11 days post-infection in HCoV-OC43 infected (OC43) and in non-infected control mice (c) and normalized by the activity in non-infected WT mice. Values are means ± SD (n=4, tested in triplicate). * $p<0.05$, ** $p<0.01$, ***$p<0.001$ vs corresponding control; # $p<0.05$, ## $p<0.01$.

Figure 5.6: Innate immune response measured in brain following HCoV-OC43 infection. Pro-inflammatory cytokines (A and B), MMPs (C) and chemokine (D) protein levels were measured in WT and Thy-1/ApoD mice at 8 and 11 DPI. Values are means ± SD (8 DPI, n=3; 11 DPI, n=2). * $p<0.05$, ***$p<0.001$ vs corresponding WT.

Figure 5.1

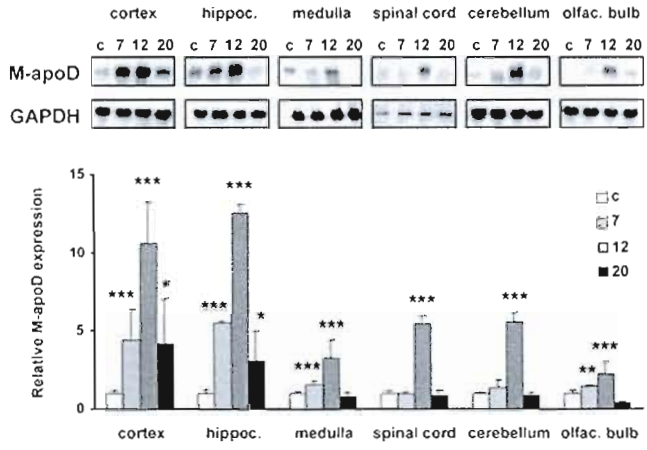
cortex
hippoc.
medulla
spinal cord
cerebellum
olfac. bulb
c 7 12 20
M-apoD
GAPDH
Relative M-apoD expression
15
10
5
0
c
7
12
20
***
**
*

Figure 5.2

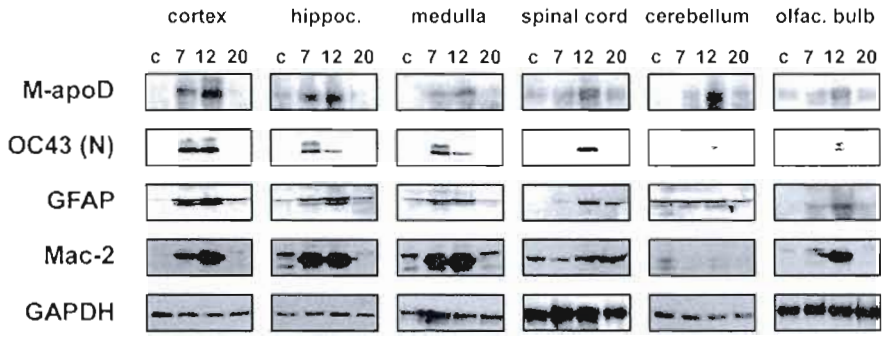
cortex
hippoc.
medulla
spinal cord
cerebellum
olfac. bulb
c 7 12 20
M-apoD
OC43 (N)
GFAP
Mac-2
GAPDH

Figure 5.3

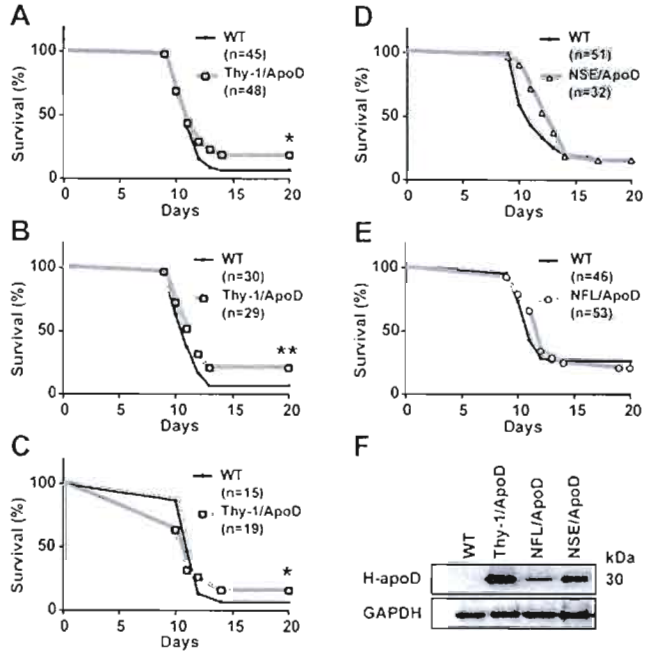
A
WT
(n=45)
Thy-1/ApoD
(n=48)
Survival (%)
Days
*
B
WT
(n=30)
Thy-1/ApoD
(n=29)
**
C
WT
(n=15)
Thy-1/ApoD
(n=19)
*
D
WT
(n=51)
NSE/ApoD
(n=32)
E
WT
(n=46)
NFL/ApoD
(n=53)
F
WT
Thy-1/ApoD
NFL/ApoD
NSE/ApoD
kDa
H-apoD
30
GAPDH

Figure 5.4

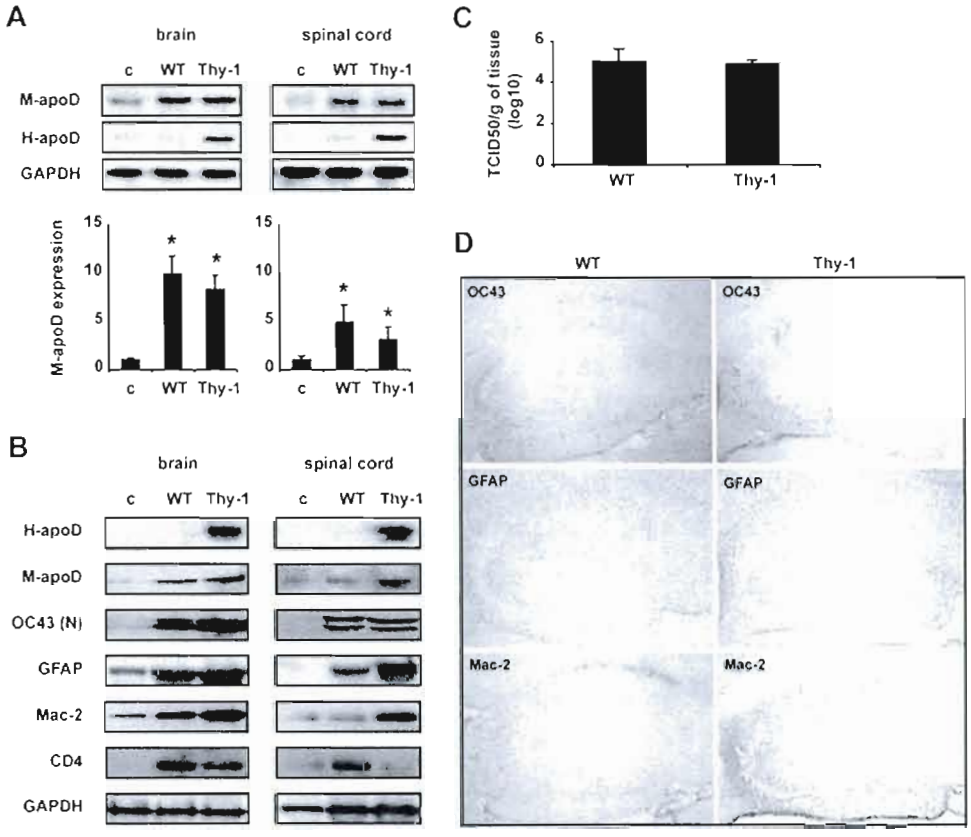
A
brain
spinal cord
c WT Thy-1
c WT Thy-1
M-apoD
H-apoD
GAPDH
M-apoD expression
15
10
5
0
*
B
brain
spinal cord
H-apoD
M-apoD
OC43 (N)
GFAP
Mac-2
CD4
GAPDH
C
TCID50/g of tissue (log10)
6
4
2
0
WT
Thy-1
D
WT
Thy-1
OC43
GFAP
Mac-2

Figure 5.5

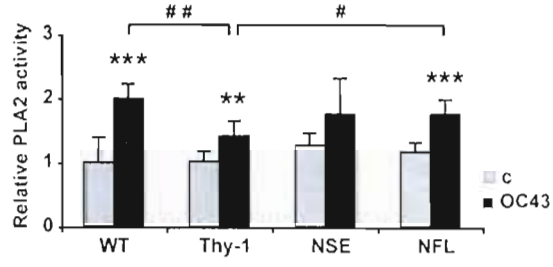

Figure 5.6

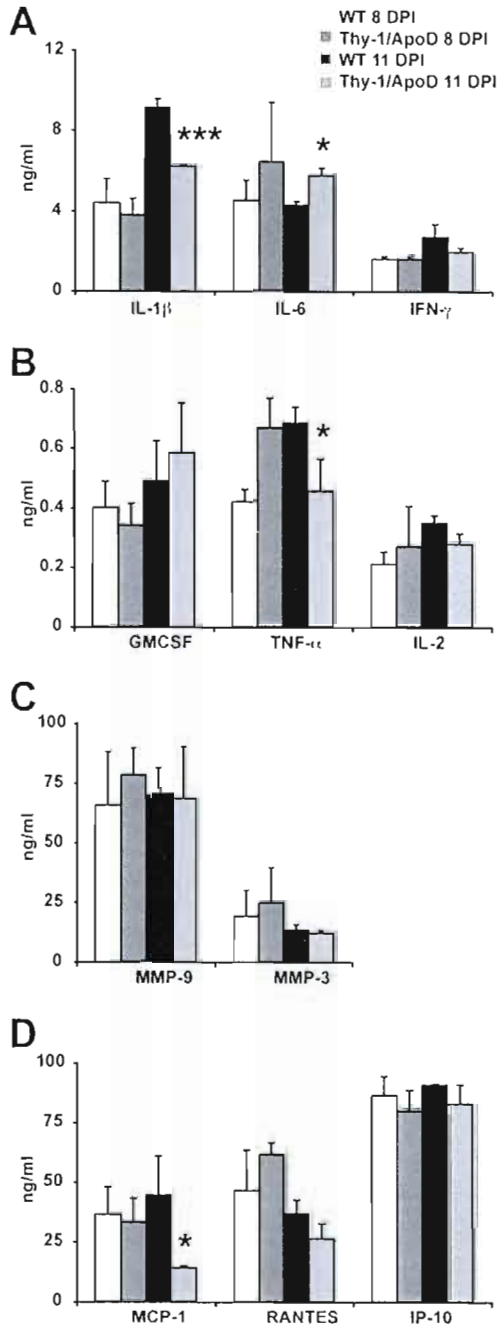
A
WT 8 DPI
Thy-1/ApoD 8 DPI
WT 11 DPI
Thy-1/ApoD 11 DPI
ng/ml
12
8
4
0
***
*
IL-1β
IL-6
IFN-γ
B
ng/ml
0.8
0.6
0.4
0.2
0
*
GMCSF
TNF-α
IL-2
C
ng/ml
100
75
50
25
0
MMP-9
MMP-3
D
ng/ml
100
75
50
25
0
*
MCP-1
RANTES
IP-10

5.9 Supplemental material

Figure 5.1S: T cell infiltration into HCoV-OC43-infected brain. FACS analysis of CD4+ and CD8+ T cells in total brain extracts of mice at various times after intracranial inoculation with HCoV-OC43 or saline solution (control). Data from one representative mouse per genotype and time-point are shown.

Figure 5.1S

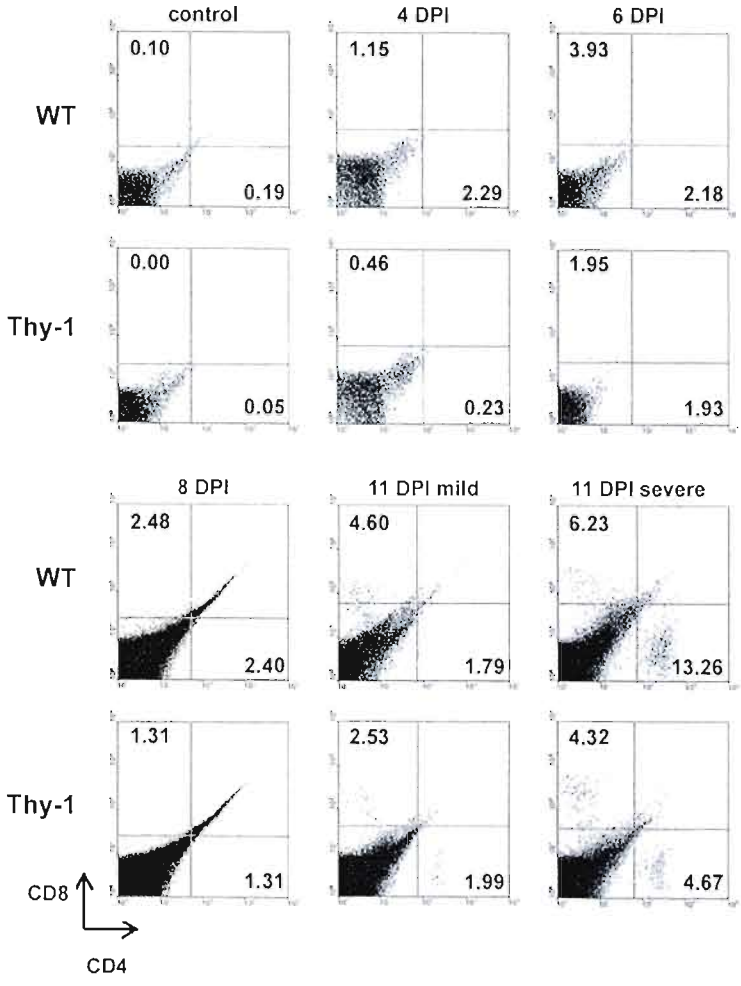
control
4 DPI
6 DPI
WT
0.10
0.19
1.15
2.29
3.93
2.18
Thy-1
0.00
0.05
0.46
0.23
1.95
1.93
8 DPI
11 DPI mild
11 DPI severe
WT
2.48
2.40
4.60
1.79
6.23
13.26
Thy-1
1.31
1.31
2.53
1.99
4.32
4.67
CD8
CD4

CHAPITRE VI

Conclusions et perspectives

6.1 Conclusions générales

Les travaux réalisés dans le cadre de ce projet ont permis d'établir que l'apoD est induite en réponse à des stress cellulaires spécifiques, incluant le stress oxydatif et l'inflammation. Ces travaux sont également les premiers à démontrer que cette induction de l'apoD est bénéfique et favorise la survie en réponse à ces stress chez les mammifères.

Nous avons d'abord déterminé *in vitro* que l'expression de l'apoD est déclenchée par des signaux spécifiques ayant une composante oxydante (peroxyde d'hydrogène et rayons UV) ou inflammatoire (LPS). Cependant, alors qu'en réponse au stress oxydatif l'expression de l'apoD est corrélée avec un arrêt de croissance, en réponse au LPS, elle est corrélée avec une stimulation de la prolifération et peut être inhibée par un traitement anti-inflammatoire. L'activation de l'expression de l'apoD a été associée à des éléments particuliers au niveau du promoteur. Les SRE avaient déjà été identifiés comme responsables de la réponse à l'arrêt de croissance. Les éléments NF-kB, AP-1 et APRE-3 ont maintenant été impliqués dans la réponse au LPS.

Nous avons également déterminé que l'apoD, une protéine glycosylée et sécrétée, est capable d'entrer dans la cellule à partir du milieu extracellulaire et qu'elle change de localisation en réponse au stress. L'apoD est normalement visible dans la cellule sous forme d'un anneau périnucléaire correspondant à l'appareil de Golgi. En réponse au stress, cependant, elle s'accumule dans le cytoplasme et dans le noyau suggérant qu'elle joue un rôle dans ces compartiments cellulaires.

De la même façon, l'expression de l'apoD est induite dans des modèles *in vivo* de neurodégénérescence causée par le stress oxydatif (paraquat) ou l'inflammation aiguë (HCoV-OC43). En utilisant des souris surexprimant l'apoD humaine dans leur système nerveux ou déficientes en apoD, nous avons établi que l'apoD joue un rôle protecteur dans ces situations et que sa surexpression améliore la survie. Les voies par lesquelles l'apoD pourrait jouer son rôle protecteur sont schématisées dans la figure 6.1. D'abord, l'apoD limite la peroxydation lipidique induite par les stress. Ensuite, l'apoD inhibe l'activation de la PLA2 et l'infiltration de cellules T dans le CNS directement ou via l'inhibition des cytokines et des chemokines. Finalement, l'apoD induit l'activation de la glie et la prolifération. Nous avons suggéré que le rôle protecteur de l'apoD est probablement lié à sa capacité à lier un ligand. L'apoD pourrait stabiliser les lipides à la membrane, empêchant leur oxydation et/ou leur conversion en AA. Elle pourrait aussi capturer le AA libre ou des lipides dans le cytoplasme, empêchant leur utilisation dans des réactions enzymatiques ou autres voies nuisibles pour la cellule. Elle pourrait également participer à l'élimination de métabolites toxiques et à l'apport de nutriments ou de facteurs nécessaires à la réparation. Finalement, elle pourrait moduler l'activité de gènes impliqués dans l'activation gliale, la prolifération, la production de cytokines, la détoxification ou ayant des propriétés anti-inflammatoires ou anti-oxydantes. Ces différents aspects seront détaillés dans la section 6.2.

Par ailleurs, l'apoD intervient également dans le métabolisme des lipides et du glucose. En plus du système nerveux, les souris H-apoD-Tg expriment l'apoD humaine dans d'autres tissus dont le foie. La surexpression d'apoD humaine dans le foie induit une accumulation de lipides dans ce tissu. Ceci provoque la diminution de la voie de signalisation de l'insuline, menant ainsi à la résistance à l'insuline chez les souris âgées. Tel qu'illustré à la figure 6.2, nous avons déterminé que l'accumulation de lipides induite par l'apoD est due à la stimulation de gènes impliqués dans la

lipogenèse *de novo*. L'apoD n'affecte pas ou très peu les autres voies pouvant causer l'accumulation de lipides. Ainsi, l'apoD ne diminue pas l'oxydation des lipides ni la production de VLDL. Donc, les souris H-apoD-Tg développent une stéatose hépatique et une résistance à l'insuline avec l'âge et présentent d'autres phénotypes entourant la résistance à l'insuline, comme l'augmentation des globules blancs et des plaquettes. Cependant, ces souris ne sont pas obèses ni diabétiques et ne présentent pas d'augmentation des marqueurs d'inflammation associés à la résistance à l'insuline. Ceci rejoint les résultats obtenus dans les modèles neurodégénératifs *in vivo* et nous mène à conclure que l'apoD joue un rôle protecteur dans l'organisme en modulant des voies intimement liées au développement de pathologies soit le stress oxydatif et l'inflammation.

L'ensemble des travaux présentés dans cette thèse de doctorat met en évidence l'importance de l'apoD dans la réponse au stress cellulaire. Il propose ainsi l'apoD comme cible thérapeutique de premier choix dans les pathologies à caractère oxydant ou inflammatoire en général et dans les maladies neurodégénératives en particulier. Il met également en valeur le rôle de l'apoD dans le métabolisme lipidique et suggère l'importance d'un contrôle serré de ses niveaux.

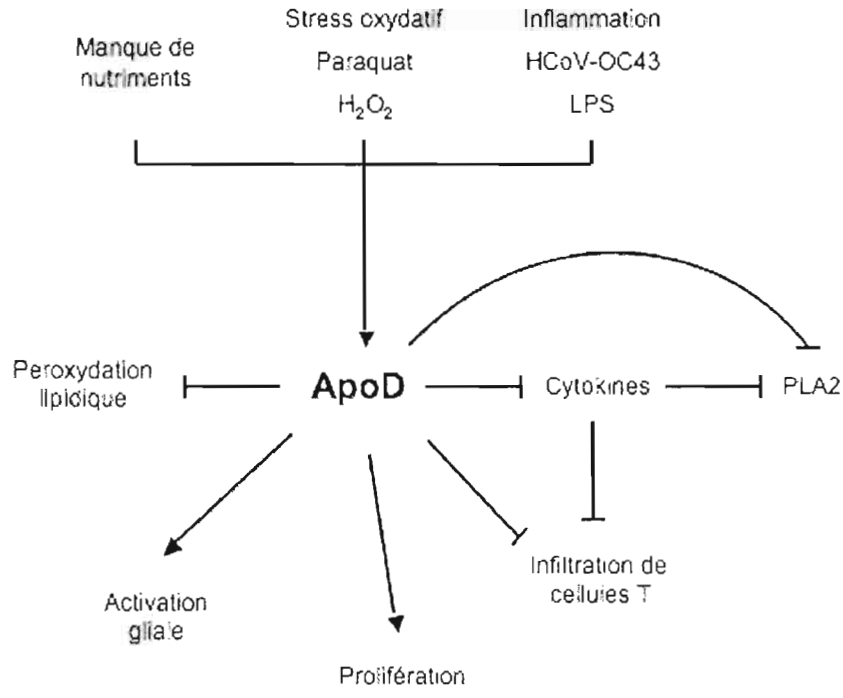

Figure 6.1: L'apoD est impliquée dans plusieurs voies régulant la protection contre diverses formes de stress cellulaire.

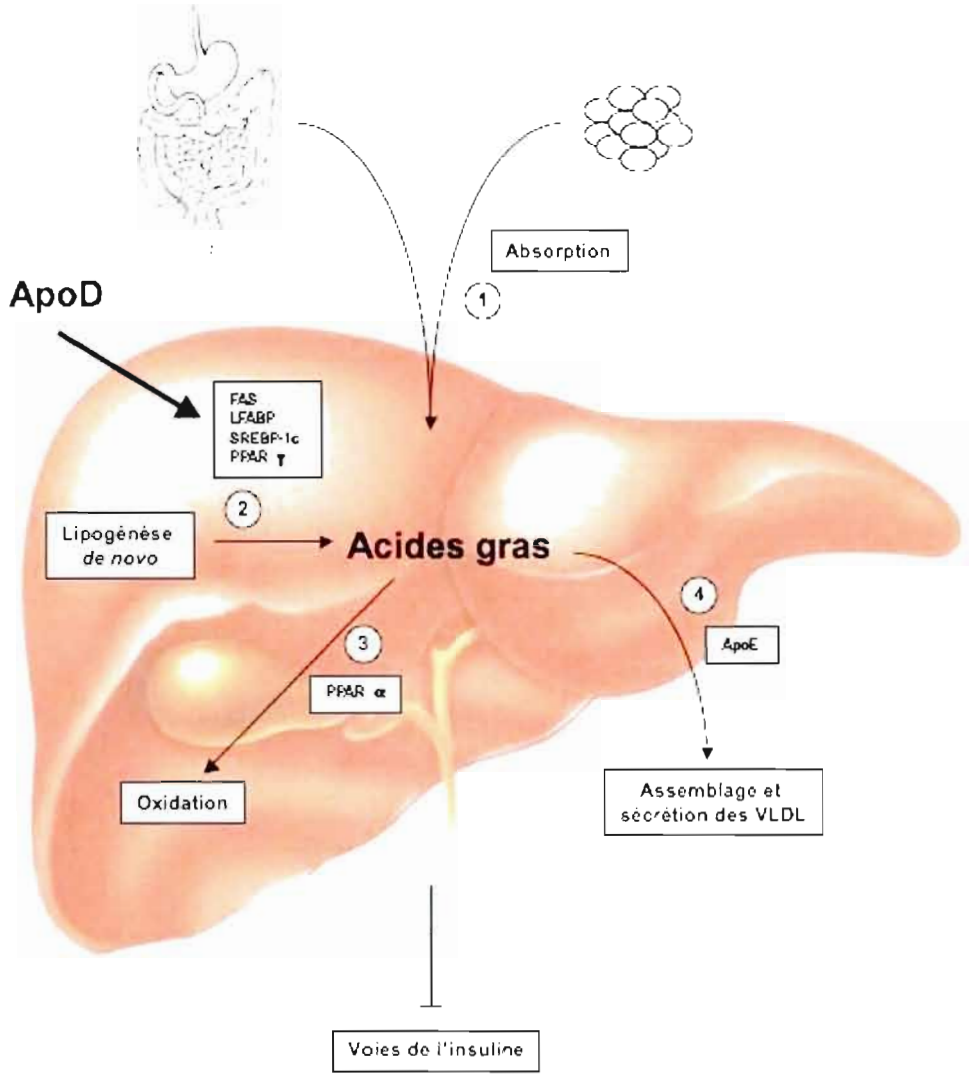

Figure 6.2: Les principales voies impliquées dans le développement de la stéatose hépatique. L'accumulation de lipides peut être causée par une augmentation de l'absorption d'acides gras périphériques obtenus par ingestion ou à partir des tissus gras (1). Elle peut aussi être causée par l'activation de gènes impliqués dans la lipogénèse *de novo* (2). Elle peut finalement être due à la diminution de l'oxidation (3) ou de la sécrétion des acides gras (4). L'apoD favorise la stéatose hépatique en stimulant la lipogénèse *de novo*, provoquant ultérieurement l'inhibition des voies de l'insuline. Adapté de Lavoie et Gauthier, 2006.

6.2 Perspectives

Les travaux présentés dans cette thèse représentent une belle avancée pour la compréhension du rôle de l'apoD. Mais bien sûr, plusieurs questions demeurent. Les expériences proposées comme perspectives visent, d'une part, à compléter les travaux présentés et, d'autre part, à comprendre les mécanismes sous-jacents aux résultats obtenus.

6.2.1 Implication dans les processus cellulaires

6.2.1.1 L'apoD comme modulateur cellulaire

L'examen des gènes modulés en aval de l'apoD peut nous informer quant aux processus dans lesquels l'apoD est impliquée. L'utilisation des micropuces d'ADN (DNA microarrays) est tout à fait indiquée pour ce type de question biologique. Les micropuces sont en fait de petits supports sur lesquels sont distribués des fragments d'ADN correspondant à des milliers de gènes ou à des portions du génome (sondes). Les micropuces sont hybridées de façon stringente avec l'ADNc que l'on désire tester. L'hybridation entre l'ADNc et les sondes est détectée et quantifiée par la flurorescence émise par le fluorophore couplé à l'ADNc. La fluorescence calculée permet de déterminer l'abondance relative des gènes dans l'ADNc. Il s'agirait donc de comparer des souris H-apoD Tg avec des souris WT et des souris ApoD-KO en situations normales et en conditions de stress. Le cerveau est le tissu idéal pour ce genre d'étude puisqu'il est le site majeur d'expression de l'apoD chez la souris et que l'apoD humaine est surexprimée dans ce tissu chez les souris H-apoD Tg. Cependant, étant donné l'implication de l'apoD dans l'accumulation de lipides au niveau du foie, l'utilisation de micro-puces avec de l'ARN extrait à partir du foie pourrait aussi être intéressante. La confirmation des résultats obtenus se fait ensuite au niveau de l'ARN par PCR en temps réel (qRT-PCR) et au niveau des protéines par immunobuvardage

et immunohistochimie. Selon les résultats, d'autres stratégies seront employées. Par exemple, dans le cas où les microarrays indiquent l'implication de l'apoD dans les voies spécifiques du métabolisme lipidique ou du glucose, celles-ci seront explorées plus en profondeur.

6.2.1.2 Identification de son récepteur et de ses interacteurs protéiques

Il est démontré en chapitre II que l'apoD est capable d'entrer dans les cellules puis de s'accumuler dans le cytoplasme et le noyau en situations de stress. Cependant, nous ne savons pas comment l'apoD est transportée. Nous ne pouvons pas éliminer la possibilité que l'entrée de l'apoD dans la cellule se fasse de façon passive. L'apoD profiterait ainsi de ses propriétés lipophiliques pour se glisser à travers la membrane. Cependant, il semble improbable que l'entrée dans le noyau se fasse de façon passive. D'abord l'apoD n'a pas de signal de localisation nucléaire (NLS). Ensuite, l'apoD-GFP utilisée dans l'étude est trop grande pour permettre la diffusion à travers la membrane nucléaire. Ainsi, il est plus probable que l'apoD entre dans la cellule et dans le noyau via l'interaction avec d'autres protéines. Il peut s'agir d'une interaction directe avec un récepteur ou de l'interaction avec une autre protéine possédant un récepteur. L'identification du récepteur de l'apoD et de ses partenaires d'interaction devient donc essentielle. Plusieurs méthodes permettent d'y arriver. On peut postuler dans un premier temps que l'apoD se lie directement à un récepteur membranaire. La visualisation d'un récepteur membranaire peut se faire à l'aide de la méthode «ligand blotting» (Todorov *et al.* 2007). Dans cette méthode, les membranes cellulaires sont solubilisées avec du Triton puis séparées par électrophorèse en conditions dénaturantes ou non-dénaturantes en une ou deux dimensions. Les protéines sont transférées sur une membrane PVDF à haute rétention (ProBlott, Applied Biosystems) puis incubées avec le ligand (dans ce cas-ci l'apoD) marqué au ^{35}S. La spécificité de liaison de ^{35}S-apoD à la membrane est vérifiée par l'incubation en

présence d'un excès d'apoD froid. Les bandes radioactives sont ensuite découpées de la membrane PVDF et identifiées par spectrométrie de masse (MALDI-TOF).

Les partenaires d'interaction de l'apoD, incluant le récepteur, peuvent également être identifiés avec le système Strep-tag (Schmidt et Skerra 2007). Le Strep-tag est un peptide contenant 8 résidus (Trp-Ser-His-Pro-Gln-Phe-Glu-Lys) et ayant une forte affinité pour la streptavine. Le système est disponible commercialement chez IBA-GmbH (One-STrEP Starter Kit cat # 2-1109-000). La protéine d'intérêt (apoD) est clonée dans un vecteur d'expression contenant le Strep-Tag. Le plasmide est ensuite transfecté dans les cellules et au stade désiré, les cellules sont lysées et les complexes apoD-partenaires d'interaction sont purifiés sur une colonne de streptavidine modifiée (Strep-Tactin). Les complexes sont décrochés de la colonne par compétition avec la D-Desthiobiotine puis les protéines sont séparées sur gel (SDS-PAGE). Les complexes non-spécifiques sont éliminés par comparaison avec des complexes provenant de cellules transfectées avec le vecteur vide. Les complexes spécifiques sont découpés du gel et identifiés par spectrométrie de masse. Cette technique a l'avantage de reposer sur un petit marqueur (tag) comparativement à d'autres comme le TAP-tag, évitant ainsi l'encombrement stérique. De plus, ses propriétés physicochimiques permettent une élution douce et rapide en une seule étape, permettant de garder intactes les protéines formant les complexes.

Une fois les partenaires de l'apoD identifiés, l'interaction entre l'apoD et chacun de ces partenaires peut être caractérisée par spectroscopie SPR (surface plasmon resonance) à l'aide de l'appareil BIAcore. Cette technologie permet de visualiser l'interaction entre deux ou plusieurs molécules en temps réel et donc de confirmer que l'interaction est bien réelle. L'apoD est liée à la surface d'une puce de détection (sensor chip) alors que l'autre (ou autres) partenaire est apporté par un flux de tampon. Chaque liaison à la surface de la puce de détection induit un changement de l'indice de réfraction qui est capté par un détecteur. Les changements d'indice de

réfraction sont enregistrés en temps réel sous forme de courbes. Ces courbes disent non seulement s'il y a eu liaison ou non, mais fournissent aussi de l'information sur la cinétique et la force de liaison (Tóth *et al.* 2000)

6.2.1.3 Fonction nucléaire

Tel que détaillé également dans le chapitre II, nous avons démontré que l'apoD accumulée dans le noyau proviendrait fort probablement du milieu extracellulaire. Entre autres raisons, nous invoquons le fait que l'apoD est une protéine sécrétée dont la localisation nucléaire lors d'un stress cellulaire est inhibée par l'application de Brefeldine A, un inhibiteur de l'appareil de Golgi et de la sécrétion protéique. Malgré cela, il est quand même possible que l'apoD nucléaire provienne directement de l'appareil de Golgi. L'appareil de Golgi est responsable de diriger les protéines vers divers compartiments. Entre autres, il peut les diriger vers le noyau via l'action de la phosphatidylinositol-4-kinase (PI4K) (Tekirian 2002). Afin de vérifier cette possibilité, des cellules transfectées avec ApoD-GFP et soumises à un stress pourraient être traitées avec de l'oxide de phenylarsine ou du orobol, des inhibiteurs de PI4K.

Par ailleurs, la localisation de l'apoD dans le noyau comble certainement une fonction. L'apoD et/ou son ligand pourraient agir comme facteur de transcription ou interférer dans des processus nucléaires comme le cycle cellulaire. Souvent, les protéines impliquées dans le cycle cellulaire subissent une modulation de leur expression et de leur localisation au cours du cycle. Pour vérifier si tel est le cas pour l'apoD, il suffit de synchroniser les cellules en phase G0/G1 par déprivation de sérum ou en phase S par double blocage avec de la thymidine, puis de vérifier l'expression et la localisation de l'apoD pendant 24 heures lorsque les cellules sont remises en cycle. La longueur du cycle cellulaire doit aussi être mesurée puisque certaines protéines altèrent la durée du cycle cellulaire. De plus, les résultats obtenus suggèrent

que l'apoD puisse agir comme signal prolifératif dans les fibroblastes. Il serait donc intéressant de mener des études de signalisation cellulaire, en particulier de vérifier l'effet de l'apoD sur l'expression et la translocation nucléaire de ERK 1/2 qui transmet les signaux extracellulaires de prolifération au noyau. De telles études avaient déjà été menées sur des cellules de muscle lisse dans lesquelles l'apoD inhibe la prolifération (Sarjeant *et al.* 2003).

Le rôle de l'apoD comme facteur de transcription requiert que l'apoD ait la capacité de lier l'ADN directement ou via l'interaction avec d'autres protéines. Pour déterminer si l'apoD lie directement l'ADN in vivo et pour connaître le lieu de cette liaison, c'est-à-dire les gènes qui sont ciblés, on peut utiliser la technique ChIP-chip. Cette technique combine l'immunoprécipitation de la chromatine (ChIP) avec la technologie des micropuces à ADN (chip). Ainsi, les cellules ou les tissus dans la condition désirée sont d'abord traités au formaldéhyde afin de lier de façon réversible (cross-link) l'ADN et les protéines qui y sont attachées. Les cellules sont ensuite récoltées et soniquées puis les complexes ADN-protéine d'intérêt sont récupérés. La récupération peut être faite de plusieurs manières. De façon classique, l'anticorps détectant l'apoD est lié à des billes de protéine G magnétiques puis l'extrait cellulaire soniqué est incubé avec ces billes. Alternativement, si l'anticorps est incapable de reconnaître l'apoD lorsque liée à l'ADN, les cellules peuvent être transfectées avec un plasmide contenant l'apoD fusionnée à un marqueur facilement purifiable, par exemple le Strep-tag décrit plus haut. La purification se fait alors sur une résine spécifique au marqueur, par exemple une résine de streptavidine permettant de purifier l'apoD-Strep-tag. Les complexes ADN-protéines sont ensuite élués de la résine et la liaison entre les protéines et l'ADN est inversée par incubation à la chaleur. Les fragments d'ADN sont ensuite amplifiés par PCR. Il est possible, à cette étape-ci, de déterminer s'il y a récupération d'ADN grâce à des méthodes ultra-sensibles. Il est possible par exemple d'évaluer la concentration d'ADN par électrophorèse microfluidique à l'aide d'un Bioanalyser (Agilent 2100). Les

fragments d'ADN sont alors couplés à un fluorophore puis hybridés à des micropuces d'ADN. L'analyse de la fluorescence obtenue permettra d'identifier les régions de l'ADN liées par l'apoD.

Alternativement, le ChIP-sequencing (ChIP-Seq) peut remplacer le ChIP-chip. Cette technique utilise aussi l'immunoprécipitation de la chromatine pour purifier l'ADN lié à la protéine d'intérêt. Cependant, au lieu d'identifier les zones de l'ADN occupées par la protéine à l'aide de micropuces, celles-ci sont identifiées par séquençage grâce à la technologie Solexa. Cette technique nécessite moins d'ADN, n'est pas limitée par le contenu d'une micropuce à ADN et permet une résolution positionnelle plus fine.

Par la suite, on doit déterminer quel est l'effet de la liaison de l'apoD à ces régions d'ADN. Si la région d'ADN identifiée avec ChIP-chip ou ChIP-Seq correspond à un promoteur, des cellules ApoD-KO peuvent être transfectées avec ce promoteur couplé au gène rapporteur de la luciférase, seul ou en combinaison avec un plasmide d'expression contenant l'apoD. On peut ainsi déterminer si l'apoD active ou réprime ce promoteur. Ensuite, on peut vérifier l'expression du gène correspondant et de sa protéine dans des conditions connues comme induisant l'expression de l'apoD, par exemple l'arrêt de croissance ou l'exposition au LPS et ce dans des cellules exprimant ou non l'apoD. Finalement, des mutants délétionnels peuvent indiquer quelle portion de l'apoD est nécessaire pour la liaison à l'ADN.

Dans le cas où l'apoD ne lie pas directement l'ADN mais fait partie d'un complexe transcriptionnel, il est possible d'identifier les composants protéiques par spectrométrie de masse suite à l'immunoprécipitation de la chromatine et l'élimination de l'apoD. L'ordre d'assemblage de ces protéines peut aussi être déterminé.

6.2.2 Études métaboliques

Il est démontré en chapitre III que la présence d'apoD humaine dans le foie de souris H-apoD-Tg provoque l'accumulation de lipides dans ce tissu et conduit à une résistance à l'insuline. Il serait intéressant de continuer l'exploration de ce phénomène.

6.2.2.1 Métabolisme du glucose et des lipides

Les travaux présentés en chapitre III pourraient être complétés avec l'analyse métabolique des souris ApoD-KO. Cependant, on ne s'attend pas à voir de différence par rapport aux souris WT puisque l'accumulation de lipides dans le foie est corrélée avec la surexpression d'apoD humaine dans ce tissu.

Il faudrait également mieux comprendre ce qui provoque l'accumulation de lipides chez les souris H-apoD-Tg. Nous avons observé que l'expression des gènes LFABP, FAS, PPAR gamma et SREBP-1c, impliqués dans la lipogenèse *de novo*, est stimulée chez les souris H-apoD-Tg. La lipogenèse *de novo* peut être quantifiée dans des cultures primaires de foie ou des tranches de foie en culture grâce à l'incorporation de ^{14}C-acétate dans les lipides. Nous avons par ailleurs postulé que la présence de l'apoD humaine pourrait provoquer un débalancement favorisant l'accumulation de lipides au niveau du foie. Il faudrait donc déterminer la composition en lipides et en acides gras du foie par chromatographie en phase liquide et gazeuse (HPLC et GC) et la comparer avec celle de souris WT. Nous avons également conclu que l'oxydation des lipides n'était pas affectée puisque l'expression de PPAR alpha, un gène-clé de l'oxydation lipidique, était stimulée. Cependant, comme il y a de nombreux autres gènes impliqués dans la beta-oxydation des lipides, une mesure globale de l'oxydation des acides gras par le foie peut se faire grâce à la libération de $^{3}H_2O$ par des coupes de foie préincubées avec du ^{3}H-acide palmitique

(Harada *et al.* 2007). Il faudrait également étudier l'influence de l'apoD sur des protéines impliquées dans la fusion puisqu'il a été démontré que les gouttelettes lipidiques visibles dans le foie des souris H-apoD-Tg sont d'abord de petites structures qui s'agrandissent par fusion avec les particules environnantes et que ce processus est dépendant des microtubules et de la dynéine. Il faudrait donc voir si le blocage de différentes protéines impliquées dans la fusion, en présence d'acide oléique, diminue le volume des gouttelettes lipidiques de la même façon dans des hépatocytes primaires de souris H-apoD-Tg et WT. Les protéines connues comme impliquées dans la fusion lipidique sont : NSF (N-ethylmaleimide-sensitive-factor), alpha-SNAP (soluble NSF attachment protein) et ses SNAREs (SNAP receptors), SNAP23 (synaptosomal-associated protein of 23 kDa), syntaxin-5 et VAMP4 (vesicle-associated membrane protein 4) (Boström *et al.* 2007).

Il faudrait aussi déterminer l'influence de la surexpression de l'apoD humaine sur le métabolisme des lipoprotéines. Une modification de la distribution des lipoprotéines circulantes a été constatée dans divers modèles de stéatose hépatique et de résistance à l'insuline (Minehira *et al.* 2008). Ainsi, le profil lipoprotéique des souris H-apoD-Tg, ApoD-KO et WT peut être analysé par FPLC. Il serait également pertinent de quantifier l'abondance de d'autres apolipoprotéines importantes dans le métabolisme lipidique comme l'apoA-I, l'apoA-II, l'apoB-48, l'apoB-100, l'apoC-III et l'apoE.

Nous pourrions aussi vérifier si la résistance à l'insuline chez les souris H-apoD-Tg peut être renversée. Le PPAR gamma, qui est impliqué dans l'adipogénèse et augmenté chez les diabétiques et les souris H-apoD-Tg, a souvent été désigné responsable de la résistance à l'insuline et est la cible de thérapies anti-diabète. Le rosiglitazone, un activateur spécifique de PPAR gamma, active l'adipogénèse induite par PPAR gamma, mais améliore, de façon paradoxale, la sensibilité à l'insuline en favorisant préférentiellement l'accumulation de gras sous-cutané (Edvardsson *et al.*

1999). La réponse à l'insuline (ITT) pourrait être testée suite à l'administration de rosiglitazone. Ceci nous indiquerait aussi l'importance véritable de l'augmentation de PPAR gamma dans le métabolisme de l'insuline chez les souris H-apoD-Tg.

Puisque la phosphorylation de Akt est diminuée presque de moitié chez les souris H-apoD-Tg, l'étude plus approfondie des voies signalétiques de l'insuline pourrait être révélatrice. Vraisemblablement, l'accumulation d'acides gras dans le foie active PKC theta, qui favorise la phosphorylation de IRS1 (insulin receptor substrate 1) (IRS1) sur les résidus sérine et tréonine plutôt que tyrosine bloquant la production de IRS2, et conséquemment l'activation de PI3K. L'inhibition de PI3K empêche finalement le recrutement à la membrane de Akt et donc sa phosphorylation. Cependant, il est possible que la présence de l'apoD induise un changement dans la composition ou la fluidité de la membrane empêchant l'insertion de Akt ou sa phosphorylation. Il faudrait donc vérifier ces deux possibilités en analysant, d'une part, les protéines en amont de Akt et d'autre part les propriétés membranaires, tel que décrit plus loin.

Pour déterminer si la résistance à l'insuline provient bien du foie et non du tissu adipeux ou des muscles, le métabolisme de l'insuline peut être davantage étudié au niveau cellulaire. Pour cela, des adipocytes, des hépatocytes et des myocytes de souris WT, ApoD-KO et H-apoD-Tg sont isolés et divers paramètres du métabolisme du glucose sont évalués. La capacité à lier l'insuline est mesurée par l'incorporation d'insuline marquée au ^{125}I. La capacité à absorber le glucose se mesure par l'incorporation de 3-oxy-methyl-D-glucose en présence ou non d'insuline. La lipolyse est mesurée à l'aide du relarguage de glycerol en réponse à l'insuline en présence ou non d'isoproterenol, un stimulateur de lipolyse (Ciaraldi *et al.* 1997).

Il faudrait aussi examiner les phénomènes entourant souvent la résistance à l'insuline comme l'hypertension, le remodelage cardiaque et l'athérosclérose.

L'athérosclérose est visualisée par microscopie de l'aorte proximale. Elle commence par des dépôts lipidiques puis progresse vers des lésions contenant des cellules spumeuses et des cellules musculaires lisses puis vers des plaques fibreuses. Le remodelage cardiaque est visualisé par échocardiographie et l'anomalie la plus courante est une hypertrophie ventriculaire.

Finalement, il serait intéressant de voir si la surexpression d'apoD humaine spécifiquement dans le foie induit une stéatose et une résistance à l'insuline comparables à celles observées lorsque l'apoD humaine est principalement dirigée vers les neurones. Cela permettrait d'évaluer si une très forte surexpression d'apoD dans le foie aggrave le phénotype observé. Cela permettrait également de dissocier l'effet neuronal de l'effet hépatique sur ces phénomènes.

6.2.2.2 Métabolisme en conditions adipogéniques

Nous avons observé que les souris H-apoD-Tg et ApoD-KO n'ont pas de différence significative de poids par rapport à des souris WT lorsque nourries avec une moulée standard. Il est possible cependant qu'avec une diète riche en gras et en carbohydrates, des différences apparaissent. Il s'agit donc de déterminer si les souris développent de l'obésité et un diabète de type 2 avec des diètes semi-synthétiques contenant divers pourcentages de gras et de carbohydrates (% carbohydrates-protéines-gras: HCLF (41:42:17); HCHF (41:16:43); LCHF (11:45:44)) et voir l'impact de ces diètes sur le métabolisme du glucose et des lipides, tel que décrit dans le chapitre III et ci-haut. En particulier, il faut examiner si la stéatose hépatique évolue vers la fibrose, la cirrhose ou le développement de tumeurs et si l'inflammation reste toujours à un faible niveau.

Si une différence au niveau du poids est constatée, ces études pourraient être complétées avec l'analyse de la composition corporelle et de la dépense énergétique.

La composition corporelle peut être analysée par DEXA (Body Dual X-Ray Absorptiometry) ou par résonnance magnétique qui nous donneront alors le pourcentage de masse maigre et de masse grasse. Le métabolisme énergétique peut être calculé de façon approximative par la consommation d'oxygène (VO2). Une mesure qui reflète mieux la dépense énergétique est le nombre de kilojoules totaux dépensés par jour. La dépense énergétique peut être aussi normalisée par la masse maigre (Trevaskis *et al.* 2005). Il serait aussi intéressant de calculer l'efficacité alimentaire, ou le taux de conversion de la nourriture en poids corporel, qui est défini comme la prise de poids relative au poids de la nourriture ingérée (Jonnson *et al.* 2002) ou aux calories ingérées (Butler et Cone 2003). La dépense énergétique peut aussi être corrélée avec l'activité physique qui peut être mesurée par la distance parcourue, l'activité spontanée (le nombre de fois que la souris déclenche le détecteur de mouvement), l'utilisation de la roue d'exercice ou les battements cardiaques.

Si une diminution de la dépense énergétique est constatée, et puisqu'une réduction de la dépense d'énergie résulte en une augmentation de l'adipogénèse, il peut être pertinent de mesurer les gènes impliqués dans la combustion d'énergie et la différentiation des adipocytes. Par exemple, l'acyl-CoA oxidase, la UCP1, la UCP2 et la carnitine palmitoyltransferase-1 sont inhibés dans le tissu adipeux brun (site de la thermogenèse) des souris p62-/-, un modèle d'obésité où le taux métabolique est réduit. Ces enzymes sont impliquées dans le taux d'oxydation des acides gras dans la mitochondrie. Par ailleurs, le PPAR-gamma est induit dans le tissu adipeux blanc (réserve énergétique de l'organisme) (Rodriguez *et al.*, 2006).

6.2.2.3 Contrôle neuronal du métabolisme

Il y a de plus en plus de preuves en faveur d'un contrôle neuronal de la résistance à l'insuline et de l'accumulation de gras. Or le site primaire d'expression de l'apoD humaine chez les souris H-apoD-Tg est les neurones. Il est possible que la

surexpression de l'apoD dans les neurones provoque, à long terme, un débalancement de ce mécanisme. Il faudrait donc regarder par immunohistochimie dans quel type de neurones s'exprime chacun des transgènes. La localisation de l'apoD dans l'hypothalamus et plus particulièrement sur les neurones NPY/AGRP et POMC/CART du noyau arqué ou les neurones du noyau paraventriculaire, impliqués dans le métabolisme énergétique, pourrait suggérer un rôle pour l'apoD dans le métabolisme du glucose contrôlé par le cerveau.

La surexpression de l'apoD pourrait bloquer directement la réponse à l'insuline ou à la leptine dans les neurones, induisant ainsi une résistance à l'insuline périphérique. Il faudrait dans un premier temps déterminer si les neurones provenant de souris H-apoD-Tg sont sensibles à l'insuline. Pour cela, on peut regarder sur des extraits de cerveau, si la phosphorylation totale sur les tyrosines médiée par l'insuline est altérée. On peut ensuite regarder de façon plus spécifique la phosphorylation de Akt, un composant majeur de la voie de l'insuline. La résistance à la leptine pourrait être causée par la liaison de l'apoD transgénique sur le récepteur de la leptine.

6.2.2.4 Inversion du phénotype

Il serait intéressant de déterminer si le blocage ou l'activation de gènes-clés du métabolisme peut moduler le phénotype des souris H-apoD-Tg. Par exemple, Pten est une phosphatase qui inhibe la voie phosphatidylinositol-3 kinase/Akt. Son inhibition dans les neurones augmente la phosphorylation de Akt, la sensibilité à l'insuline et la dépense énergétique (Plum *et al.* 2007). Par contre, sa délétion dans le foie de souris cause une hépatomégalie et une accumulation de lipides dans le foie, mais améliore la réponse à l'insuline (Stiles *et al.* 2004). Par ailleurs, il a été démontré que l'administration orale de GW3965, un agoniste de LXR, stimule la sécrétion de cholestérol à partir des cellules, ralentissant ainsi l'accumulation de lipides induite par une diète riche et améliorant la tolérance au glucose (Laffitte *et al.* 2003).

L'inhibition de Pten ou l'administration de GW3965 à des souris H-apoD-Tg sont-elles capables de renverser la stéatose hépatique ou la résistance à l'insuline?

6.2.3 Mécanismes de protection

La capacité de l'apoD à protéger les cellules, tel que démontrée en chapitre IV et V, est sûrement étroitement liée à ses propriétés de transporteur, en apportant des facteurs nutritifs ou régulateurs ou en enlevant des déchets métaboliques toxiques. On n'écarte cependant pas la possibilité que ses fonctions puissent être autres que son rôle de transporteur.

6.2.3.1 Interaction avec la membrane cellulaire

Nous avons déterminé que l'apoD protège contre le stress oxydatif en contrôlant le niveau de lipides peroxydés (chapitre IV). De plus, elle protège contre l'inflammation aiguë probablement en agissant sur les voies signalétiques impliquant la PLA2 (chapitre V). Ce rôle peut être joué a priori en stabilisant les lipides à la membrane, empêchant leur peroxydation et leur conversion en AA. Ce rôle peut également être joué a posteriori en éliminant les lipides peroxydés des membranes, prévenant ainsi les boucles de rétroaction positive qui mènent à l'amplification des dommages oxydatifs. L'apoD pourrait également capturer l'AA libre dans le cytoplasme, empêchant son utilisation dans des réactions enzymatiques (par exemple COX-2) ou autres voies nuisibles pour la cellule. Alternativement, le contrôle de la peroxydation lipidique et de l'inflammation pourrait être la conséquence de la régulation de la composition lipidique des membranes par l'apoD, qui va déterminer la susceptibilité des membranes à la peroxydation et à l'action de la PLA2.

Il a déjà été démontré que la composition lipidique du cerveau de souris ApoD-KO est altérée (Thomas et Yao 2007). Il serait donc intéressant de déterminer

la composition en lipides cérébraux des souris H-apoD-Tg, particulièrement la concentration en AA qui est un ligand préférentiel de l'apoD. Ceci peut être fait en suivant la même méthode que chez les souris ApoD-KO soit, en utilisant la méthode HPLC-ELSD (High performance liquid chromatography-Evaporative light scattering detector) pour mesurer les lipides et la méthode GC-FID (Gaz chromatography-Flame ionization detector) pour mesurer les acides gras saturés et polyinsaturés (Thomas et Yao 2007).

Il est également possible de déterminer si l'apoD est capable de lier les composants lipidiques majeurs des membranes, et donc de les stabiliser ou empêcher leur dégradation, par «Fat Western blotting» (Ching *et al.* 2007). Le principe consiste à évaluer la liaison d'une protéine d'intérêt avec des lipides immobilisés sur une membrane de nitrocellulose. Il existe des membranes commerciales contenant 100 pmol de chacun des 15 lipides membranaires les plus abondants (membrane lipid strips, cat. # P-6002, Echelon Biosciences Inc., Salt Lake City, UT). Selon le protocole du fabricant, il s'agit donc de bloquer la membrane avec un tampon contenant 3% d'albumine sérique bovine sans acides gras (fatty acid-free BSA). Ensuite, la membrane est incubée avec la protéine recombinante couplée à la GST (par exemple apoD-GST), lavée puis incubée avec un anticorps anti-GST. La membrane est ensuite incubée avec un anticorps secondaire couplé à la HRP (horse-radish peroxidase) qui est finalement détecté par chemiluminescence.

Il serait également intéressant d'étudier l'effet de l'apoD sur la stabilité membranaire. Pour ce faire, on peut comparer les propriétés structurelles et dynamiques des membranes de cellules, par exemple de neurones, provenant de souris WT, ApoD-KO et H-ApoD-Tg par la méthode ATR-FTIR (attenuated total reflection-Fourier transform infrared spectroscopy) (Gattoni et Boffi 2003). Dans cette technique, des fragments de membrane sont immobilisés sur des cristaux permettant aux rayons infrarouges de traverser, par exemple, une plaque composée de

selenide de zinc (ZnSe). Un détecteur permet alors d'analyser la structure et donc de comparer le positionnement lipidique dans des membranes provenant de différents génotypes de souris. De façon plus simple, l'effet de l'apoD sur la fluidité membranaire peut se mesurer par l'incorporation de 1,6-diphenyl-1,3,5-hexatriene (DPH), un lipide fluorescent, dans la membrane cellulaire (Beck *et al.* 1998).

Des changements de composition lipidique ou de stabilité membranaire entraînent souvent des changements morphologiques au niveau des axones. La forme et l'organisation cytosquelettique des axones sont normalement visualisées dans le nerf optique (SNC) ou dans le nerf sciatique (SNP) à l'aide de la microscopie électronique.

Afin d'analyser l'implication de l'apoD dans l'élimination des lipides peroxidés des membranes, il faut d'abord déterminer si l'apoD peut lier des produits de peroxydation lipidique comme le trans-4-hydroxy-2-nonenal (4-HNE). Le 4-HNE, un produit majeur de la peroxidation lipidique causée par le stress oxydatif, est formé par la dégradation d'acides gras ω-6-polyinsaturés comme l'acide linoléique et l'acide arachidonique, deux acides gras abondants dans les cellules (Hu *et al.* 2002).

6.2.3.2 Propriétés anti-oxydantes

L'apoD pourrait également protèger contre le stress oxydatif par une activité anti-oxydante. Cette activité antioxydante peut se faire de façon directe, c'est-à-dire en éliminant directement les radicaux libres (radical scavenging activity), bien qu'un tel mécanisme semble improbable à cause des propriétés de liaison de l'apoD. Pour le tester, plusieurs approches sont possibles (Govindarajan *et al.* 2003) : 1) L'activité antioxydante peut être quantifiée par le degré de décoloration du radical DPPH (α,α-diphenyl-β-picrylhydrazyl) mesurée par l'absorbance à 520 nm. 2) La capacité

antioxydante totale est mesurée comme l'absorbance à 695 nm en présence de 0.6 M d'acide sulfurique, 28 mM de phosphate de sodium et 4 mM d'ammonium molybdate. 3) L'activité de «scavenging» de l'oxyde nitrique (NO) se mesure par spectrophotométrie à 546 nm en présence de réactif de Griess (1% de sulphanilamide, 2% d'acide phosphorique, 0.1% de naphthyl ethelene diamine dihydrochloride). 4) L'activité «scavenger» d'acide hypochlorique (HOCl) est déterminée par spectrométrie à 412 nm en présence de 40 mM d'acide 5-Thio-2-nitrobenzoïque. 5) La capacité de chélation d'ions Fe^{2+} est estimée à l'aide de l'agent chélatant 2, 2'-bipyridyl. Ainsi, l'extrait contenant l'apoD est pré-incubé avec 50 mM de FeSO4 et 50 mM NaCl (pH 7) avant l'ajout de 1 mM 2,2'-bipyridyl. L'absorbance du complexe bipyridyl-ferreux est mesurée à 525 nm. 6) La décomposition du peroxyde d'hydrogène peut également être déterminée. À l'aide de ces méthodes, on peut donc comparer l'activité antioxydante de l'apoD avec celle de composés ayant des propriétés antioxydantes bien connues comme la vitamine E et l'acide ascorbique.

L'activité antioxydante de l'apoD peut également se faire indirectement via l'activation de voies anti-oxydantes. L'influence de l'apoD sur les enzymes antioxydantes telles que la superoxide dismutase, la catalase, la glutathione, la glutathione reductase et la glutathione peroxidase peut être mesurée par des essais spectrophotométriques (Pippenger *et al.* 1998). L'influence de l'apoD sur d'autres mécanismes de détoxification comme l'activation de la c-jun-N-terminal kinase (JNK) ou l'induction de hsp 70 (heat-shock protein 70) (Manning-Bog *et al.* 2003) peut aussi être étudiée. La JNK est un membre des MAPK (mitogen activated protein kinase). La voie des JNK peut être bloquée par la surexpression de JIP-1b/IB1. Les cellules deviennent alors insensibles à divers stimuli pro-apoptotiques. Les chaperones telles que hsp 70 sont souvent sollicitées dans la réponse au stress. Elles peuvent protéger les protéines contre les dommages oxydatifs et faciliter la dégradation des protéines oxydées via le système du protéasome.

6.2.3.3 Propriétés anti-inflammatoires

L'effet anti-inflammatoire de l'apoD lors d'encéphalite aiguë causée par HCoV-OC43 a été associé en partie avec la diminution de chemokines et de cytokines (IL-1β, TNFα et MCP-1) (Chapitre V) qui provoque une diminution de l'infiltration de leukocytes au cerveau et de la production de PLA2. La prochaine étape consiste donc à explorer les mécanismes sous-jacents à ces propriétés anti-inflammatoires.

On peut se questionner d'abord sur la façon dont l'apoD régule la production de cytokines. NF-κB est activé par les Rho GTPases et joue un rôle clé dans la régulation transcriptionnelle des cytokines, chemokines, molécules d'adhésion et les protéines de phase aiguë comme la CRP (C-reactive protein) (Pahl 1999). Il serait intéressant de comparer l'activation nucléaire de NF-κB par retard sur gel en utilisant des extraits nucléaires provenant de souris ayant divers génotypes d'apoD et un oligonucléotide contenant NF-κB. Au niveau de la voie de signalisation de NF-κB, on pourrait étudier la translocation nucléaire de la sous-unité p65, la dégradation de IκB ainsi que la phosphorylation de p38 suite à l'injection de HCoV-OC43. Plus simplement, on pourrait simplement regarder la phosphorylation de IKB.

Par ailleurs, les PPAR (peroxisome proliferator-activated receptor) α et γ, inhibent la production et les effets néfastes des chemokines et des cytokines et ont été impliqués dans les propriétés anti-inflammatoires de certains composés dont les statines. Entre autres, les PPAR lient les éléments PPRE (PPAR response elements) sur le promoteur du gène sIL-1Ra. L'IL-1Ra soluble est induit par l'IL-1β et module à son tour la réponse à l'IL-1β par sa liaison au récepteur IL-1 de type I, prévenant ainsi les effets de l'IL-1β sur les cellules cibles (François *et al.* 2006). Il est possible de démontrer l'implication de PPARα dans l'effet anti-inflammatoire de l'apoD par

diverses approches : 1) *in vitro* sur des cellules issues de souris WT, ApoD-KO et H-apoD-Tg dans lesquelles PPARα est inactivé par siRNA. On peut mesurer des marqueurs d'inflammation (Cox-2, iNOS, TNFα, IL-1α, IL-1β, IL-6) lors de conditions inflammatoires induites par un traitement au LPS. L'expérience inverse peut être faite par l'administration d'agonistes de PPARα comme le Clofibrate ou le WY-14643. 2) *in vivo* suite au croisement de souris H-apoD-Tg avec des souris PPARα-KO. Si PPARα est impliqué dans l'effet anti-inflammatoire de l'apoD, on s'attend à ce qu'une souris exprimant normalement PPARα et surexprimant l'apoD (PPARα-WT, H-apoD-TG) ait moins de marqueurs inflammatoires qu'une souris ne surexprimant pas l'apoD (PPARα-WT, apoD-WT) suite à l'application d'un modèle inflammatoire. À l'inverse, une souris déficiente en PPARα et surexprimant l'apoD (PPARα-KO, H-apoD-TG) devrait démontrer le même niveau ou une augmentation de marqueurs inflammatoires comparativement à une souris WT. 3) *in vivo* par l'administration d'apoD à des souris PPARα-KO suite à l'application d'un modèle inflammatoire. Le modèle inflammatoire le plus simple est le modèle d'œdème de la patte induit par l'injection locale de carrageenan (Guay *et al.* 2004, Paumelle *et al.* 2006). Les mêmes stratégies peuvent être employées pour étudier les effets de PPARγ. On peut aussi regarder si l'apoD participe à l'activité des PPAR soit en activant leur transcription ou en fournissant les ligands qui activent les PPAR. Les ligands des PPAR sont entre autres les acides gras libres et les eicosanoïdes. L'apoD pourrait donc stimuler les PPAR en apportant directement les acides gras ou en transportant l'acide arachidonique essentiel à la production des eicosanoïdes.

Il faudrait également déterminer si l'effet de l'apoD sur l'activité de la PLA2 est simplement lié à la réduction des cytokines et chemokines ou si l'apoD régule la PLA2 via un autre mécanisme. Il a été rapporté que les lipocortines seraient capables d'inhiber l'activité de la PLA2 en compétitionnant avec la PLA2 pour le substrat phospholipidique plutôt qu'en inhibant directement la PLA2 (Bonventre 1992).

D'autres protéines dont la PLIbeta qui a 33% d'homologie avec la leucine-rich alpha2-glycoprotein humaine sont aussi capables d'inhiber la PLA2 en la liant directement via des motifs riches en leucine (LRR) (Okumura *et al.* 1998). Pour déterminer si la présence d'apoD influence l'activité PLA2, il suffirait de mettre en présence la PLA2 et un substrat phospholipidique avec ou sans l'ajout d'apoD et de calculer l'activité de la PLA2. Il a également été rapporté que des acides gras non estérifiés cis insaturés de même que certains sous-produits de l'acide arachidonique sont capables d'inhiber la PLA2. Il faudrait donc déterminer si l'apoD est capable de lier ces acides gras. Finalement, il faudrait déterminer si l'apoD peut moduler la transcription de la PLA2.

6.2.3.4 Activation de la glie

L'effet anti-inflammatoire de l'apoD lors d'encéphalite aiguë causée par HCoV-OC43 correspondait aussi avec une plus grande activation de la microglie et des astrocytes. L'apoD humaine présente dans les neurones contribue sûrement à cette activation gliale. Cependant, on ne sait rien du mécanisme impliqué ni de la fonction de cette activation. On peut supposer que l'apoD supprime les composantes neurotoxiques tout en augmentant les composantes favorisant la survie neuronale. Afin de comprendre le mécanisme impliqué dans l'activation, il serait intéressant d'examiner si l'addition d'apoD à des cultures gliales stimulées ou non au LPS induit leur activation (activation directe) ou si la présence de neurones est requise (activation indirecte). Il est également possible que l'apoD contrôle l'activation gliale en modifiant la disponibilité de l'oestradiol (Tapia-Gonzalez *et al.* 2008). L'apoD pourrait donc capturer l'oestradiol, stimulant ainsi l'activation gliale, puis le relarguer de façon contrôlée afin d'éviter la super-activation. La visualisation par immunohistochimie des récepteurs d'œstrogène sur la glie devient donc intéressante (l'expression des récepteurs coïncide avec l'activation gliale). On ne peut non plus distinguer entre l'augmentation de la réactivité causée par l'augmentation de la

réactivité et celle causée par l'augmentation du nombre de cellules. En effet, l'encéphalite causée par HCoV-OC43 est très aiguë et il devient impossible d'avoir des images d'immunohistochimie permettant de discriminer entre ces deux effets dû au marquage inflammatoire trop intense. Il faudrait donc se tourner vers des cultures primaires de microglie ou d'astrocytes stimulées au LPS ou infectées au HCoV-OC43. Il est alors possible de quantifier et de comparer la prolifération cellulaire et l'expression des marqueurs chez les différentes lignées de souris.

Nous savons déjà que l'apoD diminue les propriétés neurotoxiques de l'activation gliale par la diminution du niveau de cytokines. Il serait également intéressant de déterminer si elle est accompagnée par une diminution de la sensibilité des neurones aux effets nocifs des cytokines ce qui contribuerait encore à la protection neuronale. Ainsi, il est possible d'analyser l'effet de milieu conditionné provenant de microglie stimulée au LPS sur des neurones provenant de souris WT, ApoD-KO et H-apoD-Tg en co-culture. Si la sensibilité des neurones aux cytokines est modulée, on s'attend à ce que les neurones H-apoD-Tg survivent mieux et les neurones ApoD-KO survivent moins bien que les neurones WT.

L'une des facettes bénéfiques de l'activation gliale est l'élimination de débris cellulaires et de molécules neurotoxiques par phagocytose. La phagocytose peut être mesurée à partir de microglie primaire provenant des divers génotypes de souris. Il suffit de stimuler cette microglie avec du LPS, par exemple, puis d'y ajouter des particules à phagocyter comme des particules de *E. coli* marquées de façon fluorescente. Après lavage, la fluorescence incorporée dans les cellules est visualisée par microscopie (Tran *et al.* 2008). L'autre facette bénéfique est l'apport de facteurs neurotrophiques ou favorisant la croissance cellulaire tel que détaillé dans la section suivante.

6.2.3.5 Transport de facteurs nutritifs et régulateurs

L'apoD pourrait contribuer au maintien, à la protection, à la réparation et à la réinervation neuronale simplement en apportant les facteurs nécessaires à la fonction cellulaire. Les acides gras à longue chaîne comme l'acide arachidonique (AA) et l'acide docosahexaénoïque (DHA) sont des composants de la membrane phospholipidique des neurones et de grandes quantités de ces gras sont donc requises après une lésion afin de permettre aux neurones survivants de s'allonger et de ré-établir des synapses lors de la réinnervation. Les neurones n'ayant pas les enzymes nécessaires pour la synthèse de novo de AA et DHA, ces acides gras sont donc fournis par l'alimentation, par leur synthèse dans le foie puis leur transport dans le cerveau ou par la synthèse de novo dans la glie. Il a été postulé que le transport de ces acides gras à partir de la circulation se fait via des transporteurs protéiques. L'albumine, qui traverse la barrière hémato-encéphalique, est un candidat potentiel (Bazan *et al.* 2005). L'apoD pourrait aussi jouer ce rôle. Cependant, la capacité de l'apoD à traverser la barrière hémato-encéphalique n'est pas établie. Afin de le démontrer, il est possible d'injecter de l'apoD humaine ou de l'apoD marquée radioactivement de façon intraveineuse à des souris puis d'extraire le cerveau de ces souris et de procéder à la visualisation de l'apoD injectée à l'aide d'anticorps ou par détection de la radioactivité. Puisque ces acides gras peuvent également être fournis par la glie environnante, il serait intéressant de déterminer in vitro si la présence d'apoD humaine dans les neurones chez les souris H-apoD-Tg ou l'absence d'apoD chez les souris ApoD-KO modifie la capture de ces acides gras par les neurones. La comparaison de l'incorporation de [^{3}H]AA par des neurones provenant des différents génotypes de souris serait très informative. Ainsi, il suffirait d'incuber des neurones avec du [^{3}H]AA pendant 72 h à 37°C. La quantité de [^{3}H]AA incorporé serait mesurée après l'élimination du [^{3}H]AA non lié par une série de lavages (Beck *et al.* 1998). Par ailleurs, il a déjà été démontré que l'application d'albumine stimule le relarguage de AA dans diverses cellules dont les myocytes (Beck *et al.* 1998). Il

serait donc intéressant de voir si l'application d'apoD sur des astrocytes stimule leur excrétion de AA. Ainsi, il suffirait d'incuber des astrocytes avec du [^{3}H]AA pendant 72 h à 37°C. Le [^{3}H]AA non lié est éliminé par une série de lavages. Le relaguage de [^{3}H]AA est mesuré suite à l'addition d'apoD dans le milieu cellulaire (Beck *et al.* 1998).

Un autre ligand de l'apoD, le cholestérol, est essentiel au maintien et à la réparation du système nerveux. La conversion du cholestérol en 24S-hydroxycholestérol, qui traverse rapidement la barrière hémato-encéphalique, est la voie majeure pour l'élimination et le maintien de l'homéostasie du cholestérol dans le système nerveux. Cependant, lorsque le transport de cholestérol est affecté, comme chez les patients atteints de la maladie d'Alzheimer et de Niemann-Pick de type C (NPC), le 24S-hydroxycholestérol s'accumule et devient neurotoxique (Bjorkhem et Meaney 2004). Il serait intéressant de déterminer si la surexpression d'apoD chez un modèle de souris NPC est capable de rétablir un niveau normal de 24S-hydroxycholestérol dans le cerveau, par exemple en croisant des souris NPC et des souris H-apoD-Tg.

L'apoD peut également jouer son rôle de neuroprotection en transportant les stéroïdes, en particulier les œstrogènes qui jouent un rôle important dans la fonction neuronale et dans la protection des neurones du cortex cérébral en situations pathologiques. Ainsi, on peut quantifier les stéroïdes chez les souris ApoD-KO et H-apoD-Tg par GCMS (Gas Chromatography Mass Spectrometry) et/ou par une méthode ELISA (enzyme-linked immunosorbent assay). On peut ensuite vérifier l'expression de leurs récepteurs à la surface des neurones et déterminer au niveau de quelles voies leur action se fait particulièrement sentir.

L'apoD peut finalement influencer la production de neurotrophines telles que le NGF (nerve growth factor), le BDNF (brain-derived neurotrophic factor), la NT-3

(neurotrophin-3), la NT-4 (neurotrophin-4) et la NNT1 (novel neurotrophin-1) et de leurs récepteurs p75 et Trk (Tyrosine kinases receptors). Ces protéines peuvent être analysées par immunobuvardage à partir d'extraits tissulaires provenant des diverses souris.

6.2.4 Études comportementales

Tel que démontré dans le chapitre IV, les souris ApoD-KO présentent une diminution de l'activité spontanée et des problèmes de coordination motrice et d'apprentissage. De plus, les souris H-apoD-Tg ont une augmentation de l'activité exploratoire. Il faudrait aussi tester la coordination motrice et l'apprentissage chez les souris H-apoD-Tg grâce au rotarod et au labyrinthe de Barnes. Ces études pourraient être complétées avec la piscine de Morris qui analyse aussi la mémoire référentielle spaciale, c'est-à-dire la capacité à apprendre à utiliser des repères visuels pour s'orienter. Des différences au niveau de ces tâches suggèrent des différences dans la plasticité synaptique. La performance lors de tâches d'apprentissage spatial a été associée au niveau de neurogénèse et de synaptogénèse des cellules granulaires dans le gyrus dentelé de l'hippocampe (Verina *et al.* 2007). Il s'agirait donc de déterminer d'abord si le niveau de neurogénèse est différent chez les différents génotypes de souris. Cela peut être fait en comparant la quantité de BrdU incorporé dans les cellules granulaires. La morphologie, la longueur et la densité des dendrites peut, quant-à-elle, être visualisée par un marquage à la doublecortine. Les connections synaptiques peuvent également être évaluées par la coloration des «mossy fiber boutons» avec la coloration de Timm, qui révèle en fait la présence de zinc à l'intérieur des vésicules synaptiques.

ANNEXE I

Autre contribution-section d'un chapitre de livre

Apolipoprotein D

Sonia Do Carmo, Eric Rassart

2006

Section de :

van Dijk W, Do Carmo S, Rassart E, Dahlbäck B, Sodetz JM
The plasma lipocalins α1-acid glycoprotein, apolipoprotein D, apolipoprotein M and complement protein C8γ.
Dans: Akerström B, Borregaard N, Flower DR, Salier JP, eds.
Lipocalins
Landes Bioscience, Georgetown, TX, USA
p.140-166

A1.1 Résumé

L'Apolipoprotéine D est une glycoprotéine de 29 kDa qui a été isolée pour la première fois en 1973 à partir d'une fraction de HDL de plasma humain. C'est une apolipoprotéine atypique puisque sa synthèse n'est pas limitée au foie et aux intestins. De plus, elle est exprimée à divers niveaux dans divers tissus chez plusieurs espèces de mammifères et chez le poulet. La large expression du gène de l'apoD chez plusieurs espèces suggère son importance chez les chordés. Des analyses de structure ont révélé que l'apoD fait partie de la famille des lipocalines. Plusieurs molécules hydrophobes ont été identifiées comme des ligands potentiels de l'apoD comme la progestérone, la prégnénolone, la bilirubine, le cholestérol, l'acide arachidonique et l'acide E-3-méthyle-2-héxénoïque. Des études de liaison récentes ont révélé que l'apoD est capable de discriminer entre des composés semblables. Étant donné son hétérogénéité apparente, il a été proposé que l'apoD ait un rôle multi-ligand : multi-fonction.

Mots-clés : lipocaline, régulation, cancer, système nerveux.

A1.2 Abstract

Apolipoprotein D is a 29-kDa glycoprotein that was isolated for the first time in 1973 from a human plasma HDL fraction. It is an atypical apolipoprotein since its synthesis is not restricted to the liver and/or the intestine. In addition, it is expressed at different levels in a wide range of tissues of several mammalian species and chicken. The wide distribution of the apoD gene in many species supports its evolutionary importance in the chordate lineage. Structural analyses revealed that the protein was part of the lipocalin family. Several candidate hydrophobic molecules were identified as potential ligand for apoD, such as progesterone, pregnenolone, bilirubin, cholesterol, arachidonic acid and E-3-methyl-2-hexenoic acid. Recent detailed ligand binding studies revealed that apoD discriminates well in its binding function between closely related compounds. Due to this apparent heterogeneity, a role as a multi-ligand:multi-function protein has been proposed.

Keywords : lipocalin, regulation, cancer, nervous system.

A1.3 Introduction

Apolipoprotein D (apoD), so called because of its association with plasma lipoproteins, belongs to the lipocalin superfamily. In human, apoD is present in many fluids, expressed in several tissues although poorly expressed in the liver and intestine, which are the major sites of synthesis of other apolipoproteins. In serum of adult healthy subjects, apoD levels vary from 50-200 mg/L plasma. Plasma apoD is mainly associated with both apoA-I and apoA-II in HDL and VHDL particles. It is also present as apoD/apoB-100 heterodimers in LDL and VLDL lipoproteins.

The gene and protein structures, the tissue distribution and known ligands of apoD have been reviewed in Rassart *et al.* (2000). Here, the role of apoD is discussed with respect to its modulation 1) by biological factors, 2) in various types of cancer, and 3) in the normal and injured nervous systems.

A1.4 Modulation of apoD levels

The regulation of apoD expression is complex and many authors have shown the importance of biological factors in the modulation of this protein.

A1.4.1 Cellular growth and differentiation

Many lines of evidence suggest an inverse relationship between apoD expression and cell proliferation (Blais *et al.* 1994, 1995, Do Carmo *et al.* 2002, Provost *et al.* 1991, Simard *et al.* 1990, 1991, 1992). Furthermore, apoD selectively suppresses the proliferative response of vascular smooth muscle cells to growth factors by a mechanism related to nuclear translocation of ERK1/2 (Sarjeant *et al.* 2003).

However, apoD expression might also be related to the differentiation period that is attained following growth arrest. Both retinoic acid (Lopez-Boado *et al.* 1994) and 1,25-dihydroxyvitamin D3 (Lopez-Boado *et al.* 1997), well known for their differentiation properties, were able to induce apoD expression in breast cancer cells. This induction was shown later to be mediated by the nuclear retinoic acid receptors (RAR) leading to a significant inhibition of cell proliferation suggesting that apoD could be a biochemical marker of RAR-mediated growth arrest and cell differenciation (Lopez-Boado *et al.* 1996).

There is also evidence for such a role *in vivo* as apoD is expressed mostly in nonproliferating or terminally differentiated prostate glandular epithelial cells (Aspinall *et al.* 1995). However, this observation can not be generalized since not all nonproliferating or terminally differentiated cells do express apoD (Do Carmo *et al.* 2002).

A1.4.2 Metabolic studies and energy homeostasis

ApoD modulation is found in pathologies such as Tangier disease (Alaupovic *et al.* 1981), familial LCAT deficiency (Albers *et al.* 1985), mutations in the apoA-I gene (Deeb *et al.* 1991), type 2 diabetes (Baker *et al.* 1994, Vijayaraghavan *et al.* 1994, Hansen *et al.* 2004), alcoholism (Lewohl *et al.* 2002, Saito *et al.* 2002), corneal Fuch's dystrophy (Gottsch *et al.* 2002), renal dysfunction (Dieplinger *et al.* 1986, DeWan *et al.* 2001) and ischemic tissue injuries (James *et al.* 1986, Lin *et al.* 2001). This association with such diseases may be fortuitous and a reflection of lipid metabolism imbalance. The apoD correlation with type 2 diabetes, obesity and hyperinsulinemia may be liver X receptor-dependent and the activation of inflammatory and pro-angiogenic pathways (Hansen *et al.* 2004, Hummasti *et al.* 2004).

In the hypothalamus, apoD interacts specifically with the cytoplasmic portion of the long form of the leptin receptor, Ob-Rb, known to play a key function in regulating food intake and body weight. Moreover, the hypothalamic level of apoD mRNA is stimulated by dietary fat, and is strongly, positively correlated with body fat mass and circulating leptin levels. This positive association with body fat, however, is lost in obese ob-/ob- and db-/db- mice, which exhibit markedly reduced levels of hypothalamic apo D mRNA compared to that of wild-type mice. These results suggest that apoD in the hypothalamus is involved in the leptin/Ob-Rb signal transduction pathway that controls body fat accumulation on a high-fat diet (Liu *et al.* 2001).

A1.4.3 Development

ApoD is also involved in gestation (Provost *et al.* 1995) and foetus development (McConathy and Lane 1980). In mouse, apoD is selectively modulated from E9 to birth in mesenchyme and neuroepithelium (Sanchez *et al.* 2002). In rat brain, during development and in the early neonatal period, maturation-associated induction of apoD gene expression coincides with the period of active myelination as well as synaptogenesis in rodent brain (Ong *et al.* 1999).

ApoD is also present in the yolk of the rapidly growing chicken oocyte. First proposed to play a role in the transport and/or mobilization of lipids during embryogenesis in oviparous species (Vieira *et al.* 1995), it is presumed to transport regulatory molecules such as vitamin A and thyroid hormones (Yao *et al.* 2002). In the chicken foetus, apoD is expressed in ectodermal derivatives in the developing feather follicles and the nervous system. Both neurons and glia express chicken apoD in a subset-dependent form, although very dynamic temporal changes of expression cannot be ruled out. By contrast with the mouse, chicken apoD was not found in pericytes and meningeal cells. It was suggested that the common ancestor of birds

and mammals might have expressed apoD in both mesenchymal and neuroectodermal derivatives. The expression profiles possibly changed after the split of mammals and birds, with chicken apoD expression being restricted to neuroectodermal derivatives (Ganfornina *et al.* 2005).

A1.4.4 Cancer

ApoD is overexpressed in several types of cancer such as breast, ovarian, endometrium, prostate, retinal, skin, pancreatic, and central nervous system (CNS) carcinomas. It is underexpressed in thyroid oncocytomas (Baris *et al.* 2004). It is silenced by DNA methylation in esophageal squamous cell carcinoma and was identified as a candidate of tumor suppression (Yamashita *et al.* 2002). However, the correlation between the degree of tumoral differentiation and apoD expression remains ambiguous. This association can either be positive or negative depending on the type of tumor analysed. It can also vary depending upon the sample analysed and there are even discrepancies within the same tumor type. Whether apoD expression is a cause or a consequence of these cellular transformations remains unclear. In breast and central nervous system cancers, high apoD expression is mostly correlated with highly differentiated, non-invasive/metastatic carcinomas and it is associated with a longer relapse-free and better survival. The presence of apoD in these tumors serves as a good prognostic indicator but could simply be a reflection of growth arrest due to cellular differentiation (Diez-Itza *et al.* 1994, Hunter *et al.* 2002, Lamelas *et al.* 2000, Porter *et al.* 2003, Serra Diaz *et al.* 1999).

In contrast, the inverse relationship between apoD and cell proliferation appears to be lost during malignant transformation and elevated apoD staining is associated with advanced invasive prostate (Ashida *et al.* 2004, Aspinall *et al.* 1995, Hall *et al.* 2004, Zhang *et al.* 1998), skin (Miranda *et al.* 2003, West *et al.* 2004) and pancreatic carcinomas (Iacobuzio-Donahue *et al.* 2002, Ryu *et al.* 2001) and may

therefore be a prognostic of unfavorable evolution. It is not known if this is due to an increased rate of cellular proliferation or a decrease in cell death (Hall *et al.* 2004). Moreover, apoD protease activity (Kesner *et al.* 1988), its implication in cell motility in response to growth factors (Leung *et al.* 2004) and its association with the progression to a more differentiated tumoral stage suggests a potential role for apoD in tumoral invasiveness.

In other cancers, like endometrial and ovarian carcinomas and retinoblastomas, there is no significant relationship between apoD immunostaining and either age of the patients, or the stage and histologic grade of the tumors (Alvarez *et al.* 2003, Rojo *et al.* 2001, Vazquez *et al.* 2000). There are also contradictions in the same cancer type. Some studies of breast and prostate cancers demonstrate no significant association between apoD expression and the degree of differentiation although an association with patient survival remains (Rodriguez *et al.* 2000, Selim *et al.* 2001).

So far, it appears that the utility of apoD as a prognostic remains uncertain and more studies are required. It was shown that apoD could be useful in the choice and follow-up of hormonal therapy to treat breast cancers (Hall *et al.* 1996, Harding *et al.* 2000, Weber-Chappuis *et al.* 1996). This observed discrepancy among a wide range of cancer could be due to the fact that some cancers show hormonal dependance for their growth and the correlation may be restricted to some specific cancer cell types. For example, differences in apoD expression between male and female breast cancer, the latter having a higher level of apoD and a better outcome, opens the field of a more selective hormonal therapy (Serra *et al.* 2000). There are numerous sterol responsive elements in the apoD promoter (Do Carmo *et al.* 2002) and one would expect a fine regulation of apoD expression by steroids.

A1.4.5 Nervous system

A1.4.5.1 Peripheral nervous system

The first report showing an implication of apoD in the nervous system was the study of Boyles *et al.* (1990a) that showed an increased expression in the regenerating sciatic nerve of the rat after a crush injury. The level of ApoD mRNA and protein transiently increased by 40- and 500-fold, respectively, at the time when axons from the proximal stump grow into the distal nerve segment (Boyles *et al.* 1990a, Spreyer *et al.* 1990). ApoE, another apolipoprotein, increased 250-fold after crush injury. ApoD also accumulated in the regenerating sciatic nerve of two other species, the rabbit and the marmoset monkey (Boyles *et al.* 1990a). Only small amounts of apoD mRNA are detected in rat non-injured mature nerve and modest expression was detected in transected nerves which were prevented from regeneration by ligation. Since peripheral neural tissue is capable of local synthesis of some apolipoproteins such as apoD and apoE, it seems probable that it would have its own independent system of lipoproteins that may serve as the vehicles for lipid movement between cells. This lipid transport system should be most active in the injured peripheral nerves, in which massive quantities of lipid are freed due to myelin degradation and are subsequently stored and reused during regeneration.

A1.4.5.2 Central nervous system

In human, apoD is produced by astrocytes and oligodendrocytes in the white matter and in some scattered neurons and protoplasmic astrocytes in the grey matter (Patel *et al.* 1995). It is also present in perivascular cells, and pericytes in the walls of blood vessels suggesting a role in the transport of sterols and small hydrophobic molecules to, or from, blood vessels to the cortex (Hu *et al.* 2001, Navarro *et al.* 1998, 2004).

All the apoD ligands, cholesterol, progesterone, pregnenolone, arachidonic acid and bilirubin are important molecules in the CNS. ApoD also binds androgens and oestrogens to a lower extent. Two ligands, progesterone and pregnenolone, are synthesized by astrocytes and oligodendrocytes. Pregnenolone was shown to accumulate as pregnenolone sulfate in the brains and sciatic nerves of humans and rats (Baulieu 1998). ApoD could, therefore, be implicated in the local transport of steroid hormones and may participate in reinnervation process.

Both apoD protein and mRNA increase in aged cerebral cortex probably due to the increased number of total and reactive astrocytes (Belloir *et al.* 201, del Valle *et al.* 2003, Kalman *et al.* 2000). The same observation is also reported in microglia of mice that lack cystatin B, a model for Unverricht-Lundborg disease, a human disorder characterized by progressive neurological dysfunction and seizures (Lieuallen *et al.* 2001). Also, an even larger increase of apoD is observed in aged PDAPP transgenic mice, a model for Alzheimer's disease that express the mutated human amyloid precursor protein (Thomas *et al.* 2001c). This may represent a glial cell compensatory response to beta-amyloid deposition in Alzheimer's disease.

ApoD is increased in the cerebrospinal fluid (CSF) and hippocampus of patients with Alzheimer disease (Terrisse *et al.* 1998). This increase is correlated with the Braak stage of neurodegeneration (Glockner *et al.* 2003). Although independent of apoE protein concentrations, it is correlated with the apoE genotype depending on the brain region analysed (Glockner *et al.* 2003, Terrisse *et al.* 1998, Thomas *et al.* 2003e). The differential association with apoE genotype may be explained by disease progression. In early stages, an apoD increase in the presence of E4 allele could be a compensatory mechanism and be indicative of ongoing reinnervation rather than cell injury and death. However, this correlation is lost during disease progression (Belloir *et al.* 2001, Thomas *et al.* 2003e). The apoD increase correlates with the number of

neurofibrillary tangles (NFT) but not with senile plaques (Glockner *et al.* 2003). Furthermore, whereas apoE is always located overlapping the amyloid core, apoD seems preferably around and near the amyloid (Navarro *et al.* 2003). Colocalization of apoD and NFT in the same neuron was rare and apoD transcription is impaired during NFT formation (Belloir *et al.* 2001), suggesting that apoD is present in stressed neurons before they possibly accumulate NFT.

ApoD levels are also elevated in the CSF of patients with stroke, meningoencephalitis, motor neuron disease, dementia (Terrisse *et al.* 1998), chronic inflammatory demyelinating polyneuropathy, Guillain-Barre Syndrome, multiple sclerosis (Reindl *et al.* 2001), and cerebrotendinous xanthomatosis (Salen *et al.* 1987). Increased ApoD transcripts were identified in glaucoma (Tomarev *et al.* 2003) and in the nervous system of virus-infected mice (Dandoy-Dron *et al.* 1998, Kang *et al.* 2003, Saha *et al.* 2003).

ApoD decreases significantly in serum samples from schizophrenic patients (Thomas *et al.* 2001b). This supports recent hypotheses involving systemic insufficiencies in lipid metabolism /signaling in schizophrenia. Deficiencies in arachidonic acid, a primary apoD ligand, were reported in schizophrenic patients (Thomas *et al.* 2003d, Yao *et al.* 2005). In contrast, apoD levels were significantly and selectively increased both in schizophrenic and bipolar subjects depending on the brain region analysed allowing the discrimination between the two disorders (Thomas *et al.* 2003b). This apoD elevation in affected CNS regions is emphasized by neuroleptic drugs, suggesting a focal compensatory response (Thomas *et al.* 2001a). Indeed, elevated apoD levels were reported in post-mortem brains, as well as plasma, of schizophrenic patients and in rodent brains after chronic treatment with clozapine and other atypical antipsychotics (Khan *et al.* 2003, Mahadik *et al.* 2002, Thomas *et al.* 2001a, 2003c,). This increase was even more significant in clozapine-treated chronic patients (Mahadik *et al.* 2002).

The Niemann-Pick disease (NPC) is another human genetic disorder affecting lipid homeostasis that shows altered apoD expression. It is an inherited lysosomal cholesterol disorder whose major phenotypic feature is a progresssive neurodegeneration. The animal model of human NPC also shows abnormalities in cholesterol metabolism and increased apoD levels in plasma, brain, adipose tissue, heart, thymus and cultured astrocytes (Suresh *et al.* 1998, Yoshida *et al.* 1996). In particular, strongly apoD-immunolabeled cells are present in the brain regions previously shown to display the most significant neurodegenerative changes (Ong *et al.* 2002). Thus, increased synthesis of apoD, a cholesterol transporter, could reflect an attempt to improve the cellular cholesterol trafficking.

ApoD is normally produced by astrocytes and oligodendrocytes (Boyles *et al.* 1990b, Patel *et al.* 1995). Following an acute brain injury in rodents, its expression is upregulated in astrocytes and is also found in neurons. It is the case following kainic acid injection (Montpied *et al.* 1999, Ong *et al.* 1997), entorhinal cortex lesion (Terrisse *et al.* 1999), traumatic brain injury (Franz *et al.* 1999) and chronic treatments with MK-801, a noncompetitive antagonist of the NMDA glutamate receptor (O'Donnell *et al.* 2003). However, apoD expression appears as a distinct event in glial and neuronal cells. Astrocyte activation is a general response after a brain lesion. The recovery of neural tissue after an injury is probably in part the result of an equilibrium between the negative effets of reactive astroglia on axon growth and the beneficial properties of the substances released by these reactive astroglia, such as sex steroids (Garcia-Segura *et al.* 1999). The latter could potentially be responsible for the local increase in apoD mRNA and protein by either a direct action on the apoD gene promoter or, indirectly, by causing a growth arrest of astrocytes that usually appears 3 to 4 days post-lesion. The production of apoD by neurons, however, could be a desperate attempt to retrieve essential survival factors such as steroids or growth factors. Alternatively, apoD expression could be devoted to the

release of toxic molecules. ApoD may be part of the antioxidant defense system and act as a scavenger to remove heme-related molecules such as bilirubin (Alvarez *et al.* 2003, Peitsch and Boguski 1990). ApoD clearly has an important function in the nervous system in both normal and pathological situations.

A1.5 Conclusion

In spite of the quantity of studies on apoD, little is known about its physiological functions. It seems possible that because of its multi-ligand properties, apoD acts through different pathways in each tissue or organ where its expression was reported. Its implication in cellular processes and pathologies highlights the importance of understanding the molecular mechanisms controlling its expression.

ANNEXE II

Autre contribution-article en préparation

Modulation of Apolipoprotein D in pregnancy and association with pre-pregnancy body mass index and gestational weight gain

Sonia Do Carmo, Jean-Claude Forest, Yves Giguère, André Masse, Julie Lafond, Eric Rassart

2009

Avant-propos

Ces travaux s'insèrent dans le cadre du projet de recherche du Dr Julie Lafond visant à mieux comprendre les échanges mère-fœtus. Il semblait judicieux de tester la modulation de l'apoD au cours de la grossesse. D'abord, les travaux présentés en chapitre III suggèrent l'importance de l'apoD dans le métabolisme lipidique alors que les travaux présentés en chapitre II, IV et V démontrent une fonction dans le stress cellulaire. La grossesse et les dérangements métaboliques qu'elle implique représentent une période de stress au niveau de l'organisme. Ensuite, la plupart des apolipoprotéines testées subissent des modulations au courant de la grossesse. De plus, l'apoD, bien qu'étant une apolipoprotéine atypique, est retrouvée à la surface des HDL dont les niveaux sont modulés au courant de la gestation. Finalement, elle est capable de transporter le cholestérol, l'acide arachidonique, la bilirubine et les hormones stéroïdes, molécules échangées entre la mère et le fœtus. Nous avons donc dosé l'apoD dans le plasma de femmes classées en neuf groupes selon leur indice de masse corporelle et leur gain de poids durant la grossesse. Le dosage a été fait à chacun des trimestres ainsi que dans le sang du nouveau-né à la naissance. Nous avons corrélé ces concentrations avec d'autres caractéristiques de la grossesse, incluant les divers dosages sanguins chez la mère, la durée de la gestation et la grosseur du nouveau-né. Nous avons également examiné les concentrations de l'apoD et sa corrélation avec divers paramètres gestationels en fonction du niveau de cholestérol de la mère. Nous avons de plus examiné la transcription de l'apoD au niveau du placenta chez les neuf groupes de femmes. Nous avons finalement dosé l'apoD deux mois après l'accouchement afin de déterminer l'effet de l'allaitement sur le retour aux niveaux de base de l'apoD.

Le design expérimental de ce travail a été réalisé par Julie Lafond. Elle a également fourni le matériel biologique et l'expertise concernant la physiologie de la grossesse. J'ai pour ma part effectué les dosages de l'apoD dans le plasma de même

que les RT-PCR quantitatifs (qRT-PCR) pour déterminer le niveau d'ARNm dans le placenta. J'ai également fait la compilation et l'analyse des données et j'ai écrit l'article.

A2.1 Résumé

L'apolipoprotéine D (ApoD) est une lipocaline impliquée dans divers processus incluant le transport lipidique, mais sa modulation au courant de la grossesse chez l'humain n'a jamais été examinée. Nous avons analysé la variation de l'ApoD dans le plasma de 151 femmes à chaque trimestre de leur grossesse et dans le placenta en relation avec leur indice de masse corporelle (IMC) et leur gain de poids gestationnel (GPG). Nos résultats démontrent que les niveaux d'ApoD plasmatique diminuent au cours de la grossesse. Cette diminution est plus prononcée chez les femmes ayant un GPG excessif et leurs nouveaux-nés. Chez ces femmes, comme chez d'autres femmes ayant un IMC ou un GPG sous-optimal, la concentration de l'ApoD était associée à plusieurs paramètres lipidiques et la durée gestationnelle, alors que dans le groupe contrôle, elle était seulement corrélée avec les concentrations de cholestérol et d'albumine. Cependant, le fait que les femmes ayant un faible ou un fort taux de cholestérol possèdent des niveaux d'ApoD similaires suggère que la variation de l'ApoD plasmatique n'est pas dépendante du cholestérol. Plus probablement, la diminution des niveaux d'ApoD chez les femmes ayant un GPG excessif est causé par une plus faible transcription de l'ApoD dans le placenta, un site majeur d'expression de l'ApoD. Ce contrôle est perdu chez les femmes obèses. Après l'accouchement, la concentration plasmatique d'ApoD est reliée à l'allaitement, celui-ci favorisant un retour plus rapide aux concentrations plasmatiques de base. Il est proposé que la diminution de la concentration plasmatique d'ApoD est une réponse adaptative destinée à maintenir l'homéostasie fœtale. Le mécanisme exact de cette adaptation n'est pas connu. Il pourrait cependant être relié à l'augmentation des niveaux d'oestrogènes durant la grossesse.

Mots-clés : cholestérol, placenta, grossesse, humain, indice de masse corporelle, gain de poids, œstrogène.

A2.2 Abstract

Apolipoprotein D (ApoD) is a lipocalin involved in many processes including lipid transport, but its modulation during human pregnancy was never examined. We investigated the changes in the levels of ApoD in the plasma of 151 women at each trimester of gestation and in placenta in relation to their prepregnancy body mass index (BMI) and gestational weight gain (GWG). Our results show that plasma ApoD levels decrease during normal uncomplicated pregnancy. ApoD is further decreased in women with excessive GWG and their newborns. In these women, as in other women with suboptimal BMI or GWG, the ApoD concentration was associated with many lipid parameters as well as gestation duration, while in the control group, it was only correlated with total cholesterol and albumin values. However, the similar ApoD levels in low cholesterol (LC) and high cholesterol (HC) women, suggested that the plasma ApoD variation is not cholesterol dependant. Most probably, the decrease in plasma ApoD levels in women with excessive GWG derived in part from their lower ApoD mRNA production by the placenta, a main site of ApoD transcription. This control was lost in overweight women. After childbirth, the plasma ApoD concentrations depended on if the mother was breast-feeding or not, lactation favoring a faster return to baseline values. It is speculated that the decrease in plasma ApoD concentration during pregnancy is an adaptive response aimed at maintaining fetal lipid homeostasis. The exact mechanism of this adaptation is not known. It may, however, be related to pregnancy-induced increase in estrogen levels.

Keywords : cholesterol, placenta, pregnancy, human, body mass index, weight gain, estrogen.

A2.3 Introduction

Human pregnancy is associated with profound changes in the maternal lipid, carbohydrate and protein metabolisms. These changes are aimed at favoring the maintenance of pregnancy, sustaining fetal growth and brain development, and facilitating parturition (DeCherney and Pernoll 1994). Maternal metabolism is intimately linked with prepregnancy body mass index (BMI) and gestational weight gain (GWG), which greatly influence the outcome of pregnancy (Nohr *et al.* 2008). In association with an unhealthy lifestyle, suboptimal prepregnancy BMI and GWG also increase the risk of birth defects and chronic health problems in the children (Kaiser *et al.* 2008).

The lipid metabolism during pregnancy is characterized by progressive increases in plasma cholesterol and triglyceride levels accompanied by increases in low density lipoprotein (LDL) and very low density lipoprotein (VLDL), leading to maternal hyperlipidemia during late pregnancy (Potter and Nestel 1979). Cholesterol is essential for optimal embryonic and fetal development. It is an important component of plasma membranes, is required for cell proliferation and differentiation and modulates morphogenesis (Porter *et al.* 1996). It is also used by the placenta for the synthesis of steroid hormones (Kallen 2004). Triglycerides are also crucial as they are used as a source of essential fatty acids for the fetus, although they do not directly cross the placental barrier (Herrera 2000).

Plasma lipid metabolism is regulated in part by the specific apolipoprotein constituents of the various lipoprotein classes. Apolipoprotein D (ApoD) is a lipocalin assigned to many putative functions including lipid transport. Its macromolecular distribution extends from VLDL into very high density lipoproteins (VHDL) with a maximum concentration in high density lipoproteins 3 (HDL_3) (McConathy and Alaupovic 1976). It is considered an atypical apolipoprotein as both

its structure and major sites of synthesis differ from the other apolipoproteins. Indeed, in human, ApoD is poorly expressed in the liver and intestine while it is highly expressed in adrenal glands, kidneys, pancreas, placenta, spleen, nervous system, lungs, ovaries and testes (Drayna *et al.* 1986, Rassart *et al.* unpublished results). Several hydrophobic molecules were identified as its potential ligands including cholesterol (Drayna *et al.* 1986), bilirubin (Peitsch and Boguski 1990), pregnenolone, progesterone, estrogens (Dilley *et al.* 1990, Simard *et al.* 1991) and arachidonic acid (Morais Cabral *et al.* 1995).

ApoD expression is modulated in many situations (for review see Rassart *et al.* 2000, van Dijk *et al.* 2006), namely cellular growth and differentiation (Do Carmo *et al.* 2002, Lopez-Boado *et al.* 1994, Simard *et al.* 1990), cancer (Hunter *et al.* 2002, Simard *et al.* 1990), nervous system pathologies (Boyles *et al.* 1990a, Terrisse *et al.* 1998, Thomas *et al.* 2001b), inflammation (Do Carmo *et al.* 2007) and oxidative stress (Ganfornia *et al.* 2008). ApoD is also involved in gestation and fetus development. In human, it is up-regulated in endometrium during the window of uterine receptivity for embryonic implantation (Kao *et al.* 2002), is highly expressed in placenta (Drayna *et al.* 1986) and is found in colustrum and milk (Palmer *et al.* 2006). Its levels are also increased in fallopian tubes and ovaries of gestating compared to non-gestating guinea pigs (Provost *et al.* 1995) but are decreased in lactating compared to virgin mouse mammary gland (Cofer and Ross 1996). During mouse development, ApoD expression is selectively modulated from E9 to birth (Sanchez *et al.* 2002) and in brain, its expression coincides with the period of active myelination and synaptogenesis (Ong *et al.* 1999). The role of ApoD in embryogenesis is not limited to mammals as it is found in the yolk of the rapidly growing chicken oocyte, where it might transport lipids or regulatory molecules such as vitamin A and thyroid hormones (Vieira *et al.* 1995, Yao and Vieira 2002), and expressed during late chicken embryogenesis (Ganfornina *et al.* 2005).

In spite of the role of ApoD in lipid transport and its expression in gestation-related tissues and during fetus development in various species, no information is available concerning the modulation of ApoD, a secreted protein, throughout human pregnancy. To address this question, we measured plasma ApoD levels at each trimester of pregnancy and two months after delivery. We also examined how ApoD levels are modified by factors affecting lipid metabolism such as maternal prepregnancy BMI, gestational weight gain and hypercholesterolemia.

A2.4 Materials and methods

A2.4.1 Population

The women participating in the study were recruited at their first prenatal visit, before their tenth week of pregnancy, at the Clinique Fidès of Montréal (Montréal, QC, Canada) and at the Saint-Luc Hospital's Perinatology Service of the Centre Hospitalier de l'Université de Montréal (Montréal, QC, Canada), from 2002-2006. This study included 151 pregnant women of similar socio-economic situation. The study was approved by the ethical committee of Saint-Luc Hospital and Université du Québec à Montréal (Montréal, QC, Canada). All subjects provided written informed consent. A group of 5 non-pregnant women of similar age was also included.

A2.4.2 Population classification

The study population was classified into nine groups according to their prepregnancy BMI and GWG. The normal values for BMI were established at 20-26 kg/m^2. The normal values for GWG were established at 11-18 kg. The normal control group was defined as: BMI 20-26 kg/m^2, GWG 11-18 kg. A classification based on the median plasmatic total cholesterol level at delivery (6,85 mM) was also established. The low cholesterol group (LC) is composed of women with a cholesterol concentration inferior to 7 mM (n=38) while the high cholesterol group (HC) is composed of women with a cholesterol concentration superior to 8 mM (n=29).

A2.4.3 Blood and tissue samples

Blood samples were collected at first (10-17 weeks), second (22-28 weeks), and third trimester (36-40 weeks) of gestation. A few blood samples were also collected two months after parturition (postpartum). Newborn blood samples were retrieved from the umbilical cord (cord blood). The blood samples were centrifuged 15 min at 3500 x g and plasma samples were kept at -20°C until analysis. The placentas, from vaginal delivery, were obtained from the Centre Hospitalier de l'Université de Montréal (Montréal, QC, Canada) and were immediately immersed in Dulbecco's Modified Eagle Medium (DMEM) (Sigma, Oakville, ON, Canada) supplemented with antibiotics (penicillin, streptomycin and neomycin, Invitrogen, Burlington, ON, Canada) and $NaHCO_3$. After the removal of the amnion, the chorion and the decidual layer, the placental tissue was cut in 5 cm^2 sections, immediately frozen in liquid nitrogen and kept at -80°C until analysis.

A2.4.4 Plasma biochemistry

The plasma levels of total cholesterol, LDL-cholesterol, HDL-cholesterol, triglycerides and glucose were individually measured using the UniCel 36 DX600 Synchron Clinical System (Beckman-Coulter, Mississauga, ON, Canada) at the Clinical Biochemistry Service of Saint-François d'Assise Hospital (Québec, QC, Canada). Total plasma fatty acids were measured by gas phase chromatography. Plasma insulin and alpha-fetoprotein were measured by an automatic enzymatic-immunological method using a Elecsys automate (Roche Diagnostics, Laval, QC, Canada) while plasma albumin was analyzed using an Hitachi 717 device (Roche Diagnostics). ApoA-1 and ApoB-100 levels were measured by RIA or ELISA methods at the Centre Hospitalier Universitaire de Québec (Québec, QC, Canada). ApoD levels were measured by competitive ELISA using the human ApoD

monoclonal antibody 2B9 as previously described (Terrisse *et al.* 1998). Briefly, microtiter plates were coated with antigen (1 µg ApoD/ml) overnight at 4°C in 5 mM glycin buffer (pH 9.2). Unreacted sites were blocked with PBS-BSA 1% for 1 h. A mixture containing diluted plasma and 2B9 antibody in PBS-BSA 1% then replaced the saturation solution. Bound 2B9 antibody was detected by peroxidase labeled anti-mouse IgG (KPL, Gaithersburg, MD) and revealed with ABTS substrate (KPL). Optical density was measured at 410 nm. All quantifications were performed in triplicate.

A2.4.5 RNA isolation and quantitative Real-Time PCR (qRT-PCR)

Total RNA was prepared from 25 mg of placental tissue using the High Pure RNA Tissue Kit (Roche Diagnostics) according to the manufacturer's instructions. Subsequently, cDNA was obtained by reverse transcription of total RNA using the Omniscript RT kit (Qiagen, Mississauga, ON, Canada). The quantification of ApoD and 18S transcripts were assessed by qRT-PCR using the LightCycler 480 SYBR Green I Master and the LightCycler 480 instrument and software (Roche Diagnostics). For each gene, diluted amounts of known templates provided quantitative standard curves from which cDNA copy number in clinical samples could be determined. ApoD transcript expression was then normalized versus the housekeeping gene 18S. The following primers were used in qRT-PCR: ApoD forward primer, 5'-CAT CTT GGG AAG TGC CCC AA-3'; ApoD reverse primer, 5'-CCA TCA GCT CTC AAC TCC TGG TTT-3'; 18S forward primer, 5'-CGC CGC TAG AGG TGA AAT TC-3'; 18S reverse primer, 5'-TTG GCA AAT GCT TTC GCT C-3'.

A2.4.6 Statistical analyses

Data were expressed as means ± SEM and analyzed with unpaired Student's *t*-test or with one-way ANOVA and Turkey–Kramer post-test for multiple comparisons. Results were considered significant at $p < 0.05$. The association between two variables of the same population was assessed using Pearson's correlation coefficient. All statistical analyses were performed using Prism 4.0 (GraphPad Software, San Diego, CA, USA).

A2.5 Results

A2.5.1 Population characteristics

As shown in Table A2.1, the 151 pregnant women participating to this study were classified into nine groups according to their prepregnancy BMI and GWG. GWG had a greater impact on group characteristics than BMI. Thus, especially in groups with normal or high BMI, high GWG was associated with lower levels of total cholesterol, LDL-cholesterol and to a less extent HDL-cholesterol. ApoB-100 and alphafetoprotein were also affected by GWG. However, while suboptimal GWG induced decreases in ApoB-100 concentration in the normal and high BMI groups, alphafetoprotein was affected by GWG mainly in low BMI groups. Suboptimal GWG had the strongest impact in the high BMI group. It decreased the duration of gestation (gestational age), total cholesterol, LDL-cholesterol and ApoB-100 values. Free fatty acids levels were decreased in the most extreme groups, that is women with low BMI and GWG and women with high BMI and GWG. Finally, some groups had distinctive characteristics. The group with high BMI and high GWG had lower levels of all lipid parameters except triglycerides and reduced albumin levels. On the other hand, the group with normal BMI and low GWG had low triglyceride and ApoB-100 concentrations and smaller newborns. In spite of these differences, all groups had similar glucose levels at their third trimester of gestation (Table A2.1).

A2.5.2 Plasma ApoD levels decrease during pregnancy

Plasma ApoD levels were measured in women at each trimester of pregnancy. In the control group (BMI 20-26 kg/m^2, GWG 11-18 kg), plasma ApoD concentration declined early in pregnancy as its levels were already reduced by 40% at the first trimester of pregnancy compared to non-pregnant women (Fig. A2.1). ApoD levels continued to progressively decrease at the second trimester and at third trimester of

gestation, ApoD levels reached only 30% of the levels in non-pregnant women (Fig. A2.1). A similar decrease of ApoD during gestation was also observed in the 8 other groups (data not shown). Interestingly, ApoD levels in the newborn were similar to the levels in the mother at third trimester of pregnancy in all groups except the normal BMI (20-26 kg/m^2), low GWG (< 11 kg) group where newborns had inferior ApoD levels than their mothers (Fig. A2.1 and Table A2.2). In spite of this, by using the Pearson's correlation coefficient, no correlation was found between ApoD plasma levels in the mother and the newborn (Table A2.3).

A2.5.3 Influence of prepregnancy BMI and GWG on plasma ApoD levels

Maternal prepregnancy BMI did not have an impact on plasma ApoD levels during the third trimester of pregnancy (Table A2.2). However, a GWG superior to 18 kg caused a decrease in maternal ApoD levels in the normal and low BMI groups but not in the high BMI group (Table A2.2). GWG but not BMI also affected newborn ApoD concentration. Newborns from mothers having a GWG superior to 18 kg had lower plasma ApoD than newborns from the other groups (Table A2.2).

A2.5.4 Association between plasma ApoD levels and pregnancy parameters

The correlation between ApoD concentration during the third trimester of pregnancy and the other pregnancy-related parameters was explored using Pearson's correlation coefficient (Table A2.3). In the control group, ApoD levels were only correlated with total-cholesterol and albumin levels, in a positive manner. In groups having suboptimal BMI or GWG, ApoD levels were correlated, as expected, mainly with lipid parameters but also with gestational age, maternal BMI and GWG. However, in the three high GWG groups, no correlation was seen between ApoD levels and any of the parameters examined, except for the negative correlation

between ApoD and gestational age in women with normal BMI (Table A2.3). The low number of women in these groups may explain the lack of correlation.

Correlations between ApoD and gestational age, maternal BMI or GWG were revealed in some groups (Table A2.3). ApoD and gestational age were inversely correlated in women with low GWG and suboptimal BMI. The same correlation was also observed in women with normal BMI and high GWG, as described above. The correlation was reversed in women with low BMI and normal GWG. In addition, ApoD was correlated with BMI in groups with low GWG and suboptimal BMI. However, although this correlation was positive in the low BMI group, it was negative in the high BMI group. Finally, when women had low GWG, whatever the BMI, ApoD was positively correlated with GWG, but this correlation was reversed in women with normal GWG and suboptimal BMI.

Moreover, correlations between ApoD and lipid levels emerged in some groups (Table A2.3). Therefore, in women with low BMI, no correlation between ApoD and total cholesterol, LDL-cholesterol, HDL-cholesterol, triglycerides or ApoB-100 was seen. However, these parameters were correlated with ApoD in women with high BMI and low or normal GWG and in women with normal BMI and low GWG. Thus, in women with normal BMI and low GWG, ApoD was positively correlated with total cholesterol, LDL-cholesterol and ApoB-100 and negatively correlated with triglycerides. In women with high BMI and low GWG, ApoD was directly correlated with total cholesterol, triglycerides and ApoB-100. Finally, in women with high BMI and normal GWG, ApoD was positively correlated with total LDL-cholesterol, HDL-cholesterol and ApoB-100 but negatively correlated with triglycerides. On the other hand, a negative correlation between ApoD and ApoA-I was seen in groups with normal GWG but suboptimal BMI. Furthermore, in women having low BMI and low or normal GWG, ApoD was inversely correlated with free

fatty acids. This correlation was reversed in women with high BMI and normal GWG (Table A2.3).

Some of the others parameters examined also demonstrated a correlation with ApoD levels (Table A2.3). ApoD was positively correlated with glucose both in the low BMI, normal GWG group and the normal BMI, low GWG group whereas ApoD was positively correlated with insulin only in the latter group. Other than in the control group, albumin was also positively correlated with ApoD in the high BMI, low GWG group. However, the only correlation between ApoD and alphafetoprotein was observed in the low BMI, normal GWG group.

Finally, maternal ApoD levels did not affect newborn parameters. Therefore, neither newborn weight nor height was correlated to maternal ApoD levels (Table A2.3). Surprisingly, although ApoD levels were similar in mothers at their third trimester of pregnancy and newborns, there was no correlation between mother and newborn ApoD levels (Table A2.2).

Because of the low number of women in the three high GWG groups, in an attempt to reveal ApoD correlations, we created a new group containing all women with high GWG, regardless of their BMI (Table A2.4). In this new group, ApoD was negatively correlated with gestational age, GWG and newborn height and directly correlated with maternal BMI. ApoD was also strongly negatively correlated with most of the lipid parameters except triglycerides with which ApoD was directly correlated. Moreover, in this group ApoD was greatly inversely related to albumin and directly correlated with insulin levels.

A2.5.5 ApoD and cholesterol

To verify if the low ApoD in women with excessive GWG was attributable to their lower cholesterol levels, and because of the correlation between plasma ApoD and cholesterol levels in the control group, we compared the ApoD levels between low cholesterol (LC) and high cholesterol (HC) women and we examined the association between ApoD and other pregnancy-related parameters (Table A2.5). The HC group had higher total and LDL-cholesterol, triglycerides, ApoA-I, ApoB-100 and albumin levels but lower GWG and alphafetoprotein levels. In spite of that, both groups displayed similar gestational age, BMI and plasma levels of ApoD, HDL-cholesterol, free fatty acids, glucose and insulin. In addition, their different range of cholesterol levels did not affect the newborn weight, height or plasma ApoD levels (Table A2.5). The two groups were also different from the control group. As expected, the LC group had lower while the HC group had higher levels of total cholesterol, LDL-cholesterol and ApoB-100. In this aspect, the LC group was similar to the high GWG groups (Tables A2.1 and A2.5). The HC group also showed lower GWG and alphafetoprotein concentration and higher triglycerides than the control group (Tables A2.1 and A2.5).

The cholesterol level greatly affected the association of ApoD with maternal and newborn characteristics, ApoD being more associated with pregnancy-related characteristics in LC than in HC women (Table A2.5). Thus, in both the LC and HC groups, ApoD was inversely correlated with free fatty acids levels. In addition, ApoD levels were directly correlated with glucose levels and newborn weight in the HC group. In contrast, in the LC women, ApoD levels were inversely correlated with GWG and total cholesterol, HDL-cholesterol, ApoA-I and ApoB-100 levels and directly correlated with LDL-cholesterol, albumin and alphafetoprotein concentrations (Table A2.5). These associations differed from the ones described for the control group (Table A2.3) but were similar to the ones in high GWG groups

(Tables A2.3 and A2.4), although the association with LDL-cholesterol was reversed and there was no correlation with triglycerides and insulin values.

A2.5.6 ApoD transcription in placenta

Because of the high levels of ApoD mRNA in human placenta and the importance of this tissue in fetal development, we examined placental ApoD expression in relation to maternal BMI and GWG. Besides its influence on plasma ApoD levels (Table A2.2), maternal GWG also affected placental ApoD transcription (Fig. A2.2). However, in contrast to plasma, ApoD transcript levels were decreased in both low and high GWG compared with normal GWG groups. This pattern was mostly noticed in women with normal or low BMI but, although not significant, this tendency was also observed in women with high BMI.

A2.5.7 Postpartum plasma ApoD levels

Given the fact that plasma ApoD levels were decreased by 70% at the end of pregnancy, we examined ApoD levels in control women after delivery and whether these levels were affected by lactation (Fig. A2.3). Two months after delivery, breast-feeding (lactating) women had plasma ApoD levels similar to non-pregnant women. However, in bottle-feeding (non-lactating) women, ApoD concentration was comparable to third trimester levels.

A2.6 Discussion

This study is the first to our knowledge to demonstrate that plasma ApoD levels decrease during pregnancy. Plasma ApoD levels were already significantly lower during first trimester of pregnancy than values detected in non-pregnant women and continued to decrease until the end of pregnancy. The mechanisms governing this decrease are currently unknown, but many potential reasons could explain it.

As for albumin, which concentration decreases from 30% during pregnancy (Maher *et al.* 1993), the decrease in plasma ApoD levels could be explained by hemodilution. Maternal blood volume increases until term and although dependant on many factors, the average increase in volume at term is 45-50% (Hytten 1985). Still, hemodilution alone cannot explain the observed 70% decrease of plasma ApoD.

Low levels of plasma ApoD could also result from decreased ApoD synthesis or secretion. Plasma ApoD can originate from many sources, one of which being the placenta. Since ApoD mRNA levels are almost as high in placenta as in adrenal glands and spleen (Drayna *et al.* 1986), major sources of ApoD in non-pregnant humans, decreased ApoD transcription is unlikely the origin of low plasma ApoD concentration. Another argument against ApoD transcriptional downregulation is the presence of oxidative and inflammatory markers mostly in complicated but also in normal pregnancies (Fialová *et al.* 2006). Oxidative stress (Do Carmo *et al.* 2007, Ganfornina *et al.* 2008) and inflammation (Do Carmo *et al.* 2007) were both reported as intensifying ApoD mRNA production. ApoD decrease could also be caused by the inhibition of its translation or the increase of its degradation rate. More likely, the decline in ApoD levels could be imputable to its reduced secretion during pregnancy. In breast or prostate cancer cells, ApoD secretion is stimulated by IL-1 alpha (Blais *et al.* 1994), androgens, glucocorticoids (Simard *et al.* 1990, 1991, 1992), retinoic acid (Lopez-Boado *et al.* 1994) and 1,25-dihydroxyvitamin D3 (Lopez-Boado *et al.* 1997)

and inhibited by IL-6 (Blais *et al.* 1995) and estrogens (Simard *et al.* 1990). Estrogens are greatly increased during pregnancy. Estrogen values, already high at first trimester, continue to increase until the third trimester to reach levels more than 100-fold higher than the non-pregnant levels (Alvarez *et al.* 1996, Soldin *et al.* 2005). As prolonged exposure to physiological concentrations of 17 beta-estradiol inhibited markedly (70-90%) ApoD secretion in human breast cells (Simard *et al.* 1990), high estrogen concentrations, as seen during gestation, could be the root of plasma ApoD decrease.

This reduction in ApoD secretion might take place not only in tissues directly related to pregnancy such as placenta, uterus and mammary gland but also in other tissues expressing high levels of ApoD mRNA and whose physiology is altered in response to gestation-induced hormonal changes, including the spleen, adrenals, pancreas and kidneys (Bender and Chickering 1985, Maymon *et al.* 2007, Novak *et al.* 2001). Assuming that ApoD synthesis and degradation rates remain unchanged, a reduced secretion will result in ApoD accumulation inside these tissues, suggesting an intratissular role for ApoD in pregnancy. In the placenta, in collaboration with other molecules, ApoD could play a key role in the transport of essential nutrients, regulation factors and toxic metabolites between the mother and the fetus, thus influencing fetal development and health in later life. Those could include cholesterol (Drayna *et al.* 1986), arachidonic acid (Lafond *et al.* 2000, Morais Cabral *et al.* 1995), steroids (Dilley *et al.* 1990, Simard *et al.* 1991), vitamin A and thyroid hormones (Yao and Vieira 2002) as well as the removal of bilirubin (Peitsch and Boguski 1990).

It was already reported that ApoD levels in newborns represent about 37% of the levels found in adults (Lane and McConathy 1983, McConathy and Lane 1980). Accordingly, we observed that the concentration of circulating ApoD in the newborn was very similar to the one of the mother at the third trimester of pregnancy, although

the levels found in the newborn and in the mother were not statistically correlated. This lack of correlation suggests that ApoD does not pass through the placental barrier. Since ApoD mRNA is expressed as early as E8.5 during mouse embryogenesis (Sanchez *et al.* 2002), the fetus might not be dependent on a maternal ApoD supply. Furthermore, the similarity in mother and newborn ApoD concentrations suggests that even if maternal plasma ApoD does not directly cross the placental barrier, both might be subjected to the same regulatory mechanisms.

An exception to the close match between maternal and newborn ApoD levels was found in the group displaying normal maternal BMI (20-26 kg/m^2) and low GWG (< 11 kg). This difference could be related to the lower maternal triglycerides and ApoB-100 levels. As triglycerides, a source of fatty acids, and ApoB-100, which influences the transfer of cholesterol and lipid soluble vitamins, are both essential for fetus development (Madsen *et al.* 2004), their low levels probably explain the smaller size of the newborns as well as the low levels of ApoD.

We also observed that, while prepregnancy maternal BMI had no incidence on plasma ApoD concentrations on both mother and newborn, high GWG (> 18 kg) significantly decreased ApoD values. This decrease is very likely multifactorial. First, it could be related to defects in lipid metabolism. Indeed, high GWG groups displayed lower levels of total cholesterol, LDL-cholesterol, and ApoB-100. This was present in normal, high and pooled BMI groups but the tendency, although not significant, was also observed in the low BMI group. In addition, in the group composed of all women with high GWG regardless of their BMI, ApoD and lipid markers were strongly correlated. An involvement of ApoD in lipid metabolism was already suggested. Because of its capacity to bind cholesterol (Drayna *et al.* 1986) and its presence on lipoprotein fractions (McConathy and Alaupovic 1976), ApoD, in collaboration with apoA-I, lecithin-cholesterol acyltransferase (LCAT) and cholesteryl ester transfer protein (CETP) (Francone *et al.* 1989), may participate in

the cholesterol transport pathway. Furthermore, genetic variation in ApoD affects the serum lipid levels (Desai *et al.* 2002).

Nevertheless, in view of the facts that high GWG groups are not the only ones presenting levels of total cholesterol, LDL-cholesterol, and ApoB-100 different from the control group as well as correlations between ApoD and lipid levels, that the low BMI group does not show a significant decrease of these lipid parameters, and that the ApoD concentration is similar in the control, HC and LC groups, the latter showing similarities with the high GWG groups, lipid levels are probably not the major factors responsible for low ApoD levels in these groups. Determinants of maternal GWG include a range of biological, metabolic, and social factors. Amongst them, studies show that higher levels of circulating insulin, leptin, IGF-1 and C-Peptide are associated with excessive amounts of weight gain during pregnancy (Delvaux *et al.* 2003, Scholl and Chen 2002, Stein *et al.* 1998). Given that: 1) the insulin levels variations are inconsistent in the three high GWG groups; 2) the only high GWG group presenting high insulin levels had ApoD levels similar to the control group; and 3) the lack of correlation between ApoD and insulin levels in these groups, it seems improbable that insulin is responsible for the decreased ApoD values in high GWG groups. ApoD levels could also be related to leptin concentration. Indeed, ApoD was found to interact specifically with the cytoplasmic portion of the long form of the leptin receptor Ob-Rb and can thus be involved in the control of energy homeostasis (Liu *et al.* 2001). However, this hypothesis is toned down by the fact that leptin levels were reported to correlate strongly with BMI (Ostlund *et al.* 1996) while ApoD levels were not affected by the mother's BMI. Another alternative is that women with excessive GWG may have had higher pregnancy hormone levels than women with GWG within the recommended range. Some studies suggested that high GWG may be associated with increased estrogen levels (Petridou *et al.* 1992), but other studies have not confirmed this observation (Wuu *et al.* 2002). As a reminder, estrogens are inhibitors of ApoD secretion.

A lower placental ApoD mRNA level in women with excessive GWG is probably at the basis of the lower circulating ApoD concentrations in these women. However, as women with low GWG also have decreased ApoD transcripts in placenta but normal circulating ApoD levels, it suggests that the levels of placental and circulating ApoD are subjected to a tight regulation. In the view that ApoD plays a key role in the control of fetal homeostasis, the regulation of ApoD levels becomes vital for the pregnancy outcome and the health of the newborn. Thus, in women with high GWG, a decrease in ApoD is desirable in order to reduce lipid transfer to fetus. In these women, as already discussed, ApoD transcription could be downregulated in response to lipid and hormone concentrations. The same factors could account for low ApoD transcription in low GWG women. In addition, in these women, low ApoD transcription could be also related to inadequate nutrient intake. In this case, the lower production of ApoD is disadvantageous and would then be compensated by an increased secretion or lower degradation resulting in adequate ApoD protein concentration in the circulation and possibly in the placenta. In overweight women (high BMI), this control is probably altered, explaining why the ApoD mRNA and plasma ApoD levels are similar in high GWG and in the control group. It also suggests that ApoD could participate to the high transfer of lipids to the fetus in these women, contributing to obesity and cardiovascular disease in later life.

The return to basal, non-pregnant, plasma ApoD levels after delivery, such as observed in breast-feeding women was expected. This correlates well with the drop in estrogen levels after childbirth (Alvarez *et al.* 1996, West and McNeilly 1979). However, the fact that bottle-feeding women still have the same plasma ApoD levels than during their third trimester of pregnancy is intriguing and suggests again that the regulation of ApoD levels is complex and does not only depend on estrogen levels. A possible explanation of this discrepancy is that two months after delivery non-lactating women may not have fully recovered their normal endocrine activity,

menstrual cycle and weight which possibly affects ApoD production. Breastfeeding mothers do not recover ovarian activity and normal weight in two months either. However, they have high levels of prolactin that exert an antagonistic action on estrogen production in order to maintain lactation (Alvarez *et al.* 1996, Wang *et al.* 1980). In addition, breast-feeding induces the production of cytokines (Shimaoka *et al.* 2000, 2001), which may contribute to the higher levels of circulating ApoD.

To summarize, plasma ApoD levels decrease during normal uncomplicated human pregnancy. ApoD is further decreased in women with excessive GWG and their newborns. The fall in circulating ApoD may be a compensation mechanism in order to achieve appropriate fetal homeostasis. The cause of this decrease, controlled in part at the transcriptional level in the placenta, is probably multifactorial and may be related to pregnancy induced increase in estrogen levels.

Table A2.1 : Clinical and biochemical characteristics of the studied population during the third trimester of pregnancy. Data are organized according to maternal body mass index (BMI) at first trimester of pregnancy and weight gain during pregnancy (GWG). Results are expressed as mean ± SE. * The same letter within one parameter means no statistical differences between groups; different letters indicate significant differences between the corresponding groups ($p < 0.01$).

	BMI < 20 kg/m²			BMI 20 -26 kg/m²			BMI > 26 kg/m²		
	GWG < 11 kg n= 9	GWG 11 -18 kg n= 14	GWG > 18 kg n= 4	GWG < 11 kg n= 28	GWG 11 -18 kg n= 48	GWG > 18 kg n= 6	GWG < 11 kg n= 20	GWG 11 -18 kg n= 18	GWG > 18 kg n= 4
Gestational age (weeks)	39.10±0.62	39.21±0.39	40.17±0.54	39.2±0.23	39.49±0.19	39.22±0.52	38.59±0.25	39.32±0.21	38.25±0.85
BMI (kg/m²)	18.81±0.31	19.06±0.16	18.69±0.50	23.09±0.27	22.66±0.22	22.90±0.54	30.81±0.75	28.43±0.45	34.40±2.6
GMG (kg)	9.07±0.29	13.37±0.36	30.04±8.29	7.80±0.45	14.19±0.28	20.21±0.57	8.04±0.52	14.54±0.44	18.7±0.29
Newborn weight (g)	3220. 00±133. 95	3405. 86±117. 19	3554. 17±209. 46	3147. 71±76.17	3373. 34±63.26	3375. 89±159. 79	3408. 22±82.74	3494. 52±99.58	3259. 25±302. 11
Newborn height (cm)	50.55±1.01	51.5±0.57	52.08±0.99	50.73±0.36	51.70±0.29	52.11±0.79	51.57±0.44	51.28±0.44	51.26±1.43
Total cholesterol (mM)	7.85±0.75	7.31± 0.46	6.81±0.28	6.81±0.21	6.99±0.19	6.25±0.36	6.26±0.39	6.97±0.31	5.11±0.40
LDL -cholesterol (mM)	4.69±0.62	4.25±0.44	3.70±0.32	3.79±0.19	3.86±0.16	3.29±0.20	3.13±0.30	3.75±0.29	2.41±0.53
HDL -cholesterol (mM)	1.70±0.10	1.85±0.15	1.66±0.11	1.86±0.08	1.83±0.06	1.68±0.30	1.64±0.11	1.73±0.12	1.34±0.23
Triglycerides (mM)	3.16±0.43	2.87±0.24	3.15±0.58	2.55±0.14	2.83±0.11	2.77±0.50	3.25±0.29	3.24±0.28	2.96±1.00
Free fatty acids (mmol/L)	0.48±0.09	0.66±0.09	0.64±0.12	0.70±0.08	0.61±0.06	0.67±0.09	0.67±0.08	0.73±0.06	0.36±0.06
ApoA -I (g/L)	2.13±0.10	2.12±0.12	2.08±0.08	2.14±0.07	2.16±0.06	2.11±0 .18	2.08±0.09	2.13±0.09	1.80±0.08
ApoB-100 (mg/L)	1.53±0.14	1.42±0.10	1.39±0.04	0.93±0.06	1.38±0.05	1.27±0.05	1.19±0.07	1.42±0.09	1.04±0.14
Albumin (g/L)	33.67±1.00	35.43±1.00	34.40±1.29	35.67±0.51	34.31±0.43	33.57 ±1.33	33.86±0.50	34.47±0.65	30.00±0.01
Alphafetoprotein (μg/L)	113.20± 24.49	177.79± 22.82	76.96±17. 55	108.78±9. 41	1029. 11±901. 35	155.60± 42.15	116.41± 17.87	304.9±1 91.75	82.31±42. 80
Glucose (mmol/L)	5.86±1.15	4.60±0.60	4.34±0.64	5.67±0.64	4.78±0.26	4.51±0.38	5.15±0.51	4.30±0.45	14.3±8.6
Insulin (pmol/L)	243.29± 119.72	133.96± 59.70	132.56± 21.01	161.68± 27.81	186.86± 34.22	124.50± 24.72	232.26± 44.55	168.52± 34.23	565.40± 30.30

Table A2.2: Plasmatic ApoD (mg/L) in the mother at third trimester of pregnancy and in the newborn depending on maternal weight gain during pregnancy and body mass index (BMI) at first trimester. Data are expressed as mean ± SE. The same letter means no statistical differences between groups; different letters indicate significant differences between the groups ($p < 0.01$). * indicates a difference between mothers and newborns of the corresponding group ($p < 0.001$).

Mother			
		BMI (kg/m^2)	
GWG (kg)	< 20	20-26	> 26
< 11	76.08 ± 31.36 (n=9) [a]	87.84 ± 21.94 (n=28) [a]	64.86 ± 21.54 (n=20) [a]
11-18	59.30 ± 16.65 (n=14) [a]	61.69 ± 10.93 (n=48) [a]	54.44 ± 11.30 (n=18) [a]
> 18	25.99 ± 14.02 (n=4) [b]	27.45 ± 9.10 (n=6) [b]	46.44 ± 20.96 (n=4) [ab]
Newborn			
		BMI (kg/m^2)	
GWG (kg)	< 20	20-26	> 26
< 11	60.35 ± 21.12 (n=9) [a]	43.48 ± 8.73 (n=28) [a, b] *	67.28 ± 17.20 (n=20) [a]
11-18	64.61 ± 22.20 (n=14) [a]	56.63 ± 8.96 (n=48) [a]	85.06 ± 70.11 (n=18) [a, b]
> 18	20.26 ± 8.56 (n=4) [b]	36.98 ± 13.00 (n=6) [b]	17.25 ± 6.51 (n=4) [b]

Table A2.3: Association of plasma ApoD levels with clinical and biochemical characteristics in women at their third trimester. Pearson correlations (r) are significant at * $p<0.05$, ** $p<0.05$, ***$p<0.001$.

	BMI < 20 kg/m²			BMI 20 -26 kg/m²			BMI > 26 kg/m²		
	GWG < 11 kg n= 9	GWG 11 -18 kg n= 14	GWG > 18 kg n= 4	GWG < 11 kg n= 28	GWG 11 -18 kg n= 48	GWG > 18 kg n= 6	GWG < 11 kg n= 20	GWG 11 -18 kg n= 18	GWG > 18 kg n=4
Gestational age (weeks)	**-0.229 ***	**0.404 ****	0.326	0.086	0.079	**-0.409 ***	**-0.280 ****	0.070	-0.899
BMI (kg/m²)	**0.284 ***	-0.046	0.984	0.160	-0.115	-0.326	**-0.233 ***	-0.143	0.035
GWG (kg)	**0.675 ***	**-0.365 ****	-0.602	**0.275 ****	-0.026	-0.249	**0.294 ***	**-0.253 * ****	-0.493
Newborn weight (g)	-0.358	0.414	-0.994	0.086	0.079	-0.136	0.155	0.224	0.092
Newborn height (cm)	0.199	0.134	-0.472	-0.044	-0.164	-0.086	0.173	0.197	0.092
Newborn ApoD (mg/L)	0.761	0.784	0.478	0.171	0.204	-0.169	-0.074	0.056	0.018
Total cholesterol (mM)	-0.561	-0.064	-0.589	**0.202 * ****	**0.253 * ****	-0.548	**0.272 * ****	0.052	0.149
LDL-cholesterol (mM)	-0.080	-0.899	-0.899	**0.226 * ****	0.179	-0.739	0.107	**0.378 * ****	-0.961
HDL-cholesterol (mM)	0.466	-0.165	-0.262	0.146	-0.146	-0.744	0.086	**0.201 * ****	-0.996
Triglycerides (mM)	-0.648	0.036	0.144	**-0.214 * ****	0.080	0.822	**0.335 * ****	0.163	0.997
Free fatty acids (mmol/L)	**-0.346 ***	**-0.416 ***	-0.589	-0.031	0.077	-0.462	-0.123	**0.266 * ****	0.534
ApoA-I (g/L)	-0.385	**-0.200 ****	-0.742	0.093	0.127	-0.582	0.018	**-0.289 * ****	1.00
ApoB-100 (mg/L)	-0.642	-0.038	-0.776	**0.332 * ****	0.126	0.355	**0.205 * ****	**0.335 * ****	-0.178
Albumin (g/L)	-0.283	-0.021	-0.940	0.133	**0.313 * ****	-0.746	**0.306 * ****	0.119	0.119
Alphafetoprotein (µg/L)	-0.200	**-0.303 ****	-0.325	-0.105	0.053	0.360	-0.011	0.074	0.050
Glucose (mmol/L)	0.037	**0.365 ****	0.772	**0.416 * ****	-0.036	0.761	0.029	0.176	1.00
Insulin (pmol/L)	0.319	0.142	0.321	**0.424 * ****	-0.073	0.955	-0.079	0.008	-0.002

Table A2.4: Association of plasma ApoD levels with clinical and biochemical characteristics in women with GWG > 18 kg at their third trimester. Women with BMI < 20 kg/m^2, 20-26 kg/m^2 and > 26 kg/m^2 were pooled (n=14). § p< 0.001 compared to the control group (BMI 20-26 kg/m^2, GWG 11-18 kg). Pearson correlations (*r*) are significant at * p<0.05, ** p<0.05, ***p<0.001.

	Mean ± SE	*r*
Gestational age (weeks)	39.32±0.37	**-0.414** ***
BMI (kg/m^2)	24.37±1.59	**0.232** ***
GMG (kg)	22.75±2.56	**-0.365** ***
Newborn weight (g)	3407.16±114.4	-0.552
Newborn height (cm)	52±0.54	**-0.559** ***
Newborn ApoD (mg/L)	28.04±7.14	-0.080
Total cholesterol (mM)	6.25±0.25 §	**-0.563** **
LDL-cholesterol (mM)	3.28±0.20 §	**-0.724** **
HDL-cholesterol (mM)	1.61±0.14	**-0.598** **
Triglycerides (mM)	2.95±0.34	**0.631** **
Free fatty acids (mmol/L)	0.60±0.06	**-0.358** **
ApoA-I (g/L)	2.04±0.09	**-0.554** **
ApoB-100 (mg/L)	1.27±0.05 §	**-0.243** **
Albumin (g/L)	33.36±0.86	**-0.647** **
Alphafetoprotein (µg/L)	117.04±24.05	0.164
Glucose (mmol/L)	5.85±1.34	-0.116
Insulin (pmol/L)	206.89±55.36	**0.464** *

Table A2.5: Characteristics of the studied population according to plasma cholesterol levels during third trimester and association with plasma ApoD levels. LC : low cholesterol; HC : high cholesterol. Results are expressed as mean ± SE. * p<0.05, ** p<0.01, *** p< 0.001 compared to the LC group. § p< 0.001 compared to the control group (BMI 20-26 kg/m^2, GWG 11-18 kg). Pearson correlations (*r*) are significant at * p<0.05, *** p<0.001.

	LC n=38	HC n=29	LC n=38	HC n=29
			r	*r*
Gestational age (weeks)	39.30 ±0.25	39.5±0.23	0.100	-0.066
BMI (kg/m^2)	22.68±0.33	23.26±0.68	0.086	0.175
GMG (kg)	14.26±0.43	12.16±0.47 § ***	**-0.321** ***	-0.054
Newborn weight (g)	3452.43±83.90	3389.27±67.13	-0.329	**0.398** *
Newborn height (cm)	51.86±0.39	51.77±0.40	0.114	0.009
Newborn ApoD (mg/L)	59.17±13.31	59.33±11.57	-0.005	0.490
Total cholesterol (mM)	5.95±0.13 §	9.08±0.17 § ***	**-0.533** ***	0.023
LDL-cholesterol (mM)	2.94±0.12 §	5.65±0.18 § ***	**0.314** ***	-0.040
HDL-cholesterol (mM)	1.75±0.09	1.79±0.10	**-0.215** ***	0.063
Triglycerides (mM)	2.76±0.18	3.59±0.18 § ***	-0.178	-0.033
Free fatty acids (mmol/L)	0.51±0.06	0.63±0.08	**-0.268** ***	**-0.310** ***
ApoA-I (g/L)	2.09±0.06	2.24±0.08 *	**-0.422** ***	0.028
ApoB-100 (mg/L)	1.18±0.04 §	1.82±0.04 § ***	**-0.413** ***	0.071
ApoD (mg/L)	57.69±14.16	63.05±11.54	-	-
Albumin (g/L)	33.70±0.51	35.14±0.71 ***	**0.340** ***	0.046
Alphafetoprotein (µg/L)	1298.73±1193.7	94.22±9.46 § **	**0.813** ***	-0.086
Glucose (mmol/L)	5.05±0.37	5.04±0.52	-0.022	**0.449** ***
Insulin (pmol/L)	186.48±37.80	194.72±39.51	-0.138	0.156

A2.7 Figure legends

Figure A2.1: Plasmatic ApoD levels during pregnancy. ApoD levels were measured in women with a BMI of 20-26 kg/m^2 and a WG of 11-18 kg at the two first trimesters of pregnancy (1st and 2nd) and at delivery (3rd) and compared with levels in non-pregnant women (BMI 20-26 kg/m^2). ApoD levels in the cord blood were also measured. Data are expressed as means ± SEM. The same letter means no statistical differences between groups; different letters indicate significant differences between the groups ($p < 0.001$)

Figure A2.2: Expression of apoD mRNA in placenta according to the pre-pregnancy BMI and gestational WG. The level of apoD expression was measured by qRT-PCR using specific primers for apoD. Data are expressed as the normalized ratio of apoD mRNA to 18S RNA (means ± SEM). The same letter means no statistical differences between groups; different letters indicate significant differences between the groups ($p < 0.01$).

Figure A2.3: The effect of breast- and bottle-feeding on plasmatic ApoD levels. ApoD concentration was measured in mothers two month after delivery (women with a BMI of 20-26 kg/m^2 and a WG of 11-18 kg) and compared with levels in non-pregnant women (BMI 20-26 kg/m^2). Data are expressed as means ± SEM. The same letter means no statistical differences between groups; different letters indicate significant differences between the groups ($p < 0.001$).

Figure A2.1

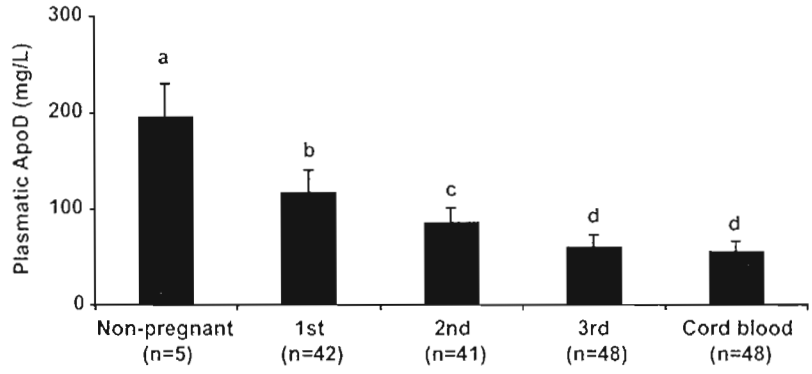
300
200
100
0
Plasmatic ApoD (mg/L)
a
b
c
d
d
Non-pregnant (n=5)
1st (n=42)
2nd (n=41)
3rd (n=48)
Cord blood (n=48)

Figure A2.2

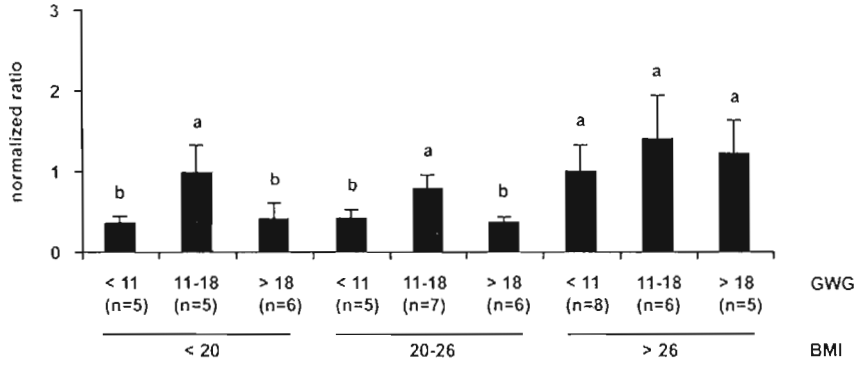
normalized ratio
3
2
1
0
b
a
b
b
a
b
a
a
a
< 11 (n=5)
11-18 (n=5)
> 18 (n=6)
< 11 (n=5)
11-18 (n=7)
> 18 (n=6)
< 11 (n=8)
11-18 (n=6)
> 18 (n=5)
GWG
< 20
20-26
> 26
BMI

Figure A2.3

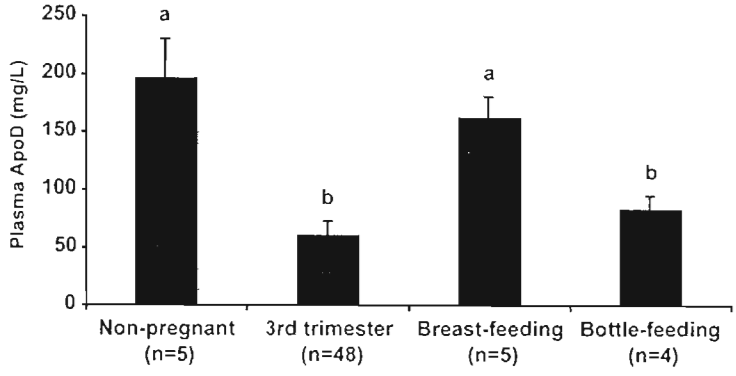
Plasma ApoD (mg/L)
250
200
150
100
50
0
a
b
a
b
Non-pregnant (n=5)
3rd trimester (n=48)
Breast-feeding (n=5)
Bottle-feeding (n=4)

ANNEXE III

Résultats supplémentaires non-publiés

Survie des souris Thy-1/ApoD et NSE/ApoD

A3.1 Résultats

Les souris Thy-1/ApoD et NSE/ApoD présentent une survie différente de celle des souris WT. Cependant, cette différence de survie est difficilement réconciliable avec le phénotype métabolique et nécessite une plus grande exploration avant publication. C'est pourquoi ces résultats n'ont pas été inclus dans le chapitre III.

Tel qu'illustré dans la figure A3.1A, la courbe de survie de Kaplan-Meier des souris Thy-1/ApoD démontre une claire divergence par rapport à la courbe des souris WT ($p=0.0045$) avec une plus grande survie médiane (753 jours comparativement à 643 jours chez les souris WT). Cependant, la longévité maximale des souris Thy-1/ApoD (824.4 ± 43.9 jours, $p>0.05$, $n=40$), n'est pas significativement différente de celle des souris WT (808.4 ± 47 jours, $n=60$). En comparaison, les souris NSE/ApoD vivent plus longtemps (909.8 ± 21.5 jours, $p<0.001$, $n=57$) et démontrent une courbe de survie différente par rapport aux souris WT ($p=0.0227$), mais ont une survie médiane similaire (629 jours) (Fig. A3.1B). Ces courbes de survie peuvent être reliées à l'expression du transgène dans le cerveau de ces souris en fonction du temps. Chez les souris Thy-1/ApoD, l'expression du transgène diminue dans le temps à partir de 500 jours pour atteindre de faibles niveaux à 900 jours. Cette diminution est probablement reliée au déclin du nombre des neurones dopaminergiques dû au vieillissement. Cependant, l'expression de H-ApoD reste constante durant la vie des souris NSE/ApoD (Fig. A3.1C).

A3.2 Légende des figures

Figure A3.1: Courbes de survie Kaplan-Meier des souris H-apoD Tg. Courbes de survie des souris Thy-1/ApoD (n=40) (A) et NSE/ApoD (n=57) (B) versus les souris WT (n=60). Puisque aucune différence n'a été constatée entre les sexes, un mélange de sexes a été utilisé pour ces courbes. C: Immunobuvardage démontrant l'expression protéique de H-apoD dans le cerveau des souris transgéniques en fonction de l'âge (jours). Un anticorps polyclonal anti-GAPDH a été utilisé pour la normalisation.

Figure A3.1

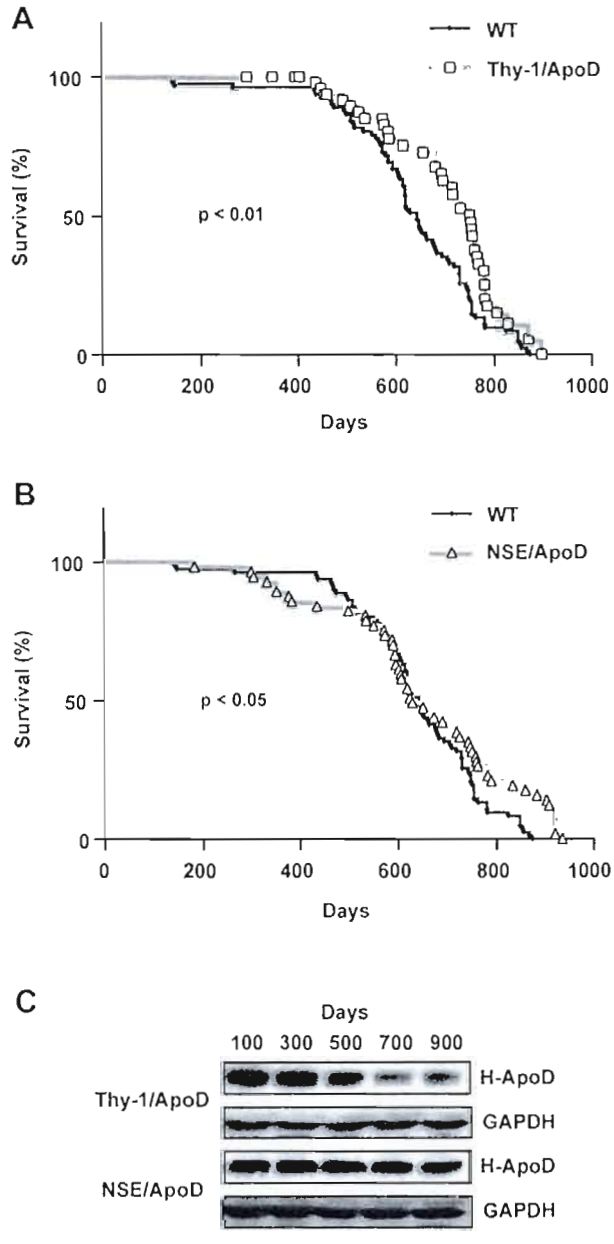
A
WT
Thy-1/ApoD
100
50
0
Survival (%)
p < 0.01
0
200
400
600
800
1000
Days
B
WT
NSE/ApoD
100
50
0
Survival (%)
p < 0.05
0
200
400
600
800
1000
Days
C
Days
100 300 500 700 900
Thy-1/ApoD
H-ApoD
GAPDH
NSE/ApoD
H-ApoD
GAPDH

ANNEXE IV

Résultats supplémentaires non-publiés

Caractérisation des souris NFL/ApoD

A4.1 Résultats

Les souris NFL/ApoD ont aussi été partiellement caractérisées. Cependant, la divergence de ces souris au niveau de la réponse au glucose et à l'insuline reste pour l'instant inexplicable et nécessite une plus grande exploration avant publication. C'est pourquoi ces résultats n'ont pas été inclus dans le chapitre III.

Les souris NFL/ApoD expriment l'apoD humaine sous le contrôle du promoteur du gène NFL (Fig. A4.1A-B). Ce promoteur est un promoteur faible qui s'exprime au niveau de tous les types de neurones. Chez ces souris, la H-apoD s'exprime dans le système nerveux, particulièrement au niveau de la medulla oblongata, du cortex et du cervelet (Fig. A4.1C). L'expression de H-apoD a aussi été retrouvée hors du système nerveux dans le sang, le muscle, le cœur, les poumons et les reins (Fig. A4.1C). Sauf pour les cellules sanguines, l'expression de NFL dans ces tissus avait déjà été rapportée.

Les souris NFL/ApoD présentent des différences par rapport aux souris WT et aux autres souris transgéniques. Ces souris ont un plus gros cerveau mais moins de gras épididymal (Table A4.1). Elles ont aussi plus de créatine kinase, un marqueur de la fonction rénale et musculaire (Table A4.2). Comme les souris NSE/ApoD (Table 3.4), elles ont aussi un plus grand nombre de globules blancs, causé par une augmentation des neutrophiles, des lymphocytes et des monocytes (Table A4.3). Cependant, les souris NFL/ApoD ont une longévité similaire à celle des souris WT (Fig. A4.2). Elles ont aussi une plus grande tolérance au glucose (Fig. A4.3A-B) et ne présentent pas de résistance à l'insuline (Fig. A4.3C). De plus, ces souris n'ont pas ou très peu d'accumulation de lipides au niveau du foie (Fig. A4.4). Finalement, ces souris ont des niveaux de pAkt, d'apoE, de LFABP, de FAS, de PPAR α et γ, de

SREBP1c, d'IL-1α, d'IL-6, d'IL-10, de TNFα, de IFNγ, de TGFβ, de leptine, d'adiponectine et de résistine semblables aux souris WT (résultats non-montrés).

La cause de ce phénotype reste inconnue. Il pourrait s'expliquer par le fait que ce promoteur est le plus faible des trois. De plus, le transgène n'est pas exprimé dans le foie ce qui explique probablement la plus petite accumulation de lipides comparativement aux autres souris transgéniques et éviterait donc l'inhibition des voies de l'insuline. Par ailleurs, la tolérance accrue au glucose reste inexpliquée, mais pourrait être corrélée avec l'expression de H-apoD dans le muscle. D'autres études seront essentielles à la clarification de ces phénomènes.

Table A4.1 : Paramètres morphométriques des souris NFL/ApoD.

	WT	NFL/ApoD
Poids (g)	38.95 ± 4.57	38.78 ± 3.12
Longueur (cm)	9.86 ± 0.40	9.90 ± 0.12
Indice de poids corporel (g/cm2)	0.40 ± 0.03	0.40 ± 0.02
Poids des tissus (g/g poids corporel, x 100)		
Cerveau	1.07 ± 0.08	1.23 ± 0.13 *
Foie	4.03 ± 0.58	4.27 ± 0.85
Gras inguinal	4.87 ± 1.54	3.18 ± 1.26
Gras mésentérique	5.26 ± 1.01	4.35 ± 1.17
Gras épididymal	0.88 ± 0.26	0.46 ± 0.19 *

Les valeurs représentent la moyenne ± l'écart-type de 12 souris par groupe. * $p<0.05$ vs les souris WT.

Table A4.2 : Paramètres sanguins des souris NFL/ApoD.

	WT	NFL/ApoD
Protéines totales (g/L)	52.20 ± 4.09	52.20 ± 5.45
Albumine (g/L)	27.40 ±7.50	26.80 ± 8.70
Glucose (mmol/L)	10.90 ± 0.75	11.68 ± 3.46
Insuline (ng/ml)	1.44 ± 0.37	1.35 ± 0.42
BUN urée (mmol/L)	8.28 ± 1.01	7.94 ± 1.67
Créatinine (µmol/L)	13.33 ± 0.58	16.00 ± 3.61
Bilirubine totale (µmol/L)	2.92 ± 0.94	2.82 ± 0.46
ALT (U/L)	39.00 ± 1.00	42.00 ± 6.89
AST (U/L)	86.00 ± 20.88	132.00 ± 61.54
Phosphatase alkaline (U/L)	82.40 ± 14.96	100.00 ± 33.07
Créatine kinase (U/L)	85.33 ± 47.51	319.25 ± 127.75 **
Cholestérol (mmol/L)	2.98 ± 0.36	2.75 ± 0.36
HDL (mmol/L)	2.42 ± 0.31	2.21 ± 0.30
Triglycérides (mmol/L)	1.15 ± 0.31	1.25 ± 0.50
Acides gras libres (mmol/L)	0.63 ± 0.38	0.51 ± 0.06

Les valeurs représentent la moyenne ± l'écart-type de 6 souris par groupe. ** $p<0.01$ vs les souris WT.

Table A4.3 : Paramètres hématologiques des souris NFL/ApoD.

	WT	NFL/ApoD
Hémoglobine (g/L)	123.50 ± 9.19	129.00 ± 5.66
Globules rouges (x 10^{12}/L)	8.07 ± 0.18	8.19 ± 0.01
Globules blancs (x 10^9/L)	3.75 ± 0.21	4.45 ± 0.35 *
Neutrophiles (x 10^9/L)	0.42 ± 0.34	0.80 ± 0.20 *
Lymphocytes (x 10^9/L)	3.27 ± 0.16	3.47 ± 0.11 *
Monocytes (x 10^9/L)	0.02± 0.03	0.10 ± 0.01 **
Éosinophils (x 10^9/L)	0.04 ± 0.06	0.09 ± 0.01
Plaquettes (x 10^9/L)	747.00 ± 241.83	830.00 ± 15.56

Les valeurs représentent la moyenne ± l'écart-type de 6 souris par groupe.* $p<0.05$, ** $p<0.01$ vs les souris WT.

A4.2 Légende des figures

Figure A4.1: Structure et expression du transgène NFL/ApoD. A) La partie codante du gène de l'H-apoD (noir) fusionnée avec le signal de polyadénylation du gène de l'hormone de croissance bovine (BGH; gris) ont été insérés dans le gène de la chaîne légère du neurofilament (NFL; blanc). B: BamHI, H: HindIII, Sac: SacI, Sma: SmaI, S/X: SalI/XhoI, X: XbaI. Le transgène a été excisé par digestion avec les enzymes SmaI et SacI (NFL/ApoD; 7 kpb). B) Analyse de type Southern des souris NFL/ApoD. L'ADN génomique (10 µg) digéré par BamHI a été analysé en utilisant le transgène comme sonde. Les témoins (gauche) correspondant à 1 (1c) ou 10 (10c) copies du transgène sont utilisés pour déterminer le nombre de copies intégrés à l'ADN. C) Analyse de divers tissus par RT-PCR semi-quantitatif en utilisant des oligonuléotides spécifiques à H-apoD. Le gène HPRT sert de témoin interne. Medulla: medulla oblongata. Muscle: muscle squelettique. Les résultats sont représentatifs de 3 expériences séparées.

Figure A4.2: Courbes de survie Kaplan-Meier des souris NFL/ApoD. NFL/ApoD (n=21) versus WT (n=60). Puisqu'il n'y avait pas de différence entre les sexes, mâles et femelles ont été inclus dans la courbe.

Figure A4.3: Analyse in vivo de la tolérance au glucose et de la sensibilité à l'insuline. A) Niveaux de glucose sanguin pendant le test de tolérance au glucose intrapéritonéal (IPGTT), démontrant une plus grande tolérance au glucose chez les souris NFL/ApoD (2 g/kg poids corporel; animaux à jeun de 12-15h). B) Concentration d'insuline plasmatique durant le IPGTT. C) Niveaux de glucose pendant le test de tolérance à l'insuline (ITT) montrant une plus grande tolérance chez les animaux NFL/ApoD. Les valeurs représentent la moyenne ± l'écart-type de 6 souris par génotype. * $p<0.01$ vs les souris WT.

Figure A4.4: Stéatose hépatique chez les souris NFL/ApoD. A-B) Coupes de foie colorées à l'hématoxyline-éosine. C-D) Cryosections de foie colorées à l'huile rougeO. Magnification originale, x 100; n=6. E) Contenu lipidique total. Les valeurs représentent la moyenne ± l'écart-type de 6 souris par génotype.

Figure A4.1

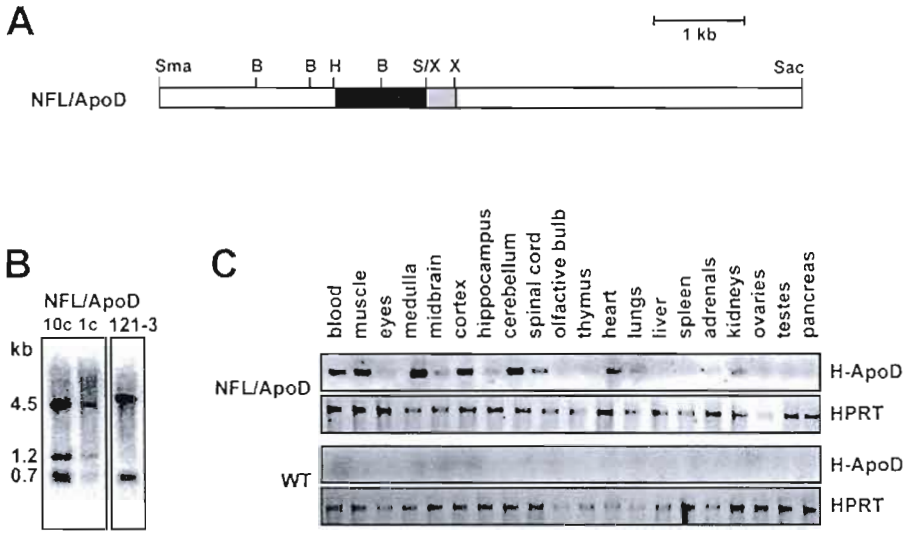
A
1 kb
Sma
B
B
H
B
S/X
X
Sac
NFL/ApoD
B
NFL/ApoD
10c 1c 121-3
kb
4.5
1.2
0.7
C
blood
muscle
eyes
medulla
midbrain
cortex
hippocampus
cerebellum
spinal cord
olfactive bulb
thymus
heart
lungs
liver
spleen
adrenals
kidneys
ovaries
testes
pancreas
NFL/ApoD
H-ApoD
HPRT
WT
H-ApoD
HPRT

Figure A4.2

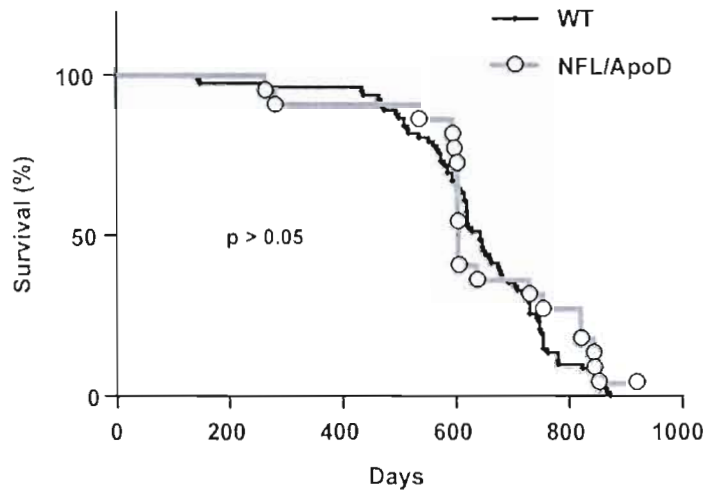

Figure A4.3

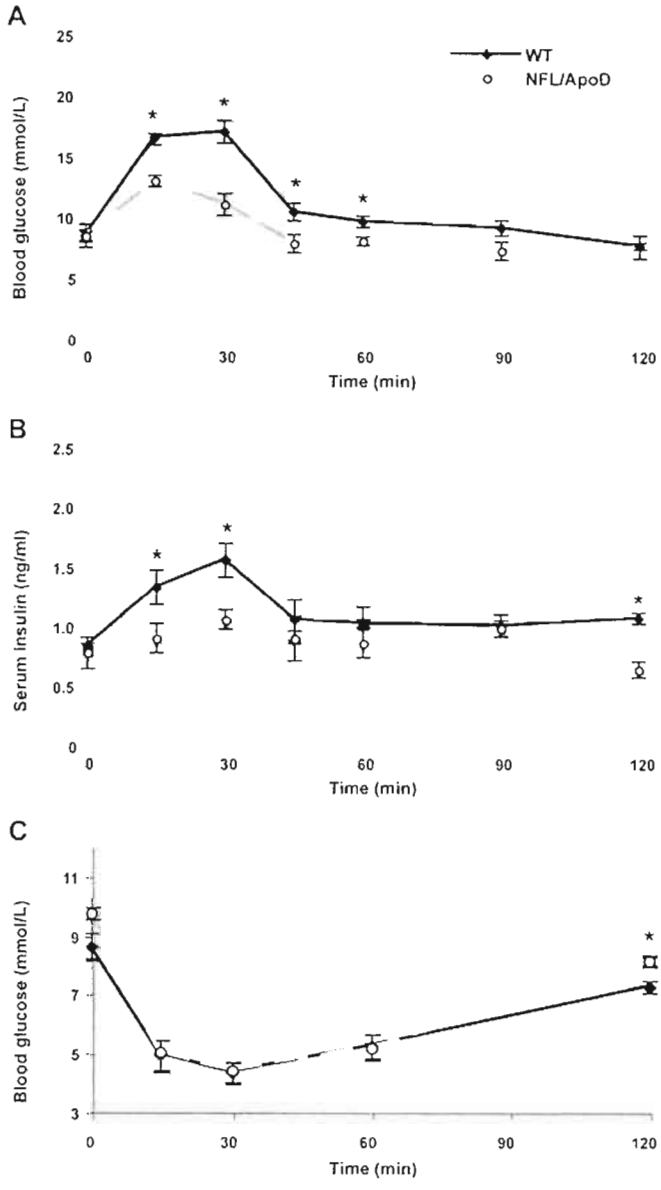
A
WT
NFL/ApoD
Blood glucose (mmol/L)
Time (min)
B
Serum insulin (ng/ml)
Time (min)
C
Blood glucose (mmol/L)
Time (min)

Figure A4.4

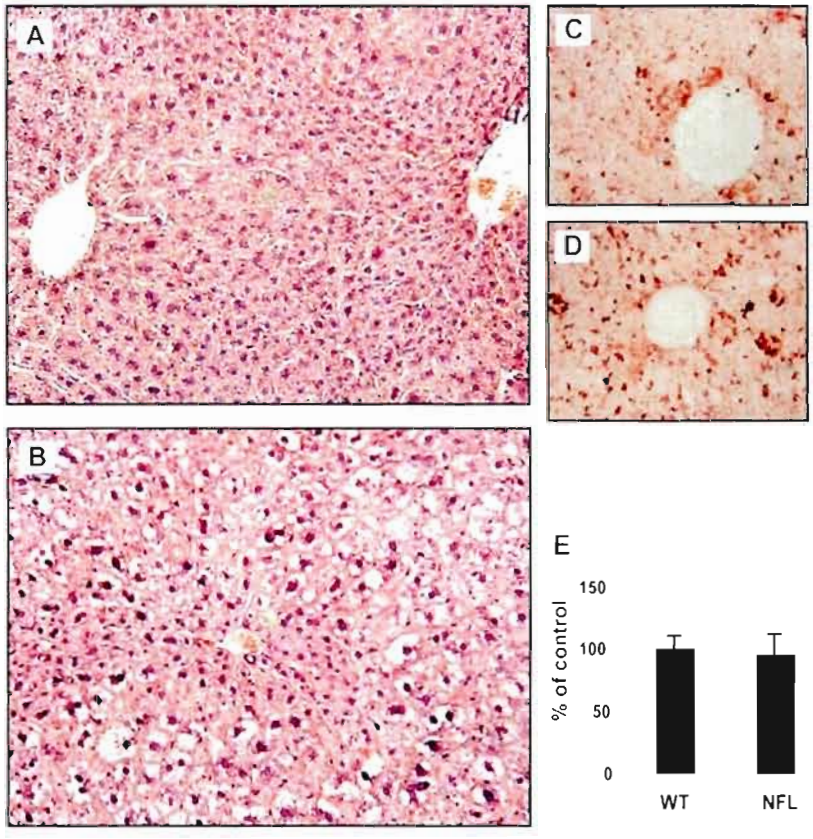

ANNEXE V

Résultats supplémentaires non-publiés

Réponse des souris ApoD-KO à l'infection par HCoV-OC43

A5.1 Résultats

Étant donné que l'expression de l'apoD humaine chez les souris transgéniques induit une protection contre l'encéphalite virale en limitant la réponse inflammatoire, nous avons examiné la réponse inflammatoire chez quelques souris déficientes en apoD (ApoD-KO). Tel qu'attendu, 11 jours post-infection (DPI), les souris ApoD-KO avaient des niveaux de GFAP et de Mac-2 inférieurs à ceux des souris WT (Fig. A4.1A) alors que le niveau de virus infectieux dans le cerveau était similaire (Fig. A4.1C). Les souris ApoD-KO avaient aussi des niveaux plus élevés de CD4 ce qui trahit une plus grande infiltration de cellules T dans le cerveau (Fig. A4.1B et E). Finalement, la quantification de l'activité PLA2 a révélé que les souris ApoD-KO ont des niveaux de PLA2 supérieurs aux souris WT autant en conditions normales qu'après infection (Fig. A4.1D).

Ces résultats concordent avec ce qui a été observé chez les souris transgéniques et appuient davantage un rôle pour l'apoD dans l'activation gliale et dans le contrôle de l'inflammation suite à l'infection. Ces résultats n'ont pas été publiés puisque nous avons été incapables de générer une courbe de survie suite à l'infection statistiquement significative. En effet, les souris ApoD-KO sont plus nerveuses et ont tendance à manger leurs petits. De plus, les souris âgées de 21 jours sont plus petites que les souris WT et transgéniques et survivaient moins bien à l'injection intracrânienne.

A5.2 Légende des figures

Figure A5.1: Analyse du cerveau de souris ApoD-KO suite à l'infection par HCoV-OC43. A) Analyse de type northern de l'apoD de souris (M-apoD) 11 DPI. GAPDH est inclus comme témoin de charge. B) Analyse de M-apoD, OC43(N), GFAP, Mac-2 et CD4 par immunobuvardage (11 DPI). GAPDH est inclus comme témoin de charge (n=3, testé en triplicata). C) Quantité de virus infectieux détecté dans le cerveau 11 DPI. Les valeurs représentent la moyenne ± l'écart-type (n=3). D) Activité PLA2 totale chez les souris non-infectées (control) et infectées par HCoV-OC43 (OC43) et normalisée par l'activité PLA2 retrouvée chez les souris WT non-infectées. Les valeurs représentent la moyenne ± l'écart-type (n=2, testé en triplicata). *** $p<0.001$ vs le contrôle correspondant; ## $p<0.01$, ### $p<0.001$ vs WT. E) Analyse par FACS d'extraits de cerveau total, 8 jours après l'injection intracrânienne de HCoV-OC43 ou de solution saline (control). Les valeurs représentent la moyenne ± l'écart-type de 3 souris par génotype, exprimé en pourcentage. Les analyses ont été faites en triplicata. * $p<0.001$ vs WT.

Figure A5.1

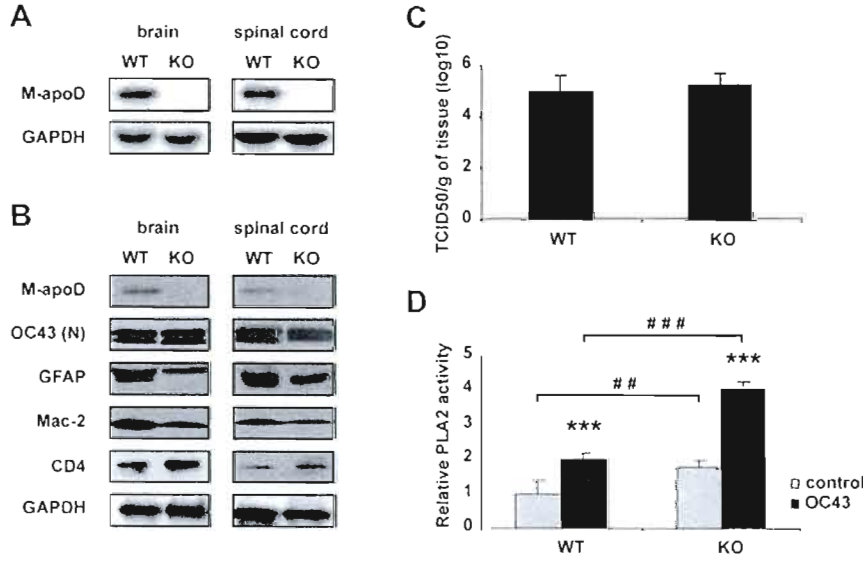

E

	Percentage of cells			
	WT		apoD-KO	
	CD4	CD8	CD4	CD8
control	0.24 ± 0.06	0.14 ± 0.03	0.06 ± 0.01*	0.00 ± 0.01*
OC43	2.45 ± 0.55	2.75 ± 0.43	3.00 ± 0.27	5.76 ± 0.94*

RÉFÉRENCES

Adibhatla, R.M., Hatcher, J.F. 2007. Secretory phospholipase A2 IIA is up-regulated by TNF-alpha and IL-1alpha/beta after transient focal cerebral ischemia in rat. Brain Res. **1134**: 199-205.

Agdeppa, E.D., Kepe, V., Liu, J., Small, G.W., Huang, S.C., Petric, A., Satyamurthy, N., Barrio, J.R. 2003. 2-Dialkylamino-6-acylmalononitrile substituted naphthalenes (DDNP analogs): novel diagnostic and therapeutic tools in Alzheimer's disease. Mol. Imaging Biol. **5**: 404-417.

Akerstrom, B., Borregaard, N., Flower, D.R., Salier, J.-P. (Eds) 2006. Lipocalins. Landes Biosciences, Georgetown, TX, USA.

Akerstrom, B., Maghzal, G., Winterbourn, C.C., Kettle, A.J. 2007. The lipocalin alpha 1-microglobulin has radical scavenger activity. J. Biol. Chem. **282**: 31493-31503.

Alaupovic, P., Schaefer, E.J., McConathy, W.J., Fesmire, J.D., Brewer, H.B. Jr 1981. Plasma apolipoprotein concentrations in familial apolipoprotein A-I and A-II deficiency (Tangier disease). Metabolism **30**: 805-809.

Albers, J.J., Adolphson, J., Chen, C.H., Murayama, N., Honma, S., Akanuma, Y. 1985. Defective enzyme causes lecithin-cholesterol acyltransferase deficiency in a Japanese kindred. Biochim. Biophys. Acta **835**: 253-257.

Albers, J.J., Cheung, M.C., Ewens, S.L., Tollefson, J.H. 1981. Characterization and immunoassay of apolipoprotein D. Atherosclerosis **39**: 395-409.

Alexander, H., Stegner, A.L., Wagner-Mann, C., Du Bois, G.C., Alexander, S., Sauter, E.R. 2004. Proteomic analysis to identify breast cancer biomarkers in nipple aspirate fluid. Clin. Cancer Res. **10** :7500-7510.

Allhorn, M., Berggard, T., Nordberg, J., Olsson, M.L., Akerstrom, B. 2002. Processing of the lipocalin alpha(1)-microglobulin by hemoglobin induces heme-binding and heme-degradation properties. Blood **99**: 1894-1901.

Allhorn, M., Klapyta, A., Akerstrom, B. 2005. Redox properties of the lipocalin alpha1-microglobulin: reduction of cytochrome c, hemoglobin, and free iron. Free Radic. Biol. Med. **38**: 557-567.

Alvarez, J.J., Montelongo, A., Iglesias, A., Lasunción, M.A,, Herrera, E. 1996. Longitudinal study on lipoprotein profile, high density lipoprotein subclass, and postheparin lipases during gestation in women. J. Lipid Res. **37**: 299-308.

Alvarez, M.L., Barbón, J.J., González, L.O., Abelairas, J., Boto, A., Vizoso, F.J. 2003. Apolipoprotein D expression in retinoblastoma. Ophthalmic Res. **35**: 111-116.

Alvarez, M.L., Barbon, J.J., Gonzalez, L.O., Lamelas, M.L., Vazquez, J., Vizoso, F.J. 2004. Expression of two androgen-induced proteins (pepsinogen C and apolipoprotein d) in epithelial skin cancers of the eyelids. Ophthalmologica **218**: 115-9.

Andrä, K., Abramowski, D., Duke, M., Probst, A., Wiederhold, K.H., Burki, K., Goedert, M., Sommer, B., Staufenbiel, M. 1996. Expression of APP in transgenic mice: a comparison of neuron-specific promoters. Neurobiol. Aging **17** :183-90.

Arbour, N., Day, R., Newcombe, J., Talbot, P.J. 2000. Neuroinvasion by human respiratory coronaviruses. J. Virol. **74**: 8913-8921.

Ashida, S., Nakagawa, H., Katagiri, T., Furihata, M., Iiizumi, M., Anazawa, Y., Tsunoda, T., Takata, R., Kasahara, K., Miki, T., Fujioka, T., Shuin, T., Nakamura, Y. 2004. Molecular features of the transition from prostatic intraepithelial neoplasia (PIN) to prostate cancer: genome-wide gene-expression profiles of prostate cancers and PINs. Cancer Res. **64**: 5963-5972.

Aspinall, J.O., Bentel, J.M., Horsfall, D.J., Haagensen, D.E., Marshall, V.R., Tilley, W.D. 1995. Differential expression of apolipoprotein-D and prostate specific antigen in benign and malignant prostate tissues. J. Urol. **154**: 622-628.

Ayrault-Jarrier, M., Levy, G., Polonovski, J. 1963a. Study of human serum alpha-lipoproteins by immunoelectrophoresis. Bull. Soc. Chim. Biol. (Paris) **45**: 703-713.

Ayrault-Jarrier, M., Levy, G., Wald, R., Polonovski J. 1963b. Separation by ultracentrifugation of the alpha-lipoproteins of normal human serum. Bull. Soc. Chim. Biol. (Paris) **45**: 349-359.

Babcock, A.A., Kuziel, W.A., Rivest, S., Owens, T. 2003. Chemokine expression by glial cells directs leukocytes to sites of axonal injury in the CNS. J. Neurosci. **23**: 7922-7930.

Baker, W.A., Hitman, G.A., Hawrami, K., McCarthy, M.I., Riikonen, A., Tuomilehto-Wolf, E., Nissinen, A., Tuomilehto, J., Mohan, V., Viswanathan, M., Snehalatha, C., Ramachandran, A., Dowse, G.K., Zimmet, P., Serjeantson, S.W. 1994. Apolipoprotein D gene polymorphism: a new genetic marker for type 2 diabetic subjects in Nauru and south India. Diabet. Med. **11**: 947-952.

Balbin, M., Freije, J.M., Fueyo, A., Sanchez, L.M., Lopez-Otin, C. 1990. Apolipoprotein D is the major protein component in cyst fluid from women with human breast gross cystic disease. Biochem. J. **271**: 803-807.

Balboa, M.A., Balsinde, J. 2006. Oxidative stress and arachidonic acid mobilization. Biochim. Biophys. Acta **1761**: 385-391.

Baris, O., Savagner, F., Nasser, V., Loriod, B., Granjeaud, S., Guyetant, S., Franc, B., Rodien, P., Rohmer, V., Bertucci, F., Birnbaum, D., Malthièry, Y., Reynier, P., Houlgatte, R. 2004. Transcriptional profiling reveals coordinated up-regulation of oxidative metabolism genes in thyroid oncocytic tumors. J. Clin. Endocrinol. Metab. **89**: 994-1005.

Barnes, C.A. 1979. Memory deficits associated with senescence: a neurophysiological and behavioral study in the rat. J. Comp. Physiol. Psychol. **93**: 74-104.

Basili, S., Pacini, G., Guagnano, M.T., Manigrasso, M.R., Santilli, F., Pettinella, C., Ciabattoni, G., Patrono, C., Davì, G. 2006. Insulin resistance as a determinant of platelet activation in obese women. J. Am. Coll. Cardiol. **48**: 2531-2538.

Baulieu, E.E. 1998. Neurosteroids: a novel function of the brain. Psychoneuroendocrinology **23**: 963-987.

Bazan, N,G,, Marcheselli, V.L., Cole-Edwards, K. 2005. Brain response to injury and neurodegeneration: endogenous neuroprotective signaling. Ann. N. Y. Acad. Sci. **1053** :137-147.

Beal, M.F. 2002. Oxidatively modified proteins in aging and disease. Free Radic. Biol. Med. **32**: 797-803.

Beck, R., Bertolino, S., Abbot, S.E., Aaronson, P.I., Smirnov, S.V. 1998. Modulation of arachidonic acid release and membrane fluidity by albumin in vascular smooth muscle and endothelial cells. Circ. Res. **83**: 923-931.

Belloir, B., Kövari, E., Surini-Demiri, M., Savioz, A. 2001. Altered apolipoprotein D expression in the brain of patients with Alzheimer disease. J. Neurosci. Res. **64**: 61-69.

Bender, H.S., Chickering, W.R. 1985. Pregnancy and diabetes: the maternal response. Life Sci. **37**: 1-9.

Biernacki, K., Prat, A., Blain, M., Antel, J.P. 2004. Regulation of cellular and molecular trafficking across human brain endothelial cells by Th1- and Th2-polarized lymphocytes. J. Neuropathol. Exp. Neurol. **63**: 223-232.

Bishop, R.E., Penfold, S.S., Frost, L.S., Holtje, J.V., Weiner, J.H. 1995. Stationary phase expression of a novel Escherichia coli outer membrane lipoprotein and its relationship with mammalian apolipoprotein D. Implications for the origin of lipocalins. J. Biol. Chem. **270**: 23097-23103.

Bjorkhem, I., Meaney, S. 2004. Brain cholesterol: long secret life behind a barrier. Arterioscler. Thromb. Vasc. Biol. **24**: 806-815.

Blais, Y., Sugimoto, K., Carrière, M.C., Haagensen, D.E., Labrie, F., Simard, J. 1995. Interleukin-6 inhibits the potent stimulatory action of androgens, glucocorticoids and interleukin-1 alpha on apolipoprotein D and GCDFP-15 expression in human breast cancer cells. Int. J. Cancer **62**: 732-737.

Blais, Y., Sugimoto, K., Carrière, M.C., Haagensen, D.E., Labrie, F., Simard, J. 1994. Potent stimulatory effect of interleukin-1 alpha on apolipoprotein D and gross

cystic disease fluid protein-15 expression in human breast-cancer cells. Int. J. Cancer **59**: 400-407.

Blanco-Vaca, F., Via, D.P., Yang, C.Y., Massey, J.B., Pownall, H.J. 1992. Characterization of disulfide-linked heterodimers containing apolipoprotein D in human plasma lipoproteins. J. Lipid Res. **33**: 1785-1796.

Bojanovski, D., Alaupovic, P., McConathy, W.J., Kelly, J.L. 1980. Isolation and partial characterization of apolipoprotein D and lipoprotein D from baboon plasma. FEBS Lett. **112**: 251-254.

Bonavia, A., Arbour, N., Yong, V.W., Talbot, P.J. 1997. Infection of primary cultures of human neural cells by human coronaviruses 229E and OC43. J. Virol. **71**: 800-806.

Bonventre, J.V. 1992. Phospholipase A2 and signal transduction. J. Am. Soc. Nephrol. **3**: 128-150.

Borghini, I., Barja, F., Pometta, D., James, R.W. 1995. Characterization of subpopulations of lipoprotein particles isolated from human cerebrospinal fluid. Biochim. Biophys. Acta **1255**: 192-200.

Boström, P., Andersson, L., Rutberg, M., Perman, J., Lidberg, U., Johansson, B.R., Fernandez-Rodriguez, J., Ericson, J., Nilsson, T., Borén, J., Olofsson, S.O. 2007. SNARE proteins mediate fusion between cytosolic lipid droplets and are implicated in insulin sensitivity. Nat. Cell. Biol. **9**: 1286-1293.

Boucher, A., Desforges, M., Duquette, P., Talbot, P.J. 2007. Long-term human coronavirus-myelin cross-reactive T-cell clones derived from multiple sclerosis patients. Clin. Immunol. **123**: 258-267.

Boyles, J.K., Notterpek, L.M., Anderson, L.J. 1990a. Accumulation of apolipoproteins in the regenerating and remyelinating mammalian peripheral nerve. Identification of apolipoprotein D, apolipoprotein A-IV, apolipoprotein E, and apolipoprotein A-I. J. Biol. Chem. **265**: 17805-17815.

Boyles, J.K., Notterpek, L.M., Wardell, M.R., Rall, S.C. Jr. 1990b. Identification, characterization, and tissue distribution of apolipoprotein D in the rat. J. Lipid Res. **31**: 2243-2256.

Brasier, A.R., Ron, D., Tate, J.E., Habener, J.F. 1990. A family of constitutive C/EBP-like DNA binding proteins attenuate the IL-1 alpha induced, NF kappa B mediated trans-activation of the angiotensinogen gene acute-phas response element. EMBO J. **9**: 3933-3944.

Breustedt, D.A., Schonfeld, D.L., Skerra, A. 2006. Comparative ligand-binding analysis of ten human lipocalins. Biochim. Biophys. Acta. **1764**: 161-173.

Bujalska, I.J., Quinkler, M., Tomlinson, J.W., Montague, C.T., Smith, D.M., Stewart, P.M. 2006. Expression profiling of 11beta-hydroxysteroid dehydrogenase type-1 and glucocorticoid-target genes in subcutaneous and omental human preadipocytes. J. Mol. Endocrinol. **37**: 327-340.

Busacchi, P., De Giorgio, R., Santini, D., Bellavia, E., Perri, T., Oliverio, C., Paradisi, R., Corinaldesi, R., Flamigni, C. 1999. A histological and immunohistochemical study of neuropeptide containing somatic nerves in the levator ani muscle of women with genitourinary prolapse. Acta Obstet. Gynecol. Scand. **78**: 2-5.

Bush, T.G., Puvanachandra, N., Horner, C.H., Polito, A., Ostenfeld, T., Svendsen, C.N., Mucke, L., Johnson, M.H., Sofroniew, M.V. 1999. Leukocyte infiltration, neuronal degeneration, and neurite outgrowth after ablation of scar-forming, reactive astrocytes in adult transgenic mice. Neuron **23**: 297-308.

Buss, H., Chan, T.P., Sluis, K.B., Domigan, N.M., Winterbourn, C.C. 1997. Protein carbonyl measurement by a sensitive ELISA method. Free Radic. Biol. Med. **23**: 361-366.

Butler, A.A., Cone, R.D. 2003. Knockout studies defining different roles for melanocortin receptors in energy homeostasis. Ann. N. Y. Acad. Sci. **994**: 240-245.

Butler, N., Pewe, L., Trandem, K., Perlman, S. 2006. Murine encephalitis caused by HCoV-OC43, a human coronavirus with broad species specificity, is partly immune-mediated. Virology **347**: 410-421.

Calder, P.C. 2005. Polyunsaturated fatty acids and inflammation. Biochem. Soc. Trans. **33**: 423-427.

Calvo, C.F., Yoshimura, T., Gelman, M., Mallat, M. 1996. Production of monocyte chemotactic protein-1 by rat brain macrophages. Eur. J. Neurosci. **8**: 1725-1734.

Carr, D.J., Chodosh, J., Ash, J., Lane, T.E. 2003. Effect of anti-CXCL10 monoclonal antibody on herpes simplex virus type 1 keratitis and retinal infection. J. Virol. **77**: 10037-10046.

Chan, P.H., Epstein, C.J., Li, Y., Huang, T.T., Carlson, E., Kinouchi, H., Yang, G., Kamii, H., Mikawa, S., Kondo, T., *et al.* 1995. Transgenic mice and knockout mutants in the study of oxidative stress in brain injury. J. Neurotrauma **12**: 815-824.

Charron JB, Ouellet F, Houde M, Sarhan F. 2008. The plant Apolipoprotein D ortholog protects Arabidopsis against oxidative stress. BMC Plant Biol. 8: 86 [Epub ahead of print].

Ching, K.H., Kisailus, A.E., Burbelo, P.D. 2007. Biochemical characterization of distinct regions of SPEC molecules and their role in phagocytosis. Exp. Cell. Res. **313**: 10-21.

Ciaraldi, T.P., Morales, A.J., Hickman, M.G., Odom-Ford, R., Olefsky, J.M., Yen, S.S. 1997. Cellular insulin resistance in adipocytes from obese polycystic ovary syndrome subjects involves adenosine modulation of insulin sensitivity. J. Clin. Endocrinol. Metab. **82**: 1421-1425.

Clements, J.A., Rohde, P., Allen, V., Hyland, V.J., Samaratunga, M.L., Tilley, W.D., Lavin, M.F., Gardiner, R.A. 1999. Molecular detection of prostate cells in ejaculate and urethral washings in men with suspected prostate cancer. J. Urol. **161**: 1337-1343.

Cofer, S., Ross, S.R. 1996. The murine gene encoding apolipoprotein D exhibits a unique expression pattern as compared to other species. Gene **171**: 261-263.

Crawley, J. 2000. What's wrong with my mouse?: behavioral phenotyping of transgenic and knockout mice. Wiley-Liss, New York, NY, USA.

Dakhale, G., Khanzode, S., Khanzode, S., Saoji, A., Khobragade, L., Turankar, A. 2004. Oxidative damage and schizophrenia: the potential benefit by atypical antipsychotics. Neuropsychobiology **49**: 205-209.

Dandoy-Dron, F., Guillo, F., Benboudjema, L., Deslys, J.P., Lasmezas, C., Dormont, D., Tovey, M.G., Dron, M. 1998. Gene expression in scrapie. Cloning of a new scrapie-responsive gene and the identification of increased levels of seven other mRNA transcripts. J. Biol. Chem. **273**: 7691-7697.

Davies, K.J. 1999. The broad spectrum of responses to oxidants in proliferating cells: a new paradigm for oxidative stress. IUBMB Life **48**: 41-47.

DeCherney, A., Pernoll, M.L. 1994. Current Obstetric & Gynecologic Diagnosis & Treatment 8th edition. McGraw-Hill Companies, East Norwalk, Connecticut, USA.

Deeb, S.S., Cheung, M.C., Peng, R.L., Wolf, A.C., Stern, R., Albers, J.J., Knopp, R.H. 1991. A mutation in the human apolipoprotein A-I gene. Dominant effect on the level and characteristics of plasma high density lipoproteins. J. Biol. Chem. **266**: 13654-13660.

del Valle, E., Navarro, A., Astudillo, A., Tolivia, J. 2003. Apolipoprotein D expression in human brain reactive astrocytes. J. Histochem. Cytochem. **51**: 1285-1290.

Delvaux, T., Buekens, P., Thoumsin, H., Dramaix, M., Collette, J. 2003. Cord C-peptide and insulin-like growth factor-I, birth weight, and placenta weight among North African and Belgian neonates. Am. J. Obstet. Gynecol. **189**: 1779-1784.

Demeester, N., Castro, G., Desrumaux, C., De Geitere, C., Fruchart, J.C., Santens, P., Mulleners, E., Engelborghs, S., De Deyn, P.P., Vandekerckhove, J., Rosseneu, M., Labeur, C. 2000. Characterization and functional studies of lipoproteins, lipid

transfer proteins, and lecithin:cholesterol acyltransferase in CSF of normal individuals and patients with Alzheimer's disease. J. Lipid Res. **41**: 963-974.

Desai, P.P., Bunker, C.H., Ukoli, F.A., Kamboh, M.I. 2002. Genetic variation in the apolipoprotein D gene among African blacks and its significance in lipid metabolism. Atherosclerosis **163**: 329-338.

Desai, P.P., Hendrie, H.C., Evans, R.M., Murrell, J.R., DeKosky, S.T., Kamboh, M.I. 2003. Genetic variation in apolipoprotein D affects the risk of Alzheimer disease in African-Americans. Am. J. Med. Genet. **116B**: 98-101.

Desai, P.P., Ikonomovic, M.D., Abrahamson, E.E., Hamilton, R.L., Isanski, B.A., Hope, C.E., Klunk, W.E., DeKosky, S.T., Kamboh, M.I. 2005. Apolipoprotein D is a component of compact but not diffuse amyloid-beta plaques in Alzheimer's disease temporal cortex. Neurobiol Dis. **20**: 574-582.

DeWan, A.T., Arnett, D.K., Atwood, L.D., Province, M.A., Lewis, C.E., Hunt, S.C., Eckfeldt, J. 2001. A genome scan for renal function among hypertensives: the HyperGEN study. Am. J. Hum. Genet. **68**: 136-144.

Diau, G.Y., Hsieh, A.T., Sarkadi-Nagy, E.A., Wijendran, V., Nathanielsz, P.W., Brenna, J.T. 2005. The influence of long chain polyunsaturate supplementation on docosahexaenoic acid and arachidonic acid in baboon neonate central nervous system. BMC Med. **3**: 11.

Dieplinger, H., Schoenfeld, P.Y., Fielding, C.J. 1986. Plasma cholesterol metabolism in end-stage renal disease. Difference between treatment by hemodialysis or peritoneal dialysis. J. Clin. Invest. **77**: 1071-1083.

Diez-Itza, I., Vizoso, F., Merino, A.M., Sanchez, L.M., Tolivia, J., Fernandez, J., Ruibal, A., Lopez-Otin, C. 1994. Expression and prognostic significance of apolipoprotein D in breast cancer. Am. J. Pathol. **144**: 310-320.

Dilley, W.G., Haagensen, D.E., Cox, C.E., Wells, S.A. Jr. 1990. Immunologic and steroid binding properties of the GCDFP-24 protein isolated from human breast gross cystic disease fluid. Breast Cancer Res. Treat. **16**: 253-260.

Do Carmo S, Levros LC Jr, Rassart E. 2007. Modulation of apolipoprotein D expression and translocation under specific stress conditions. Biochim Biophys Acta. **1773**: 954-969.

Do Carmo, S., Séguin, D., Milne, R., Rassart, E. 2002. Modulation of apolipoprotein D and apolipoprotein E mRNA expression by growth arrest and identification of key elements in the promoter. J. Biol. Chem. **277**: 5514-5523.

Drayna, D., Fielding, C., McLean, J., Baer, B., Castro, G., Chen, E., Comstock, L., Henzel, W., Kohr, W., Rhee, L., Wion, K., Lawn, R. 1986. Cloning and expression of human apolipoprotein D cDNA. J. Biol. Chem. **261**: 16535-16539.

Drayna, D.T., McLean, J.W., Wion, K.L., Trent, J.M., Drabkin, H.A., Lawn, R.M. 1987. Human apolipoprotein D gene: gene sequence, chromosome localization, and homology to the alpha 2u-globulin superfamily. DNA **6**: 199-204.

Dudas, J., Mansuroglu, T., Batusic, D., Saile, B., Ramadori, G. 2007. Thy-1 is an in vivo and in vitro marker of liver myofibroblasts. Cell Tissue Res. **329**: 503-514.

Edvardsson, U., Bergström, M., Alexandersson, M., Bamberg, K., Ljung, B., Dahllöf, B. 1999. Rosiglitazone (BRL49653), a PPARgamma-selective agonist, causes peroxisome proliferator-like liver effects in obese mice. J. Lipid Res. **40**: 1177-1184.

Eichinger, A., Nasreen, A., Kim, H.J., Skerra, A. 2007. Structural insight into the dual ligand specificity and mode of high density lipoprotein association of apolipoprotein D. J. Biol. Chem. **282**: 31068-31075.

Elkabes, S., DiCicco-Bloom, E.M., Black, I.B. 1996. Brain microglia/macrophages express neurotrophins that selectively regulate microglial proliferation and function. J. Neurosci. **16**: 2508-2521.

Facchini, F.S., Hua, N., Abbasi, F., Reaven, G.M. 2001. Insulin resistance as a predictor of age-related diseases. J. Clin. Endocrinol. Metab. **86**: 3574-3578.

Farooqui, A.A., Horrocks, L.A., Farooqui, T. 2007. Modulation of inflammation in brain: a matter of fat. J. Neurochem. **101**: 577-599.

Farooqui, A.A., Ong, W.Y., Horrocks, L.A. 2004. Biochemical aspects of neurodegeneration in human brain: involvement of neural membrane phospholipids and phospholipases A2. Neurochem. Res. **29**: 1961-1977.

Farooqui, A.A., Yang, H.C., Horrocks, L. 1997. Involvement of phospholipase A2 in neurodegeneration. Neurochem. Int. **30**: 517-522.

Faulkner, J.R., Herrmann, J.E., Woo, M.J., Tansey, K.E., Doan, N.B., Sofroniew, M.V. 2004. Reactive astrocytes protect tissue and preserve function after spinal cord injury. J. Neurosci. **24**: 2143-2155.

Fialová, L., Malbohan, I., Kalousová, M., Soukupová, J., Krofta, L., Stípek, S., Zima, T. 2006. Oxidative stress and inflammation in pregnancy. Scand. J. Clin. Lab. Invest. **66**: 121-127.

Fielding, P.E., Fielding, C.J. 1980. A cholesteryl ester transfer complex in human plasma. Proc. Natl Acad. Sci. USA **77**: 3327-3330.

Flatscher-Bader, T., Wilce, P.A. 2006. Chronic smoking and alcoholism change expression of selective genes in the human prefrontal cortex. Alcohol Clin. Exp. Res. **30**: 908-915.

Flo, T.H., Smith, K.D., Sato, S., Rodriguez, D.J., Holmes, M.A., Strong, R.K., Akira, S., Aderem, A. 2004. Lipocalin 2 mediates an innate immune response to bacterial infection by sequestrating iron. Nature **432**: 917-921.

Flower, D.R., North, A.C.T., Sansom, C.E. 2000. The lipocalin protein family: structural and sequence overview. Biochim. Biophys. Acta. **1482**: 9-24.

Forss-Petter, S., Danielson, P.E., Catsicas, S., Battenberg, E., Price, J., Nerenberg, M., Sutcliffe, J.G. 1990. Transgenic mice expressing beta-galactosidase in mature neurons under neuron-specific enolase promoter control. Neuron **5**: 187-197.

François, M., Richette, P., Tsagris, L., Fitting, C., Lemay, C., Benallaoua, M., Tahiri, K., Corvol, M.T. 2006. Activation of the peroxisome proliferator-activated receptor alpha pathway potentiates interleukin-1 receptor antagonist production in cytokine-treated chondrocytes. Arthritis Rheum. **54**: 1233-1245.

Francone, O.L., Gurakar, A., Fielding, C. 1989. Distribution and functions of lecithin:cholesterol acyltransferase and cholesteryl ester transfer protein in plasma lipoproteins. Evidence for a functional unit containing these activities together with apolipoproteins A-I and D that catalyzes the esterification and transfer of cell-derived cholesterol. J. Biol. Chem. **264** :7066-7072.

Franz, G., Reindl, M., Patel, S.C., Beer, R., Unterrichter, I., Berger, T., Schmutzhard, E., Poewe, W., Kampfl, A. 1999. Increased expression of apolipoprotein D following experimental traumatic brain injury. J. Neurochem. **73**: 1615-1625.

Frenette Charron, J.B., Breton, G., Badawi, M., Sarhan, F. 2002. Molecular and structural analyses of a novel temperature stress-induced lipocalin from wheat and Arabidopsis. FEBS Lett. **517**: 129-32.

Ganfornina, M.D., Do Carmo, S., Lora, J.M., Torres-Schumann, S., Vogel, M., Allhorn, M., Gonzalez, C., Bastiani, M.J., Rassart, E., Sanchez, D. 2008. Apolipoprotein D is involved in the mechanisms regulating protection from oxidative stress. Aging cell **7**: 506-515.

Ganfornina, M.D., Sanchez, D., Pagano, A., Tonachini, L., Descalzi-Cancedda, F., Martinez, S. 2005. Molecular characterization and developmental expression pattern of the chicken apolipoprotein D gene: implications for the evolution of vertebrate lipocalines. Dev. Dyn. **232**: 191-199.

Garcia-Segura, L.M., Naftolin, F., Hutchison, J.B., Azcoitia, I., Chowen, J.A. 1999. Role of astroglia in estrogen regulation of synaptic plasticity and brain repair. J. Neurobiol. **40**: 574-584.

Gattoni, M., Boffi, A. 2003. The effect of isoflurane on erythrocyte membranes studied by ATR-FTIR. Biochim Biophys Acta **1613**: 72-78.

Gebicke-Haerter, P.J. 2005. Microarrays and expression profiling in microglia research and in inflammatory brain disorders. J. Neurosci. Res. **81**: 327-341.

Ghoumari, A.M., Ibanez, C., El-Etr, M., Leclerc, P., Eychenne, B., O'Malley, B.W., Baulieu, E.E., Schumacher, M. 2003. Progesterone and its metabolites increase

myelin basic protein expression in organotypic slice cultures of rat cerebellum. J. Neurochem. **86**: 848-859.

Giovannoni, G., Baker, D. 2003. Inflammatory disorders of the central nervous system. Curr. Opin. Neurol. **16**: 347-350.

Glockner, F., Ohm, T.G. 2003. Hippocampal apolipoprotein D level depends on Braak stage and APOE genotype. Neuroscience **122**: 103-110.

Goessling, W., Zucker, S.D. 2000. Role of apolipoprotein D in the transport of bilirubin in plasma. Am. J. Physiol. Gastrointest. Liver Physiol. **279**: G356-G365.

Goetz, D.H., Holmes, M.A., Borregaard, N., Bluhm, M.E., Raymond, K.N., Strong, R.K. 2002. The neutrophil lipocalin NGAL is a bacteriostatic agent that interferes with siderophore-mediated iron acquisition. Mol. Cell. **10**: 1033-1043.

Gordon, J.W., Chesa, P.G., Nishimura, H., Rettig, W.J., Maccari, J.E., Endo, T., Seravalli, E., Seki, T., Silver, J. 1987. Regulation of Thy-1 gene expression in transgenic mice. Cell **50**: 445-452.

Gottsch, J.D., Bowers, A.L., Margulies, E.H., Seitzman, G.D., Kim, S.W., Saha, S., Jun, A.S., Stark, W.J., Liu, S.H. 2003. Serial analysis of gene expression in the corneal endothelium of Fuchs' dystrophy. Invest. Ophthalmol. Vis. Sci. **44**: 594-599.

Govindarajan, R., Rastogi, S., Vijayakumar, M., Shirwaikar, A., Rawat, A.K., Mehrotra, S., Pushpangadan, P. 2003. Studies on the antioxidant activities of Desmodium gangeticum. Biol. Pharm. Bull. **26**: 1424-1427.

Guay, J., Bateman, K., Gordon, R., Mancini, J., Riendeau, D. 2004. Carrageenan-induced paw edema in rat elicits a predominant prostaglandin E2 (PGE2) response in the central nervous system associated with the induction of microsomal PGE2 synthase-1. J. Biol. Chem. **279**: 24866-24872.

Hall, R.E., Aspinall, J.O., Horsfall, D.J., Birrell, S.N., Bentel, J.M., Sutherland, R.L., Tilley, W.D. 1996. Expression of the androgen receptor and an androgen-responsive protein, apolipoprotein D, in human breast cancer. Br. J. Cancer **74**: 1175-1180.

Hall, R.E., Horsfall, D.J., Stahl, J., Vivekanandan, S., Ricciardelli, C., Stapleton, A.M., Scardino, P.T., Neufing, P., Tilley, W.D. 2004. Apolipoprotein-D: a novel cellular marker for HGPIN and prostate cancer. Prostate **58**: 103-108.

Hansen, L., Gaster, M., Oakeley, E.J., Brusgaard, K., Damsgaard Nielsen, E.M., Beck-Nielsen, H., Pedersen, O., Hemmings, B.A. 2004. Expression profiling of insulin action in human myotubes: induction of inflammatory and pro-angiogenic pathways in relationship with glycogen synthesis and type 2 diabetes. Biochem. Biophys. Res. Commun. **323**: 685-695.

Harada, N., Oda, Z., Hara, Y., Fujinami, K., Okawa, M., Ohbuchi, K., Yonemoto, M., Ikeda, Y., Ohwaki, K., Aragane, K., Tamai, Y., Kusunoki, J. 2007. Hepatic de novo lipogenesis is present in liver-specific ACC1-deficient mice. Mol. Cell. Biol. **27**: 1881-1888.

Harding, C., Osundeko, O., Tetlow, L., Faragher, E.B., Howell, A., Bundred, N.J. 2000. Hormonally-regulated proteins in breast secretions are markers of target organ sensitivity. Br. J. Cancer **82**: 354-360.

Helisalmi, S., Hiltunen, M., Vepsalainen, S., Iivonen, S., Corder, E.H., Lehtovirta, M., Mannermaa, A., Koivisto, A.M., Soininen, H. 2004. Genetic variation in apolipoprotein D and Alzheimer's disease. J. Neurol. **251**: 951-957.

Herrera, E. 2000. Metabolic adaptations in pregnancy and their implications for the availability of substrates to the fetus. Eur. J. Clin. Nutr. **54**: S47-S51.

Hitman, G.A., McCarthy, M.I., Mohan, V., Viswanathan, M. 1992. The genetics of non-insulin-dependent diabetes mellitus in south India: an overview. Ann. Med. **24**: 491-497.

Hu, B., Wu, Z., Jin, H., Hashimoto, N., Liu, T., Phan, S.H. 2004. CCAAT/enhancer-binding protein beta isoforms and the regulation of alpha-smooth muscle actin gene expression by IL-1 beta. J. Immunol. **173**: 4661-4668.

Hu, C.Y., Ong, W.Y., Sundaram, R.K., Chan, C., Patel, S.C. 2001. Immunocytochemical localization of apolipoprotein D in oligodendrocyte

precursor-like cells, perivascular cells, and pericytes in the human cerebral cortex. J. Neurocytol. **30**: 209-218.

Hu, W., Feng, Z., Eveleigh, J., Iyer, G., Pan, J., Amin, S., Chung, F.L., Tang, M.S. 2002. The major lipid peroxidation product, trans-4-hydroxy-2-nonenal, preferentially forms DNA adducts at codon 249 of human p53 gene, a unique mutational hotspot in hepatocellular carcinoma. Carcinogenesis **23**: 1781-1789.

Hu, Z.Y., Bourreau, E., Jung-Testas, I., Robel, P., Baulieu, E.E. 1987. Neurosteroids: oligodendrocyte mitochondria convert cholesterol to pregnenolone. Proc. Natl Acad. Sci. USA **84**: 8215-8219.

Hudon-David, F., Bouzeghrane, F., Couture, P., Thibault, G. 2007. Thy-1 expression by cardiac fibroblasts: lack of association with myofibroblast contractile markers. J. Mol. Cell. Cardiol. **42**: 991-1000.

Hulbert, A.J. 2005. On the importance of fatty acid composition of membranes for aging. J. Theor. Biol. **234**: 277-288.

Hummasti, S., Laffitte, B.A., Watson, M.A., Galardi, C., Chao, L.C., Ramamurthy, L., Moore, J.T., Tontonoz, P. 2004. Liver X receptors are regulators of adipocyte gene expression but not differentiation: identification of apoD as a direct target. J. Lipid Res. **45**: 616-625.

Hunter, S., Young, A., Olson, J., Brat, D.J., Bowers, G., Wilcox, J.N., Jaye, D., Mendrinos, S., Neish, A. 2002. Differential expression between pilocytic and anaplastic astrocytomas: identification of apolipoprotein D as a marker for low-grade, non-infiltrating primary CNS neoplasms. J. Neuropathol. Exp. Neurol. **61**: 275-281.

Hytten, F. 1985. Blood volume changes in normal pregnancy. Clin. Haematol. **14**: 601-12.

Iacobuzio-Donahue, C.A., Maitra, A., Shen-Ong, G.L., van Heek, T., Ashfaq, R., Meyer, R., Walter, K., Berg, K., Hollingsworth, M.A., Cameron, J.L., Yeo, C.J., Kern, S.E., Goggins, M., Hruban, R.H. 2002a. Discovery of novel tumor markers

of pancreatic cancer using global gene expression technology. Am. J. Pathol. **160**: 1239-1249.

Iacobuzio-Donahue, C.A., Ryu, B., Hruban, R.H., Kern, S.E. 2002b. Exploring the host desmoplastic response to pancreatic carcinoma: gene expression of stromal and neoplastic cells at the site of primary invasion. Am. J. Pathol. **160**: 91-99.

Irani, D.N., Griffin, D.E. 1996. Regulation of lymphocyte homing into the brain during viral encephalitis at various stages of infection. J. Immunol. **156**: 3850-3857.

Jacomy, H., Fragoso, G., Almazan, G., Mushynski, W.E., Talbot, P.J. 2006. Human coronavirus OC43 infection induces chronic encephalitis leading to disabilities in BALB/C mice. Virology **349**: 335-346.

Jacomy, H., Talbot, P.J. 2003. Vacuolating encephalitis in mice infected by human coronavirus OC43. Virology **315**: 20-33.

Jamaluddin, M. Meng, T. Sun, J. Boldogh, I. Han, Y. Brasier, A.R. 2000. Angiotensin II induces nuclear factor (NF)-kappaB1 isoforms to bind the angiotensinogen gene acute-phase response element: a stimulus-specific pathway for NF-kappaB activation. Mol. Endocrinol. **14**: 99-113.

James, R.W., Martin, B., Pometta, D., Grab, B., Suenram, A. 1986. Apoprotein D in a healthy, male population and in male myocardial infarction patients and their male, first-degree relatives. Atherosclerosis **60**: 49-53.

Jin, D., El-Tanani, M., Campbell, F.C. 2006. Identification of apolipoprotein D as a novel inhibitor of osteopontin-induced neoplastic transformation. Int. J. Oncol. **29**: 1591-1599.

Johnston, C., Jiang, W., Chu, T., Levine, B. 2001. Identification of genes involved in the host response to neurovirulent alphavirus infection. J. Virol. **75**: 10431-10445.

Jonsson, L., Skarphedinsson, J.O., Skuladottir, G.V., Watanobe, H., Schioth, H.B. 2002. Food conversion is transiently affected during 4-week chronic administration of melanocortin agonist and antagonist in rats. J. Endocrinol. **173**: 517-523.

Kaiser, L., Allen, L.H.; American Dietetic Association. 2008. Position of the American Dietetic Association: nutrition and lifestyle for a healthy pregnancy outcome. J. Am. Diet. Assoc. **108**: 553-561.

Kallen, C.B. 2004. Steroid hormone synthesis in pregnancy. Obstet. Gynecol. Clin. North. Am. **31**: 795-816.

Kalman, J., McConathy, W., Araoz, C., Kasa, P., Lacko, A.G. 2000. Apolipoprotein D in the aging brain and in Alzheimer's dementia. Neurol. Res. **22**: 330-336.

Kang, S., Seo, S., Hill, J., Kwon, B., Lee, H., Cho, H., Vinay, D., Kwon, B. 2003. Changes in gene expression in latent HSV-1-infected rabbit trigeminal ganglia following epinephrine iontophoresis. Curr. Eye Res. **26**: 225-229.

Kao, L.C., Tulac, S., Lobo, S., Imani, B., Yang, J.P., Germeyer, A., Osteen, K., Taylor, R.N., Lessey, B.A., Giudice, L.C. 2002. Global gene profiling in human endometrium during the window of implantation. Endocrinology **143**: 2119-2138.

Kesner, L., Yu, W.S., Bradlow, H.L., Breed, C.W., Fleisher, M. 1988. Proteases in cyst fluid from human gross cyst breast disease. Cancer Res. **48**: 6379-6383.

Khan, M.M., Parikh, V.V., Mahadik, S.P. 2003. Antipsychotic drugs differentially modulate apolipoprotein D in rat brain. J. Neurochem. **86**: 1089-1100.

Khanzode, S.S., Muddeshwar, M.G., Khanzode, S.D., Dakhale, G.N. 2004. Antioxidant enzymes and lipid peroxidation in different stages of breast cancer. Free Radic. Res. **38**: 81-85.

Kim, H.J., Je, H.J., Cheon, H.M., Kong, S.Y., Han, J., Yun, C.Y., Han, Y.S., Lee, I.H., Kang, Y.J., Seo, S.J. 2005. Accumulation of 23 kDa lipocalin during brain development and injury in Hyphantria cunea. Insect Biochem. Mol. Biol. **35**: 1133-1141.

Klein, R.S. 2004. Regulation of neuroinflammation: the role of CXCL10 in lymphocyte infiltration during autoimmune encephalomyelitis. J. Cell. Biochem. **92**: 213-222.

Kolodny, E.H. 2000. Niemann-Pick disease. Curr. Opin. Hematol. **7**: 48-52.

Kostner, G.M., Schaupp, K., Stvarnik, G. 1988. Exchange and transfer of apolipoproteins and lipids: impact on lipoprotein metabolism. Adv. Exp. Med. Biol. **243**: 333-338.

Kraegen, E.W., Cooney, G.J., Ye, J., Thompson, A.L. 2001. Triglycerides, fatty acids and insulin resistance hyperinsulinemia. Exp. Clin. Endocrinol. Diabetes **109**: S516–S526.

Kushner, P.J., Agard, D.A., Greene, G.L., Scanlan, T.S., Shiau, A.K., Uht, R.M., Webb, P. 2000. Estrogen receptor pathways to AP-1, J. Steroid Biochem. Mol. Biol. **74**: 311-317.

Laffitte, B.A., Chao, L.C., Li, J., Walczak, R., Hummasti, S., Joseph, S.B., Castrillo, A., Wilpitz, D.C., Mangelsdorf, D.J., Collins, J.L., Saez, E., Tontonoz, P. 2003. Activation of liver X receptor improves glucose tolerance through coordinate regulation of glucose metabolism in liver and adipose tissue. Proc Natl Acad Sci USA **100**: 5419-5424.

Lafond, J., Moukdar, F., Rioux, A., Ech-Chadli, H., Brissette, L., Robidoux, J., Masse, A., Simoneau, L. 2000. Implication of ATP and sodium in arachidonic acid incorporation by placental syncytiotrophoblast brush border and basal plasma membranes in the human. Placenta **21**: 661-669.

Lambert, J., Provost, P.R., Marcel, Y.L., Rassart, E. 1993. Structure of the human apolipoprotein D gene promoter region. Biochim. Biophys. Acta. **1172**: 190-192.

Lamelas, M.L., Vazquez, J., Enguita, M.I., Rodriguez, J.C., Gonzalez, L.O., Merino, A.M., Vizoso, F. 2000. Apolipoprotein D expression in metastasic lymph nodes of breast cancer. Int. J. Surg. Investig. **2**: 285-293.

Lane, D.M., McConathy, W.J. 1983. Factors affecting the lipid and apolipoprotein levels of cord sera. Pediatr. Res. **17**: 83-91.

Lavoie, J.M., Gauthier, M.S. 2006. Regulation of fat metabolism in the liver: link to non-alcoholic hepatic steatosis and impact of physical exercise. Cell. Mol. Life Sci. **63**: 1393-1409.

Lea, O.A. 1988. Binding properties of progesterone-binding Cyst protein, PBCP. Steroids **52**: 337-338.

Lechner, M., Wojnar, P., Redl, B. 2001. Human tear lipocalin acts as an oxidative-stress-induced scavenger of potentially harmful lipid peroxidation products in a cell culture system. Biochem. J. **356**: 129-135.

Lee, A.K. Sung, S.H. Kim, Y.C. Kim, S.G. 2003. Inhibition of lipopolysaccharide-inducible nitric oxide synthase, TNF-alpha and COX-2 expression by sauchinone effects on I-kappaBalpha phosphorylation, C/EBP and AP-1 activation. Br. J. Pharmacol. **139**: 11-20.

Leung, W.C., Lawrie, A., Demaries, S., Massaeli, H., Burry, A., Yablonsky, S., Sarjeant, J.M., Fera, E., Rassart, E., Pickering, J.G., Rabinovitch, M. 2004. Apolipoprotein D and platelet-derived growth factor-BB synergism mediates vascular smooth muscle cell migration. Circ. Res. **95**: 179-186.

Lewohl, J.M., Wang, L., Miles, M.F., Zhang, L., Dodd, P.R., Harris, R.A. 2000. Gene expression in human alcoholism: microarray analysis of frontal cortex. Alcohol Clin. Exp. Res. **24**: 1873-1882.

Li, X., Miyajima, M., Mineki, R., Taka, H., Murayama, K., Arai, H. 2006. Analysis of potential diagnostic biomarkers in cerebrospinal fluid of idiopathic normal pressure hydrocephalus by proteomics. Acta Neurochir. (Wien). **148**: 859-864.

Lieuallen, K., Pennacchio, L.A., Park, M., Myers, R.M., Lennon, G.G. 2001. Cystatin B-deficient mice have increased expression of apoptosis and glial activation genes. Hum. Mol. Genet. **10**: 1867-1871.

Lin, C.S., Ho, H.C., Gholami, S., Chen, K.C., Jad, A., Lue, T.F. 2001. Gene expression profiling of an arteriogenic impotence model. Biochem. Biophys. Res. Commun. **285**: 565-569.

Liu, Z. Chang, G.Q. Leibowitz, S.F. 2001. Apolipoprotein D interacts with the long-form leptin receptor: a hypothalamic function in the control of energy homeostasis. FASEB J. **15**: 1329-1331.

Lopez-Boado, Y.S., Klaus, M., Dawson, M.I., Lopez-Otin, C. 1996. Retinoic acid-induced expression of apolipoprotein D and concomitant growth arrest in human breast cancer cells are mediated through a retinoic acid receptor RARalpha-dependent signaling pathway, J. Biol. Chem. **271**: 32105-32111.

Lopez-Boado, Y.S., Puente, X.S., Alvarez, S., Tolivia, J., Binderup, L., Lopez-Otin, C. 1997. Growth inhibition of human breast cancer cells by 1,25-dihydroxyvitamin D3 is accompanied by induction of apolipoprotein D expression. Cancer Res. **57**: 4091-4097.

Lopez-Boado, Y.S., Tolivia, J., Lopez-Otin, C. 1994. Apolipoprotein D gene induction by retinoic acid is concomitant with growth arrest and cell differentiation in human breast cancer cells. J. Biol. Chem. **269**: 26871-26878.

Lynch, J.R., Morgan, D., Mance, J., Matthew, W.D., Laskowitz, D.T. 2001. Apolipoprotein E modulates glial activation and the endogenous central nervous system inflammatory response. J. Neuroimmunol. **114**: 107-113.

Madsen, E.M., Lindegaard, M.L., Andersen, C.B., Damm, P., Nielsen, L.B. 2004. Human placenta secretes apolipoprotein B-100-containing lipoproteins. J. Biol. Chem. **279**: 55271-55276.

Mahadik, S.P., Khan, M.M., Evans, D.R., Parikh, V.V. 2002. Elevated plasma level of apolipoprotein D in schizophrenia and its treatment and outcome. Schizophr. Res. **58**: 55-62.

Maher, J.E., Goldenberg, R.L., Tamura, T., Cliver, S.P., Hoffman, H.J., Davis, R.O., Boots, L. 1993. Albumin levels in pregnancy: a hypothesis--decreased levels of albumin are related to increased levels of alpha-fetoprotein. Early Hum. Dev. **34**: 209-215.

Manning-Bog, A.B., McCormack, A.L., Purisai, M.G., Bolin, L.M., Di Monte, D.A. 2003. Alpha-synuclein overexpression protects against paraquat-induced neurodegeneration. J. Neurosci. **23**: 3095-3099.

Marques, C.P., Hu, S., Sheng, W., Lokensgard, J.R. 2006. Microglial cells initiate vigorous yet non-protective immune responses during HSV-1 brain infection. Virus Res. **121**: 1-10.

Marques, F., Rodrigues, A.J., Sousa, J.C., Coppola, G., Geschwind, D.H., Sousa, N., Correia-Neves, M., Palha, J.A. 2008. Lipocalin 2 is a choroid plexus acute-phase protein. J. Cereb. Blood Flow Metab. **28**: 450-455.

Masliah, E., Mallory, M., Ge, N., Alford, M., Veinbergs, I., Roses, A.D. 1995. Neurodegeneration in the central nervous system of apoE-deficient mice. Exp. Neurol. **136**: 107-122.

Maymon, R., Zimerman, A.L., Strauss, S., Gayer, G. 2007. Maternal spleen size throughout normal pregnancy. Semin. Ultrasound CT MR. **28**: 64-66.

McConathy, W.J., Alaupovic, P. 1976. Studies on the isolation and partial characterization of apolipoprotein D and lipoprotein D of human plasma. Biochemistry **15**: 515-520.

McConathy, W.J., Lane, D.M. 1980. Studies on the apolipoproteins and lipoproteins of cord serum. Pediatr. Res. **14**: 757-761.

McCormack, A.L., Atienza, J.G., Johnston, L.C., Andersen, J.K., Vu, S., Di Monte, D.A. 2005. Role of oxidative stress in paraquat-induced dopaminergic cell degeneration. J. Neurochem. **93**: 1030-1037.

McEwen, B.S. 1994. How do sex and stress hormones affect nerve cells? Ann. N Y Acad. Sci. **743**: 1-16.

Mensenkamp, A.R., Havekes, L.M., Romijn, J.A., Kuipers, F. 2001. Hepatic steatosis and very low density lipoprotein secretion: the involvement of apolipoprotein E. J. Hepatol. **35**: 816-822.

Milne, R., Rassart, E., Marcel, Y. 1993. Molecular biology of apolipoprotein D. Current Op. in lipidol. **4**: 100-106.

Minehira, K., Young, S.G., Villanueva, C.J., Yetukuri, L., Oresic, M., Hellerstein, M.K., Farese, R.V. Jr, Horton, J.D., Preitner, F., Thorens, B., Tappy, L. 2008.

Blocking VLDL secretion causes hepatic steatosis but does not affect peripheral lipid stores or insulin sensitivity in mice. J. Lipid Res. [Epub ahead of print]

Miranda, E., Vizoso, F., Martin, A., Quintela, I., Corte, M.D., Segui, M.E., Ordiz, I., Merino, A.M. 2003. Apolipoprotein D expression in cutaneous malignant melanoma. J. Surg. Oncol. **83**: 99-105.

Montpied, P., de Bock, F., Lerner-Natoli, M., Bockaert, J., Rondouin, G. 1999. Hippocampal alterations of apolipoprotein E and D mRNA levels in vivo and in vitro following kainate excitotoxicity. Epilepsy Res. **35**: 135-146.

Morais Cabral, J.H., Atkins, G.L., Sanchez, L.M., Lopez-Boado, Y.S., Lopez-Otin, C., Sawyer, L. 1995. Arachidonic acid binds to apolipoprotein D: implications for the protein's function. FEBS Lett. **366**: 53-56.

Muffat J, Walker DW, Benzer S. 2008. Human ApoD, an apolipoprotein up-regulated in neurodegenerative diseases, extends lifespan and increases stress resistance in Drosophila. Proc Natl Acad Sci USA **105**: 7088-7093.

Myint, S., Johnston, S., Sanderson, G., Simpson, H. 1994. Evaluation of nested polymerase chain methods for the detection of human coronaviruses 229E and OC43. Mol. Cell. Probes **8**: 357-364.

Nakajima, K., Honda, S., Tohyama, Y., Imai, Y., Kohsaka, S., Kurihara, T. 2001. Neurotrophin secretion from cultured microglia. J. Neurosci. Res. **65**: 322-331.

Navarro, A., del Valle, E., Astudillo, A., Gonzalez del Rey, C., Tolivia, J. 2003. Immunohistochemical study of distribution of apolipoproteins E and D in human cerebral beta amyloid deposits. Exp. Neurol. **184**: 697-704.

Navarro, A., del Valle, E., Tolivia, J. 2004. Differential expression of apolipoprotein D in human astroglial and oligodendroglial cells. J. Histochem. Cytochem. **52**: 1031-1036.

Navarro, A., Tolivia, J., Astudillo, A., del Valle, E. 1998. Pattern of apolipoprotein D immunoreactivity in human brain. Neurosci Lett. Sep **254**: 17-20.

Nguyen, K.D. Lee, D.A. 1993. In vitro evaluation of antiproliferative potential of topical cyclooxygenase inhibitors in human Tenon's fibroblasts. Exp. Eye Res. **57**: 97-105.

Nohr, E.A., Vaeth, M., Baker, J.L., Sørensen, T.I.A., Olsen, J., Rasmussen, K.M. 2008. Combined associations of prepregnancy body mass index and gestational weight gain with the outcome of pregnancy. Am. J. Clin. Nutr. **87**: 1750-1759.

Novak, J., Danielson, L.A., Kerchner, L.J., Sherwood, O.D., Ramirez, R.J., Moalli, P.A., Conrad, K.P. 2001. Relaxin is essential for renal vasodilation during pregnancy in conscious rats. J. Clin. Invest. **107**: 1469-1475.

O'Donnell, J., Stemmelin, J., Nitta, A., Brouillette, J., Quirion, R. 2003. Gene expression profiling following chronic NMDA receptor blockade-induced learning deficits in rats. Synapse **50**: 171-180.

Ogawa, K., Utsunomiya, T., Mimori, K., Yamashita, K., Okamoto, M., Tanaka, F., Inoue, H., Ikeda, Y., Saku, M., Murayama, S., Mori, M. 2005. Genomic screens for genes upregulated by demethylation in colorectal cancer: possible usefulness for clinical application. Int. J. Oncol. **27**: 417-426.

Ohm, T.G., Treiber-Held, S., Distl, R., Glockner, F., Schonheit, B., Tamanai, M., Meske,V. 2003. Cholesterol and tau protein--findings in Alzheimer's and Niemann Pick C's disease. Pharmacopsychiatry **36**: S120-S126.

Okumura, K., Ohkura, N., Inoue, S., Ikeda, K., Hayashi, K. 1998. A novel phospholipase A2 inhibitor with leucine-rich repeats from the blood plasma of Agkistrodon blomhoffii siniticus. Sequence homologies with human leucine-rich alpha2-glycoprotein. J. Biol. Chem. **273**: 19469-19475.

O'Neill, L, 2000. The Toll/interleukin-1 receptor domain: a molecular switch for inflammation and host defence. Biochem. Soc. Trans. **28**: 557-563.

Ong, W.Y., He, Y., Suresh, S., Patel, S.C. 1997. Differential expression of apolipoprotein D and apolipoprotein E in the kainic acid-lesioned rat hippocampus. Neuroscience **79**: 359-367.

Ong, W.Y., Hu, C.Y., Patel, S.C. 2002. Apolipoprotein D in the Niemann-Pick type C disease mouse brain: an ultrastructural immunocytochemical analysis. J. Neurocytol. **31**: 121-129.

Ong, W.Y., Lau, C.P., Leong, S.K., Kumar, U., Suresh, S., Patel, S.C. 1999. Apolipoprotein D gene expression in the rat brain and light and electron microscopic immunocytochemistry of apolipoprotein D expression in the cerebellum of neonatal, immature and adult rats. Neuroscience **90**: 913-922.

Ordoñez, C. Navarro, A. Perez, C. Astudillo, A. Martinez, E. Tolivia, J. 2006. Apolipoprotein D expression in substantia nigra of Parkinson disease. Histol. Histopathol. **21**: 361-366.

Ostlund, R.E. Jr, Yang, J.W., Klein, S., Gingerich, R. 1996. Relation between plasma leptin concentration and body fat, gender, diet, age, and metabolic covariates. J. Clin. Endocrinol. Metab. **81**: 3909-3913.

Pacifico, L., Di Renzo, L., Anania, C., Osborn, J.F., Ippoliti, F., Schiavo, E., Chiesa, C. 2006. Increased T-helper interferon-gamma-secreting cells in obese children. Eur J Endocrinol **154**: 691-697.

Pahl, H.L. 1999. Activators and target genes of Rel/NF-κB transcription factors. Oncogene **18**: 6853-6866.

Palmer, D.J., Kelly, V.C., Smit, A.M., Kuy, S., Knight, C.G., Cooper, G.J. 2006. Human colostrum: Identification of minor proteins in the aqueous phase by proteomics. Proteomics **6**: 2208-2216.

Patel, R.C., Lange, D., McConathy, W.J., Patel, Y.C., Patel, S.C. 1997. Probing the structure of the ligand binding cavity of lipocalins by fluorescence spectroscopy. Protein Eng. **10**: 621-625.

Patel, S.C., Asotra, K., Patel, Y.C., McConathy, W.J., Patel, R.C., Suresh, S. 1995. Astrocytes synthesize and secrete the lipophilic ligand carrier apolipoprotein D. Neuroreport **6**: 653-657.

Paumelle, R., Blanquart, C., Briand, O., Barbier, O., Duhem, C., Woerly, G., Percevault, F., Fruchart, J.C., Dombrowicz, D., Glineur, C., Staels, B. 2006. Acute

antiinflammatory properties of statins involve peroxisome proliferator-activated receptor-alpha via inhibition of the protein kinase C signaling pathway. Circ. Res. **98**: 361-369.

Pearlman, W.H., Guériguian, J.L., Sawyer, M.E. 1973. A specific progesterone-binding component of human breast cyst fluid. J. Biol. Chem. **248**: 5736-5741.

Pechumer, H., Bender-Götze, C., Ziegler-Heitbrock, H.W. 1993. Detection of neuron-specific gamma-enolase messenger ribonucleic acid in normal human leukocytes by polymerase chain reaction amplification with nested primers. Lab. Invest. **69**: 743-749.

Peitsch, M.C., Boguski, M.S. 1990. Is apolipoprotein D a mammalian bilin-binding protein? New Biol. **2**: 197-206.

Peng, J., Mao, X.O., Stevenson, F.F., Hsu, M., Andersen, J.K. 2004. The herbicide paraquat induces dopaminergic nigral apoptosis through sustained activation of the JNK pathway. J. Biol. Chem. **279**: 32626-32632.

Pippenger, C.E., Browne, R.W., Armstrong, D. 1998. Regulatory antioxidant enzymes. Methods Mol. Biol. **108**: 299-313.

Petersen, K.F., Shulman, G.I. 2006. Etiology of insulin resistance. Am. J. Med. **119**: S10-S16.

Peterson, P.K., Hu, S., Salak-Johnson, J., Molitor, T.W., Chao, C.C. 1997. Differential production of and migratory response to beta chemokines by human microglia and astrocytes. J. Infect. Dis. **175**: 478-481.

Petridou, E., Katsouyanni, K., Hsieh, C.C., Antsaklis, A., Trichopoulos, D. 1992. Diet, pregnancy estrogens and their possible relevance to cancer risk in the offspring. Oncology **49**: 127-132.

Phipps, R.P., Penney, D.P., Keng, P., Quill, H., Paxhia, A., Derdak, S., Felch, M.E. 1989. Characterization of two major populations of lung fibroblasts: distinguishing morphology and discordant display of Thy 1 and class II MHC. Am. J. Respir. Cell. Mol. Biol. **1**: 65-74

Pippenger, C.E., Browne, R.W., Armstrong, D. 1998. Regulatory antioxidant enzymes. Methods Mol. Biol. **108**: 299-313.

Plum, L., Rother, E., Münzberg, H., Wunderlich, F.T., Morgan, D.A., Hampel, B., Shanabrough, M., Janoschek, R., Könner, A.C., Alber, J., Suzuki, A., Krone, W., Horvath, T.L., Rahmouni, K., Brüning, J.C. 2007. Enhanced leptin-stimulated Pi3k activation in the CNS promotes white adipose tissue transdifferentiation. Cell. Metab. **6**: 431-445.

Porter, D., Lahti-Domenici, J., Keshaviah, A., Bae, Y.K., Argani, P., Marks, J., Richardson, A., Cooper, A., Strausberg, R., Riggins, G.J., Schnitt, S., Gabrielson, E., Gelman, R., Polyak, K. 2003. Molecular markers in ductal carcinoma in situ of the breast. Mol. Cancer Res. **1**: 362-375.

Porter, J.A., Young, K.E., Beachy, P.A. 1996. Cholesterol modification of hedgehog signaling proteins in animal development. Science **274**: 255-259.

Potter, J.M., Nestel, P.J. 1979. The hyperlipidemia of pregnancy in normal and complicated pregnancies. Am. J. Obstet. Gynecol. **133**: 165-170.

Prosniak, M., Hooper, D.C., Dietzschold, B., Koprowski, H. 2001. Effect of rabies virus infection on gene expression in mouse brain. Proc. Natl Acad. Sci. U S A **98**: 2758-2763.

Provost, P.R., Marcel, Y.L., Milne, R.W., Weech, P.K., Rassart, E. 1991a. Apolipoprotein D transcription occurs specifically in nonproliferating quiescent and senescent fibroblast cultures. FEBS Lett. **290**: 139-141.

Provost, P.R., Tremblay, Y., el-Amine, M., Belanger, A. 1995. Guinea pig apolipoprotein D RNA diversity, and developmental and gestational modulation of mRNA levels. Mol. Cell. Endocrinol. **109**: 225-236.

Provost, P.R., Villeneuve, L., Weech, P.K., Milne, R.W., Marcel, Y.L., Rassart, E. 1991b. Localization of the major sites of rabbit apolipoprotein D gene transcription by in situ hybridization. J. Lipid Res. **32**: 1959-1970.

Provost, P.R., Weech, P.K., Tremblay, N.M., Marcel, Y.L., Rassart, E. 1990. Molecular characterization and differential mRNA tissue distribution of rabbit apolipoprotein D. J. Lipid Res. 31: 2057-2065.

Rassart, E., Bedirian, A., Do Carmo, S., Guinard, O., Sirois, J., Terrisse, L., Milne, R. 2000. Apolipoprotein D. Biochim. Biophys. Acta. **1482**: 185-198.

Reindl, M., Knipping, G., Wicher, I., Dilitz, E., Egg, R., Deisenhammer, F., Berger, T. 2001. Increased intrathecal production of apolipoprotein D in multiple sclerosis. J. Neuroimmunol. **119**: 327-332.

Rickhag, M., Deierborg, T., Patel, S., Ruscher, K., Wieloch, T. 2008. Apolipoprotein D is elevated in oligodendrocytes in the peri-infarct region after experimental stroke: influence of enriched environment. J. Cereb. Blood Flow Metab. **28**: 551-562.

Rickhag, M., Wieloch, T., Gidö, G., Elmér, E., Krogh, M., Murray, J., Lohr, S., Bitter, H., Chin, D.J., von Schack, D., Shamloo, M., Nikolich, K. 2006. Comprehensive regional and temporal gene expression profiling of the rat brain during the first 24 h after experimental stroke identifies dynamic ischemia-induced gene expression patterns, and reveals a biphasic activation of genes in surviving tissue. J. Neurochem. **96**: 14-29.

Rinaldi, P., Polidori, M.C., Metastasio, A., Mariani, E., Mattioli, P., Cherubini, A., Catani, M., Cecchetti, R., Senin, U., Mecocci, P. 2003. Plasma antioxidants are similarly depleted in mild cognitive impairment and in Alzheimer's disease. Neurobiol. Aging **24**: 915-919.

Rodriguez, J.C., Diaz, M., Gonzalez, L.O., Sanchez, J., Sanchez, M.T., Merino, A.M., Vizoso, F. 2000. Apolipoprotein D expression in benign and malignant prostate tissues. Int. J. Surg. Investig. **2**: 319-326.

Rodriguez, A., Durán, A., Selloum, M., Champy, M.F., Diez-Guerra, F.J., Flores, J.M., Serrano, M., Auwerx, J., Diaz-Meco, M.T., Moscat, J. 2006. Mature-onset obesity and insulin resistance in mice deficient in the signaling adapter p62. Cell Metab. **3**: 211-222.

Rojo, J.V., Gonzalez, L.O., Lamelas, M.L., Merino, A., Vizoso, F. 2001. Apolipoprotein D expression in endometrial carcinomas. Acta Obstet. Gynecol. Scand. **80**: 158-161.

Ruhlen, R.L., Sauter E.R., Proteomics of nipple aspirate fluid, breast cyst fluid, milk, and colostrum. Proteomics **1**: 845-852.

Ryu, B., Jones, J., Hollingsworth, M.A., Hruban, R.H., Kern, S.E. 2001. Invasion-specific genes in malignancy: serial analysis of gene expression comparisons of primary and passaged cancers. Cancer Res. **61**: 1833-1838.

Saha, S., Rangarajan, P.N. 2003. Common host genes are activated in mouse brain by Japanese encephalitis and rabies viruses. J. Gen. Virol. **84**: 1729-1735.

Saito, M., Smiley, J., Toth, R., Vadasz, C. 2002. Microarray analysis of gene expression in rat hippocampus after chronic ethanol treatment. Neurochem. Res. **27**: 1221-1229.

Salen, G., Berginer, V., Shore, V., Horak, I., Horak, E., Tint, G.S., Shefer, S. 1987. Increased concentrations of cholestanol and apolipoprotein B in the cerebrospinal fluid of patients with cerebrotendinous xanthomatosis. Effect of chenodeoxycholic acid. N. Engl. J. Med. **316**: 1233-1238.

Sanchez, D., Ganfornina, M.D., Martínez, S. 2002. Expression pattern of the lipocalin apolipoprotein D during mouse embryogenesis. Mech. Dev. **110**: 225-229.

Sanchez, D., López-Arias, B., Torroja, L., Canal, I., Wang, X., Bastiani, M.J., Ganfornina, M.D. 2006. Loss of glial lazarillo, a homolog of apolipoprotein D, reduces lifespan and stress resistance in Drosophila. Curr. Biol. **16**: 680-686.

Sandhya, T.L., Ong, W.Y., Horrocks, L.A., Farooqui, A.A. 1998. A light and electron microscopic study of cytoplasmic phospholipase A2 and cyclooxygenase-2 in the hippocampus after kainate lesions. Brain Res. **788**: 223-231.

Sarjeant, J.M., Lawrie, A., Kinnear, C., Yablonsky, S., Leung, W., Massaeli, H., Prichett, W., Veinot, J.P., Rassart, E., Rabinovitch, M. 2003. Apolipoprotein D inhibits platelet derived growth factor-BB-induced vascular smooth muscle cell proliferated by preventing translocation of phosphorylated extracellular signal

regulated kinase 1/2 to the nucleus. Arterioscler. Thromb. Vasc. Biol. **23**: 2172-2177.

Sato, N., Fujii, K., Yuge, O., Morio, M. 1992. Changes in lipid peroxidation levels and lipid composition in the lungs, livers, kidneys and brains of mice treated with paraquat. J. Appl. Toxicol. **12**: 365-368.

Schaeren-Wiemers, N., Schaefer, C., Valenzuela, D.M., Yancopoulos, G.D., Schwab, M.E. 1995. Identification of new oligodendrocyte- and myelin-specific genes by a differential screening approach. J. Neurochem. **65**: 10-22.

Schinner, S., Scherbaum, W.A., Bornstein, S.R., Barthel, A. 2005. Molecular mechanisms of insulin resistance. Diabet. Med. **22**: 674-682.

Schmidt, S., Barcellos, L.F., DeSombre, K., Rimmler, J.B., Lincoln, R.R., Bucher, P., Saunders, A.M., Lai, E., Martin, E.R., Vance, J.M., Oksenberg, J.R., Hauser, S.L., Pericak-Vance, M.A., Haines, J.L. 2002. Association of polymorphisms in the apolipoprotein E region with susceptibility to and progression of multiple sclerosis. Am. J. Hum. Genet. **70**: 708-717.

Schmidt, T.G., Skerra, A. 2007. The Strep-tag system for one-step purification and high-affinity detection or capturing of proteins. Nat Protoc. **2**: 1528-1535.

Scholl, T.O., Chen, X. 2002. Insulin and the "thrifty" woman: the influence of insulin during pregnancy on gestational weight gain and postpartum weight retention. Matern. Child. Health J. **6**: 255-261.

Séguin, D., Desforges, M., Rassart, E. 1995. Molecular characterization and differential mRNA tissue distribution of mouse apolipoprotein D. Brain Res. Mol. Brain Res. **30**: 242-250.

Selim, A.A., El-Ayat, G., Wells, C.A. 2001. Immunohistochemical localization of gross cystic disease fluid protein-15, -24 and -44 in ductal carcinoma in situ of the breast: relationship to the degree of differentiation. Histopathology **39**: 198-202.

Serra Diaz, C., Vizoso, F., Lamelas, M.L., Rodriguez, J.C., Gonzalez, L.O., Baltasar, A., Medrano, J. 1999. Expression and clinical significance of apolipoprotein D in male breast cancer and gynaecomastia. Br. J. Surg. **86**: 1190-1197.

Serra, C., Vizoso, F., Lamelas, M.L., Rodriguez, J.C., Gonzalez, L.O., Merino, A.M., Baltasar, A., Perez-Vazquez, M.T., Medrano, J. 2000. Comparative study of two androgen-induced markers (apolipoprotein D and pepsinogen C) in female and male breast carcinoma. Int. J. Surg. Investig. **2**: 183-192.

Shimaoka, Y., Hidaka, Y., Tada, H., Nakamura, T., Mitsuda, N., Morimoto, Y., Murata, Y., Amino, N. 2000. Changes in cytokine production during and after normal pregnancy. Am. J. Reprod. Immunol. **44**: 143-147.

Shimaoka, Y., Hidaka, Y., Tada, H., Takeoka, K., Morimoto, Y., Amino, N. 2001. Influence of breast-feeding on the production of cytokines. Am. J. Reprod. Immunol. **45**: 100-102.

Shintaku, K., Arima, Y., Dan, Y., Takeda, T., Kogushi, K., Tsujimoto, M., Nagata, H., Satoh, S., Tsukimori, K., Nakano, H., Hori, S., Ohtani, H., Sawada, Y. 2007. Kinetic analysis of the transport of salicylic acid, a nonsteroidal anti-inflammatory drug, across human placenta. Drug Metab. Dispos. **35**: 772-778.

Simard, A.R., Rivest, S. 2007. Neuroprotective effects of resident microglia following acute brain injury. J. Comp. Neurol. **504**: 716-729.

Simard, J., Dauvois, S., Haagensen, D.E., Levesque, C., Merand, Y., Labrie, F. 1990. Regulation of progesterone-binding breast cyst protein GCDFP-24 secretion by estrogens and androgens in human breast cancer cells: a new marker of steroid action in breast cancer. Endocrinology **126**: 3223-3231.

Simard, J., de Launoit, Y., Haagensen, D.E., Labrie, F. 1992. Additive stimulatory action of glucocorticoids and androgens on basal and estrogen-repressed apolipoprotein-D messenger ribonucleic acid levels and secretion in human breast cancer cells. Endocrinology **130**: 1115-1121.

Simard, J., Veilleux, R., de Launoit, Y., Haagensen, D.E., Labrie, F. 1991. Stimulation of apolipoprotein D secretion by steroids coincides with inhibition of cell proliferation in human LNCaP prostate cancer cells. Cancer Res. **51**: 4336-4341.

Smith, C., Andreakos, E., Crawley, J.B., Brennan, F.M., Feldmann, M., Foxwell, B.M., 2001. NF-kappaB-inducing kinase is dispensable for activation of NF-kappaB in inflammatory settings but essential for lymphotoxin beta receptor activation of NF-kappaB in primary human fibroblasts. J. Immunol. **167**: 5895-5903.

Smith, K.M., Lawn, R.M., Wilcox, J.N. 1990. Cellular localization of apolipoprotein D and lecithin:cholesterol acyltransferase mRNA in rhesus monkey tissues by in situ hybridization. J. Lipid Res. **31**: 995-1004.

Soldin, O.P., Guo, T., Weiderpass, E., Tractenberg, R.E., Hilakivi-Clarke, L., Soldin, S.J. 2005. Steroid hormone levels in pregnancy and 1 year postpartum using isotope dilution tandem mass spectrometry. Fertil. Steril. **84**: 701-710.

Song, H., Jin, X., Lin, J. 2004. Stat3 upregulates MEK5 expression in human breast cancer cells. Oncogene **23**: 8301-8309.

Spreyer, P., Schaal, H., Kuhn, G., Rothe, T., Unterbeck, A., Olek, K., Muller, H.W. 1990. Regeneration-associated high level expression of apolipoprotein D mRNA in endoneurial fibroblasts of peripheral nerve. EMBO J. **9**: 2479-2484.

Stein, T.P., Scholl ,T.O., Schluter, M.D., Schroeder, C.M. 1998. Plasma leptin influences gestational weight gain and postpartum weight retention. Am. J. Clin. Nutr. **68**: 1236-1240.

Stephenson, D.T., Lemere, C.A., Selkoe, D.J., Clemens, J.A. 1996. Cytosolic phospholipase A2 (cPLA2) immunoreactivity is elevated in Alzheimer's disease brain. Neurobiol. Dis. **3**: 51-63.

Steyrer, E., Kostner, G.M. 1988. Activation of lecithin-cholesterol acyltransferase by apolipoprotein D: comparison of proteoliposomes containing apolipoprotein D, A-I or C-I. Biochim. Biophys. Acta **958**: 484-491.

Stiles, B., Wang, Y., Stahl, A., Bassilian, S., Lee, W.P., Kim, Y.J., Sherwin, R., Devaskar, S., Lesche, R., Magnuson, M.A., Wu, H. 2004. Liver-specific deletion of negative regulator Pten results in fatty liver and insulin hypersensitivity. Proc. Natl Acad. Sci. U S A. **101**: 2082-2087.

Stohlman, S.A., Bergmann, C.C., van der Veen, R.C., Hinton, D.R. 1995. Mouse hepatitis virus-specific cytotoxic T lymphocytes protect from lethal infection without eliminating virus from the central nervous system. J. Virol. **69**: 684-694.

Stoll, G., Jander, S., Schroeter, M. 2000. Cytokines in CNS disorders: neurotoxicity versus neuroprotection. J. Neural Transm. Suppl. **59**: 81-89.

Strehlow, I., Seegert, D., Frick, C., Bange, F.C., Schindler, C., Bottger, E.C., Decker, T. 1993. The gene encoding IFP 53/tryptophanyl-tRNA synthetase is regulated by the gamma-interferon activation factor. J. Biol. Chem. **268**: 16590-16595.

Streit, W.J., Mrak, R.E., Griffin, W.S. 2004. Microglia and neuroinflammation: a pathological perspective. J. Neuroinflammation **1**: 14.

Strittmatter, W.J., Roses, A.D. 1996. Apolipoprotein E and Alzheimer's disease. Annu. Rev. Neurosci. **19**: 53-77.

Sugimoto, K., Simard, J., Haagensen, D.E., Labrie, F. 1994. Inverse relationships between cell proliferation and basal or androgen-stimulated apolipoprotein D secretion in LNCaP human prostate cancer cells. J. Steroid Biochem. Mol. Biol. **51**: 167-174.

Suresh, S., Yan, Z., Patel, R.C., Patel, Y.C., Patel, S.C. 1998. Cellular cholesterol storage in the Niemann-Pick disease type C mouse is associated with increased expression and defective processing of apolipoproteinD. J. Neurochem. **70**: 242-251.

Suzuki, S., Gerhold, L.M., Böttner, M., Rau, S.W., Dela Cruz, C., Yang, E., Zhu, H., Yu, J., Cashion, A.B., Kindy, M.S., Merchenthaler, I., Gage, F.H., Wise, P.M. 2007. Estradiol enhances neurogenesis following ischemic stroke through estrogen receptors alpha and beta. J. Comp. Neurol. **500**: 1064-1075.

Talbot, P.J., Arnold, D., Antel, J.P. 2001. Virus-induced autoimmune reactions in the CNS. Curr. Top. Microbiol. Immunol. **253**: 247-271.

Talbot, P.J., Jacomy, H.J., Desforges, M. 2008. Pathogenesis of Human Coronaviruses other than severe acute respiratory syndrome coronavirus. In:

Perlman, S., Gallagher, T., Snijder, E.J. (eds). Nidovirus. ASM Press. Washington, DC, USA, pp313-324.

Tanigawa, T., Iso, H., Yamagishi, K., Muraki, I., Kawamura, N., Nakata, A., Sakurai, S., Ohira, T., Shimamoto, T. 2004. Association of lymphocyte sub-populations with clustered features of metabolic syndrome in middle-aged Japanese men. Atherosclerosis **173**: 295-300.

Tapia-Gonzalez, S., Carrero, P., Pernia, O., Garcia-Segura, L., Diz-Chaves, Y. 2008. Selective oestrogen receptor modulators reduce microglia reactivity in vivo after peripheral inflammation: potential role of microglial oestrogen receptors. J. Endocrinol. **198**: 219-230.

Tardif, F. Ross, G. Rouabhia, M. 2004. Gingival and dermal fibroblasts produce interleukin-1 beta converting enzyme and interleukin-1 beta but not interleukin-18 even after stimulation with lipopolysaccharide. J. Cell Physiol. **198**: 125-132.

Tekirian, T.L. 2002. The central role of the trans-Golgi network as a gateway of the early secretory pathway: physiologic vs nonphysiologic protein transit. Exp. Cell. Res. **281**: 9-18.

Terrisse, L., Poirier, J., Bertrand, P., Merched, A., Visvikis, S., Siest, G., Milne, R., Rassart, E. 1998. Increased levels of apolipoprotein D in cerebrospinal fluid and hippocampus of Alzheimer's patients. J. Neurochem. **71**: 1643-1650.

Terrisse, L., Séguin, D., Bertrand, P., Poirier, J., Milne, R.W., Rassart, E. 1999. Modulation of Apolipoprotein D and apolipoprotein E mRNA expression in rat hippocampus after enthorinal cortex lesion. Mol. Brain Res. **70**: 26-35.

Thiruchelvam, M., Richfield, E.K., Baggs, R.B., Tank, A.W., Cory-Slechta, D.A. 2000. The nigrostriatal dopaminergic system as a preferential target of repeated exposures to combined paraquat and maneb: implications for Parkinson's disease. J Neurosci. **20**: 9207-9214.

Thomas, E.A., Copolov, D.L., Sutcliffe, J.G. 2003a. From pharmacotherapy to pathophysiology: emerging mechanisms of apolipoprotein D in psychiatric disorders. Curr. Mol. Med. **3**: 408-418.

Thomas, E.A., Danielson, P.E., Nelson, P.A., Pribyl, T.M., Hilbush, B.S., Hasel, K.W., Sutcliffe, J.G. 2001a. Clozapine increases apolipoprotein D expression in rodent brain: towards a mechanism for neuroleptic pharmacotherapy. J. Neurochem. **76**: 789-796.

Thomas, E.A., Dean, B., Pavey, G., Sutcliffe, J.G. 2001b. Increased CNS levels of apolipoprotein D in schizophrenic and bipolar subjects: implications for the pathophysiology of psychiatric disorders. Proc. Natl Acad. Sci. USA **98**: 4066-4071.

Thomas, E.A., Dean, B., Scarr, E., Copolov, D., Sutcliffe, J.G. 2003b. Differences in neuroanatomical sites of apoD elevation discriminate between schizophrenia and bipolar disorder. Mol. Psychiatry **8**: 167-175.

Thomas, E.A., George, R.C., Danielson, P.E., Nelson, P.A., Warren, A.J., Lo, D., Sutcliffe, J.G. 2003c. Antipsychotic drug treatment alters expression of mRNAs encoding lipid metabolism-related proteins. Mol. Psychiatry **8**: 983-393.

Thomas, E.A., George, R.C., Sutcliffe, J.G. 2003d. Apolipoprotein D modulates arachidonic acid signaling in cultured cells: implications for psychiatric disorders. Prostaglandins Leukot. Essent. Fatty Acids. **69**: 421-427.

Thomas, E.A., Laws, S.M., Sutcliffe, J.G., Harper, C., Dean, B., McClean, C., Masters, C., Lautenschlager, N., Gandy, S.E., Martins, R.N. 2003e. Apolipoprotein D levels are elevated in prefrontal cortex of subjects with Alzheimer's disease: no relation to apolipoprotein E expression or genotype. Biol. Psychiatry **54**: 136-141.

Thomas, E.A., Sautkulis, L.N., Criado, J.R., Games, D., Sutcliffe, J.G. 2001c. Apolipoprotein D mRNA expression is elevated in PDAPP transgenic mice. J. Neurochem. **79**: 1059-1064.

Thomas, E.A., Yao, J.K. 2007. Clozapine specifically alters the arachidonic acid pathway in mice lacking apolipoprotein D. Schizophr. Res. **89**: 147-153.

Thompson, G.N., Halliday, D. 1992. Protein turnover in pregnancy. Eur. J. Clin. Nutr. **46**: 411-417.

Tilg, H., Moschen, A.R. 2008. Inflammatory mechanisms in the regulation of insulin resistance. Mol. Med. **14**: 222-231.

Todorov, P.T., Wyke, S.M., Tisdale, M.J. 2007. Identification and characterization of a membrane receptor for proteolysis-inducing factor on skeletal muscle. Cancer Res. **67**: 11419-11427.

Tokugawa, Y., Koyama, M., Silver, J. 1997. A molecular basis for species differences in Thy-1 expression patterns. Mol. Immunol. **34**: 1263-1272.

Tomarev, S.I., Wistow, G., Raymond, V., Dubois, S., Malyukova, I. 2003. Gene expression profile of the human trabecular meshwork: NEIBank sequence tag analysis. Invest. Ophthalmol. Vis. Sci. **44**: 2588-2596.

Tomita, M., Okuyama, T., Katsuyama, H., Ishikawa, T. 2006a. Paraquat-induced gene expression in rat kidney. Arch. Toxicol. **80**: 687-693.

Tomita, M., Okuyama, T., Katsuyama, H., Hidaka, K., Otsuki, T., Ishikawa, T. 2006b. Gene expression in rat lungs during early response to paraquat-induced oxidative stress. Int. J. Mol. Med. **17**: 37-44.

Tóth, A., Kiss, E., Herberg, F.W., Gergely, P., Hartshorne, D.J., Erdödi, F. 2000. Study of the subunit interactions in myosin phosphatase by surface plasmon resonance. Eur. J. Biochem. **267**: 1687-1697.

Tran, T.A., McCoy, M.K., Sporn, M.B., Tansey, M.G. 2008. The synthetic triterpenoid CDDO-methyl ester modulates microglial activities, inhibits TNF production, and provides dopaminergic neuroprotection. J. Neuroinflammation **5**: 14.

Trevaskis, J., Walder, K., Foletta, V., Kerr-Bayles, L., McMillan, J., Cooper, A., Lee, S., Bolton, K., Prior, M., Fahey, R., Whitecross, K., Morton, G.J., Schwartz, M.W., Collier, G.R. 2005. Src homology 3-domain growth factor receptor-bound 2-like (endophilin) interacting protein 1, a novel neuronal protein that regulates energy balance. Endocrinology **146**: 3757-3764.

Uematsu, S., Matsumoto, M., Takeda, K., Akira, S. 2002. Lipopolysaccharide-dependent prostaglandin E(2) production is regulated by the glutathione-dependent

prostaglandin E(2) synthase gene induced by the Toll-like receptor 4/MyD88/NF-IL6 pathway. J. Immunol. **168**: 5811-5816.

Ulmer, A.J. Flad, H. Rietschel, T. Mattern, T. 2000. Induction of proliferation and cytokine production in human T lymphocytes by lipopolysaccharide (LPS). Toxicology **152**: 37-45.

Utsunomiya, T., Ogawa, K., Yoshinaga, K., Ohta, M., Yamashita, K., Mimori, K., Inoue, H., Ezaki, T., Yoshikawa, Y., Mori, M. 2005. Clinicopathologic and prognostic values of apolipoprotein D alterations in hepatocellular carcinoma. Int. J. Cancer **116**: 105-109.

Vajragupta, O., Monthakantirat, O., Wongkrajang, Y., Watanabe, H., Peungvicha, P. 2000. Chroman amide 12P inhibition of lipid peroxidation and protection against learning and memory impairment. Life Sci. **67**: 1725-1734.

van Dijk, W., Do Carmo, S., Rassart, E., Dahlbäck, B., Sodetz, J.M. 2006. The plasma lipocalins α1-acid glycoprotein, apolipoprotein D, apolipoprotein M and complement protein C8γ, in: B. Akerström, N. Borregaard, D.R. Flower, J.-P. Salier (Eds.), Lipocalins, Landes Bioscience, Georgetown, TX, USA. pp.140-166.

Vazquez, J., Gonzalez, L., Merino, A, Vizoso, F. 2000. Expression and clinical significance of apolipoprotein D in epithelial ovarian carcinomas. Gynecol. Oncol. **76**: 340-347.

Verina, T., Rohde, C.A., Guilarte, T.R. 2007. Environmental lead exposure during early life alters granule cell neurogenesis and morphology in the hippocampus of young adult rats. Neuroscience **145**: 1037-1047.

Vieira, A.V., Lindstedt, K., Schneider, W.J., Vieira, P.M. 1995. Identification of a circulatory and oocytic avian apolipoprotein D. Mol. Reprod. Dev. **42**: 443-446.

Vijayaraghavan, S., Hitman, G.A., Kopelman, P.G. 1994. Apolipoprotein-D polymorphism: a genetic marker for obesity and hyperinsulinemia. J. Clin. Endocrinol. Metab. **79**: 568-570.

Vogt, M., Skerra, A. 2001. Bacterially produced apolipoprotein D binds progesterone and arachidonic acid, but not bilirubin or E-3M2H. J. Mol. Recognit. **14**: 79-86.

Volontc, D. Zhang, K. Lisanti, M.P. Galbiati, F. 2002. Expression of caveolin-1 induces premature cellular senescence in primary cultures of murine fibroblasts. Mol. Biol. Cell. **13**: 2502-2517.

Walker, D.W., Muffat, J., Rundel, C., Benzer, S. 2006. Overexpression of a Drosophila homolog of apolipoprotein D leads to increased stress resistance and extended lifespan. Curr. Biol. **16**: 674-679.

Walton, M., Sirimanne, E., Williams, C., Gluckman, P.D., Keelan, J., Mitchell, M.D., Dragunow, M. 1997. Prostaglandin H synthase-2 and cytosolic phospholipase A2 in the hypoxic-ischemic brain: role in neuronal death or survival? Brain Res. Mol. Brain Res. **50**: 165-170.

Wang, C., Hsueh, A.J., Erickson, G.F. 1980. Prolactin inhibition of estrogen production by cultured rat granulosa cells. Mol. Cell. Endocrinol. **20**: 135-144.

Wang, L., Zhang S, Liu Z, Li H, Wang Y, Jiang S. 2007. Characterization and expression of amphioxus ApoD gene encoding an archetype of vertebrate ApoD proteins. Cell. Biol. Int. **31**: 74-81.

Warner, R.L. Bhagavathula, N. Nerusu, K.C. Lateef, H. Younkin, E. Johnson, K.J. Varani, J. 2004. Matrix metalloproteinases in acute inflammation: induction of MMP-3 and MMP-9 in fibroblasts and epithelial cells following exposure to pro-inflammatory mediators in vitro. Exp. Mol. Pathol. **76**: 189-195.

Weber-Chappuis, K., Bieri-Burger, S., Hurlimann, J. 1996. Comparison of prognostic markers detected by immunohistochemistry in male and female breast carcinomas. Eur. J. Cancer **32A**: 1686-1692.

Weech, P.K., Camato, R., Milne, R.W., Marcel, Y.L. 1986. Apolipoprotein D and cross-reacting human plasma apolipoproteins identified using monoclonal antibodies. J. Biol. Chem. **261**: 7941-7951.

Weiss, J.M., Downie, S.A., Lyman, W.D., Berman, J.W. 1998. Astrocyte-derived monocyte-chemoattractant protein-1 directs the transmigration of leukocytes across a model of the human blood-brain barrier. J. Immunol. **161**: 6896-6903.

West, C.P., McNeilly, A.S. 1979. Hormonal profiles in lactating and non-lactating women immediately after delivery and their relationship to breast engorgement. Br. J. Obstet. Gynaecol. **86**: 501-506.

West, R.B., Harvell, J., Linn, S.C., Liu, C.L., Prapong, W., Hernandez-Boussard, T., Montgomery, K., Nielsen, T.O., Rubin, B.P., Patel, R., Goldblum, J.R., Brown, P.O., van de Rijn, M., Lui, C.L. 2004. Apo D in soft tissue tumors: a novel marker for dermatofibrosarcoma protuberans. Am. J. Surg Pathol. **28**: 1063-1069.

Wuu, J., Hellerstein, S., Lipworth, L., Wide, L., Xu, B., Yu, G.P., Kuper, H., Lagiou, P., Hankinson, S.E., Ekbom, A., Carlström, K., Trichopoulos, D., Adami, H.O., Hsieh, C.C. 2002. Correlates of pregnancy oestrogen, progesterone and sex hormone-binding globulin in the USA and China. Eur. J. Cancer Prev. **11**: 283-293.

Yamashita, K., Upadhyay, S., Osada, M., Hoque, M.O., Xiao, Y., Mori, M., Sato, F., Meltzer, S.J., Sidransky, D. 2002. Pharmacologic unmasking of epigenetically silenced tumor suppressor genes in esophageal squamous cell carcinoma. Cancer Cell. **2**: 485-495.

Yang, C.Y., Gu, Z.W., Blanco-Vaca, F., Gaskell, S.J., Yang, M., Massey, J.B., Gotto, A.M. Jr, Pownall, H.J. 1994. Structure of human apolipoprotein D: locations of the intermolecular and intramolecular disulfide links. Biochemistry **33**: 12451-12455.

Yao, J.K., Thomas, E.A., Reddy, R.D., Keshavan, M.S. 2005. Association of plasma apolipoproteins D with RBC membrane arachidonic acid levels in schizophrenia. Schizophr. Res. **72**: 259-266.

Yao, Y., Vieira, A. 2002. Comparative 17beta-estradiol response and lipoprotein interactions of an avian apolipoprotein. Gen. Comp. Endocrinol. **127**: 89-93.

Yoshida, K., Cleaveland, E.S., Nagle, J.W., French, S., Yaswen, L., Ohshima, T., Brady, R.O., Pentchev, P.G., Kulkarni, A.B. 1996. Molecular cloning of the mouse apolipoprotein D gene and its upregulated expression in Niemann-Pick disease type C mouse model. DNA Cell Biol. **15** :873-882.

Yoshikawa, T., Shimano, H., Yahagi, N., Ide, T., Amemiya-Kudo, M., Matsuzaka, T., Nakakuki, M., Tomita, S., Okazaki, H., Tamura, Y., Iizuka, Y., Ohashi, K., Takahashi, A., Sone, H., Osuga Ji, J., Gotoda, T., Ishibashi, S., Yamada, N. 2002. Polyunsaturated fatty acids suppress sterol regulatory element-binding protein 1c promoter activity by inhibition of liver X receptor (LXR) binding to LXR response elements. J. Biol. Chem. **277**:1705-1711.

Yuan, J., Wegenka, U.M., Lutticken, C., Buschmann, J., Decker, T., Schindler, C., Heinrich, P.C., Horn, F. 1994. The signalling pathways of interleukin-6 and gamma interferon converge by the activation of different transcription factors which bind to common responsive DNA elements. Mol. Cell. Biol. **14**: 1657-1668.

Zandi, P.P. Anthony, J.C. Hayden, K.M. Mehta, K. Mayer, L. Breitner, J.C. 2002. Reduced incidence of AD with NSAID but not H2 receptor antagonists: the Cache County Study. Neurology **59**: 880-886.

Zeng, C., Spielman, A.I., Vowels, B.R., Leyden, J.J., Biemann, K., Preti, G. 1996. A human axillary odorant is carried by apolipoprotein D. Proc. Natl Acad. Sci. U S A **93**: 6626-6630.

Zhang, J., He, Q., Liu, Q.Y., Guo, W., Deng, X.M., Zhang, W.W., Hu, X.X., Li, N. 2007. Differential gene expression profile in pig adipose tissue treated with/without clenbuterol. BMC Genomics **8**: 433.

Zhang, S.X., Bentel, J.M., Ricciardelli, C., Horsfall, D.J., Haagensen, D.E., Marshall, V.R., Tilley, W.D. 1998. Immunolocalization of apolipoprotein D, androgen receptor and prostate specific antigen in early stage prostate cancers. J. Urol. **159**: 548-554.